UNIVERSITÉ DU QUÉBEC

MÉMOIRE PRÉSENTÉ À
L'UNIVERSITÉ DU QUÉBEC À CHICOUTIMI
COMME EXIGENCE PARTIELLE
DE LA MAÎTRISE EN SCIENCES DE LA TERRE

Par
MATTHIAS QUEFFURUS

L'UTILISATION DU RAPPORT S/SE DANS LES GISEMENTS MAGMATIQUES À SULFURES DE NI-CU-EGP ET SES IMPLICATIONS DANS LA CARACTÉRISATION DES PROCESSUS PÉTROGÉNÉTIQUES : APPLICATION AU COMPLEXE DE DULUTH (MINNESOTA, USA).

Août 2012

RÉSUMÉ

L'utilisation du rapport soufre/sélénium (S/Se) dans les gisements magmatiques à Ni-Cu-Eléments du Groupe du Platine (EGP), ses implications dans la caractérisation des processus pétrogénétiques ainsi qu'une application au complexe de Duluth sont présentés dans ce mémoire de Maîtrise en Sciences de la Terre. Depuis 30 ans, cet outil est régulièrement utilisé en tant qu'indicateur pétrogénétique de processus de formation à l'origine des gisements de Ni-Cu-EGP. Cependant, le rapport S/Se est parfois appliqué de manière arbitraire et en omettant de nombreux processus modifiant ses valeurs et donc son interprétation. L'absence d'étude consacrée spécifiquement au rapport S/Se dans ce type de gisement est la base de ce projet. Une revue bibliographique des données en S, Se, $\delta^{34}S$ et métaux des principaux gisements de Ni-Cu-EGP a été réalisée afin de mieux contraindre le domaine d'application du rapport S/Se. À travers ce travail de compilation, nous avons répertoriés deux grands types de processus affectant le rapport S/Se: les processus magmatiques et les processus tardi- à post-magmatiques. 1) Les processus magmatiques incluent la contamination par le S d'origine crustal, les variations dans le rapport de volume entre le liquide sulfuré et le liquide silicaté (facteur R) durant la ségrégation du liquide sulfuré, l'appauvrissement en Se du magma silicaté par ségrégation précoce du liquide sulfuré et l'incompatibilité modérée du Se dans les premières phases sulfurées cristallisant à partir du liquide sulfuré, la solution-solide monosulfurée (SSM). Cette légère incompatibilité entraine des variations dans le rapport S/Se des sulfures magmatiques, entre la phase riche en Fe et la phase résiduelle riche en Cu, dérivée de solution-solide intermédiaire (SSI). Le fractionnement du Se pendant la cristallisation du liquide sulfuré n'avait jamais été identifié jusqu'à maintenant. 2) Les processus tardi- à post-magmatiques, incluant l'hydrothermalisme, le métamorphisme de haute grade, la serpentinisation et l'altération météorique, entraînent une remobilisation préférentielle du S par rapport au Se conduisant généralement à une diminution relative du rapport S/Se des roches minéralisées. Les diagrammes synthétiques S/Se *versus* Pt+Pd à 100% sulfures permettent de distinguer les différents domaines du rapport S/Se en fonction du type de dépôt, de l'origine du S et des processus subis. La majeure partie des gisements de Ni-Cu possède des rapports S/Se supérieurs ou égal au manteau associés à de faibles concentrations en Pt+Pd et de faibles facteurs R tandis que les gisements d'EGP ont des rapports S/Se faibles, des concentrations Pt+Pd élevées, des facteurs R élevés et sont constitués de S provenant du manteau. Les exceptions

notables à ce modèle sont les gisements de Ni-Cu ayant subi une perte significative de S, vraisemblablement lors d'un épisode métamorphique de haut grade, marqués par de faibles rapports S/Se associés à de faibles concentrations en Pt+Pd, ainsi que les phases sulfurées riches en Cu enrichies en Se et en Pt+Pd lors du fractionnement du liquide sulfuré. Le rapport S/Se des roches minéralisées est donc le résultat d'une évolution complexe d'une série de processus magmatiques puis tardi-magmatiques et enfin post-magmatiques survenant depuis la fusion partielle mantellique jusqu'à l'altération des roches postérieurement à la mise en place du magma dans la croûte. Parmi la liste des processus répertoriés, la contamination par le S d'origine crustale peut générer des variations importantes dans le rapport S/Se initial des roches ignées contaminées. Dans le but de mieux contraindre ce mécanisme, de nouvelles analyses en S, Se et $\delta^{34}S$ sur les roches encaissantes de la formation métasédimentaire de Virginia localisées au voisinage du complexe de Duluth (MN, USA) ont été réalisées. Le Se a été mesuré par TCF-INAA (*Thiol Cotton Fiber - Instrumental Neutron Activation Analysis)*, une technique adaptée pour les roches présentant de faibles concentrations. Contrairement aux études précédentes, les résultats obtenus montrent que la majeure partie des sédiments possèdent des rapports S/Se et des valeurs $\delta^{34}S$ inférieurs à ceux des dépôts de Cu-Ni-(EGP) soulignant l'impossibilité que ces sédiments soient la source du S des roches minéralisées. Seule l'Unité de Pyrrhotite Litée (UPL) possède des valeurs du rapport S/Se et $\delta^{34}S$ suffisamment élevées pour accroître le rapport S/Se et les valeurs $\delta^{34}S$ des roches minéralisées. Ces résultats, associés à la diminution progressive du rapport S/Se et des valeurs $\delta^{34}S$ depuis la marge vers le centre de l'intrusion et à l'analyse texturale des xénolithes de la BPU, suggèrent un modèle de contamination en S par l'assimilation *in situ* de xénolithes dérivés de l'Unité de Pyrrhotite Litée. L'exemple du complexe de Duluth souligne l'influence fondamentale du rapport S/Se des roches encaissantes dans l'interprétation de l'origine du S des dépôts magmatiques de Ni-Cu-EGP, d'où la nécessité de déterminer la concentration en Se avec une précision acceptable.

AVANT-PROPOS

Le modèle de ce mémoire de Maîtrise en Sciences de la Terre est sous la forme de publications. Deux manuscrits ont été rédigés en anglais et ils font l'objet d'une soumission dans le journal *Economic Geology*. Ce mémoire débute par une introduction générale afin de replacer le projet dans son contexte scientifique et de rappeler les problématiques concernées. Avant chaque manuscrit, un résumé en français est présenté ainsi que les contributions scientifiques relatives à chacun des auteurs, incluant ceux du candidat à la maîtrise. Les deux manuscrits sont ensuite présentés et forment le corps principal du mémoire. Enfin, la conclusion générale synthétise les aboutissements principaux résultant de cette étude, ses retombées académiques et les travaux futurs envisageables. L'ensemble des données utilisées dans le premier manuscrit est présenté en annexe 1 et 2 tandis que les données produites dans le second manuscrit sont incluses dans ce dernier.

REMERCIEMENTS

Je tiens tout d'abord à exprimer mes plus profonds et sincères remerciements envers ma directrice de recherche, Madame la professeure Sarah-Jane Barnes, pour son encadrement, sa très grande disponibilité, son soutien indéfectible, ses nombreux conseils et encouragements durant l'ensemble du projet. Je ne saurais exprimer ma gratitude autant que le respect que m'inspire sa profonde érudition. La réalisation de ce projet n'aurait pu être possible sans le support financier de la Chaire de Recherche du Canada en Métallogénie Magmatique et du Conseil de Recherche en Sciences Naturelles et en Génie du Canada. Mes remerciements s'adressent également aux Dr. Sarah Dare et Philippe Pagé dont les multiples discussions et conseils avisés m'ont permis de mener à bien ce projet. Je remercie Dany Savard et Dr. Paul Bédard pour leur aide dans la réalisation des analyses au laboratoire. Merci également à Judith Ozoray pour la correction de la grammaire anglaise des deux manuscrits présentés.

Je remercie tous mes collègues de l'université avec qui j'ai partagé de nombreux moments de travail, ainsi que de non moins nombreux moment de détentes, notamment: Clifford Patten, Lucas Briao Koth, Charley Duran, Moïse-Lionnel N'Gue Djon, Jérôme Augustin, Dominique Genna, Sandra Richard, Daphnée Pino, Laetitia Amisse, Samuel Morfin, Levin Castillo-Guimond, Pamela Tremblay, Moussa Sinare, Géraldine St-Pierre, Julien Méric, Carlos Ore, Carlos Munoz, Stéphanie Lavaure, Gabriel Coté et Jean-Philippe Arguin, ainsi que tous les étudiants du baccalauréat et l'ensemble du corps professoral de l'UQAC.

Enfin, je tiens à remercier ma copine Gaëlle présente à mes côtés, ainsi que mes amis et ma famille qui m'ont encouragé depuis la Bretagne. Ils m'ont chacun accompagné et soutenu tout au long de mon parcours, en partageant avec moi tout le panel d'émotions que peut générer la réalisation d'une maîtrise. Ils ont contribué pleinement à l'accomplissement de ce projet.

TABLE DES MATIÈRES

LISTE DES TABLEAUX

LISTE DES FIGURES

Article #1

Article #2

À mon cousin, mon grand-père et ma grand-mère

INTRODUCTION GÉNÉRALE

L'exploitation des dépôts magmatiques de Ni-Cu et d'Eléments du Groupe du Platine (EGP) représente 60% du nickel, 2% du cuivre et 99% des platinoïdes produits mondialement (Naldrett, 2004). Ces gisements sont génétiquement associés à des roches mafiques et ultramafiques provenant de la cristallisation de magmas générés par un haut degré de fusion partielle mantellique. La distribution des éléments chalcophiles et sidérophiles est largement contrôlée par la répartition des sulfures magmatiques. Ces sulfures sont dérivés de la cristallisation d'un liquide sulfuré immiscible ségrégué dans le magma silicaté qui a interagi avec le magma silicaté en collectant les éléments chalcophiles. La formation de ce liquide sulfuré implique que le magma silicaté atteigne la saturation en S au cours de son évolution. Plusieurs mécanismes permettant cette saturation sont régulièrement évoqués : 1) Soit une modification des paramètres physico-chimiques du magma a permis la saturation en sulfure avec la concentration en S mantellique du magma initial, telle qu'une diminution de température ou de la fugacité du S, une augmentation de la pression ou de la fugacité de l'oxygène, ou un changement dans la composition du magma (e.g., Wallace et Carmichael, 1992; Mavrogenes et O'Neill, 1999; Li et Ripley, 2005; Liu et al., 2007). 2) Soit un apport de S d'origine externe par contamination crustale permet la saturation. Le processus d'assimilation *in situ* de roches sédimentaires encaissantes riches en S est considéré comme fondamental par de nombreuses études (e.g., Lesher et Keays, 2002). Par conséquent, la détermination de l'origine du S impliquée dans la saturation du magma reste une question essentielle dans la genèse des gisements magmatiques à sulfures de Ni-Cu-EGP.

Dans un premier temps, le rapport S/Se a été développé dans le but de mettre en évidence l'ajout du S dans le magma et, le cas échéant, de retracer son origine (e.g., Eckstrand et Cogulu, 1986). La proximité du comportement chimique du Se avec le S permet de l'utiliser comme témoin des processus géochimiques et géologiques à l'origine de la formation des systèmes magmatiques minéralisés. Un rapport S/Se proche de la valeur du manteau primitif (≈ 3000) indique que le S ayant saturé le magma serait d'origine mantellique, tandis qu'un rapport S/Se élevé (> 10 000) suggère que du S d'origine externe a été ajouté au magma initial. Depuis, le rapport S/Se est régulièrement employé en association avec l'analyse des isotopes du S ($\delta^{34}S$) pour retrouver la source du S de nombreux dépôts de Ni-Cu-EGP. Dans un second temps et jusqu'à récemment, le rapport S/Se a été utilisé pour mettre en évidence toute une série de processus modifiant les valeurs de ce dernier, comme par exemple, la remobilisation du S (e.g., Peck et Keays, 1990) ou la ségrégation du liquide sulfuré (Barnes et al., 2009). Ces processus influencent significativement les concentrations en S et en Se, et donc le rapport S/Se, et peuvent souvent masquer la source originale du S impliqué dans la genèse de la minéralisation. L'utilisation récurrente du rapport S/Se dans la caractérisation des gisements, la quantité de données accumulées sur le rapport S/Se depuis trois décennies pour l'ensemble des gisements, ainsi que les différents processus évoqués, nous ont incité à réaliser une étude spécifiquement consacrée à l'utilisation du rapport S/Se.

L'objectif principal du projet de recherche est de vérifier si le rapport S/Se est un outil efficace pour l'exploration et la caractérisation des processus de formation dans les dépôts magmatiques à sulfures de Ni-Cu et d'EGP. Afin de parvenir à cette conclusion, une série d'objectifs secondaires a été définie :

1) Réaliser le bilan des connaissances sur l'utilisation du rapport S/Se dans les gisements magmatiques de Ni-Cu et d'EGP.

2) Répertorier les processus modifiant le rapport S/Se et leurs influences sur son interprétation.

3) Contraindre le domaine d'application du rapport S/Se.

4) Combler les lacunes sur l'utilisation du rapport S/Se en réalisant de nouvelles mesures grâce à une approche scientifique originale, couplée au progrès analytique dans la détermination du Se dans les roches.

Afin d'atteindre chacun des objectifs présentés précédemment, la méthodologie a été divisée en deux parties distinctes : la revue bibliographique des travaux antérieurs et la réalisation de nouvelles analyses. L'approche méthodologique a consisté en une succession de différentes étapes décrites en détail ci-après.

Le projet a débuté par l'élaboration d'une base de données répertoriant la majeure partie des analyses en S, Se et $\delta^{34}S$ des gisements magmatiques à sulfures de Ni-Cu-EGP à partir de publications arbitrées, de thèses et de tableaux de données brutes (Annexes 1 et 2). Les connaissances acquises sur les rapports S/Se de plus de 50 gisements ont ainsi été classées en fonction du type de gisement et des processus subis, à l'aide d'une série de graphiques synthétisées dans la création d'un modèle chronologique sur l'évolution du rapport S/Se. Le travail de compilation a mené à la rédaction d'un manuscrit, présenté dans le chapitre I et prochainement soumis dans la revue *Economic Geology*. Cet ouvrage a pour objectif de devenir un article de référence afin de servir de base de travail pour toutes études impliquant l'utilisation du rapport S/Se.

Les prémices du travail de compilation ont rapidement mis en évidence l'absence fréquente de mesures en Se, et donc du rapport S/Se, dans les roches encaissantes susceptibles d'être la source du S. Dans les rares cas où ces analyses avaient été effectuées, la proximité des valeurs en Se avec les limites de détection respectives des techniques utilisées, notamment dans les roches sédimentaires pauvres en S, entrainent des incertitudes et des erreurs. Dans le but de mieux contraindre l'influence du rapport S/Se des roches encaissantes sur celui des roches minéralisées, une série de mesures du Se sur les roches encaissantes d'un gisement donné a été entrepris.

Le complexe de Duluth (USA) a été jugé comme étant un des gisements les plus appropriés pour servir de cadre d'étude, et ce pour les raisons suivantes: 1) De nombreuses études antérieures ont souligné le rôle essentiel de la contamination en S par les roches encaissantes de la Formation sédimentaire de Virginia dans la genèse des dépôts à Cu-Ni-(EGP) ; 2) Certaines études passées ont utilisé le rapport S/Se dans la caractérisation des minéralisations et ont montré la grande dispersion des valeurs obtenues ; 3) Le métamorphisme régional de faciès Schiste Vert n'a pas modifié les concentrations en S et en Se des roches minéralisées et encaissantes. La Chaire de Recherche du Canada en Métallogénie Magmatique dispose de nombreux échantillons en provenance du complexe de Duluth prélevés lors des campagnes d'échantillonnage antérieures successives de Robert Thériault (1997-2000), Jean Lafrance (1999) et Louise Duschène (2004). Une quantité satisfaisante d'échantillons de roches encaissantes de la Formation de Virginia et de xénolithes des intrusions magmatiques a été collectée sur une dizaine de sections de forage pour permettre la réalisation de cette étude. Une sélection rigoureuse des échantillons a été effectuée en fonction du site de prélèvement, de la pétrologie (lithologie, métamorphisme, altération), de la pertinence des analyses antérieures et de la disponibilité du matériel.

La plupart des échantillons de roches utilisés avait préalablement été analysés pour leur concentration en éléments majeurs et en traces. Le Se a été analysé une nouvelle fois et de manière systématique par TCF-INAA, hormis pour quelques échantillons de sulfures massifs où la technique de mesure par INAA était applicable. Ces échantillons ont tous été préparés au laboratoire LabMaTer de l'Université du Québec à Chicoutimi, avant d'être envoyés au réacteur du laboratoire SLOWPOKE de l'Ecole Polytechnique de Montréal (QC, Canada) pour l'activation neutronique. Le S a été mesuré par spectrométrie infrarouge S-C pour les rares échantillons où la concentration était manquante. Pour compléter la base de données, des analyses isotopiques du S ($\delta^{34}S$) ont été réalisées par spectrométrie de masse au laboratoire isotopique de l'Université de Waterloo (ON, Canada). Les résultats obtenus ont permis d'améliorer le modèle génétique supposé de la contamination en S d'origine crustale ce qui a mené à la rédaction d'un second manuscrit, présenté dans le chapitre II, soumis et accepté récemment dans la revue *Economic geology*.

RÉFÉRENCES

Barnes, S.-J., Savard, D., Bedard, P., et Maier, W.D., 2009, Selenium and sulfur concentrations in the Bushveld Complex of South Africa and implications for formation of the platinum-group element deposits: Mineralium Deposita, v. 44, p. 647–663.

Eckstrand, O.R., et Cogolu, E., 1986, Se/S evidence relating to genesis of sulphides in the Crystal Lake gabbro, Thunder Bay, Ontario [abs.]: Geological Association Canada–Mineralogical Association Canada Program with Abstracts, v. 11, p. 66.

Lesher, C.M., et Keays, R.R., 2002, Komatiite-associated Ni-Cu-(PGE) deposits:Geology, mineralogy, geochemistry and genesis: Canadian Institute of Mining, Metallurgy and Petroleum Special Volume 54, p. 579–618.

Li, C., et Ripley, E.M., 2005, Empirical equations to predict the sulfur content of mafic magmas at sulfide saturation and applications to magmatic sulfide deposits: Mineralium Deposita, v. 40, p. 218–230.

Liu, Y., Samaha, N.T. et Baker, D.R., 2007, Sulfur concentration at sulfide saturation (SCSS) in magmatic silicate melts: Geochimica et Cosmochimica Acta, v. 71, p. 1783–1799.

Mavrogenes, J.A., et O'Neill, H.S.C., 1999, The relative effects of pressure, temperature and oxygen fugacity on the solubility of sulfide in mafic magmas: Geochimica et Cosmochimica Acta, v. 63, p. 1173–1180.

Naldrett, A.J., 2004, Magmatic sulfide deposits: Geology, geochemistry, and exploration: Berlin, Springer, 727 p.

Peck, D.C., et Keays, R.R., 1990, Insights into the behavior of precious metals in primitive, S-undersaturated magmas; evidence from the Heazlewood River Complex, Tasmania: Canadian Mineralogist, v. 28, p. 553–577.

Wallace, P., et Carmichael I.S.E., 1992, Sulfur in basaltic magmas. Geochimica et Cosmochimica Acta, v. 56, p. 1863–1874.

CHAPITRE I

L'UTILISATION DU RAPPORT S/SE DANS LES GISEMENTS MAGMATIQUES À SULFURES DE NI-CU-EGP ET SES IMPLICATIONS DANS LA CARACTÉRISATION DES PROCESSUS PÉTROGÉNÉTIQUES

Titre du manuscrit (pour la soumission à Economic Geology):

"Processes affecting the S/Se ratio in magmatic nickel-copper and platinum-group element deposits."

Auteurs:

Matthias Queffurus et Sarah-Jane Barnes

Résumé:

Dans les gisements magmatiques à sulfures de Ni-Cu-Eléments du groupe du platine (EGP), les déviations du rapport Soufre/Sélénium (S/Se) par rapport aux valeurs mantelliques ont été interprétées comme étant: soit le résultat de l'effet de la contamination crustale des roches sédimentaires riches en S sur les magmas mantelliques, induisant des rapports S/Se supérieurs aux valeurs du manteau, soit comme le résultat d'une perte de S postérieurement à la cristallisation, produisant des rapports S/Se inférieurs aux valeurs du manteau. Cependant, il existe de nombreux autres processus impliqués dans la genèse d'un gisement et il est probable que ces derniers aient exercés un contrôle important dans les variations du rapport S/Se. Dans le but de mieux contraindre l'influence relative de chacun de ces processus, une revue

bibliographique des données en S, Se, $\delta^{34}S$ et métaux des principaux gisements de Ni-Cu-EGP a été effectuée. Ce travail de compilation démontre que les processus affectant le rapport S/Se sont divisés en deux grands types: les processus magmatiques et les processus tardi- à post-magmatiques.

1) Les processus magmatiques incluent la contamination par le S d'origine crustal, les variations dans le rapport de volume entre le liquide sulfuré et le liquide silicaté (facteur R) durant la ségrégation du liquide sulfuré, l'appauvrissement en Se du magma silicaté par ségrégation précoce du liquide sulfuré et l'incompatibilité modérée du Se dans les premières phases sulfurées cristallisant à partir du liquide sulfuré, la solution-solide monosulfurée (SSM). Cette légère incompatibilité entraine des variations dans le rapport S/Se des sulfures magmatiques, entre la phase riche en Fe et la phase résiduelle riche en Cu, dérivée de solution-solide intermédiaire (SSI). Le fractionnement du Se pendant la cristallisation du liquide sulfuré n'avait jamais été identifié jusqu'à maintenant.

2) Les processus tardi- à post-magmatiques incluent le métamorphisme de haute grade, l'hydrothermalisme, la serpentinisation et l'altération météorique. Certains gisements de Cu métamorphisés possèdent de faibles rapports S/Se suggérant une perte de S générée par la destruction des sulfures durant l'évènement métamorphique de haute température. Néanmoins, l'efficacité de ce processus reste mal définie et des modèles alternatifs existent. La remobilisation préférentielle du S par rapport au Se pendant l'hydrothermalisme, la serpentinisation et l'altération météorique entraîne une diminution modérée des valeurs du rapport S/Se et peut masquer le rapport S/Se initial.

Les diagrammes synthétiques S/Se *versus* Pt+Pd à 100% sulfures permettent de distinguer les différents domaines du rapport S/Se en fonction du type de dépôt, de l'origine du S et des processus subis. La majeure partie des gisements de Ni-Cu possède des rapports S/Se supérieurs

ou égaux au manteau associés à de faibles concentrations en Pt+Pd et de faibles facteurs R tandis que les gisements d'EGP ont des rapports S/Se faibles, des concentrations Pt+Pd élevées, des facteurs R élevés et sont constitués de S provenant du manteau. Les exceptions notables à ce modèle sont les gisements de Ni-Cu ayant subi une perte significative de S, vraisemblablement lors d'un épisode métamorphique de haut grade, marqués par de faibles rapports S/Se associés à de faibles concentrations en Pt+Pd, ainsi que les phases sulfurées riches en Cu enrichies en Se et en Pt+Pd lors du fractionnement du liquide sulfuré.

Le rapport S/Se est le résultat d'une évolution complexe de processus influençant significativement les concentrations en S et en Se des roches minéralisées, et donc le rapport S/Se, et pouvant occulter la source originelle du S et modifier l'interprétation de la genèse du dépôt.

Contributions des auteurs:

1er auteur : Matthias Queffurus

- Création de la base de données et compilation des résultats.
- Rédaction de l'ensemble du manuscrit.
- Production de tous les tableaux et figures.
- Mise en forme de l'article suivant les critères de l'éditeur.

2ème auteur : Sarah-Jane Barnes

- Planification et direction du projet.
- Aide à la rédaction de l'ensemble du manuscrit.

Processes affecting the sulfur to selenium ratio in magmatic nickel-copper and platinum-group element deposits

Matthias Queffurus* **and Sarah-Jane Barnes**

Université du Québec à Chicoutimi, 555 boulevard de l'Université, Saguenay, QC, G7H 2B1, Canada

(*corresponding author: e-mail: matthias.queffurus@uqac.ca)

Keywords: S/Se ratio, Selenium, Sulfur, Sulfur isotope, Ni-Cu-PGE deposits, Contamination, Assimilation.

Abstract

Deviations in the Sulfur to Selenium ratios (S/Se) from mantle values in magmatic Ni-Cu-Platinum Group Elements (PGE) sulfide deposits have been largely interpreted to be the result of contamination of the mantle derived magma by S-rich sedimentary rocks, which produced rocks with the ratios greater than mantle values, or as the result of S loss during post crystallizations, which produced rocks with the ratio is less than mantle values. However, there are many other processes involved in producing an ore deposit and it is possible that these may be also be important in controlling S/Se ratios. In order to investigate the relative importance of these processes, we have compiled a data base of S, Se, $\delta^{34}S$ and metal values from numerous, important Ni-Cu-PGE sulfide deposits. This compilation shows that processes affecting S/Se ratios can be divided into two main classes: magmatic processes and late- to post-magmatic processes.

1) Magmatic processes include the well-known addition of S from sedimentary rocks, variations in the sulfide to silicate liquid ratio (R-factor) during sulfide liquid segregation, depletion of the silicate magma in Se by prior segregation of the sulfide liquid, and the moderate incompatibility of Se into the first sulfide minerals to crystallize from a sulfide liquid, the Monosulfide Solid-Solution (MSS). This incompatibility results in a change in S/Se ratio between the Fe-rich and Cu-rich zones of magmatic sulfide ores. The fractionation of Se during crystallization of sulfide liquids has not previously been appreciated.

2) Late- to post-magmatic processes include: hydrothermalism, high-grade metamorphism, serpentinization and supergene weathering. Some metamorphosed Cu-deposits (Curaçà Valley, Brazil; O'Kiep, South-Africa; and some thick crust mafic-ultramafic intrusions of the Grenville Province, Canada) have low S/Se ratios suggesting S-loss by breakdown of

sulfide minerals during a high-grade metamorphic event. However, the effectiveness of this process remains unclear and alternative models exist. The preferential remobilization of S relative to Se during hydrothermalism, serpentinization and supergene weathering leads to a moderate decrease of S/Se ratios values and can mask the initial S/Se ratio.

Plots of S/Se versus Pt+Pd in 100 % sulfide are useful in distinguishing the various ore types and processes. Most of the Ni-Cu deposits have S/Se ratios similar to or higher than mantle ratios. These high S/Se ratios are combined with low Pt+Pd contents in 100 % sulfides compared with PGE-deposits which have low S/Se ratios and high Pt+Pd contents that indicate a formation by mantle-derived S. Exceptions to this are the Ni-Cu deposits that have undergone S-loss, possibly during metamorphism, resulting in low S/Se ratios combined with relatively low Pt+Pd contents and Cu-rich ores which have are enriched both in Se and Pt+Pd due to fractionation of the sulfide liquid.

The S/Se ratio is a result of a complex evolution of various processes that influence significantly the concentrations of S and Se in mineralized rocks, i.e. S/Se ratio, and may commonly overprint the original source of S and the interpretation of the genesis of the deposit.

Introduction

For the past 30 years, S/Se ratios have been used in the study of magmatic Ni-Cu sulfide deposits and Platinum-Group Element (PGE) deposits as a petrogenetic indicator of ore forming processes (e.g., Eckstrand and Cogulu, 1986; Eckstrand et al., 1989; Peck and Keays, 1990; Ripley, 1990; Thériault and Barnes, 1998; Hinchey and Hattori, 2005; Maier et al., 2008). Sulfur/Se ratios in magmatic Ni-Cu sulfide or PGE deposits vary from 100 to 100 000. The S/Se ratio of the mantle was estimated at between 2850 and 4350 by Eckstrand and Hulbert (1987). Later studies indicate average mantle values of 3333 (McDonough and Sun, 1995) and 3150 (Lorand et al., 2003). Most igneous rocks have a S/Se ratio close to the mantle value, as in the case of Merensky Reef of the Bushveld Complex (Barnes and Maier, 2002; Godel et al., 2007) and suggesting that the S that saturated the mafic magma had a mantle origin. S/Se ratios greater than mantle values has been interpreted to signify that a large S contribution from the country rock has occurred, (e.g., Lesher and Burnham, 2001; Maier and Barnes, 2010). In contrast, S/Se ratios less than the mantle values are taken to indicate a S-loss such as the Heazlewood River, the Lac des Iles Complex or the PGE-rich reef of the Penikat intrusion (Peck and Keays, 1990; Hinchey and Hattori, 2005; Barnes et al., 2008). Recently, it has been suggested that S/Se ratios can also be affected by: 1) Preferential retention of Se during partial melting (Hattori et al., 2002); 2) Refertilization of mantle lithosphere by metal-rich sulfide melts (Lorand and Alard, 2010); 3) Changes in the silicate to sulfide liquid ratio, i.e. the R-factor (Thériault and Barnes, 1998); 4) Segregation of the sulfide liquid (Barnes et al., 2009); 5) Partial desulfurization caused by a S-undersaturated fluid (Godel and Barnes, 2008).

Following the pioneering compilation work of Eckstrand (unpublished data, 1988), S/Se ratios have been determined in many deposits and as a result there is a large amount of data

available in the literature. However, the S/Se ratio is generally applied without considering the many processes that could modify the S/Se ratio. Despite the utility of S/Se ratios, no study has been dedicated specifically to considering these processes and their implications on the interpretation of the S/Se ratio. This work proposes to update the available S/Se database and fill in the gaps on the use of the S/Se ratio.

We have compiled S, Se, $\delta^{34}S$ and metals data from most of the major magmatic Ni-Cu and PGE deposits and added some new data with the aims of: a) characterizing the deposits, b) considering the wider range of processes than have been discussed in the past and, c) making recommendations on the application of the S/Se ratio. The behavior of S/Se ratio will be analyzed at each step involved in the formation of a Ni-Cu or PGE sulfide deposit: 1) Partial melting; 2) S-saturation and the contribution from the country rocks, especially the S-rich sediments; 3) Interaction between sulfide and silicate liquid (i.e. R-factor); 4) Collection of the sulfide liquid; 5) Fractional crystallization of sulfide liquid; 6) Post-cumulate processes. The project's main objective is to determine whether the S/Se ratio is a reliable tool for petrogenesis, exploration and characterization of ore mineralizing processes in magmatic Ni-Cu-PGE sulfide deposits.

Methodology

The available S/Se or Se data for the Ni-Cu-PGE deposits of the world (Fig. 1) are listed in Table 1 where they are classified according to Barnes and Lightfoot's (2005) system. The geometric mean (geomean), although very close to the arithmetic mean in most cases, was used with the aim of overcoming deviation generated by the extreme values in the concentrations of chalcophile elements. The S/Se ratios were also calculated using the geomean. In some publications, the S/Se ratio is presented as whole rock data but in others it is normalized to 100

percent sulfides. Some recalculation methods appear to introduce systematic errors, therefore whenever possible we calculated the S/Se ratio based on the whole rock data. To estimate the Pt+Pd concentrations in 100 percent sulfides, we have applied the formula of Barnes and Lightfoot (2005):

$$C_{(100\%\ sul)} = C_{wr} \times 100/(2.527 \times S + 0.3408 \times Cu + 0.4715 \times Ni) \qquad (1)$$

where $C_{(100\%\ sul)}$ is the concentration of an element in 100 percent sulfides, C_{wr} is the concentration of the element in the whole rock and S, Cu, Ni are the concentration in weight percent of these elements in the whole rock.

To complete the database, four samples of massive ore from the Ovoïd Zone of the Voisey's Bay deposit were analyzed for S and Se. Sulfur was determined by infrared spectrometry carbon-sulfur analyser (HORIBA EMIA-220V) according to the method of Bédard et al. (2008). Selenium was determined by Instrumental Neutron Activation Analysis (INAA) after irradiation for 90 min (neutron flux of 4.63 to 5.58 $\times$ 10^{11} n cm^{-2} sec^{-1}) in the SLOWPOKE reactor at the *École Polytechnique*, Montreal.

One of the reasons for our lack of a detailed understanding for the variations in S/Se ratios in ore deposits is that the concentration of Se in the country rocks that are thought to contaminate the mafic magmas and bring about sulfide saturation is poorly known. In part because very few studies determine Se in the country rocks to the deposits and in part because until recently it was difficult to determine Se in sediments due to the very low Se concentrations and matrix effects. For some deposits, analytical techniques used for the determination of the concentration of Se were very close to the detection limit, causing a dispersion of values. Particular attention was given to evaluating the quality and adequacy of Se measurements.

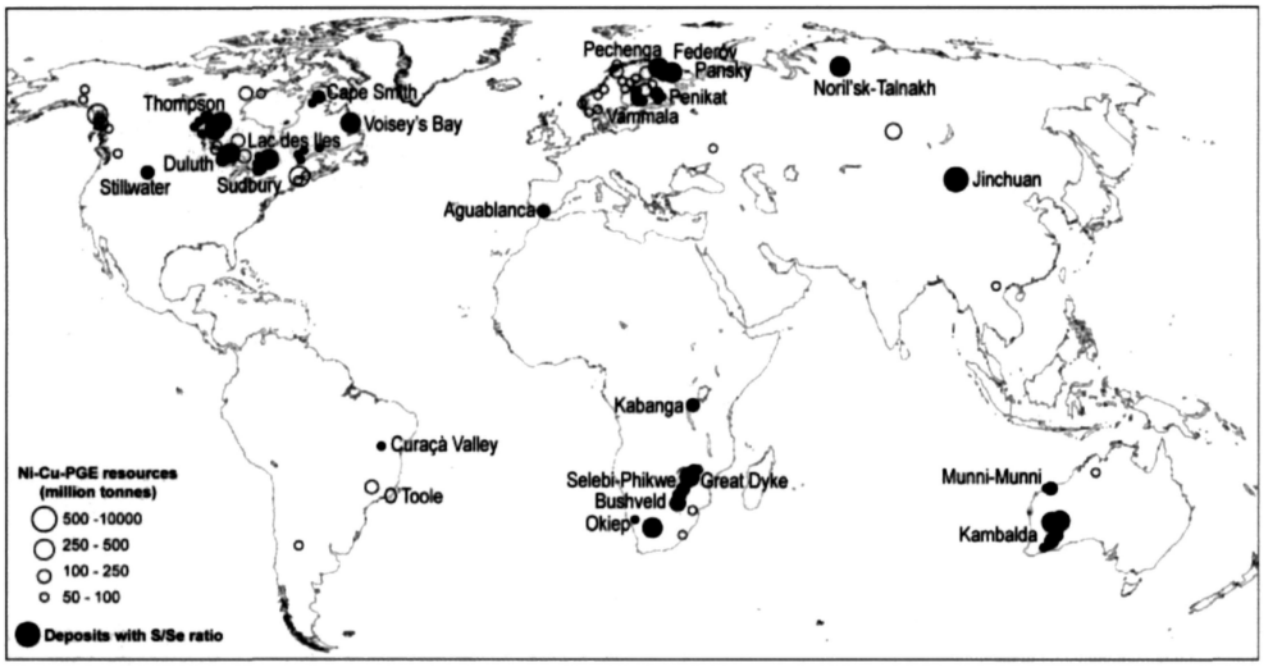

FIG. 1. Location of Ni-Cu-PGE sulfides deposits (modified from Eckstrand and Hulbert, 2007). As indicated by solids dots, S/Se ratios or Se data are available for most of the deposits. The bulk of the data was collected from published work.

Deposit type	Deposits	Rock type/ore	n	Whole rock - geomean						100% S	$\delta^{34}S$		S/Se	references
Mining Camp				S (%)	Se (ppm)	Ni (%)	Cu (%)	Pt (ppb)	Pd (ppb)	Pt+Pd (ppm)	mean	stdevpa		
Ni-Cu deposit - Class 1(i): Astrobleme – Meteorite impact														
Sudbury	Levack (N-Range)	Granophyre	2	0.02	0.03	<0,01	<0,01	0.05	0.25	0.58			7 164	Keays and Lightfoot, 2004
		Quartz gabbro	1	0.07	0.05	<0,01	<0,01	0.05	0.89	0.57			13 000	Keays and Lightfoot, 2004
		Felsic norite	13	0.06	0.08	0.01	<0,01	0.27	0.40	0.42			7 634	Keays and Lightfoot, 2004
		Mafic norite	5	0.28	0.47	0.05	0.04	3.12	4.19	0.99			6 011	Keays and Lightfoot, 2004
		Sublayer	9	0.26	0.51	0.04	0.04	16.9	15.9	4.80			5 115	Keays and Lightfoot, 2004
	Nickel Rim (N-Range)	Quartz gabbro	2	0.05	0.08	<0,01	<0,01	0.30	0.30	0.45			6 558	Keays and Lightfoot, 2004
		Felsic norite	4	0.10	0.11	0.01	<0,01	0.52	0.53	0.42			9 111	Keays and Lightfoot, 2004
		Mafic norite	4	0.51	0.87	0.06	0.05	3.93	4.88	0.66			5 908	Keays and Lightfoot, 2004
		Sublayer	7	0.38	0.86	0.06	0.05	21.8	18.4	4.04			4 348	Keays and Lightfoot, 2004
		All ores	-								+0.00	2.00		Naldrett, 1981
	Creighton	SF-Diss	3	6.59	14.2	0.94	0.19	49.0	29.1	0.46			4 632	Dare et al., 2010
		SF-Mtr	3	17.6	45.3	2.50	1.35	46.6	91.6	0.30			3 885	Dare et al., 2010
		SF-MS	13	33.8	95.2	7.74	2.01	108	342	0.50			3 548	Dare et al., 2010
	Strathcona	SF-Diss	2	1.13	2.13	0.13	0.16	114	134	8.01			5 157	Barnes and Lightfoot, 2005
	Mc Creedy	East 153 Cu veins Mtr	1	34.7	107	1.32	16.5	853	298	1.22			3 248	Dare et al., 2011
		East 153 Cu-rich veins	7	31.6	214	1.39	27.0	9 969	18 725	32.0			1 481	Dare et al., 2011
		East Main MSS	6	32.0	60.4	3.98	0.70	604	807	1.70			5 292	Dare et al., 2011
Ni-Cu deposit - Class 1(ii): Rift related mafic-ultramafic intrusions														
Duluth Complex	Dunka Road	Gabbronorite	7	1.43	1.60	0.06	0.17	13.8	49.3	1.71	+11.61	2.48	8 928	Thériault and Barnes, 1998
		Olivine-gabbronorite	6	0.96	2.18	0.13	0.42	72.2	286	13.6	+7.77	1.01	4 432	Thériault and Barnes, 1998
		PGE-rich layer	2	1.00	3.95	0.25	0.64	410	1 918	81.4	+2.05	0.45	2 530	Thériault and Barnes, 1998
		SF-MS	3	27.7	24.1	1.11	0.91	19.0	871	1.26	+12.13	3.10	11 516	Thériault and Barnes, 1998
	Virginia Formation	Pelites	1	0.31	0.20	0.01	<0,01	<0,01	2.40	0.30	+8.60	0.00	15 500	Thériault and Barnes, 1998
		Pelites	1	1.08	0.20	0.01	0.01	3.50	2.60	0.22	+5.10	0.00	54 000	Thériault and Barnes, 1998
		Bedded Pyrrhotite Unit	1	4.45	1.40	0.01	0.02	<0,01	3.50	0.03	+15.80	0.00	29 000	Thériault and Barnes, 1998
		Pelites	16	0.47	0.62						+6.88	3.76	7 635	Ripley, 1990
		Xenoliths (Dunka Road)	1	1.38	1.70								8 118	Ripley, 1990
		Footwall (Dunka Road	8	0.63	0.95								6 608	Ripley, 1990
		Xenoliths (Babbitt)	27	0.87	1.02						+5.43	1.75	8 520	Ripley, 1990
		Footwall (Babbitt)	4	0.39	0.38						+6.40	0.00	10 264	Ripley, 1990
Noril'sk - Talnakh	Medvezhy (Noril'sk 1)	SF-MS	4	33.5	222	6.88	21.1	88 105	182 213	284			1 509	Czamanske et al., 1992
	Komsolmolsky (Talnakh)	SF-MS	1	32.0	59.0	4.97	3.94	5 200	26 000	36.9			5 424	Czamanske et al., 1992
	Oktyabr'sk (Kharaelakh)	SF-MS - MSS	4	33.1	63.4	3.65	7.28	2 597	16 502	21.7			5 220	Czamanske et al., 1992
		SF-MS	4	33.2	92.8	1.76	21.8	4 306	25 779	32.7			3 576	Czamanske et al., 1992
		SF-MS - ISS	4	31.9	164	2.96	27.5	34 313	107 378	155			1 939	Czamanske et al., 1992
Jinchuan		All ores	-										3 500	Chai and Naldrett, 1992
			17								+1.71	1.31		Chai and Naldrett, 1992
			95								+1.49	1.73		Ripley et al., 2005

Deposit type	Deposits	Rock type/ore	n	Whole rock - geomean						100% S	$\delta^{34}S$		S/Se	references
Mining Camp				S (%)	Se (ppm)	Ni (%)	Cu (%)	Pt (ppb)	Pd (ppb)	Pt+Pd (ppm)	mean	stdevpa		
Molson Dykes		All ores	12	0.07	0.23						-1.05	1.10	2 799	Ecktrand et al., 1989
Fox River Sill		All ores	30	0.11	0.25						+9.27	3.83	4 279	Ecktrand et al., 1989
Ni-Cu deposit - Class 1(iii): Arc-related mafic-ultramafic intrusions														
Belleterre	Lorraine Mine	SF-Diss	4	9.07	17.1	0.36	1.66	150	253	1.70			5 315	Bouchaib, 1992
		SF-MS Cu-poor	9	31.1	77.5	2.22	0.57	134	375	0.64			4 015	Bouchaib, 1992
		SF-MS Cu-rich	3	28.2	86.1	1.49	8.94	312	351	0.88			3 271	Bouchaib, 1992
Aguablanca		All ores	25	11.0	29.3	2.05	0.99	373	510	3.05			3 747	Pina et al., 2008
		SF-MS	9	24.0	60.1	5.20	0.82	392	963	2.14			3 992	Pina et al., 2008
		SF-Mtr	6	15.8	39.0	3.28	1.13	750	823	3.76			4 048	Pina et al., 2008
		SF-Diss	10	4.35	12.9	0.67	1.08	236	216	3.87			3 379	Pina et al., 2008
		Veins	3	5.76	15.1	0.98	2.78	182	479	4.14			3 818	Pina et al., 2008
		All ores	19								+7.42	0.19		Casquet et al., 1998
	Serie Negra F.	Country rocks	-	0.52									1 436	Pina et al., 2008
Ni-Cu deposit - Class 1(iv): Province boundary														
Voisey's Bay	Ovoïd	SF-MS - MSS	2	33.6	47.4			15.20	206	0.22			7 083	this study
		SF-MS - ISS	2	31.2	89.6			0.90	347	0.35			3 482	this study
		All ores	18								-1.52	0.43		Ripley et al., 1999
	Country rocks	Tasiuyak Gneiss (Outcrop)	9	0.07	2.48						-5.41	4.50	270	Ripley et al., 2002
		Tasiuyak Gneiss	43	0.27	0.50						-0.40	7.85	5 399	Ripley et al., 2002
Ni-Cu deposit - Class 1(v): Thick crust mafic-ultramafic intrusions														
Lac Volant	Ores	SF-MS	13	37.4	29.9	1.79	1.57	41.00	317	0.37	+1.36	0.09	12 507	Nabil et al., 2004
		SF-Mtr	4	14.6	14.0	0.93	1.26	14.35	124	0.37	+1.00	0.00	10 467	Nabil et al., 2004
		SF-Diss	6	4.66	5.35	0.33	0.18	6.06	27.58	0.28	+1.35	0.35	8 723	Nabil et al., 2004
		All Ores	24	18.8	17.3	0.97	0.95	21.25	136	0.33	+1.34	0.24	10 856	Nabil et al., 2004
	Paragneiss	Country rocks	1	3.41	3.60	0.01	0.02	0.00	0.00		+3.20	0.00	9 472	Nabil et al., 2004
Lac à Paul		SF-Diss	15	2.11	2.28	0.07	0.06	1.59	5.53	0.13			9 238	Huss, 2002
		SF-Mtr	5	17.4	8.00	0.47	0.90	11.52	32.44	0.10			21 685	Huss, 2002
		SF-MS	2	31.0	13.5	0.93	0.15	2.21	80.77	0.11			22 987	Huss, 2002
Lac Kénogami	Dumont	SF-Diss	8	1.40	4.98	0.20	0.08	5.93	60.11	1.80			2 821	Vaillancourt, 2001
	Gagnon	SF-Diss	7	0.44	2.95	0.12	0.14	18.26	30.41	4.01			1 487	Vaillancourt, 2001
Portneuf-Mauricie	Lac Edouard	SF-Diss	4	4.45	6.06	0.57	0.15	1.38	3.51	0.04	+1.44	0.99	7 336	Sappin et al., 2011
	Lac Kennedy	SF-Diss	2	1.02	2.48	0.15	0.10	1.10	1.98	0.11	+1.03	0.86	4 119	Sappin et al., 2011
	Lac Matte	SF-Diss	4	1.40	2.34	0.29	0.12	2.34	1.59	0.11	+1.47	0.67	5 991	Sappin et al., 2011
	Rousseau	SF-Diss	4	0.84	4.57	0.37	0.24	34.30	73.60	4.54	-0.53	1.43	1 834	Sappin et al., 2011
	Lac Nadeau	SF-Diss	3	0.58	3.01	0.26	0.13	185	277	28.1	+0.06	1.49	1 944	Sappin et al., 2011
Ni-Cu deposit - Class 1(vi): Other mafic-ultramafic intrusions (Metamorphosed, deformed or unknown)														
Curaçà Valley		SF-MS	2	15.7	237	0.65	25.9	449	406	1.75			662	Maier and Barnes, 1999
		SF-Diss	53	0.82	9.68	0.07	1.15	34.97	18.93	2.15			852	Maier and Barnes, 1999
Okiep	Koperberg Suite	SF-Diss	12	1.11	11.7	0.03	2.34	6.19	16.62	0.63			942	Cawthorn and Meyer, 1993
		SF-Diss	-								-3.00	1.10		Boer et al., 1994

Deposit type	Deposits	Rock type/ore	n	Whole rock - geomean						100% S	$\delta^{34}S$		S/Se	references
Mining Camp				S (%)	Sc (ppm)	Ni (%)	Cu (%)	Pt (ppb)	Pd (ppb)	Pt+Pd (ppm)	mean	stdevpa		
Vammala	Ores	Deep Ore	3	3.74	9.92						-0.90	0.95	3 765	Peltonen, 1995
		Sokta Ore	5	6.58	25.4						-1.00	0.66	2 588	Peltonen, 1995
		Ekojoki Ores	7	5.48	17.1						-	-	3 206	Peltonen, 1995
		Veins	6	19.5	43.8						+0.30	0.85	4 462	Peltonen, 1995
	Unmineralised rocks	Murto	4	0.34	0.29								11 777	Peltonen, 1995
		Posionlahti	4	0.51	0.16								31 560	Peltonen, 1995
	Country rocks	Svecofennian Formation	28	2.97	4.18						+0.70	3.65	7 108	Peltonen, 1995
Selebi-Phikwe	Tati Belt	Phoenix	21	6.28	21.6	0.69	0.31	53.18	17.44	0.43			2 907	Maier et al., 2008
	Tati Belt	Selkirk	11	9.25	15.1	0.73	0.14	167	46.96	0.90			6 141	Maier et al., 2008
	Tati Belt	Tekwane	2	1.36	3.63	0.29	0.04	214	34.79	6.92			3 760	Maier et al., 2008
	Phikwe Belt	Dikoloti	2	15.1	4.47	0.40	0.63	94.39	23.14	0.31			33 781	Maier et al., 2008
	Phikwe Belt	Phikwe	5	16.0	19.6	0.80	0.34	20.93	34.05	0.13			8 128	Maier et al., 2008
	Phikwe Belt	Phokoje	2	12.8	12.7	0.86	0.11	23.24	46.59	0.21			10 077	Maier et al., 2008
Ni-Cu deposit - Class 2(i): Komattitic flows and intrusions														
Kambalda	Ores	All ores	11							4.18			9 430	Cowden et al., 1986
		All ores	-								+2.50	1.50		Groves et al., 1979
		interpillow sulfide	-							794			8 805	Lesher and Keays, 1984
		MS sdt-enriched	-							914			7 435	Lesher and Keays, 1984
		Ni sdt enriched	-							2 947			1 250	Lesher and Keays, 1984
		Hydrothermal veins	3							574			3 469	Lesher and Keays, 1984
Mt Keith	Ores	Dunite	4	0.30	0.24	0.94	<0,01	<0,01	15.40	1.28			12 728	Groves and Keays, 1979
		Serpentinite	12	0.97	0.48	0.62	0.02	<0,01	41.80	1.52			20 202	Groves and Keays, 1979
		All ores	2								-2.30	0.00		Donnelly et al., 1978
	Country rocks	S-rich metasediments	-										38 000	Groves et al., 1979
Langmuir	Langmuir 1 et 2	All ores	42	19.5	10.5	6.52	0.26	322	606	1.77			18 571	Green and Naldrett, 1981
			17								+0.00	2.20		Green and Naldrett, 1981
		Pyrrhotite-rich ores	18	25.6	11.0	7.97	0.25	395	566	1.40			23 273	Green and Naldrett, 1981
		Pyrite-rich ores	8	23.5	9.80	8.20	0.29	256	703	1.51			23 980	Green and Naldrett, 1981
		Millerite-rich ores	12	11.6	11.6	5.54	0.21	386	720	3.46			10 000	Green and Naldrett, 1981
		Metasedimentary ores	4	6.50	6.50	1.79	0.26	125	350	2.74			10 000	Green and Naldrett, 1981
	Country rocks	Cherty Iron Formation	5								-4.81	2.35	50 000	Green and Naldrett, 1981
	Mc Watters	All ores	1	21.3	13.0	10.6	0.24	174	474	1.10			16 385	Green and Naldrett, 1981
	South End Fault Zones	SF-MS	5	32.5	15.1	11.1	0.13	209	319	0.60			21 559	Green and Naldrett, 1981
		Country rocks	2	4.32	1.53	0.43	0.06	48.50	14.83	0.57			28 284	Green and Naldrett, 1981
Thompson		SF-MS	6							3.66			12 800	Bleeker, 1990
		SF-Breccia	7							1.77			16 186	Bleeker, 1990
		All Ores	-								+4.25	1.75		Bleeker, 1990
		Ni-SED	14							1.00			30 659	Bleeker, 1990
Pipe II		SF-MS	3							0.11			23 926	Bleeker, 1990
Namew Lake		SF-Diss	18							10.5			1 851	Menard et al., 1996
Cape Smith	All ores	SF-Diss	89							13.1			3 189	Barnes et al., 1997b
Cape Smith (Delta)	Delta 8	SF-MS	12	30.2	78.6	7.08	0.81	845	422	1.58			3 849	Giovenazzo, 1991

Deposit type	Deposits	Rock type/ore	n	Whole rock - geomean						100% S	$\delta^{34}S$		S/Se	references
Mining Camp				S (%)	Sc (ppm)	Ni (%)	Cu (%)	Pt (ppb)	Pd (ppb)	Pt+Pd (ppm)	mean	stdevpa		
		SF-Diss	3	2.82	11.5	0.78	0.96	379	1 190	20.0			2 454	Giovenazzo, 1991
		Veins	1	5.50	46.9	0.33	0.49	3 250	17 465	146			1 173	Giovenazzo, 1991
	Delta 9	SF-MS	13	28.4	111	5.33	0.92	899	1 775	3.58			2 555	Giovenazzo, 1991
		SF-Diss	1	12.6	63.5	2.52	0.98	1 201	2 975	12.5			1 983	Giovenazzo, 1991
		Veins	1	1.30	5.20	0.14	1.06	12.00	36.00	1.29			2 500	Giovenazzo, 1991
	Méquillon	Dyke	5	1.31	3.15	0.20	0.12	112	235	10.1	+4.52	0.41	4 174	Tremblay, 1990
		sediment	3	4.13	3.00	0.01	0.03	14.00	17.00	0.30	+1.33	1.20	13 781	Tremblay, 1990
Cape Smith (Raglan)	2-3		12							12.2			6 343	Barnes et al., 1992
	Donaldson West	SF-Diss	14							61.8			3 834	Dillon-Leitch et al., 1986
		SF-Net textured	12							22.1			12 471	Dillon-Leitch et al., 1986
		SF-MS	3							3.78			4 957	Dillon-Leitch et al., 1986
		Veins	11							21.2			5 626	Dillon-Leitch et al., 1986
	Frontier	komatiite	13	1.11	1.46	0.28	0.07	17.28	90.50	3.63			7 635	Dionne-Foster, 2007
		basalte komatiite/ophi	9	0.83	0.55	0.01	0.01	2.32	5.00	0.35			15 049	Dionne-Foster, 2007
		SF-Diss	5	1.64	3.63	0.57	0.30	57.03	340	8.81			4 507	Dionne-Foster, 2007
		SF-Mtr	4	12.4	19.5	1.86	0.66	178	1 217	4.31			6 344	Dionne-Foster, 2007
		SF-MS	1	31.1	46.3	6.01	1.29	419	1 669	2.55			6 719	Dionne-Foster, 2007
		SF-MS R	6	19.7	17.9	1.19	0.93	205	1 250	2.87			11 003	Dionne-Foster, 2007
	Raglan	All ores	-								+4.50	1.50		Lesher et al., 1999a
Ni-Cu deposit - Class 2(ii): Picritic flows and intrusions														
Pechenga	Flows (West Ore)	SF-MS	13	29.9	62.0	6.75	1.17	373	421	1.00	+0.00		4 823	Barnes et al., 2001b
		SF-Diss	16	6.09	15.5	1.54	0.64	142	149	1.78	-0.30		3 921	Barnes et al., 2001b
		SF-Breccia	16	18.6	32.5	3.45	0.68	218	108	0.67	+0.00		5 708	Barnes et al., 2001b
	Country rocks	Sulfidic black shales	4	2.63	2.00	0.04	0.05	4.00	4.00	0.12	-1.25		13 150	Barnes et al., 2001b
		Sulfidic black shales	90								-1.20			Melezhik et al., 1998
	Intrusions (East Ore)	SF-MS	4	31.4	70.0	9.57	4.35	131	219	0.41	+4.05		4 491	Barnes et al., 2001b
		SF-Diss	3	5.26	15.9	1.98	0.64	127	182	2.14	+5.40		3 308	Barnes et al., 2001b
		SF-Breccia	2	22.5	64.0	7.57	1.51	357	377	1.20	+3.55		3 517	Barnes et al., 2001b
		Veins	1	20.4	40.0	2.49	19.90	156	78.00	0.39	+4.00		5 108	Barnes et al., 2001b
	Country rocks	Sulfidic black shales	1	18.7	10.0	0.04	0.02	12.00	7.00	0.04	+11.07		18 710	Barnes et al., 2001b
		Sulfidic black shales	101								+10.40			Melezhik et al., 1998
Kabanga		SF-MS	27	27.2	6.42	1.42	0.14	62.81	43.56	0.15	+18.84	2.99	42 358	Maier et al., 2010
		SF-Breccia	7	28.1	7.11	2.07	0.09	148	62.10	0.29	+20.50	2.96	39 478	Maier et al., 2010
		M-UM rocks	18	7.27	2.01	0.35	0.07	52.07	56.95	0.59	+17.23	3.87	36 078	Maier et al., 2010
PGE-deposits														
Stillwater	J-M Reef	Reef	4	0.51	2.76	0.14	0.09	24 157	64 154	6 362			1 852	Godel and Barnes, 2008
			54								+1.01	1.17		Zientek and Ripley, 1990
Bushveld	Upper C		14	0.52	0.67		0.01						7 746	Barnes et al., 2009
	Upper B		14	0.19	0.33		0.01						5 744	Barnes et al., 2009
	Upper A		22	0.17	0.63		0.05						2 602	Barnes et al., 2009
	Main Zone		30	0.01	0.03		<0,01						2 933	Barnes et al., 2009
	Critical Zone		1	0.01	0.03		<0,01						2 438	Barnes et al., 2009

Deposit type	Deposits	Rock type/ore	n	Whole rock - geomean						100% S	$\delta^{34}S$		S/Se	references
Mining Camp				S (%)	Se (ppm)	Ni (%)	Cu (%)	Pt (ppb)	Pd (ppb)	Pt+Pd (ppm)	mean	stdevpa		
	Bastard Zone		2	0.04	0.12		0.01						3 614	Barnes et al., 2009
	Merensky Reef	Reef	7	0.48	1.80		0.07	7 499	4 724	821			2 660	Barnes et al., 2009
		Reef	-								-0.60	0.00		Buchanan et al., 1981
	UG-2		3	0.02	0.06		<0,01						2 900	Barnes et al., 2009
	UG-1		2	0.01	0.02		<0,01						5 212	Barnes et al., 2009
	LG		13	0.01	0.02		<0,01						3 041	Barnes et al., 2009
	MG		14	<0,01	0.02		<0,01						2 128	Barnes et al., 2009
	Critical Zone		2	0.01	0.02		<0,01						3 873	Barnes et al., 2009
	Lower Zone		15	0.01	0.04		<0,01						3 413	Barnes et al., 2009
	Marginal Zone		13	0.02	0.07		<0,01						3 104	Barnes et al., 2009
Great Dyke	Mimosa Mine	Main Sulfide Zone	1	0.82	3.30	0.26	0.23	470	631	48.4			2 485	Barnes et al., 2008
Penikat	AP-Reef	FI-02-06	1	1.51	11.6	0.35	0.58	6 150	26 060	771			1 302	Barnes et al., 2008
	PV-Reef	FI-03-04	1	3.83	24.6	0.71	1.20	10 550	11 450	211			1 557	Barnes et al., 2008
Munni-Munni		Serpentinite (UM Zone)	7	<0,01	0.02	0.11	<0,01	1.95	2.48	7.35			1 969	Hoatson and Keays, 1989
		UM Zone	7	0.05	0.10	0.06	0.01	4.39	2.83	4.81			4 857	Hoatson and Keays, 1989
		PGE-rich (UM Zone)	2	0.08	0.38	0.07	0.06	15.13	10.33	10.4			1 967	Hoatson and Keays, 1989
		Gabbroïc Zone	10	0.04	0.12	0.01	0.02	1.04	2.18	2.63			3 508	Hoatson and Keays, 1989
		All ores	-								+2.40	0.10		Hoatson and Keays, 1989
Federov Pansky		Gabbronorite	8	0.55	2.55						+0.80	0.60	2 146	Schissel et al., 2002
East Bull Lake	Intrusion	Contact-type PGE-rich	177	0.26	1.57	0.06	0.11	161	473	89.4			1 706	Peck et al., 2001
	Parisien Lake	Structurally PGE-rich	37	5.50	14.5	0.21	0.69	212	768	6.88			4 600	Peck et al., 2001
Lac des Iles	Roby Zone		6	0.84	5.89	0.18	0.24	651	5 616	274	+0.44	0.27	1 424	Hinchey and Hattori, 2005
	Twilight Zone		2	0.62	4.32	0.16	0.20	513	4 034	267			1 432	Hinchey and Hattori, 2005
	High Grade Zone		8	0.95	9.56	0.27	0.25	904	12 468	511	+0.79	0.37	998	Hinchey and Hattori, 2005

Table 1. Summary of magmatic Ni-Cu-PGE sulfide deposits including S, Se, S/Se and δ34S values
See Barnes and Lightfoot (2005) for the description of the classification.
Abbreviations: n = number of samples, stdev = standard deviation, SF-MS = massive sulfide, SF-MS R = remobilized massive sulfide, SF-Mtr = matrix sulfide, SF-Diss = Disseminated sulfide, MSS = Monosulfide Solid-Solution, ISS = Intermediate Solid-Solution, ophi = Basalt ophitic, UM = ultramafic, M = mafic.

Results

The S/Se ratios from Ni-Cu-PGE deposits vary by 3 orders of magnitude, from ~500 to ~40 000. The lowest values are associated with the granulite facies Cu-rich deposits of the Curaçà Valley (Brazil) and O'Kiep deposits (South Africa) and the highest with the Kabanga picrite-hosted Ni-Cu deposits of Tanzania (Fig. 2 and Table 1). With the exception of the Curaçà Valley and O'Kiep deposits, there appears to be a negative correlation between S/Se ratios and the Pd+Pt contents in 100 percent sulfides.

The PGE-deposits have the lowest S/Se ratios and highest Pt+Pd contents (Fig. 2 and Table 1). These includes most of the largest PGE-deposits of the world, such as the J-M Reef of the Stillwater Complex (USA), the Merensky Reef of the Bushveld Complex (South Africa), the Main Sulfide Zone of the Great Dyke (Zimbabwe), the AP- and PV-Reefs of the Penikat Intrusion (Finland), the East Bull Lake Intrusion (Canada), the Roby, Twilight and High Grade Zones of the Lac des Iles Complex (Canada) and to a lesser extent, the Munni Munni Complex (Australia) and the Federov Pansky layered intrusion (Russia). In contrast, many komatiitic and picritic ores (e.g., Kabanga, Kambalda, Thompson, Mount Keith, Langmuir) and some thick crust mafic-ultramafic intrusions (e.g., Lac Volant, Lac à Paul) have high S/Se ratios and low Pt+Pd contents (Fig. 2).

A wide range in S/Se ratios and in Pt+Pd in 100 % sulfides is observed for deposits where there are data for different types of ores textures or ore compositions such as the Ni-Cu deposits of the Sudbury Igneous Complex (Canada), the Noril'sk-Talnakh (Russia), the Duluth Complex (USA), Voisey's Bay (Canada), Pechenga (Finland). An extreme example of this is the Dunka Road deposit of the Duluth Complex where the S/Se ratio ranges from ~11 500 in the massive sulfides to ~2500 in the PGE-rich disseminated sulfides. In general, massive sulfides tend to have

higher S/Se ratios and lower Pt+Pd in 100 % sulfides than disseminated sulfides (Fig. 2 and Table 1). However, not all massive sulfides have high S/Se ratios. At some deposits such as the Oktyabr'sk deposit (Noril'sk-Talnakh) or the McCreedy deposit (Sudbury) the composition of the massive ore ranges from the more common Fe-rich type to Cu-rich type. The Fe-rich massive sulfides have higher S/Se and lower Pt+Pd in 100 % sulfide than in Cu-rich massive sulfides (Fig. 2 and Table 1). The following discussion considers each of the effects of the processes that could have affected the S/Se ratios.

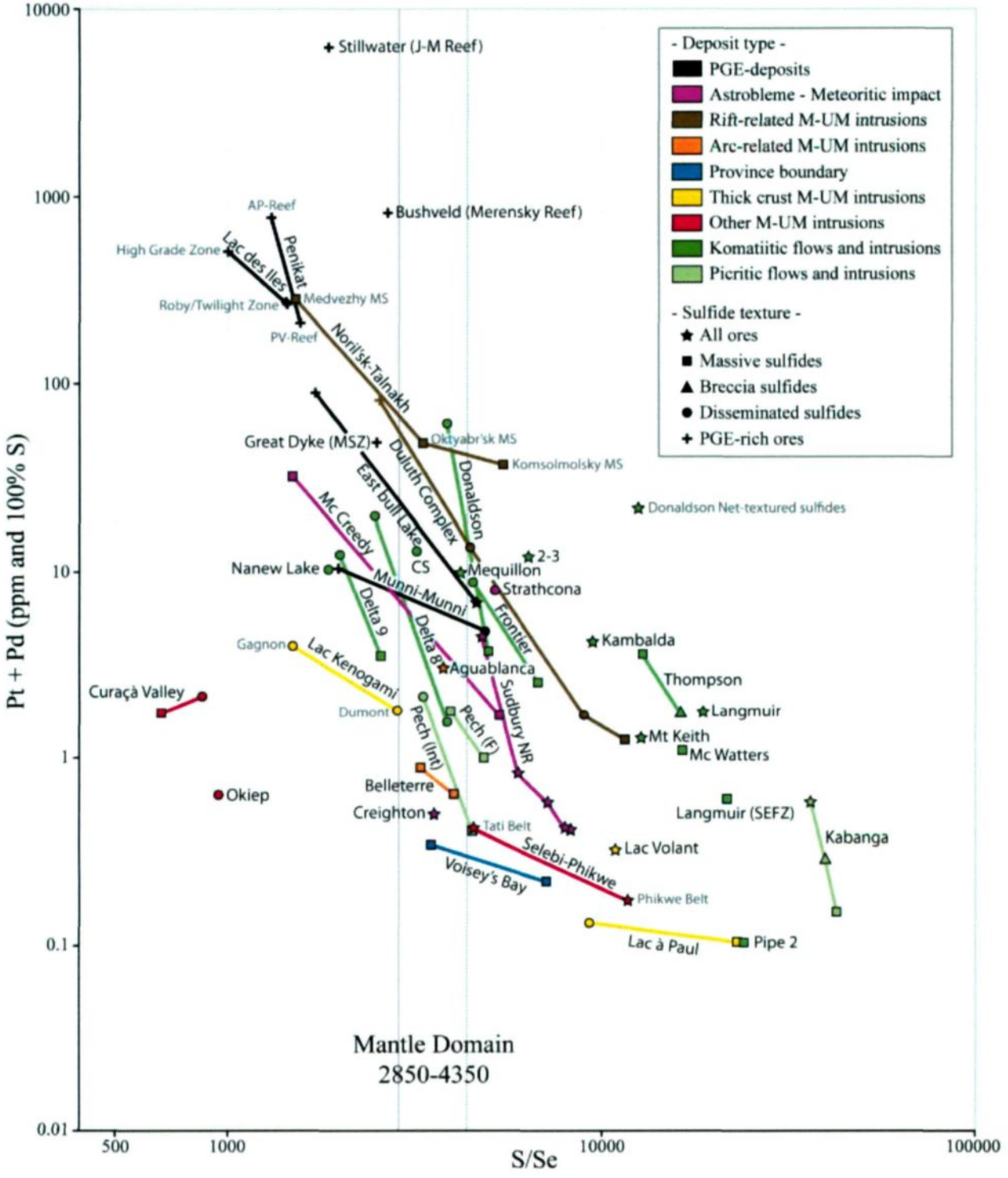

FIG. 2. Plot of Pt+Pd (ppm and 100% sulfide) versus S/Se for magmatic Ni-Cu-PGE sulfide deposits. The mantle domain S/Se values are from Eckstrand and Hulbert (1987). The bulk of the mining camps are indicated except those without Pt and Pd concentrations found. Note that PGE-deposits have lower S/Se ratios than mantle domain and high Pt+Pd contents, while Ni-Cu deposits have generally higher S/Se ratios than or equal to the mantle values and low Pt+Pd contents. Please refer to the Table 1 for the metal contents and the source of data.
Abbreviations: CS = Cape Smith (All ores) ; M-UM = mafic-ultramafic rocks.

The S contamination

The source of the S found in magmatic Ni-Cu-PGE sulfide deposits has long been debated (e.g., Naldrett, 1997; Lesher and Campbell, 1993) and remains an important question in the ore forming process. S/Se ratios and the $\delta^{34}S$ data values are commonly used to determine whether the S was derived from the crust or not. For many deposits, the S/Se ratios higher than the upper limit of the mantle values (> 4350), and the $\delta^{34}S$ values also show deviation from the mantle ones ($\delta^{34}S = 0 \pm 2‰$; Ripley, 1999), indicating that some S in the deposits is from the crust (Fig. 3). The addition of S is considered essential to the formation of large S-rich Ni-Cu deposits (e.g., Lesher and Burnham, 2001; Ripley and Li, 2003).

Komatiitic and picritic flows and intrusions

Most Ni-Cu-PGE komatiitic or picritic deposits have high S/Se ratios that are thought to be the result of S-addition from the adjacent sulfide-bearing metasedimentary country rocks (Lesher and Burnham, 2001; Lesher and Keays, 2002). The Kabanga deposit has the lowest Pt+Pd contents and the highest S/Se ratios of all known Ni-Cu-(PGE) deposits (Maier and Barnes, 2010) and is thought to represents an extreme example of crustal S contamination. The very high S/Se ratios of massive sulfides, breccia sulfides and disseminated sulfides (Table 1; Fig. 2) are thought to have been generated by multiple steps of S assimilation from country rock sulfides, which have contributed up to 50% of the total sulfur in the ore (Maier and Barnes, 2010). The extreme dispersion of S/Se ratios values (11 600-285 000), the very low Se concentration (i.e., only 7.1 ppm Se in the massive sulfides), the low metal contents and the very high $\delta^{34}S$ values (+10 to +24‰) of the sulfide-bearing igneous rocks are all strong evidence of S contamination from the country rocks.

The high S/Se ratios (≥ 10 000: Table 1; Fig. 2) of the Kambalda, Thompson, Langmuir, Mt Keith and Pipe 2 deposits are all consistent with addition of crustally derived S. The mineralogical, geochemical and geological characteristics of the komatiitic and picritic deposits have been extensively reviewed by Lesher and Keays (2002). The $\delta^{34}S$ values of the Kambalda and Thompson ores (Table 1; Fig. 3) are higher than the mantle values, consistent with crustal derived S. Moreover, Eckstrand et al. (1989) showed that the S/Se ratios and the $\delta^{34}S$ values of the Thompson ores fall between the mantle and the S-rich metasedimentary sulfides, suggesting a smaller proportion of sedimentary sulfides. The $\delta^{34}S$ values of the Langmuir and Mt Keith deposits are close to mantle values (Table 1; Fig. 3), indicating that no external S was added to the magma, but the S/Se ratios are greater than the mantle. The Archean footwall rocks at Langmuir have low $\delta^{34}S$ values (Green and Naldrett, 1981), demonstrating that the results of sulfur isotope analyses alone cannot be used to determine the origin of S in the ores. The negative $\delta^{34}S$ values of Mt Keith ores can possibly be attributed to the interaction between the low sulfide contents and the effect of the serpentinization (Groves and Keays, 1979; Lesher and Keays, 2002). In both cases, the S contamination is more easily recognized with the high S/Se values. Samples from the Pipe deposit have similar high S/Se values (Table 1; Fig. 2) but they are strongly depleted in PGEs and base metals, probably due to an extremely low R-factor (Campbell and Naldrett, 1979, Campbell and Barnes, 1984). The addition of crustal S into the komatiitic magma triggered by the assimilation of associated S-rich metasedimentary rocks is favored by numerous studies (e.g., Lesher and Keays, 2002).

However, not all the komatiitic and picritic deposits have high S/Se ratios and $\delta^{34}S$ values indicating that S contamination occurred. Exceptions exist and the identification of the source of the S based only on the S/Se ratio is not evident for some deposits. The Namew Lake deposit has the lowest S/Se ratio (1851: Table 1; Fig. 2) of all komatiitic and picritic deposits. These low

values can be explained by the ore being enriched in Se (Paktunc et al., 1990), Cu, Zn and Pb relative to Ni and Co (Lesher and Keays, 2002), as a result of the assimilation of VMS-type metasedimentary horizons (Menard et al., 1996). These values show that S contamination took place, despite the low S/Se ratios of the ores.

The S/Se ratios of the Ni-deposits from the Raglan (Cross Lake, 2–3, Katinniq, and Donaldson) and Delta (Delta, Bravo, Mequillon and Expo) horizons of the Cape Smith Belt are close to but fall on either side to the mantle domain (Fig. 2), indicating that the source of S is not well established. The S/Se ratios of sulfide-bearing komatiitic-lava channels forming the Raglan horizon (Table 1), including the mineralized rocks from the 2–3 deposits, the massive sulfides and net-textured sulfides from the Donaldson deposits and the sulfide-bearing igneous rocks of the Frontier Zone (link to the Raglan horizon) suggest that crustal S was added. On the other hand, the disseminated sulfides of the Donaldson deposits have S/Se ratios in the range of magmatic sulfides and the other indicators of a crustal contamination (e.g. Re-Os, LREE, Th, Ta, Nb) in the Frontier Zone are not very clear (Dionne-Foster, 2007). In the Delta horizon, the S/Se ratios of the massive sulfides from the Delta 8 and 9 deposits (3944 and 2546, respectively) are typical of mantle values. In addition, the S/Se ratios (geomean of 4174) and the $\delta^{34}S$ values (4.1 to 5.1‰) of the Mequillon Dyke contrast with those of the surrounding country rocks (S/Se = 13781, $\delta^{34}S$ = 0.2 to 3.0‰), indicating that the S is mantle derived (Tremblay, 1990). This dispersion in the S/Se ratios of the Cape Smith ores suggests that some deposits scale variation does occur in the S contamination derived from the country rocks. Using the S/Se ratios alone cannot determine clearly if S contamination took place in the Cape Smith Belt. However, considering other indicators (e.g., Th/La ratio, sedimentary and granophyre inclusions), some studies have emphasized the contaminated nature of the magma (e.g., Barnes et al., 1992). The komatiitic lava erupted onto a thick sequence of metasedimentary rocks of the Povungituk Group

which consist mainly of siltstone and shale (Lesher and Keays, 2002; Barnes and Lightfoot, 2005). Lesher et al. (1999a) proposed that the sulfidic semi-pelitic horizon could be the S source.

The Pechenga Ni-sulfide deposits have S/Se ratios slightly higher than the mantle values, indicating S contamination. Based on work by Melezhick et al. (1998), Barnes et al. (2001) showed some differences in crustal S contamination between the sulfide-bearing intrusions (Eastern Ore) and the sulfide-bearing flows (Western Ore) related to the nature of the country rocks. The sulfide-bearing intrusions have high S/Se ratios (3308 to 5108) and $\delta^{34}S$ values (+3.6 to +5.4‰) suggesting S contamination from the surrounding sulfidic black shales ($\delta^{34}S$ = +11.1‰ and +10.4‰, S/Se = 18 710: Table 1). The sulfide-bearing flows have low $\delta^{34}S$ values (-0.3 to 0.0‰), typical of the mantle, but the S/Se ratios (3921 to 5708) are higher than the mantle domain (2850-4350) and suggest S contamination. The country rocks of the sulfide-bearing flows are also sulfidic black shales but these are characterized by low $\delta^{34}S$ values (-1.2‰ and -1.3‰: Table 1) with high S/Se ratios (geomean of 13 150). Therefore, the S contamination by these black shales did not modify the $\delta^{34}S$ values of the ore significantly, but it nevertheless increased its S/Se ratio. Melezhick et al. (1998) argued that difference in the $\delta^{34}S$ values between the western and eastern sedimentary sulfide is because although both sedimentary sulfides were formed by bacterial sulfate reduction, the western sulfides had not undergone diagenesis at the time of contamination and hence the $\delta^{34}S$ values was not heavy.

Rift related mafic-ultramafic intrusions

Numerous studies on the genesis of the sill-hosted Ni-Cu-(PGE) deposits of the Noril'sk-Talnakh mining district emphasized the crustal contamination (e.g., Fedorenko, 1994; Lightfoot et al., 1994; Walker et al., 1994; Czamanske et al., 1994, 1995). Many of these studies suggest that the S from the anhydrite country rocks were added to the primary magma at a shallow level

(Li et al., 2003; Naldrett, 2004; Arndt et al., 2005, Barnes and Lightfoot, 2005). The strongest evidence is given by the scattered and positive $\delta^{34}S$ values of the ores (+8 to +14‰, Grinenko, 1985; +7.3 to +12.6‰, Li et al., 2003) relative to those of the anhydrite country rocks, which have similarly high $\delta^{34}S$ values (+20‰, Gorbachev and Grinenko, 1973). The S/Se ratios of Monosulfide Solid-Solution (MSS) cumulate phases of massive sulfides from Komsolmolsky and Oktyabr'sk mines (5424 and 5220, respectively: Czamanske et al., 1992) are higher than the mantle domain and are in agreement with an addition of crustally derived S.

The Duluth Complex is one of the best examples where the process of crustal contamination has a significant petrogenetic link with the development of the Cu-Ni deposits (e.g., Mainwaring and Naldrett, 1977; Andrews and Ripley, 1989; Thériault et al., 1997; Thériault and Barnes, 1998; Ripley et al., 2007). The location of the Cu-Ni deposits at the base of the intrusions, as well as the high S/Se ratios and $\delta^{34}S$ values of the gabbronorite-hosted sulfides and most of the olivine-gabbronorite hosted sulfides (Table 1; Fig. 2, 3) associated with the underlying Virginia Formation (Table 1; Fig. 2, 3) are consistent with crustal derived S (Ripley, 1990; Thériault and Barnes, 1998). However, the debate continues about the S contamination: by S-rich fluids migrating from the country rocks into the magma (e.g. Ripley and Alawi, 1986; Ripley and Al-Jassar, 1987; Andrews and Ripley, 1989) or by *in situ* assimilation of the S-rich country rocks (e.g., Ripley, 1981, Thériault and Barnes, 1998, Thériault et al., 2000). Using new S, Se and $\delta^{34}S$ data, a recent study favors the *in situ* assimilation of the Bedded Pyrrhotite Unit, a particularly S-rich horizon in the Virginia Formation (Queffurus and Barnes, accepted). The low S/Se ratios of PGE-rich layer are thought to have formed by an injection of an uncontaminated magma associated with a high R-factor.

Selenium data for the Jinchuan Ni-Cu sulfide deposit are not currently available but the S/Se ratios of the ores are estimated between 3000 and 4000 (Chai and Naldrett, 1992). The $\delta^{34}S$

values (+1.49‰: Table 1, Fig. 3) are within the mantle-derived S range, but Ripley et al. (2005) noted that local high $\delta^{34}S$ values suggest a punctual contribution of externally-derived S.

The Molson Dykes ores have low S/Se ratios and $\delta^{34}S$ values (2799 and -1.05‰, respectively: Table 1; Fig. 3) emphasizing a mantle origin for the S (Eckstrand et al., 1989). In contrast, the S/Se ratios (626 to 21 600) and the $\delta^{34}S$ values (+0.7 to +17.4‰) of the Fox River Sill ores suggest a mixing of S from both mantle and crustal sources (Fig. 3).

Arc-related mafic-ultramafic intrusions

This class contains the mafic-ultramafic intrusions formed in arc-related geological contexts (e.g., Aguablanca, Belleterre). The Aguablanca Ni-Cu deposit has S/Se ratios (3379 to 4048: Table 1; Fig. 2) characteristic of mantle-derived S. However, the $\delta^{34}S$ values of the ores (+7.42‰: Table 1; Fig. 3), as well as the lead isotopes and the existence of digested country rock xenoliths, favor a process of S-saturation triggered by the incorporation of crustal S (e.g., Casquet et al., 1998, Piña et al., 2008). Piña et al. (2008) suggested that the lack of variation in the S/Se ratios of the ores was caused by S contamination due to the unusually low S/Se ratios of the S-rich contaminant (average of 1436: Table 1).

The Meteorite impact of the Sudbury Igneous Complex

Studies agree that the Sudbury Igneous Complex represents a unique case in the genesis of Ni-Cu-PGE deposits: the flash melting of the continental crust induced by meteorite impact (e.g., Lightfoot, 2001; Keays and Lightfoot, 2004 and references therein). Our database shows that most of the deposits of the Sudbury Igneous Complex (e.g., Nickel Rim, Levack, Strathcona, MSS-massive sulfide phases of McCreedy and disseminated sulfides from the Creighton deposit) have S/Se ratios higher than the mantle domain (Table 1; Fig. 2), consistent with formation from

the crust. Ripley and Li (2003) noted that the $\delta^{34}S$ values of the Sudbury ores remain close to mantle values (0 ± 2‰: Naldrett, 1981). This could be explained by the fact that the much of the crust was Archean in age and the $\delta^{34}S$ values of such a crust would have been similar to the mantle values because of the limited S isotope fractionation process of the sedimentary rocks early in earth's history (discussed below). An exception to the high S/Se ratios are those found in the Cu-rich veins of the McCreedy deposit which have S/Se ratios (1199 to 1833 with a geomean of 1481: Dare et al., 2011) lower than the mantle domain. This is thought to be the product of concentration of Se into the fractionated Cu-rich liquid. (See Fractionation of Se between MSS and ISS).

Thick crust mafic-ultramafic intrusions

Several of the mafic-ultramafic intrusions emplaced into thick crust present some evidence of crustal S contamination marked by high S/Se ratios, such as the Lac Volant (> 8800: Table 1, Fig. 2) and Lac à Paul (> 8000: Table 1, Fig. 2 and 8C) deposits from the Grenville Province (Canada). Nabil et al. (2004) calculated that the Lac Volant deposit have undergone a contamination rate of 15 percent from the paragneiss.

Province boundary type

The province boundary type contains Voisey's Bay Ni sulfide ores. The strongly contaminated nature of the troctolitic magmas forming the Voisey's Bay deposit by crustal rocks was pointed out by numerous studies (Lambert et al., 1999, Ripley et al., 1999, Li and Naldrett, 2000, Amelin et al., 2000, Ripley et al., 2002; Lightfoot et al., 2011). Based on the S/Se ratios and the isotopic ratios ($\delta^{34}S$ and $\delta^{13}C$), Ripley et al. (2002) argued that the sulfide- and graphite-rich metapelitic rocks of the Tasiuyak Gneiss represent the source of the contaminating crustal S.

The high S/Se ratios of the MSS phases (Table 1) and the Tasiuyak Gneiss (1146 to 33 000, with 90% of the samples higher than 3300, Ripley et al., 2002) are consistent with the mixing of crustal derived S with primary mantle-derived S. Our data of the MSS phase from the Ovoïd Zone show high S/Se ratios (> 7000: Table 1) and confirm this hypothesis. However, the recognition of the S contamination process is not apparent using the $\delta^{34}S$ values because of the large dispersion (-17.0 to +18.3‰: Fig. 3) around a geomean ($\delta^{34}S$ = -0.4‰: Table 1; Fig. 3) close to the mantle values. Ripley et al., (2002) favor the incorporation of crustal S into the magma by *in situ* assimilation of the Tasiuyak Gneiss (see discussion by Ripley et al., 2002). The S/Se ratios of Cu-rich ores are control by the fractionation of Se in massive sulfides (see below).

Other mafic-ultramafic intrusions (metamorphosed, deformed or unknown)

The other mafic-ultramafic intrusions include Ni sulfide deposits formed in metamorphosed (e.g., Curaçà Valley, Okiep), deformed (e.g., Selebi-Phikwe) or unknown (e.g., Vammala) geological contexts. The high S/Se ratios of the Tati and Phikwe belt deposits (Table 1; Fig. 2) suggest S contamination by crustal rocks. The Deep, Sokta and Ekojoki ores of the Vammala Nickel Belt have S/Se ratios (3765, 2588 and 3206 respectively: Table 1; Fig. 3) close to the magmatic values. The $\delta^{34}S$ values (-1.0 to -0.9‰: Table 1; Fig. 3) are within the range of the mantle domain. Nevertheless, the high zinc content of the sulfides and spinels from the ores were interpreted by Peltonen (1995) as the result of an addition of zinc during crustal contamination, in association with the addition of S. The dispersion of the S/Se ratios of the Svecofennian metasedimentary rocks (2427 to 23 256), the suspected contaminant, between mantle- and crustally-derived S, and especially the local contamination by Se-rich sedimentary sulfides will not increase the S/Se ratios of the contaminated ores significantly, but will allow S-saturation (Peltonen, 1995). Furthermore, the higher S/Se ratios (3765) and the higher Zn content

of the Deep ores compared to the Sokta ores (S/Se = 2588) suggest that the addition of crustal S was more effective. The $\delta^{34}S$ values of the Svecofennian country rocks (+0.7‰: Table 1; Fig. 3), close to the mantle values, are not indicative of a contamination by crustal S.

Mechanisms of S contamination

The mechanisms causing the S contamination of the magma by sulfide-bearing country rocks are not fully understood (e.g., Barnes et al., 2001; Arndt et al., 2005). Indeed, the efficiency of the S contamination is controlled by numerous geological, physical and geochemical parameters specific to each magma and contaminant (e.g., Lesher et al., 2001; Lesher and Burnham, 2001). Different hypotheses have been proposed: a) the bulk assimilation of crustal rocks followed by their complete melting and mixing into the magma (e.g., Lesher and Burnham, 2001); b) the assimilation of S-rich liquids produced by incongruent melting of crustal rocks (e.g., Arndt et al., 2005); c) the *in situ* assimilation of S-rich crustal rocks as xenoliths (e.g., Thériault and Barnes, 1998; Barnes and Lightfoot, 2005) or xenomelts (Lesher and Burnham, 2001); d) the devolatilization of a S-rich fluid or gas phase migrating from the country rocks into the magma (Pechenga: Barnes et al., 2001), in most cases below the level of its final emplacement (e.g., Duluth: Ripley, 1981; Noril'sk-Talnakh: Grinenko, 1985; Vammala: Peltonen, 1995); e) the assimilation of oxidized crustal rocks containing S in the form of sulfate, coupled with a reducing agent (e.g., Noril'sk-Talnakh: Naldrett, 2004). For the komatiite- and picrite-hosted Ni-Cu sulfide deposits, as well as for the Voisey's Bay deposit, the *in situ* assimilation model of S-rich sediments is strongly promoted (e.g., Lesher and Campbell, 1993; Lesher and Burnham, 2001, Ripley et al., 2002; Maier and Barnes, 2010).

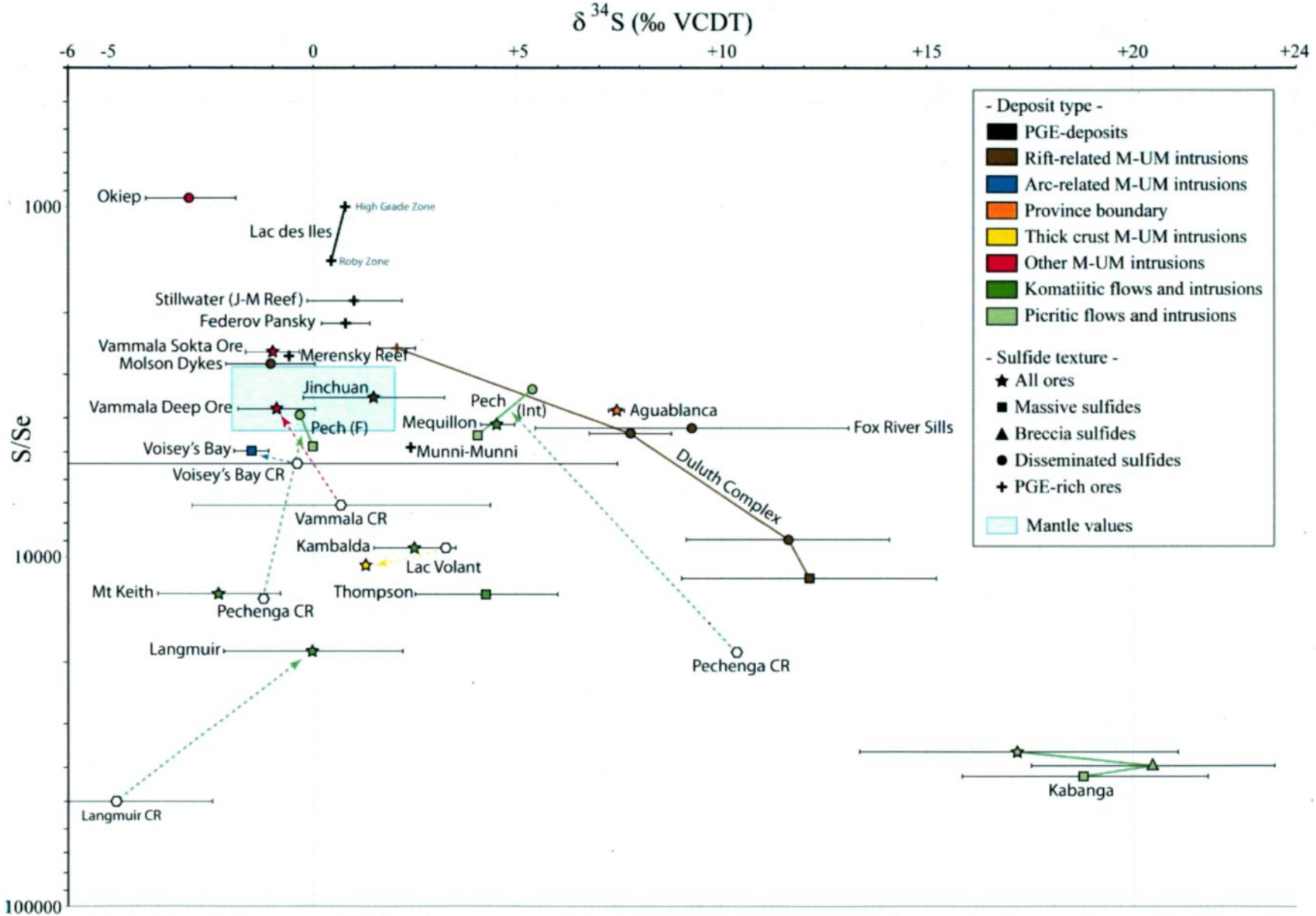

FIG. 3. Plot of S/Se versus $\delta^{34}S$ for the magmatic Ni-Cu-PGE sulfides deposits and their associated contaminants. The S/Se ratios and $\delta^{34}S$ values of mantle domain are taken from Eckstrand and Hulbert (1987) and Ripley (1999) respectively. The bulk of the mining camps are indicated except those without S/Se ratios and $\delta^{34}S$ data available. Abbreviations: Pech (Int) = Pechenga Intrusions, Pech (F) = Pechenga Flows, CR = Country rocks, VCDT = Vienna Cañon Diablo Troilite (international standard).

Influence of the $\delta^{34}S$ values of the contaminating country rocks

In many cases, the deviation in the $\delta^{34}S$ values of the Ni-Cu-PGE ores from the mantle domain led to the suggestion that the source of S was the crustal rocks because most have strongly positive or negative $\delta^{34}S$ values (Ripley and Li, 2003). However, in some cases, the sedimentary country rocks have $\delta^{34}S$ values close to mantle values ($\delta^{34}S = 0 \pm 2‰$) such as the Svecofennian metasedimentary rocks (+0.7‰, Peltonen, 1995) of the Vammala deposits and the sedimentary sulfidic black shales (-1.2 ‰ and -1.3 ‰, Melezhick et al., 1998, Barnes et al., 2001) of the Pechenga Flows. Alternatively Ripley and co-workers have argued that although the country rock $\delta^{34}S$ values may lie outside the mantle range, they may span the mantle values with the result that the net $\delta^{34}S$ of the contamination is close to zero e.g. the Tasiuyak Gneiss (geomean of -0.4 ‰, Ripley et al., 2002) of the Voisey's Bay deposit and the metasedimentary rocks melted by the meteor impact at Sudbury (close to 0‰, Ripley and Li, 2003). These may prevent any distinctions between the potential sources of S (Fig. 3). One of the main reasons for the lack of fractionation of S isotope values in the sediments is that the bacterial process responsible of the decoupling between heavy and light isotopes was limited during the Archean (e.g., Lambert et al., 1979; Groves et al., 1979; Green and Naldrett, 1981; Habicht and Canfield, 1997; Ripley, 1999; Ripley and Li, 2003). Therefore, the $\delta^{34}S$ values of the ores contaminated by the Archean sediments do not show large variations relative to the primary mantle values and stay close to 0 per mil (e.g., Langmuir, Vammala and Sudbury). As a result, the $\delta^{34}S$ isotope ratio is not a useful tool when considering whether contamination of magmas by Archean sedimentary rocks took place and the S/Se ratios present a significant advantage in the search for determining the origin of the S.

Influence of the S/Se values of the contaminating country rocks

The S/Se ratio of the contaminated magma depends largely on the S/Se ratio of the contaminant and not all country rocks have high values (Fig. 4). A high S/Se ratio of the contaminant, e.g., S-rich sediments, provides a significant increase in the S/Se ratios of the contaminated magma and is evidence that the S-saturation was triggered by the crustal S contamination (Fig. 4). If the S/Se ratio of the contaminant is in the range of mantle values and if the amount of S is low, the S/Se ratio of the contaminated magma will not display large variations from the primitive mantle values and other mechanisms should be considered for the S-saturation. A major problem is that crustal-S can be responsible of the S-saturation of the magma without causing an increase in the S/Se ratios because the S/Se ratios of the contaminants are less than or close to the mantle values. Two scenarios may be responsible of the low S/Se ratios of the contaminants.

First scenario: the contaminant is enriched in Se (Fig. 4). For example, some samples of the Svecofennian metasedimentary country rocks of the Vammala Nickel Belt have low S/Se ratios due to the locally Se-rich nature (Se > 10 ppm) of the sedimentary sulfides (Peltonen, 1995). Due to the high S concentration in the sediment, the magma is able to reach S-saturation but, at the same time, a large concentration of Se is incorporated into the magma. Despite the addition of external S, the S/Se ratios of the contaminated ores can remain in the mantle domain.

Second scenario: the contaminant is sufficiently rich in S to generate saturation, but having undergone a prior S-depletion relative to Se (Fig. 4). A mechanism regularly discussed is the S-loss by devolatilization reactions due to the transformation of pyrite to pyrrhotite during metamorphism. This process was recognized in the Virginia Formation, the country rocks surrounding the Duluth complex (Ripley, 1981; Andrews and Ripley, 1989; Thériault and Barnes, 1998). Nevertheless, Andrews and Ripley (1989) and Ripley (1990) suggested that S has been

conserved in the country rocks, leading to limited variation in the S/Se ratios. In contrast, Piña et al. (2008) interpreted the low values of the S/Se ratios (184 to 3300) of the S-rich Serie Negra black slates (up to 0.5 %), metamorphosed to greenschist facies and located at the contact with the Aguablanca intrusion, as resulting from S-loss probably by devolatilization. Even though isotope signatures and the presence of xenoliths indicate a significant country rock contamination, crustal S did not increase the S/Se ratio of the Aguablanca ore (average of 1436: Table 1).

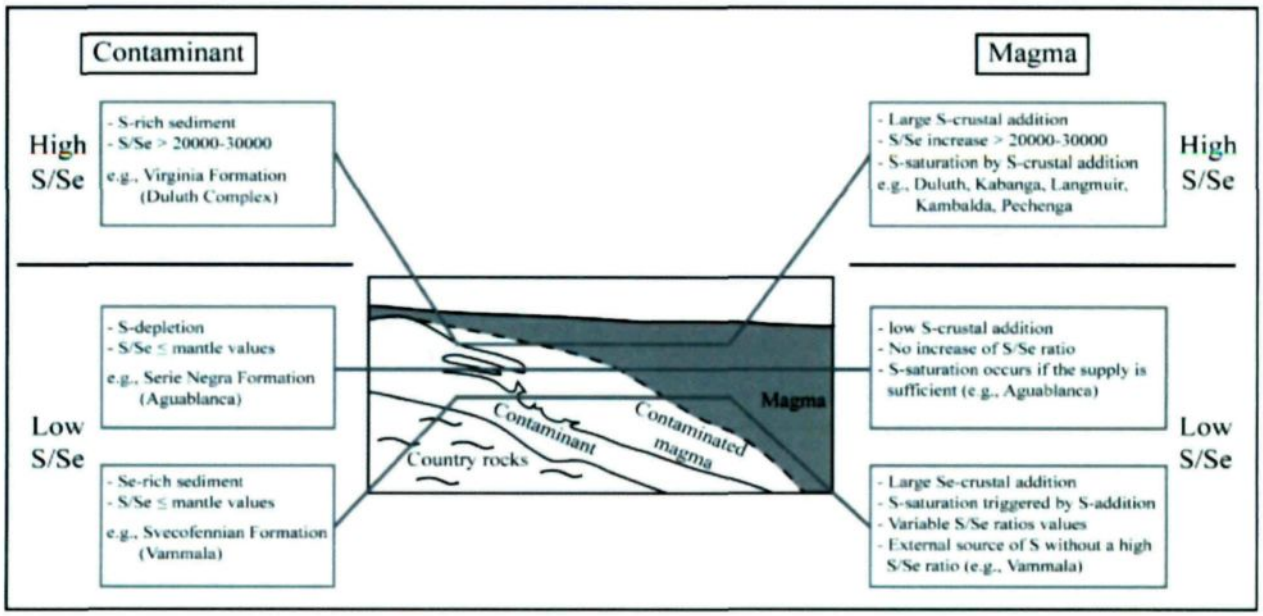

FIG. 4. Schematic model illustrating the different possibles cases of S contamination by the crustal rocks, considering the effect of the S/Se ratio of the contaminant on the S/Se ratio of the contaminated magma.

R-factor

The R-factor is an essential parameter controlling the degree of metal enrichment before and during the segregation of the sulfide liquid. The R-factor represents the mass ratio of silicate magma to sulfide liquid (Campbell & Naldrett, 1979) and can be calculated by the following equation:

$$R = D^{sul/sil}[(C_{Sil} - C_{Sul})/(C_{Sul} - D^{sul/sil})] \quad (2)$$

where $D^{sul/sil}$ is the equilibrium partition coefficient for each elements between the sulfide and the silicate liquids, C_{sil} is the concentration of an element in the initial silicate liquid and C_{Sul} is the concentration of this same element in the sulfide melt. Therefore, the chalcophile elements with a high partition coefficient between the sulfide and silicate liquids ($D^{sul/sil}$), such as Se and other metals including PGEs, will be concentrated in the sulfide liquid. Thus, during the segregation of the sulfide liquid, the Se concentration and the S/Se ratio is affected by variations in the R-factor values (e.g., Thériault and Barnes, 1998).

The R-factors have been calculated for most of the deposits, but not for all (Table 2). To validate the published R-factors and to fill any gaps, we have re-calculated R-factors for all the deposits to provide a consistent database. To estimate the R-factor, the $D^{sul/sil}$ of the element chosen for the calculations must be ten times greater than the R-factor (Campbell and Barnes, 1984). Therefore, Pd with its extremely high partition coefficients into sulfide liquid (e.g., $D^{sul/sil}$ = 43 000; Peach et al., 1994) with a low D between olivine and sulfide liquid (Lesher and Burnham, 2001) was chosen. The resulting R-factors and the parameters used are given in Table 2.

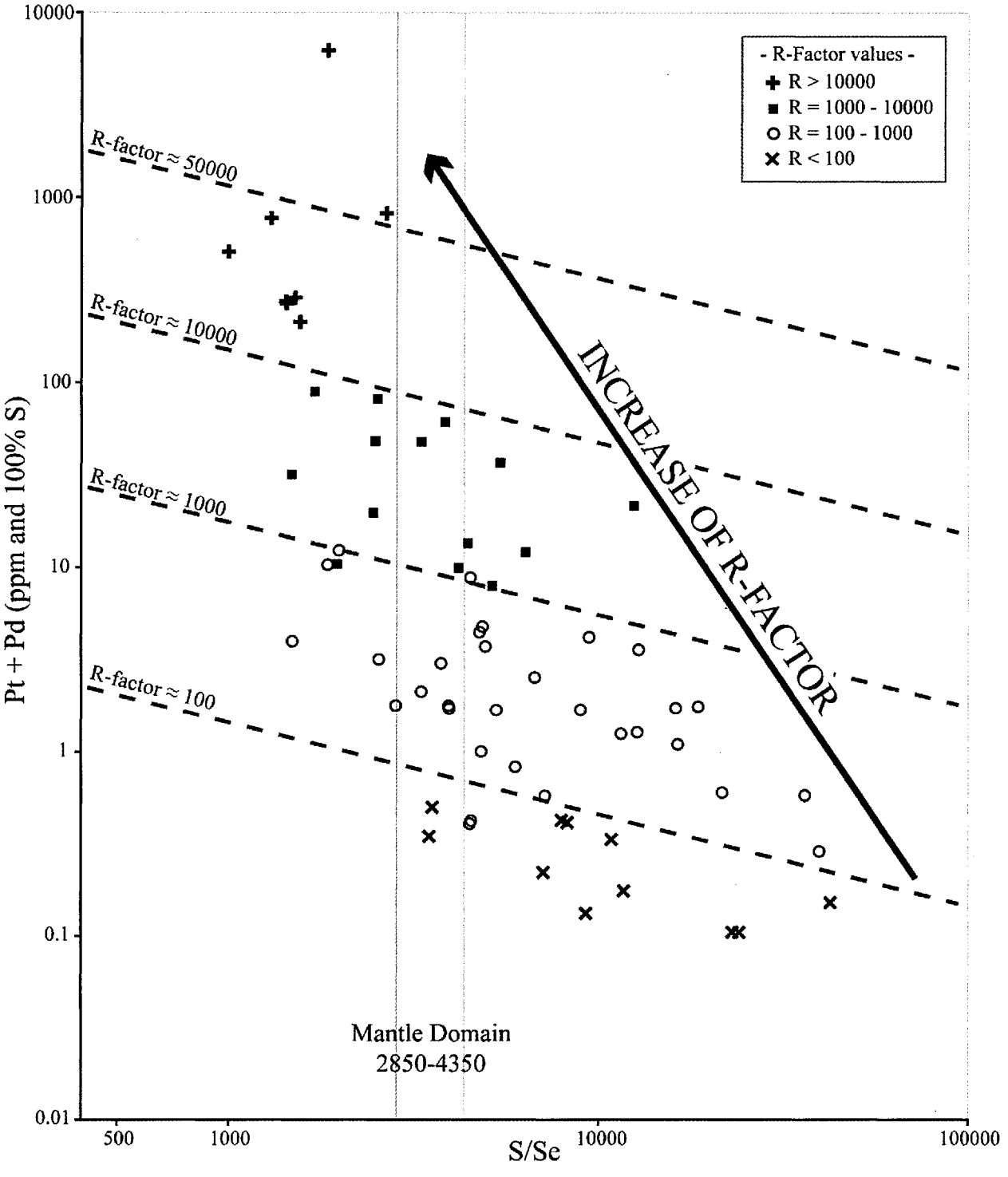

FIG. 5. Plot of Pt+Pd versus S/Se of the Ni-Cu-PGE deposits, classified using R-factor values published or recalculated from the literature. The mantle domain S/Se values are taken from Eckstrand and Hulbert (1987).

Table 2. R-factors values for each deposits taken from the literature and recalculated

Deposit type	Deposits	Rocktype/Ore	Literature		this study		
Mining Camp			R-factor	References	Csul (ppm)	Csil (ppb)	R-factor
Ni-Cu deposit - Class 1(i): Astrobleme – Meteorite impact							
Sudbury	Levack (N-Range)	Granophyre	400 - 4000	Keays and Lightfoot, 2004	0.481	4.01	40 - 370
		Quartz gabbro	400 - 4000	Keays and Lightfoot, 2004	0.537	4.01	130
		Felsic norite	400 - 4000	Keays and Lightfoot, 2004	0.252	1.1	360
		Mafic norite	400 - 4000	Keays and Lightfoot, 2004	0.565	1.1	600
		Sublayer	400 - 4000	Keays and Lightfoot, 2004	2.324	2.3	1500
	Nickel Rim (N-Range)	Quartz gabbro	400 - 4000	Keays and Lightfoot, 2004	0.224	4.01	20 - 140
		Felsic norite	400 - 4000	Keays and Lightfoot, 2004	0.21	1.1	330
		Mafic norite	400 - 4000	Keays and Lightfoot, 2004	0.364	1.1	315
		Sublayer	400 - 4000	Keays and Lightfoot, 2004	0.185	2.3	1600
	Creighton	All ores	-	Dare et al., 2010	0.365	2.3	30 - 600
	Strathcona	SF-Diss	-	Barnes and Lightfoot, 2005	-	-	≈ 1000
	Mc Creedy	Cu-rich veins	-	Dare et al., 2011	20.852	2.3	1500 - 3100
		East Main MSS	-	Dare et al., 2011	0.973	2.3	20 - 250
Ni-Cu deposit - Class 1(ii): Rift related mafic-ultramafic intrusions							
Duluth Complex	Dunka Road	Norite	50 - 400	Thériault et al., 1997	1.334	9.5	170
		Troctolite	700 - 2000	Thériault et al., 1997	10.819	9.5	1220
		PGE-rich layer	5000 - 11000	Thériault et al., 1997	67.065	9.5	8170
		SF-MS	-	Thériault and Barnes, 1998	1.229	9.5	130
Noril'sk - Talnakh	Medvezhy (N1)	SF-MS	-	Czamanske et al., 1992	191.627	8	> 10000
	Komsolmolsky	SF-MS	-	Czamanske et al., 1992	30.751	8	4200
	Oktyabr'sk	SF-MS - MSS	-	Czamanske et al., 1992	18.788	8	1700 - 3300
		SF-MS	-	Czamanske et al., 1992	27.985	8	1500 - 6000
		SF-MS - ISS	-	Czamanske et al., 1992	177.55	8	15000 - 34000
Jinchuan		All Ores	30 - 1300	Chai and Naldrett, 1992	-	-	n.d.
Ni-Cu deposit - Class 1(iii): Arc-related mafic-ultramafic intrusions							
Aguablanca		All Ores	-	Piña et al., 2008	1.758	10	50 - 370
Ni-Cu deposit - Class 1(iv): Province boundary							
Voisey's Bay		All Ores	50 - 500	Naldrett et Li, 2007	-	-	n.d.
				Li et al., 2000	-	-	n.d.
Ni-Cu deposit - Class 1(v): Thick crust mafic-ultramafic intrusions							
Curaçà Valley		All Ores	-	Maier and Barnes, 1999	-	-	n.d.
Okiep	Koperberg Suite	All Ores	-	Maier, 2000	-	-	n.d.
Lac Volant		All Ores	100 - 200	Nabil, 1999	0.282	3	20 - 270
Lac à Paul		SF-Diss	50 - 400	Huss, 2002	0.103	3	5 - 500
		SF-MS	50 - 400	Huss, 2002	0.102	3	10 - 60
Lac Kenogami		All Ores	10000 - 20000	Vaillancourt, 2001	42.757	3	≈ 1000
Ni-Cu deposit - Class 1(vi): Other mafic-ultramafic intrusions (Metamorphosed, deformed or unknown)							
Selebi-Phikwe	Tati Belt	All Ores	-	Maier et al., 2008	0.096	10	50 - 4000
	Phikwe Belt	All Ores	-	Maier et al., 2008	0.087	10	5 - 200
Ni-Cu deposit - Class 2(i): Komattitic flows and intrusions							
Kambalda		All Ores	500	Naldrett, 1981	2.46	10.3	250
			300	Campbell and Barnes, 1984			
			6500	Duke, 1990			
Mt Keith - Betheno		Dunite	-	Groves and Keays, 1979	1.279	10.3	250
Langmuir	Langmuir 1 and 2	All ores	-	Green and Naldrett, 1981	1.156	10.3	100 - 200
	Mc Watters		-	Green and Naldrett, 1981	0.805	10.3	≈ 100

	South End Fault Zones	SF-MS	-	Green and Naldrett, 1981	0.366	10.3	≈ 100
Thompson		SF-MS	100 - 200	Naldrett, 2004	3.655	10.3	300
Pipe II		SF-MS	-	Bleeker, 1990	0.077	10.3	≈ 10
Namew Lake		SF-Diss	-	Menard et al., 1996	5.32	10.3	500
Cape Smith (Delta)	Delta 8	SF-MS	300	Barnes and Picard, 1993	0.527	12	10 -300
		SF-Diss	300	Barnes and Picard, 1993	15.195	12	2000
	Delta 9	SF-Diss	300	Barnes and Picard, 1993	8.924	12	750
		SF-MS	300	Barnes and Picard, 1993	2.156	12	470
	Méquillon	Dyke	1000	Barnes and Picard, 1993	6.808	12	800
Cape Smith (Raglan)	2-3		1000	Barnes and Picard, 1993	6.909	12	800
	Donaldson West	SF-Diss	1000	Barnes and Picard, 1993	25.087	12	2000
		SF-Net textured	1000	Barnes and Picard, 1993	12.688	12	1000
		SF-MS	-	Barnes and Picard, 1993	1.105	12	100
	Frontier	SF-Diss	100 - 500	Dionne-Foster, 2007	7.546	12	500 - 1000
		SF-Mtr	-	Dionne-Foster, 2007	3.761	12	200 - 450
		SF-MS	-	Dionne-Foster, 2007	2.038	12	170
Ni-Cu deposit - Class 2(ii): Picritic flows and intrusions							
Pechenga	Flows (West Ore)	SF-MS	250	Barnes et al., 2001	0.532	12	100 - 200
		SF-Diss	100 - 2500	Barnes et al., 2001	0.912	12	100 - 500
	Intrusions (East Ore)	SF-MS	250	Barnes et al., 2001	0.256	12	100 - 200
		SF-Diss	100 - 2500	Barnes et al., 2001	1.26	12	100 - 500
Kabanga		SF-MS	10 - 400	Maier et al., 2010	0.063	12	5- 150
		SF-MS breccia	10 - 400	Maier et al., 2010	0.086	12	170
		M-UM rocks	10 - 400	Maier et al., 2010	0.307	12	5 - 450
PGE-deposits							
Stillwater	J-M Reef	Reef	30000 - 45000	Godel and Barnes, 2008	4533.807	10	45000
Bushveld	Merensky Reef	Reef	45000	Godel et al., 2007	317.137	9.8	6500 - 75000
Great Dyke	Mimosa Mine	MSZ	-	Barnes et al., 2008	27.759	10	3000
Penikat	AP-Reef	FI-02-06	-	Barnes et al., 2008	623.675	10	10000 - 100000
	PV-Reef	FI-03-04	-	Barnes et al., 2008	109.862	10	10000 - 100000
Munni-Munni		UM Zone	-	Hoatson and Keays, 1989	1.885	15	300
		PGE-rich	-	Hoatson and Keays, 1989	4.239	15	1000
Federov Pansky		Gabbronorite	10000 - 100000	Schissel et al., 2002	-	-	n.d.
East Bull Lake	Intrusion	Contact-type	1000 - 10000	Peck et al., 2001	66.735	18.1	1500 - 10000
Lac des Iles	Roby Zone		-	Hinchey and Hattori, 2005	245.127	10	10000 - 100000
	Twilight Zone		-	Hinchey and Hattori, 2005	236.712	10	10000 - 100000
	High Grade Zone		-	Hinchey and Hattori, 2005	476.077	10	10000 - 100000

See Table 1 for the metal contents and Barnes and Lightfoot (2005) for the description of the classification.

Abbreviations: SF-MS = massive sulfide, SF-Mtr = matrix sulfide, SF-Diss = disseminated sulfide, MSS = Monosulfide Solid-Solution, ISS = Intermediate Solid-Solution, UM = ultramafic, M = mafic.

There is a strong correlation between the S/Se ratios, the PGE contents and the R-factor values (Fig. 5). The deposits with the highest R-factor values have the lowest S/Se values. Most of the PGE-poor, Ni-Cu deposits were formed at extremely low ($\leq$ 100) or low (100 to 1000) R-factors and they are characterized by S/Se ratios higher or close to the mantle values (Fig. 5). This is true for all deposits where crustally-derived S was involved in the formation of the ores (see above). The range of moderate R-factor values (1000 to 10 000, Table 2; Fig. 5) includes the deposits which have S/Se ratios on either side of the mantle domain at relatively high PGE contents (10 to 100 ppm at 100% S). The PGE-rich deposits were formed by mantle-derived S and the sulfide liquid equilibrated at high R-factors (> 10 000, Table 2; Fig. 5).

This correlation is closely linked to the behavior of PGEs and Se during the segregation of the sulfide liquid. Due to their high $D^{sul/sil}$, PGEs and Se are strongly partitioned into the sulfide liquid. A low R-factor indicates that only a limited volume of silicate magma interacted with the sulfide liquid and only small amounts of PGEs and Se were available for incorporation into the sulfide liquid and the sulfides are poor in PGE and Se. Several parameters may explain the low R-factors and they seem closely related to the crustal contamination process. The S contamination from the S-rich crustal rocks allowed the formation of a large volume of sulfide liquid. Therefore, the chalcophile elements were diluted in the sulfide liquid, explaining the low PGE and Se content, and thus the high S/Se ratios. In addition, contamination by Se-poor crustal rocks increased the S/Se ratios of the contaminated magma considerably. Moreover, the large amount of sulfide liquid formed by the addition of crustal S led to a decrease in S solubility and reduced the time of interaction between the silicate magma and the sulfide liquid, i.e., low R-factor, and resulted in a rapid segregation of the sulfide liquid. Therefore, the sulfide liquid did not have time to collect the Se and the S/Se ratios remained high and close to the S/Se ratios of

the contaminants. S contamination by S-rich crustal rocks associated with low R-factors form large deposits but with low PGE contents.

The more silicate magma and the sulfide liquid interact, the more the PGEs and Se are concentrated in the sulfide liquid, decreasing the S/Se ratio. This increase of R-factor is coupled with the progressive decrease in the impact of crustally-derived S. The S/Se ratios values of the sulfides are the result of an interaction between two parameters: the R-factor and the amount of S contamination. For example, the R-factor values of the sulfide-bearing igneous rocks of the Duluth Complex increase from the margin to the center of the intrusion, in association with the decrease of the S contamination (Thériault et al., 1997): from the gabbronorite (R = 50 to 400), to olivine-gabbronorite (R = 700 to 2000) and to the PGE-rich layer (R = 5000 to 11 000).

The maximum enrichment of Se in sulfide is in part controlled by the R-factor and in part by the partition coefficient of Se into sulfides. Peach et al. (1990) obtained an empirical value of $D_{Se}^{sul/sil} = 1770$. However recent experimental and empirical work indicates lower values: 397-793 in Brenan et al., as quoted in Barnes et al. (2009); and 323 in Patten et al. (accepted). Assuming that these lower values are correct, the maximum enrichment of Se in a sulfide liquid would be ~300-800 times the value of silicate liquid. As originally pointed out by Campbell and Barnes (1984), when the R-factor is ten times greater than D then the enrichment factor in the sulfides is equal to D, thus for R-factors >3000, Se would be enriched in the sulfides by 300-800 times. Interestingly the enrichment of S into the sulfide liquid is similar. If we assume for instance that the sulfide saturation is attained in a basalt at approximately 1000 ppm (e.g., Li and Ripley, 2005) and the sulfide liquid contains 35 percent S, the enrichment factor would be 350. In other words, the both Se and S would be enriched in similar amounts at R-factors >3000 and thus the S/Se ratio of the silicate melt would be preserved. The sulfide liquid forming the PGE-rich deposits

interacted with a volume of silicate magma over 10 000 times more abundant than the sulfide liquid. The sulfide liquid collected a large amount of Se from the silicate magma, in a dynamic system, explaining the low S/Se ratios associated with high PGE contents (Fig. 5). All known PGE-deposits are associated with very large R-factors (e.g., Campbell et al., 1983).

Generally, massive and matrix sulfides have lower S/Se ratios, PGE contents and R-factor values than associated disseminated sulfides. Possibly the sulfide droplets forming the disseminated sulfides interacted for a longer time, with a larger volume of magma, than the massive and matrix ores. Therefore, the high R-factor of disseminated sulfides leads to a higher concentration of PGEs and Se in the sulfide liquid. By this mechanism, Se is enriched and the S/Se is lowered in disseminated sulfides with respect to massive and matrix sulfides.

At low R-factors, the enrichment of Se in the sulfides would be diluted somewhat the R-factor has a significant influence on the S/Se values of the ores, which can cause either increase or decrease. However, during contamination by S-rich crustal rocks, the effect of the R-factor on the S/Se ratios seems relatively limited compare to the variations generated by the contamination. On the other hand, the R-factor governs the S/Se values of uncontaminated mantle-derived magma significantly as in the case of the PGE-deposits.

Segregation of the sulfide liquid

In the Upper Zone of the Bushveld Complex, the variation in the S/Se ratios may result from the segregation of the sulfide liquid (Barnes et al., 2009). The ultramafic-mafic section of the Rustenburg Layered Suite consists of five zones called from the base to the top: Marginal Zone, Lower Zone, Critical Zone, Main Zone and Upper Zone. Samples from the first four zones have S/Se ratios that vary between 3100 and 3300 (Table 1; Fig. 6), close to mantle values. However, the S/Se ratio increases substantially in the Upper Zone from sub-Zone A (S/Se $\approx$ 2700) at the base to Sub-Zones B and C (S/Se $\approx$ 7000) at the top (Fig. 6). Due to high partition coefficient of Se between the sulfide liquid and the silicate melt, the extraction of the sulfide liquid from the silicate magma during the formation of sub-Zone A could have depleted the silicate magma in Se. Thus, the sulfides that segregated from the fractional residual silicate magma during the formation of sub-Zones B and C were depleted in Se resulting in an increase in the S/Se ratios in these two zones.

This process has not been investigated at other intrusions. The process could be identified because of the systematical analysis of a large number of samples in two borehole sections representative of the complete stratigraphic suite of the Bushveld Complex. However, the segregation of a sulfide liquid is probably not restricted to the Bushveld and the process may yet be found in similar mafic-ultramafic intrusions if a sufficiently large number of S and Se analyses are carried out.

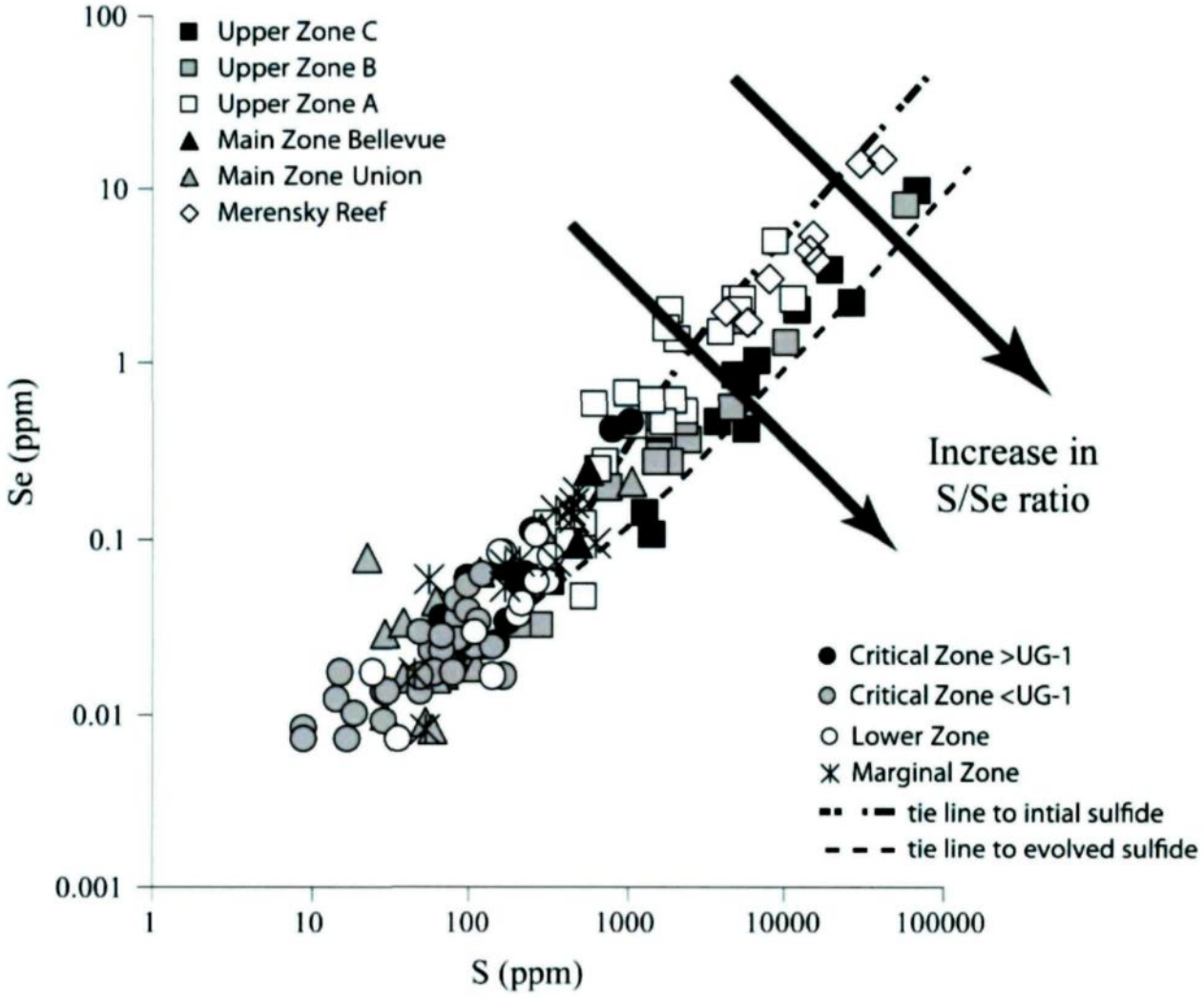

FIG. 6. Plot of Se versus S versus S/Se of rocks of the Rustenburg Layered Suite, Bushveld Complex (modified from Barnes et al., 2009), showing an increase in S/Se ratios from the Upper sub-Zone A to the Upper sub-Zones B and C.

Fractionation of Se between MSS and ISS

In the absence of metamorphism and alteration, the geochemical distribution of Se in magmatic Ni-Cu-PGE sulfide deposits is controlled by the main magmatic sulfide phases, i.e. pyrrhotite, pentlandite and chalcopyrite, formed by the crystallization of the sulfide liquid. Massive sulfides cover a wide range of S/Se ratios values (1000 to 43 000: Fig. 7) and show a fractionation of Se between the Fe-rich phase (interpreted as monosulfide solid-solution, MSS) and their respective residual Cu-rich phase (interpreted as intermediate solid-solution, ISS). Focusing on MSS and ISS phases from Voisey's Bay, Sudbury and Noril'sk-Talnakh mining camps (Fig. 7) illustrates this process. The MSS phases have lower Se concentrations (33 to 91 ppm) than the ISS phases, resulting in higher S/Se ratios (3625 to 9885: Fig. 7). Moreover, most of S/Se ratios from the MSS massive sulfides are higher than the mantle domain (> 4350: Fig. 7). By contrast, the ISS phases have higher Se concentrations (72 to 328 ppm) and lower S/Se ratios values (1005 to 3968) than the associated MSS ores. These higher Se concentrations in the ISS relative to MSS generate lower S/Se ratios, less than or equal to the mantle domain. Phases between MSS and ISS have Se concentrations (72 to 141 ppm) and S/Se ratios (2457 to 4573) indicating a mixing between the two phases. The S/Se ratios display strong variations due to various Se-enrichment in the different massive sulfide types.

Previous empirical work had shown that Fe-rich ore which are thought to represent MSS cumulates are poorer in Se than Cu-rich ores thought to represent the fractionated liquid. These observations suggest that that Se is slightly incompatible in the MSS (e.g., Thériault and Barnes, 1998, Barnes and Lightfoot, 2005). This has recently been confirmed by experimental work Helmy et al. (2010) who determined the partition coefficient for Se between MSS and the sulfide liquid with a value of $D_{Se}^{MSS/sul} \sim 0.6$. Platinum and Pd are incompatible with the MSS

($D_{Pt}^{MSS/Sulf\,liq}$ = 0.05-0.13 and $D_{Pd}^{MSS/Sulf\,liq}$ = 0.09-0.2, Barnes et al., 1997a) and are concentrated in the residual Cu-rich phase, resulting in high Pt+Pd values associated with low S/Se ratios. The Cu-rich veins have also lower S/Se ratios. The same process of preferential concentration of Se in the Cu-rich phases relative to Fe-rich phases were recognized in mantle xenoliths (Lorand and Alard, 2001; Lorand et al., 2003).

The disseminated sulfides are generally thought to represent the trapped sulfide liquid, not segregate from the mafic magma, and thus might be expected to have S/Se ratios similar to the initial liquid because MSS and ISS phases are associated in the sulfide liquid fraction. In general, it is true that disseminated sulfides at a particular deposit have lower S/Se ratios than the associated massive ores which is thought to represent the MSS cumulate. Therefore, whole rock S and Se analyses will not distinguish MSS and ISS phases and the S/Se ratio will reflect the mixing of S/Se ratio values of MSS and ISS.

Care should be taken when determining S/Se ratios in ore samples, especially for massive-sulfides, which may have undergone MSS fractionation. The influence of Se fractionation overlaps the effect of S contamination and the R-factor in the variations of the S/Se ratios. In the same ore deposit, the S/Se ratio of the Fe-rich ore can be greater than mantle values and the Cu-rich ore lower than mantle values due to MSS fractionation.

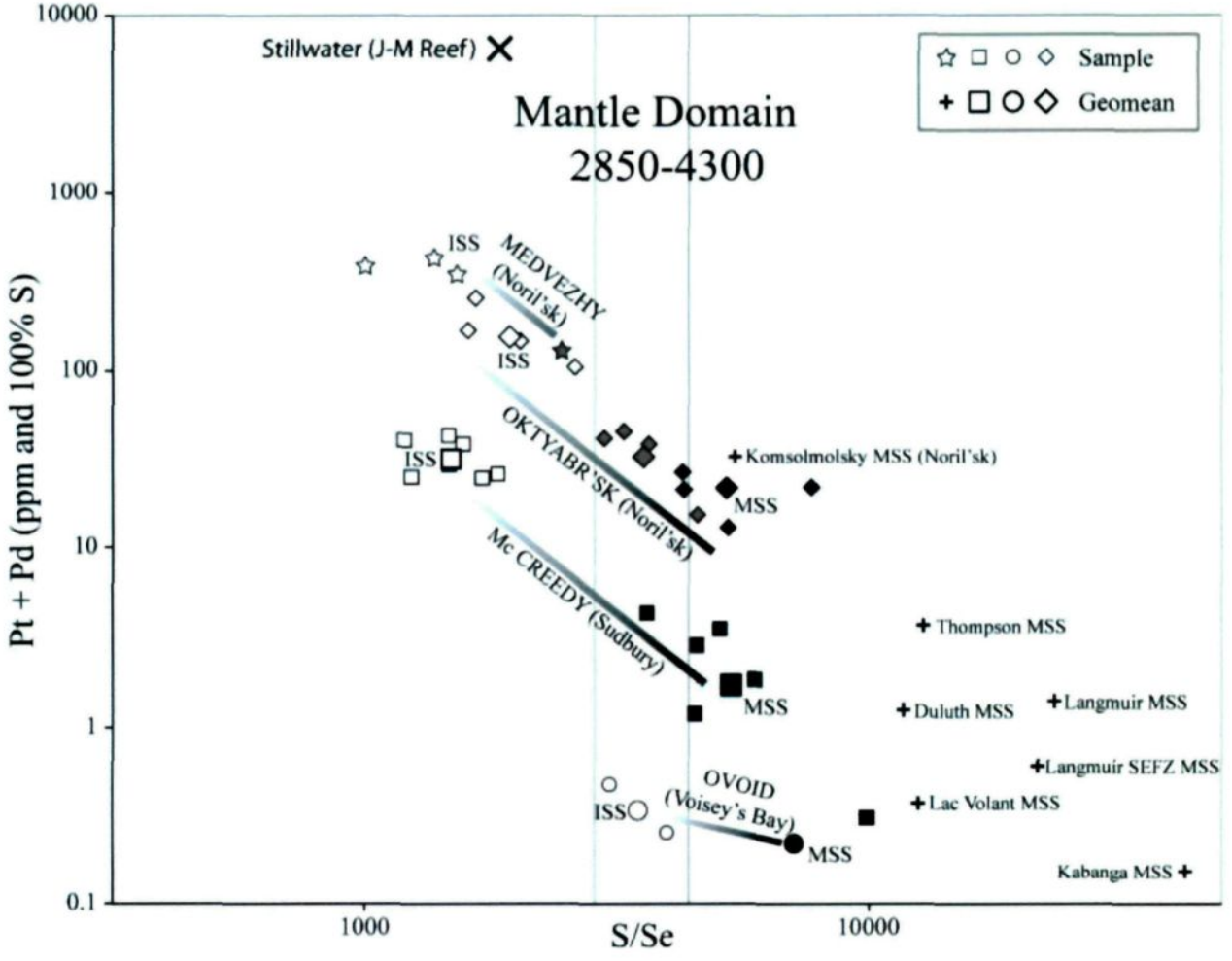

FIG. 7. Plot of Pt+Pd (100% sulfide) versus S/Se of massive sulfides from some Ni-Cu-PGE deposits. Abbreviations: MSS = Fe-rich massive sulfides interpreted as monosulfide solid-solution, ISS = Cu-rich ores interpreted as intermediate solid-solution crystallized from fractionated liquid. Stillwater (J-M Reef) is indicated as a reference point. Mantle Domain S/Se ratios values are taken from Eckstrand and Hulbert (1987). Massive sulfide data are taken from this study (Voisey's Bay) and Green and Naldrett (1981), Bleeker (1990), Czamanske et al. (1992), Thériault and Barnes (1998), Nabil (2004), Maier et al. (2010), Dare et al. (2011).

Hydrothermalism

Some magmatic Ni-Cu-PGE sulfide deposits show some petrographic and chemical evidence of remobilization of chalcophile elements by circulating fluids during late- to post-magmatic processes. Compared to S, Se is relatively immobile during hydrothermal alteration (Yamamoto, 1976; Howard, 1977) and is conserved in the altered rock while S is preferentially incorporated into the aqueous fluid. The leaching of partially or totally crystallized rocks by the circulation of fluids leads to the dissolution, transportation and crystallization into secondary minerals of mobile-elements, including S and mobile metals (e.g., Pd, Cu, Bi, As, Sb). Generally, because of the S loss, the S/Se ratios are lower in leached rocks, but the heterogeneous distribution of the mobile elements leads to some strong variations in concentration resulting in local depletion or enrichment. Consequently, the S/Se ratios could be scattered, depending on the depletion or enrichment in S. The fluids could be late-magmatic, metamorphic or superficial. Late-magmatic fluids can be expelled from the magma during its solidification; they can not only remobilize elements, but also precipitate these elements in another part of the intrusion or on the country rocks. The examples below illustrate the effect of the fluid activity on the S/Se ratios.

The low S/Se ratios (1412 to 2263; Table 1; Fig. 9C) in the PGE-rich samples of the J-M Reef (Stillwater Complex, USA), coupled with the occurrence of secondary magnetite and some recrystallization textures in the primary sulfides, suggest S loss during the post-cumulate process. Godel and Barnes (2008) argued that S loss results of the desulfurization of base-metal sulfide and their calculation indicates a removal of 20 to 50 percent of the initial S content. These authors favor a model involving a partial desulfurization caused by S undersaturated fluids percolating through the cumulate pile. Schissel et al. (2002) mentioned that some of the mineralization in the Federov Pansky layered mafic intrusion (Kola Peninsula, Russia) were

remobilized by late-stage intercumulus fluids, as evidenced by the coarse pegmatitic and/or taxitic textures of gabbronorites, and by the remobilization of Platinum-Group Minerals (PGMs) and chalcopyrite grains. The low S/Se ratios of the gabbronorite-hosted Cu-Ni-PGE (1050 to 3300: Fig. 9B, Table 1) could support this hypothesis. However, the high estimated R-factor (10 000 to 100 000, Schissel et al., 2002) could alone explain the low S/Se ratios.

The Roby, Twilight and High Grade Zones of the Lac des Iles (Canada) Pd-deposits are characterized by S/Se ratios in the range of mantle values. However, many authors have underline the fundamental role played by low temperature fluids in the ore genesis (e.g., Lavigne and Michaud, 2001; Watkinson et al., 2002; Hinchey and Hattori, 2005; Barnes and Gomwe, 2011) and especially in the Pd-enrichment (Pd/Pt = 12.3) of the High Grade Zone. Hinchey and Hattori (2005) showed that the High Grade Zone has a wider range in S/Se ratios than the Roby and Twilight Zones (Fig. 9A) with some values as low as 600. This might be thought to be due the presence of a very fractionated sulfide liquid. However, the sulfide component of the High Grade Zone is not Cu-rich (Barnes and Gomwe, 2011). Another possibility is loss of S but Hinchey and Hattori (2005) argued that the correlation between S, Cu, Ir and Se indicate that no S remobilization occurred in the High Grade Zone. Consequently, Hinchey and Hattori (2005) suggested that the S/Se ratios reflect those of the parental magma, although it is not clear why the magma would have such low S/Se ratios.

The contact-type PGE disseminated sulfides of the East Bull Lake Intrusion (Canada) are characterized by S/Se ratios lower than the range of magmatic sulfides (geomean range from 1160 to 2240: Fig. 9D) which Peck et al. (2001) explained by a high R-factor (~6600). However, greenschist to amphibolite facies metamorphism has strongly modified the primary mineralogy of mafic igneous rocks (Card, 1978; Chubb, 1994; Peck et al., 2001) and the textures of pre-existing magmatic sulfides. The structurally controlled PGE-rich sulfides in the Parisien Lake

Deformation Zone are the best example of this recrystallization. Their S/Se ratios display a wide range (468-559 000 with a geomean value of 4600: Fig. 9D) and point to a non-magmatic origin. Peck et al. (2001) indicate that these sulfides were formed by the circulation of metamorphic fluids that provoke the dissolution of pre-existing PGE-rich disseminated sulfides and their recrystallization in shear zones cutting the intrusion with the formation of low temperature Pd-Bi-Te minerals. In addition, it is quite possible that the circulation of metamorphic fluids has remobilized the S from the contact-type PGE mineralization and subsequently reprecipitates PGE and Se-poor sulfide in the permeable shear zone.

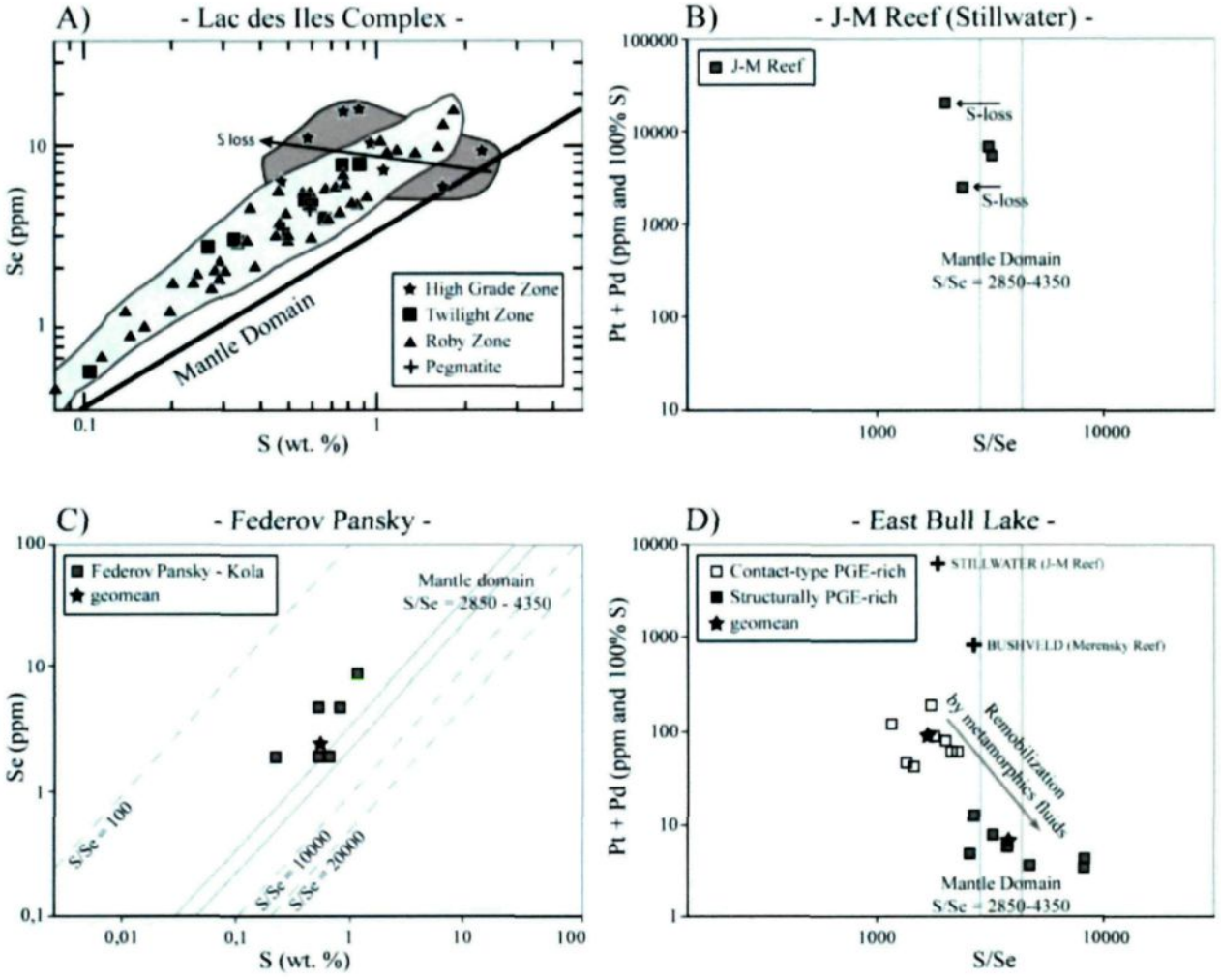

FIG. 9. Plots of Se versus S of the Lac des Iles Intrusive Complex (A) and the Federov Pansky layered mafic intrusion (B), and of Pt+Pd (100% S) vs S/Se of the J-M Reef, Stillwater Complex (C) and the East Bull Lake Intrusion (D). Data are taken from Hinchey and Hattori (2005), Schissel et al. (2002), Godel and Barnes (2008) and Peck et al. (2001)

Metamorphism

Metamorphism is one of the post-magmatic processes that can modify the mineralogical and the chemical composition of the primary magmatic ore. Some authors attribute large variations in S/Se ratios of metamorphosed magmatic Ni-Cu-(PGE) sulfide deposits to a high-grade metamorphic event (e.g., Cawthorn and Meyer, 1993; Maier and Barnes, 1996). The hypothesis is that S is mobile during metamorphism while Se is thought to be relatively immobile (e.g., Paktunc et al., 1990), leading to a dispersion and general decrease in the S/Se ratios. This process is control by the breakdown of sulfide minerals, at high temperature (> 600°C), typically during a metamorphic episode at upper amphibolite to granulite facies, where S can be released from sulfide phases. In association with mineralogical, textural and chemical observations, some studies reported extremely low S/Se ratios (< 1000) in Ni-Cu-(PGE) ores. These could be explained as the effect of high-grade metamorphism and examples are presented below.

The S/Se ratios of Cu-rich deposits of the Curaçà Valley (Brazil) and O'Kiep (South Africa) are low (< 3000: Table 1; Fig. 8A, B) and could reflect a destabilization of sulfides and S-loss (Cawthorn and Meyer, 1993; Maier and Barnes, 1996; Maier and Barnes, 1999). The main point of these deposits is that oxides, mainly magnetite, form 50 percent of the opaque phases. The sulfide assemblage consists of bornite and chalcopyrite, and the Cu/Ni is high (≤ 40). The O'Kiep deposit was metamorphosed at 750-820°C and 5-6 kbar (Raith and Harley, 1998) and the Curaçà Valley deposits reached granulite facies (Maier and Barnes, 1999). Some genetic models suggested a metamorphic oxidation (Cawthorn and Meyer, 1993; Maier and Barnes, 1996) and a replacement of the primary magmatic sulfide assemblage by desulfurization during metamorphism according to the reaction:

$$5CuFeS_2 + 5FeS + 6H_2O + 16O = Cu_5FeS_4 + 3Fe_3O_4 + 6H_2S + 5SO_2 \qquad (3)$$

The genetic model by metamorphic control is supported by the low S/Se ratios of the two deposits (Fig. 8A, B) and explains the abundance of bornite and magnetite (See discussion by Maier and Barnes, 1999 and Maier, 2000).

Some magmatic Ni-Cu-PGE sulfide occurrences associated with thick crust type mafic-ultramafic intrusions of the Grenville Province, Canada, display scattered S/Se ratios in response to high pressure granulite-facies metamorphism. Most of the samples from the Lac à Paul deposits have high S/Se ratios (8000 to 26 000: Table 1), indicating S contamination by crustal rocks (Fig. 8C). However, two samples which have undergone intense metamorphism (i.e., hornblende and/or cummingtonite form more than 60% of the rock mineralogical composition) and two samples of disseminated sulfides have lower S/Se ratios (Huss, 2002). We suggest that initially all of the rocks had high S/Se ratios as a result of crustal contamination and then, S was remobilized during high-grade metamorphism, lowering the S/Se ratios below the mantle domain.

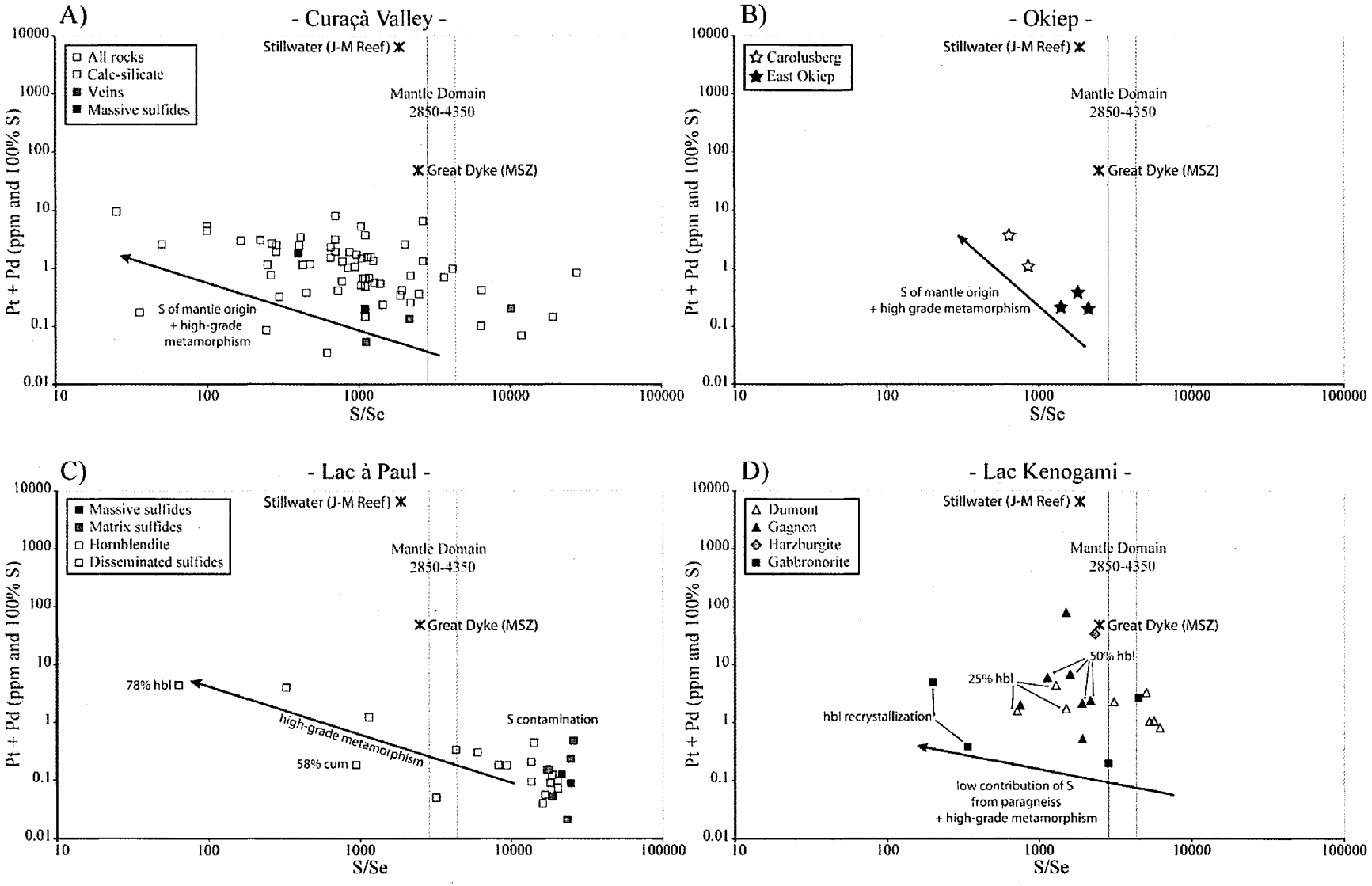

FIG. 8. Plots of Pt+Pd versus S/Se of metamorphosed magmatic Ni-Cu-(PGE) sulfide deposits. A. Curaçà Valley from Maier and Barnes (1999). B. O'Kiep from Maier (2000). C. Lac à Paul from Huss (2002). D. Lac Kenogami from Vaillancourt (2001). Mantle domain S/Se ratios are from Eckstrand and Hulbert (1987). The J-M Reef (Stillwater) and the Main Sulfide Zone (Great Dyke) are indicated as references. Abbreviations: hbl = hornblende, Cum = Cummingtonite, MSZ = Main Sulfide Zone.

S remobilization may also have occurred at the Lac Kenogami sulfide occurrences. Some samples of sulfide-bearing igneous rocks have higher S/Se ratios than the mantle domain (Fig. 8D), suggesting a S-contamination by the paragneiss country rocks. The amount of contamination at Lac Kenogami is calculated to be ~10 percent by Vaillancourt (2001). This interpretation is reinforced by the location of the sulfides at the margins of the intrusion and negative Ta anomalies (Vaillancourt, 2001). However, most of the samples of sulfide-bearing igneous rocks have S/Se ratios values near or lower than mantle values (Fig. 8D). These samples are characterized by recrystallization textures, with between 25 to 50 percent hornblende, and interstitial sulfides forming pressure shadows around porphyroclasts (Vaillancourt, 2001). These observations indicate a destabilization of sulfides during the granulite-facies metamorphism. The decrease in S/Se values of the sulfide-bearing igneous rocks after S-contamination by the country rocks suggests a S-loss sufficient to lower the S/Se ratios of the sulfide occurrences below mantle domain.

High-grade metamorphism does not necessary lead to S mobility. Some deposits affected by high-grade metamorphism show no strong evidence of S loss relative to Se. The Thompson Nickel Belt (TNB) contains several magmatic Ni-Cu-(PGE) sulfide deposits that were affected by upper-amphibolite facies metamorphism (e.g., Layton-Matthews et al., 2007) but Bleeker (1990) reported no decoupling between S and Se. The Ni-Cu-(PGE) sulfide deposits of the Tati and the Selebi-Phikwe belts have undergone variable degrees of metamorphism (lower amphibolite and granulite, Maier et al., 2008) but the interpretation of S/Se ratios remain difficult.

Low temperature alteration

In oxidizing environments and during low temperature alterations (< 300°C), S and Se have a different geochemical behavior that changes the S/Se ratio of sulfide-bearing igneous rocks. Sulfur is characterized by higher mobility compared to Se (Howard, 1977) and it is remobilized as an oxidized species (SO_2 or SO_3 : Dreibus et al., 1995) associated with a hydrous phase (Yamamoto, 1976). Selenium is much less mobile and remains adsorbed onto hydrous iron oxides as solid compound such as metallic Se (McGoldrick and Keays, 1981) or SeO_2 (Dreibus et al., 1995). This fractionation could generate variations in the S/Se ratios of sulfide-bearing rocks.

The serpentinization of the rocks, produced by the circulation of the seawater in the crust, is one of the mechanisms that could occur at low temperature. The ultramafic cumulates of the Heazlewood River Complex (Tasmania) contains low S concentrations (< 100 ppm) formed by a S-undersaturated magma (Peck and Keays, 1990) derived from a depleted mantle (Hamlyn and Keays, 1986). These rocks were strongly serpentinized and most of the S/Se ratios are located outside the field of igneous rocks (Fig. 10A), demonstrating the greater mobility of S relative to Se during low temperature alterations. The serpentinization is marked mainly by S loss, associated with the replacement of base metals sulfides by alloys. However, some authors interpret the presence of heazlewoodite in faults to be due to the addition of S by serpentinizing fluids (Eckstrand, 1975; Peck and Keays, 1990).

Some ultramafic rocks of the layered intrusions forming the Munni Munni Complex (Australia) are characterized by low S/Se ratios, below the mantle field, indicating a removal of S during serpentinization. The unaltered samples have S/Se ratios typical of magmatic sulfides (geomean of 4857, Table 1, Fig. 10B) but the S/Se ratios of serpentinized samples (geomean of 1969, Table 1, Fig. 10B) show S loss which can reach 85-90 percent (Hoatson and Keays, 1989).

In some cases, the impact of serpentinization on the variation in S/Se ratios could be overprinted by other contemporaneous processes such as the S contamination. The altered dunites from the Mount Keith-Betheno area (Australia) were strongly serpentinized, but their S/Se ratios remain high (> 20 000: Table 1, Fig. 10C). High S/Se ratios could indicate a contamination by S of crustal origin derived from sulfide-rich metasedimentary country rocks (S/Se = 38 000). Groves and Keays (1979) argued that this external S combined with Fe released during the progressive serpentinization to produce newly formed sulfides (pyrrhotite-valleriite-heazlewoodite) and the replacement of pre-existing magmatic sulfides (e.g., pentlandite). The S loss expected to occur during the serpentinization on the S/Se ratio is obscured by the crustal S addition.

Supergene weathering is another low temperature mechanism. The S/Se ratio is commonly used to monitor the effect of weathering (e.g., Peck et al., 2001; Ripley, 2002; Lorand et al., 2003) and to provide help in determining if the S content of the rock is representative of its initial composition. For example, in country rocks outcropping at the Voisey's Bay deposit, the weathering remobilized the S, leading to depletion (Table 1), while Se is immobile and its concentration remains unchanged (Ripley, 2002). As a result, the S/Se ratios of surface rocks are much lower than the rocks from boreholes.

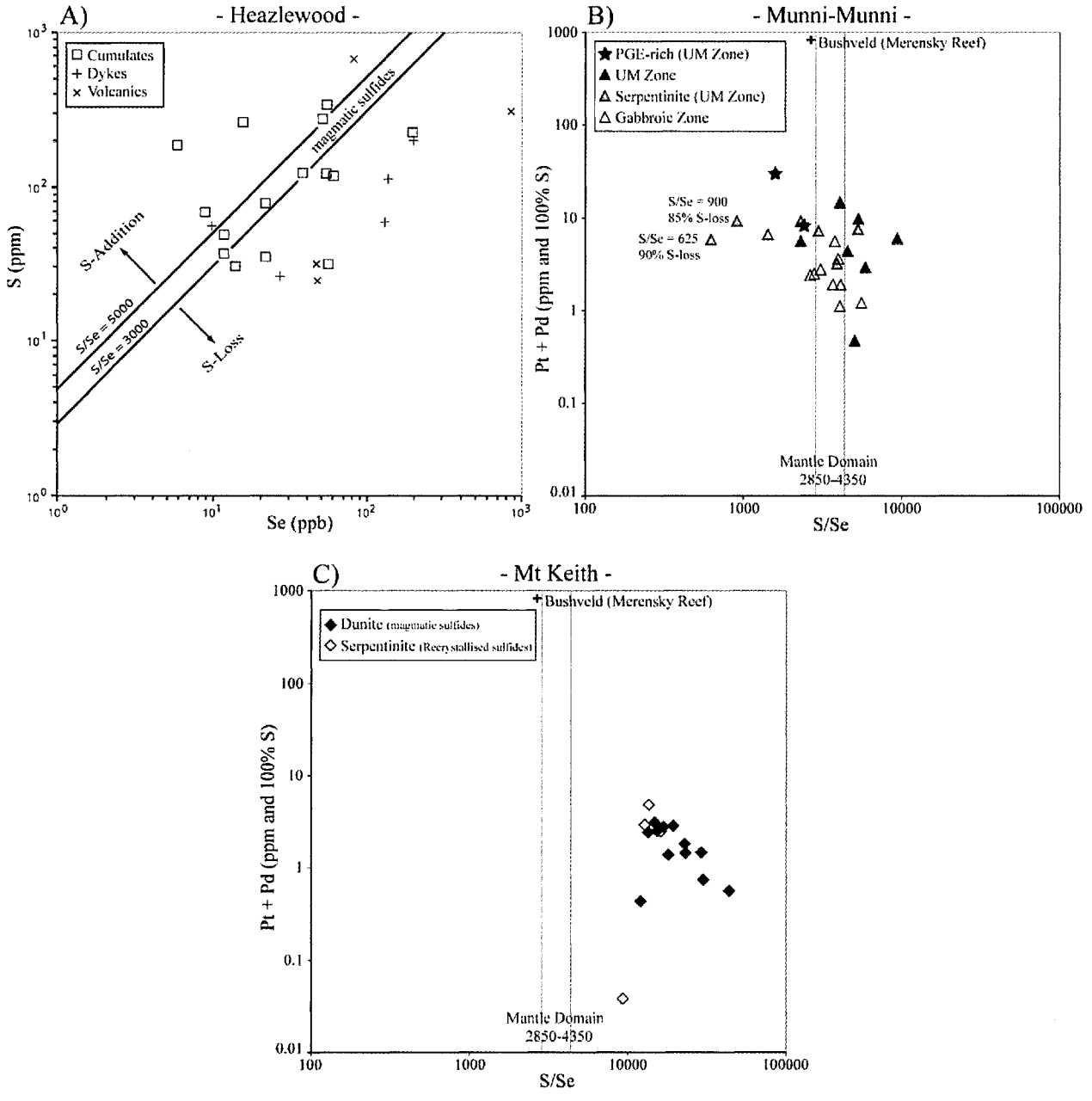

FIG. 10. Ni-Cu-(PGE) deposits showing evidence of S-mobility relative to Se during serpentinization. A. Plots of S versus Se of Heazlewood River Complex from Peck and Keays (1990). B. Pt+Pd (100% S) vs S/Se of Munni Munni Complex from Groves and Keays (1979). C. Pt+Pd (100% S) vs S/Se of Mt Keith from Hoatson and Keays (1989). The Merensky Reef (Bushveld Complex) is indicated as reference.

Discussion

The domains of the S/Se ratio

A schematic plot of Pt+Pd in 100 percent sulfides versus S/Se of magmatic Ni-Cu-PGE sulfide deposits may be divided into different fields based on a number of factors: the type of deposits, the origin of S and the processes which influence the S/Se ratio (Fig. 11). In general, the Ni-Cu deposits have high to very high S/Se ratios, low Pt+Pd contents, due to their moderate to low R-factors and crustally derived S. This is true for most of the komatiitic and picritic deposits and some thick crust mafic-ultramafic intrusions (e.g., Lac à Paul, Lac Volant). The Fe-rich massive sulfides (MSS cumulates) are also found within this range. Some mining camp display a wide range in the S/Se ratios values (2850 to 10 000), such as the meteoritic impact of Sudbury, the Ni-sulfide deposits of Pechenga and Cape Smith Belt and the Ni-Cu ores of the Duluth Complex, indicating in most cases that the S saturation is triggered by the mixing between the S of mantle origin and the S from an external source (Fig. 11B). The PGE-deposits and the PGE-rich layers of Ni-Cu deposit class have low S/Se ratios (Fig. 11A) and high Pt+Pd contents as a result of high R-factors (Fig. 11C). The S/Se ratios and the $\delta^{34}S$ values close to the mantle values (Figs. 2 and 3; Table 1) combined with the low S concentration, indicate that little crustal S contamination occurred and that the S in the reefs is largely of mantle origin (Fig. 11B). Therefore, the initiation of the S-saturation is not triggered by an addition of S and other mechanisms must be considered (e.g., Li and Ripley, 2005). The variations of the S/Se ratios values of the PGE-deposits at the local scale are link to the initial enrichment of the magma and/or to subsequent processes of the S-saturation. Due to the process of the Se fractionation, the S/Se ratios of Cu-rich ISS phases are found in the same range of values (Fig. 11C).

All the processes identified have a significant influence on the S and Se contents, and consequently on the S/Se ratios, of the magmatic Ni-Cu-PGE sulfide deposits. These processes can be divided in two main classes: 1) The magmatic processes which include the increase in S in the magma due to contamination of the magma by crustally derived S, variations in the degree of interaction between the sulfide melt and the silicate melt (R-factor), the concentration of Se into the fractionated Cu-rich sulfide liquid due to MSS crystallization and the lowering of Se concentrations in the silicate melt due to sulfide segregation resulting in subsequent sulfides being depleted in Se. 2) The late- to post-magmatic processes which include high-grade metamorphism, hydrothermalism, serpentinization and supergene weathering. However, the impact of each process on the S/Se ratios is not equal. For most of the deposits, the origin of S controls largely the S/Se ratios. The fractionation of Se between MSS and the Cu-rich sulfide liquid can result in a wide variation in S/Se ratios in the massive and matrix ores. To date, the influence of the segregation of the sulfide liquid on the S/Se ratios has been identified only in the Bushveld Complex. High-grade metamorphism affects only a limited number of deposits and the impact of this process on the S/Se ratios remains controversial. The late- to post-magmatic processes modify the S/Se ratio moderately, which remain close to the range of values generated during the magmatic processes.

During its history, a rock may be subjected to most of these processes resulting in strong variations in S/Se ratios. Based on some examples studied during this work, several paths of this dynamic evolution of the S/Se ratio are presented (Fig. 11D). A negative impact of these combinations of processes is the possible overprinting of the original source of the S that led to the saturation of the mafic magma. For example, it is possible to interpret a low S/Se ratio as an indication of mantle-derived S. But in the example of Lac à Paul and Lac Kenogami sulfide occurences (Fig. 8C, D), the parental magma underwent S contamination marked by an increase

in the S/Se ratio, then some post-magmatic processes (e.g., high-grade metamorphism) generated S loss, lowering the S/Se ratio and bringing it in the field of S/Se ratios for mantle origin. Consequently, an interpretation of S origin based exclusively on the final S/Se ratios is not reliable if the evolution of the rocks is not considered.

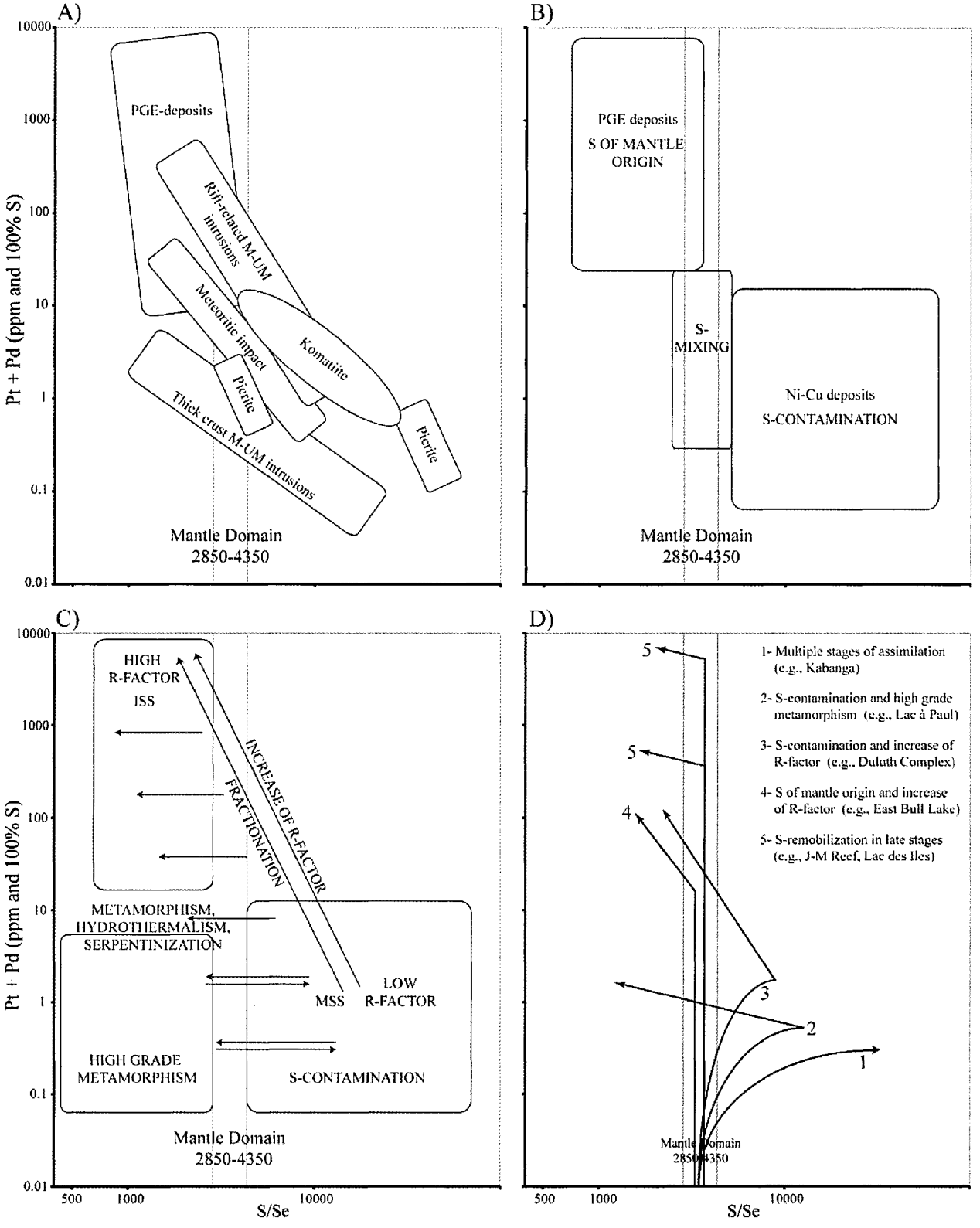

FIG. 11. Schematic plots of Pt+Pd (100% S) versus S/Se showing the distribution of Ni-Cu-PGE deposits (A), the origin of S (B), the domains of each processes (C) and some examples of different paths of the evolution of the S/Se ratio (D).

Model of the evolution of the S/Se ratio

The evolution of the S/Se ratio can be modeled from the partial melting of the mantle to the emplacement of the magma in the crust, to crystallization and enrichment processes and finally to the late- to post-magmatic processes.

1) In the mantle, the abundance of Se is controlled by the base metal sulfides (Fig. 12A), which represent less than 0.1 weight percent of the mantle (Fig. 12A). Due to the slight incompatibly of Se with the MSS, Se is more enriched in the Cu-rich phases (e.g., Lorand et al., 2001).

2) A high degree of partial melting is required (> 25%: Barnes et al., 1985) to consume all the mantle sulfides and generate the formation of a magmatic melt enriched in chalcophile elements and PGE (Fig. 12B). Like S, Se is incorporated into the magmatic melt (Fig. 12B). Although some studies suggest that the S/Se ratio of a mantle-derived magma may vary depending on the mantle source (e.g., Hattori et al., 2002; Lorand et al., 2010), the S/Se ratio of the melt formed during the partial melting will reflect the S/Se ratio of the mantle and, in most cases, can be estimated to be between 2850 and 4350 (Eckstrand and Hulbert, 1987).

3) The emplaced magma must attain S saturation in order to generate an immiscible sulfide liquid which can then collect the chalcophile elements, including Se, and the PGE. If contamination by S-rich country rocks occurs, the addition of crustal S triggered the S saturation in the magma and the S/Se ratio is increased significantly (Fig. 12C). In contrast, if the S saturation is not triggered by the addition of S, such as in the case of the PGE-deposits, other mechanisms leading to the saturation should be considered and the S/Se ratio remains close to the primary mantle values (Fig. 12D).

4) The R-factor also affects the amount of Se incorporated into the sulfide liquid, and thus the S/Se ratios (Fig. 12E). At high R-factors, Se can attain a maximum enrichment equivalent to the partition coefficient of Se between silicate and sulfide liquid resulting in low S/Se ratio values

(e.g., PGE-deposits: Table 1, 2; Figs. 2,5, 11), while at low R-factors, Se- and PGE-enrichment of the sulfide liquid is reduced resulting in the formation of Ni-Cu deposits with high S/Se ratio values (Table 1, 2; Figs. 2, 5, 11).

5) An extraction of the sulfide liquid during the differentiation can produce some strong variations in the S/Se ratio values (Barnes et al., 2009). In the case of the Bushveld Complex, due to the extraction of the sulfide liquid during the formation of the sub-Zone A, the magma that formed the sub-Zones B and C is Se-depleted and the S/Se ratio is higher (Fig. 12F).

6) During the crystallization of MSS from a sulfide liquid, Se is moderately incompatible resulting in enrichment in the residual Cu-rich liquid which will form the ISS (Fig. 12G). Consequently, the S/Se ratios of the Cu-rich ISS phases are lower than those of the associated Fe-rich MSS phases. Pt and Pd are also incompatible with the MSS and the residual sulfide liquid forming the ISS have higher Pt+Pd values associated with low S/Se ratio values.

7) During alteration (< 300°C), S may be remobilized by oxidized hydrous fluids as SO_2 or SO_3 species, while Se remains relatively immobile. Consequently, hydrothermalism, high-grade metamorphism, serpentinization and supergene weathering lead to the preferential redistribution of S relative to Se (Fig. 12H, I, J); in most cases, this generates a decrease in the S/Se ratios of the sulfide-bearing igneous rocks.

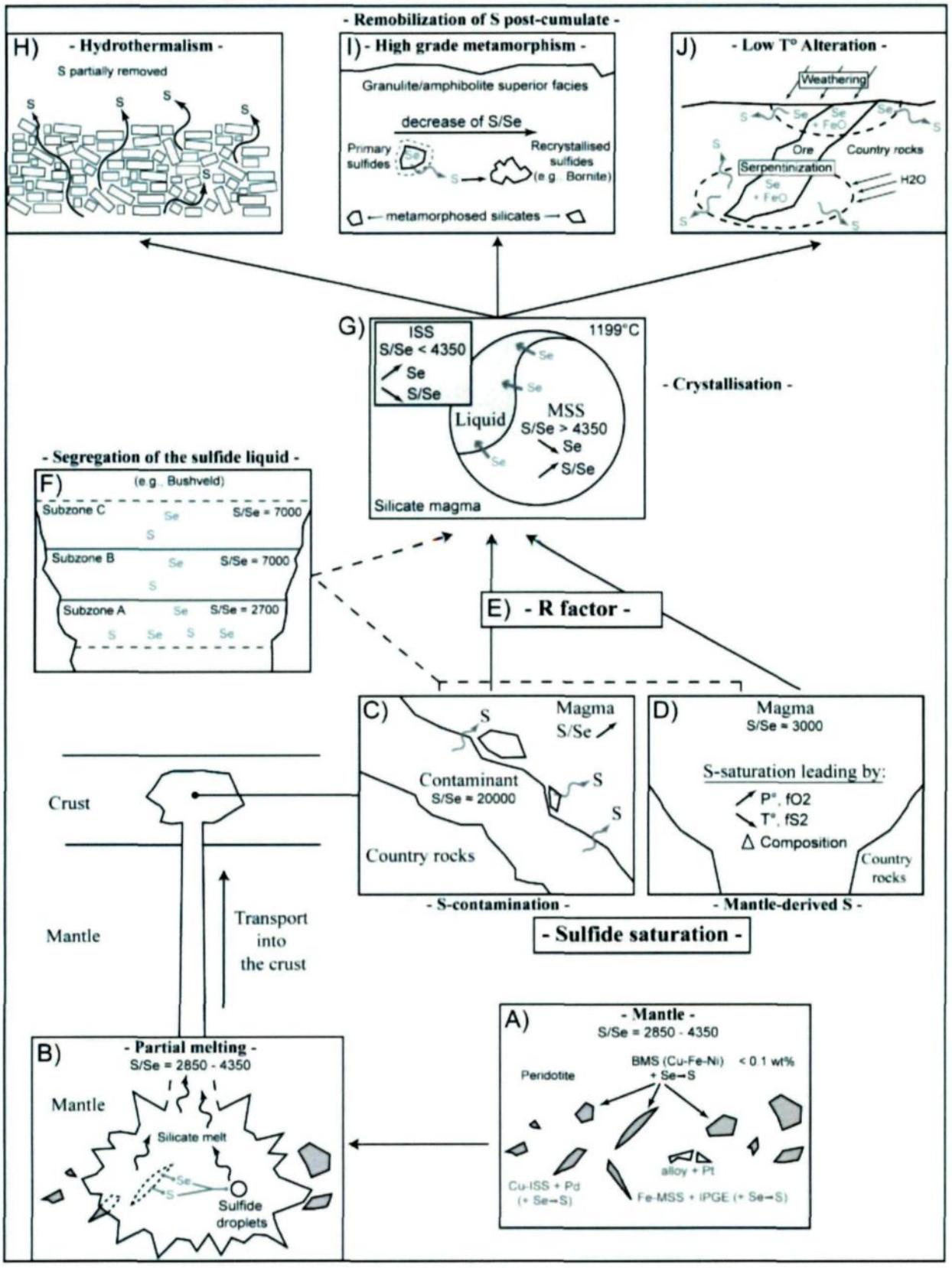

FIG. 12. Synthetical model of the evolution of the S/Se ratio. Please refer to text for further description of each step.

Conclusion

The S/Se ratio is a powerful tool in the characterization of petrogenetic processes involved in the formation of magmatic Ni-Cu-PGE sulfide deposits. This compilation allows the establishment of different domains for Ni-Cu-PGE deposits, based on: the deposit types, the origin of S and subsequent processes. The association between S/Se ratio and sulfur isotope ($\delta^{34}S$) is necessary to determine the origin of S of the ore. However, the S/Se ratio alone can provide insight into a complex evolution of magmatic processes followed by late- to post-magmatic processes that form Ni-Cu-PGE deposits.

Some precautions must be taken before using the S/Se ratio. Firstly, sample selection for the S and Se analyses has a direct influence on S/Se ratio values obtained. The degree of metamorphism, the presence of alteration or the fractionation of the Se between MSS and ISS can all modify the S/Se ratio at the scale of individual samples. Consequently, identification of processes undergone by each sample is essential before an interpretation of the S/Se ratio.

Secondly, it is necessary to combine the analysis of S and Se in both mineralized rocks and the host crustal rocks, in order to consider whether the S was derived *in situ*. The S/Se ratios of the mineralized rocks of magmatic Ni-Cu-PGE sulfide deposits taken alone do not indicate magma contamination sufficiently if they are not compared with the S/Se ratios of potential contaminants. Unfortunately, this combination of data is rarely found in the literature and the future work should integrate the S/Se ratio of the country rocks.

Finally, the method of Se-determination in rock samples should have an adequate accuracy, especially for rocks with low Se concentrations, typical for a number of Ni-Cu-PGE deposit host rocks. Analytical values of S and Se are numerous in the literature but of variable quality, especially for Se. Despite the utility of the S/Se ratio, the geochemical behavior of Se is

relatively unknown due to its very low concentration in crustal rocks. The determination of Se is difficult and some analytical techniques used in the past have been limited by poor precision. Therefore, low quality Se data will affect the S/Se ratio and distort any following interpretations and conclusions. Consequently, an accurate Se determination is required.

Acknowledgments

Dany Savard and Dr. Paul Bédard are thanked for their support with the INAA analyses and the sulfur determinations of the Voisey's Bay samples. Dr. Sarah Dare is thanked for providing the Creighton and McCreedy analyses. The helpful comments by Dr. Philippe Pagé are appreciated. This publication is part on a M.Sc. thesis funded by the Canadian Research Chair in Magmatic Metallogeny and the Natural Sciences and Engineering Research Council of Canada.

REFERENCES

Amelin, Y., Li, C., Valayev, O., and Naldrett, A.J., 2000, Nd-Pb-Sr isotope systematics of crustal assimilation in the Voisey's Bay and Mushuau intrusions, Labrador, Canada: Economic Geology, v. 95, p. 815–830.

Andrews, M.S., and Ripley E.M., 1989, Mass transfer and sulfur fixation in the contact aureole of the Duluth Complex, Dunka Road Cu–Ni deposit, Minnesota: Canadian Mineralogist, v. 27, p. 293–310.

Arndt, N.T., Lesher, C.M., and Czamanske, G.K., 2005, Mantle-derived magmas and magmatic Ni-Cu-(PGE) deposits: Economic Geology 100th Anniversary Volume, p. 5–23.

Barnes, S.-J., and Gomwe, T.S., 2011, The Pd-deposits of the Lac des Iles Complex, north-western Ontario: Reviews in Economic Geology, v. 17, p. 351–370.

Barnes, S.-J., and Lightfoot, P.C., 2005, Formation of magmatic nickel-sulfide ore deposits and processes affecting their copper and platinum-group element contents, *in* Hedenquist, J.W., Thompson, J.F.H., Goldfarb, R.J., and Richards, J.P., ed., Economic Geology 100th Anniversary Volume, p. 179–213.

Barnes, S.-J., and Maier, W.D., 2002, Platinum-group elements and microstructures of normal Merensky Reef from Impala platinum mines, Bushveld Complex: Journal of Petrology, v. 43, p.

103–128.

Barnes, S.-J., and Picard, C.P., 1993, The behaviour of platinum-group elements during partial melting, crystal fractionation, and sulphide segregation: An example from the Cape Smith Fold Belt, northern Québec: Geochimica et Cosmochimica Acta, v. 57, p. 79–87.

Barnes, S.-J., Naldrett, A.J., and Gorton, M.P., 1985, The origin of the fractionation of the platinum group elements in terrestrial magmas: Chemical Geology, v. 53, p. 303–323.

Barnes, S.-J., Picard, C., Giovennazzo, D., and Tremblay, C., 1992, The composition of nickel-copper sulphide deposits and their host rocks from the Cape Smith Fold Belt, Northern Quebec: Australian Journal of Earth Sciences, v. 39, p. 335–347.

Barnes, S.-J., Makovicky, E., Makovicky, M., Rose-Hansen, J., and Karup-Moller, S., 1997a, Partition coefficients for Ni, Cu, Pd, Pt, Rh, and Ir between monosulphide solid solution and sulphide liquid and the formation of compositionally zoned Ni-Cu sulphide bodies by fractional crystallization of sulphide liquid: Canadian Journal of Earth Sciences, v. 34, p. 366–374.

Barnes, S.-J., Zientek, M.L., and Severson, M.J., 1997b, Ni, Cu, Au, and platinum-group element contents of sulphides associated with intraplate magmatism: a synthesis: Canadian Journal of Earth Sciences, v. 34, p. 337–351.

Barnes, S.-J., Melezhick, V.A., and Sokolov, S.V., 2001, The composition and mode of formation of the Pechenga Nickel deposits, Kola Peninsula, Northwestern Russia: Canadian Mineralogist, v. 39, p. 447–471.

Barnes, S.-J., Prichard, H.M., Cox, R.A., Fisher, P.C., and Godel, B., 2008, The location of the chalcophile and siderophile elements in platinum-group element ore deposits (a textural, microbeam and whole rock geochemical study): Implications for the formation of the deposits: Chemical Geology, v. 248, p. 295–317.

Barnes, S.-J., Savard, D., Bédard, P., and Maier, W.D., 2009, Selenium and sulfur concentrations in the Bushveld Complex of South Africa and implications for formation of the platinum-group element deposits: Mineralium Deposita, v. 44, p. 647–663.

Bédard, L.P., Savard, D., and Barnes, S.-J., 2008, Total sulfur concentration in geological reference materials by elemental infrared analyzer: Journal of Geostandards and Geoanalytical Research, v. 32, p. 203–208.

Bleeker, W., 1990, Evolution of the Thompson Nickel Belt and its nickel deposits, Manitoba, Canada: Unpublished Ph.D. thesis, University of New Brunswick, Fredericton, 444 p.

Boer, R.H., Meyer, F.M., and Cawthorn, R.G., 1994, Stable isotopic evidence for crustal contamination and desulfidation of the cupriferous Koperberg Suite, Namaqualand, South Africa: Geochimica et Cosmochimica Acta, v. 58, p. 2677–2687.

Bouchaïb, C., 1992, Distribution du Cu, Ni, Co, ÉGP, Au et Ag dans les sulfures de la Mine Lorraine: Unpublished M.Sc. thesis, Université du Québec à Chicoutimi, 90 p.

Buchanan, D.L., Nolan, J., Suddaby, P., Rouse, J.E., Viljoen, M.J., and Davenport, J.W.J., 1981, The genesis of sulfide mineralization in a portion of the Potgietersrus limb of the Bushveld Complex: Economic Geology, v. 76, p. 568–579.

Campbell, I.H., and Barnes, S.J., 1984, A model for the geochemistry of the platinum group elements in magmatic sulphide deposits: Canadian Mineralogist, v. 22, p. 151–160.

Campbell, I.H., and Naldrett, A.J., 1979, The influence of silicate:sulfide ratios on the geochemistry of magmatic sulfides: Economic Geology, v. 74, p. 1503–1505.

Campbell, I.H., Naldrett, A.J., and Barnes, S.J., 1983, A model for the origin of the platinum-rich sulfide horizons in the Bushveld and Stillwater Complexes: Journal of Petrology, v. 24, p. 133–165.

Card, K.D., 1978, Metamorphism in the Middle Precambrian (Aphebian) rocks of the Southern province: Geological Survey of Canada Paper 78-10, p. 269–282.

Casquet, C., Eguiluz, L., Galindo, C., Tornos, F., and Velasco, F., 1998, The Aguablanca Cu-Ni-(PGE) intraplutonic ore deposit (Extremadura, Spain). Isotope (Sr, Nd, S) constraints on the source and evolution of magmas and sulphides: Geogaceta,v. 24, p. 71–72.

Cawthorn, R.G., and Meyer, F.M., 1993, Petrochemistry of the Okiep copper district basic intrusive bodies, northwestern Cape province, South Africa: Economic Geology, v. 88, p. 590–605.

Chai, G., and Naldrett, A.J., 1992, Characteristics of Ni-Cu-PGE mineralization and genesis of the Jinchuan deposit, northwest China: Economic Geology, v. 87, p. 1475–1495.

Chubb, P.T., 1994, Petrogenesis of the eastern portion of the East Bull Lake gabbro-anorthosite intrusion, District of Sudbury/Algoma, Ontario: Unpublished M.Sc. thesis, Sudbury, Ontario, Laurentian University, 230 p.

Cowden, A., Donaldson, M.J., Naldrett, A.J., and Campbell, I.H., 1986, Platinum-group elements and gold in the komatiite-hosted Fe-Ni-Cu sulfide deposits at Kambalda, Western Australia: Economic Geology, v. 81, p. 1226–1235.

Czamanske, G.K., Kunilov, V.E., Zientek, M.L., Cabri, L.J., Likhachev, A.P., Calk, L.C., and Oscarson, R.L., 1992, A proton-microprobe study of magmatic sulfides ores from the Noril'sk-Talnakh District, Siberia: Canadian Mineralogist, v. 30, p. 249–287.

Czamanske, G.K, Wooden, J.L., Zientek, M.L., Fedorenko, V.A., Zen'ko, T.E., Kent, J., King, B-S.W., Knight, R.J., and Siems, D.F., 1994, Geochemical and isotopic constraints on the petrogenesis of the Noril'sk Talnakh ore-forming system: Ontario Geological Survey Special Publication 5, p. 313–342.

Czamanske, G.K., Zen'ko, T.E., Fedorenko, V.A., Calk, L.C., Budahn, J.R., Bullock, J.H., Jr., Fries, T.L., King, B-S.W., and Siems, D.F., 1995, Petrographic and geochemical characterization of ore-bearing intrusions of the Noril'sk type, Siberia: With discussion of their origin: Resource Geology Special Issue 18, p. 1–48.

Dare, S.A.S., Barnes, S.-J., Prichard, H., and Fisher, P.C., 2010, The timing and formation of platinum-group minerals from the Creighton Ni-Cu-Platinum-Group Element sulfide deposit, Sudbury, Canada: early crystallization of PGE-rich sulfarsenides: Economic Geology, v. 105, p. 1071–1096.

Dare, S.A.S., Barnes, S.-J., Prichard, H., and Fisher, P.C., 2011, Chalcophile and platinum-group element (PGE) concentrations in the sulfide minerals from the McCreedy East deposit, Sudbury, Canada, and the origin of PGE in pyrite: Mineralium Deposita, v. 46, p. 381–407.

Dillon-Leitch, H.C.H., Watkinson, D.H., and Coats, C.J.A., 1986, Distribution of platinum-group elements in the Donaldson West deposit, Cape Smith Belt, Québec: Economic Geology, v. 81, p. 1147–1158.

Dionne-Foster, C., 2007, Géologie et indices de Ni-Cu-EGP de la zone Frontier dans la ceinture de Cape Smith, Nouveau Québec: Unpublished M.Sc. thesis, Université du Québec à Chicoutimi, 342 p.

Djon, M.L.N., 2010, Changement de la minéralogie des sulfures, des minéraux du groupe du platine et des textures avec le degree d'altération des zones Roby, Twilight et High-Grade du Complex du Lac-Des-Iles (Ontario, Canada): Unpublished M.Sc. thesis, Université du Québec à Chicoutimi, 95 p.

Donnelly, T.H., Lambert, I.B., Oehler, D.Z., Hallberg, J.A., Hudson, D.R., Smith, J.W., Bavinton, O.A., and Golding, L.Y., 1978, A reconnaissance study of stable isotope ratios in Archaean rocks from the Yilgarn Block, Western Australia. Journal of the Geological Society of Australia, v. 24, p. 409-420.

Dreibus, G., Palme, H., Spettel, B., Zipfel, J., and Wänke, H., 1995, Sulphur and selenium in chondritic meteorites: Meteoritics, v. 30, p. 439–445.

Duke, J.M., 1990, Mineral deposit models: Nickel sulfide deposit of the Kambalda type: Canadian Mineralogist, v. 28, p. 379–388.

Eckstrand, O.R., 1975, The Dumont serpentinite: a model for control of nickeliferous opaque assemblages by alteration reactions in ultramafic rocks: Economic Geology, v. 70, p. 183–201.

Eckstrand, O.R., and Cogolu, E., 1986, Se/S evidence relating to genesis of sulphides in the Crystal Lake gabbro, Thunder Bay, Ontario [abs.]: Geological Association Canada–Mineralogical Association Canada Program with Abstracts, v. 11, p. 66.

Eckstrand, O.R., and Hulbert, L.J., 1987, Selenium and the source of sulfur in magmatic nickel and platinum deposits [abs.]: Geological Association of Canada–Mineralogical Association Canada Program with Abstracts, v. 12, p. 40.

Eckstrand, O.R., and Hulbert, L.J., 2007, Magmatic nickel-copper-platinum group element deposits, *in* Goodfellow, W.D., ed., Mineral deposits of Canada: a synthesis of major deposit types, district metallogeny, the evolution of geological provinces, and exploration methods: Geological Association of Canada, Mineral Deposits Division, Special Publication No. 5, p. 205–222.

Eckstrand, O.R., Grinenko, L.N., Krouse, H.R., Paktunc, A.D., Schwann. P.L., and Scoates, R.F., 1989, Preliminary data on sulphur isotopes and Se/S ratios, and the source of sulphur in magmatic sulphur in magmatic sulphides from the Fox River Sill, Molson Dykes and Thompson nickel deposits, northern Manitoba. In: Current Research, Part C. Geological Survey of Canada 89–1C, p. 235–242.

Fedorenko, V.A., 1994, Evolution of magmatism as reflected in the volcanic sequence of the Noril'sk region: Ontario Geological Survey Special Publication 5, p. 171–184.

Giovenazzo, D., 1991, Geologie et caracteristiques geochimique des mineralisations Ni-Cu-EGP de la region de Delta, Ceinture de Cape-Smith, Nouveau Quebec: Unpublished M.Sc. thesis, Université du Québec à Chicoutimi, 257 p.

Godel, B., and Barnes, S.-J., 2008, Platinum-group elements in sulfide minerals and the whole rocks of the J-M Reef (Stillwater Complex): implication for the formation of the reef: Chemical Geology, v. 248, p. 272–294.

Godel, B., Barnes, S.-J., and Maier, W.D., 2007, Platinum-group elements in sulphide minerals, platinum-group minerals, and the whole rocks of the Merensky Reef (Bushveld Complex, South Africa): Implication for the formation of the Reef: Journal of Petrology, v. 48, p. 1569–1604.

Gorbachev, N.S., and Grinenko, L.N., 1973, The sulfur-isotope ratios of the sulfides and sulfates of the Oktyabr'sky sulfide deposit, Noril'sk region, and the problem of its origin: Geokhimiya, v. 8, p. 1127–1136.

Groves, D.I., and Keays, R.R., 1979, Mobilization of ore-forming elements during alteration of dunites, Mt. Keith-Betheno, Western Australia: Canadian Mineralogist, v. 17, p. 373–389.

Groves, D.I., Barrett, F.M., and McQueen, K.G., 1979, The relative roles of magmatic segregation, volcanic exhalation and regional metamorphism in the generation of volcanic-associated nickel ores of Western Australia: Canadian Mineralogist, v. 17, p. 319-336.

Green, A.H., and Naldrett, A.J., 1981, The Langmuir volcanic peridotite-associated nickel deposits; Canadian equivalents of the Western Australian occurences: Economic Geology, v. 76, p. 1503–1523.

Grinenko, L.I., 1985, Sources of sulfur of the nickeliferous and barren gabbro-dolerite intrusions of the northwestern Siberian platform: International Geology Review, v. 27, p. 695–708.

Habicht, K. and Canfield, D.E., 1997, Sulfur isotope fractionation during bacterial sulfate reduction in organic-rich sediments: Geochimica et Cosmochimica Acta, v. 61, p. 5351–5361.

Hamlyn, P.R., and Keays, 1986, Sulfur-saturation and second-stage melts: application to the Bushveld platinum metal deposits: Economic Geology, v. 81, p. 1431–1445.

Hattori, K.H., Arai, S., and Clarke, D.B., 2002, Selenium, tellurium, arsenic and antimony contents of primary mantle sulfides: Canadian Mineralogist, v. 40, p. 637–650.

Helmy, H.M., Ballhaus, C., Wohlgemuth-Ueberwasser, C., Fonseca, R.O.C., and Laurenz, V., 2010, Partitioning of Se, As, Sb, Te and Bi between monosulfide solid solution and sulfide melt–application to magmatic sulfide deposits: Geochimica et Cosmochimica Acta, v. 74, p. 6174–6179.

Hinchey, J.G., and Hattori, K.H., 2005, Magmatic mineralization and hydrothermal enrichment of the High Grade Zone at the Lac des Iles palladium mine, northern Ontario, Canada : Mineralium Deposita, v. 40, p. 13–23.

Hoatson, D.M., and Keays, R.R., 1989, Formation of Platiniferous sulfide horizons by crystal fractionation and magma mixing in the Munni Munni layered intrusion, West Pilbara Block, Western Australia: Economic Geology, v. 84, p. 1775–1804.

Howard, J.H., 1977, Geochemistry of selenium: formation of ferroselite and selenium behavior in the vicinity of oxidizing sulfide and uranium deposits: Geochimica et Cosmochimica Acta, v. 41, p.1665–1678.

Huss, L., 2002, Caractérisation de la mineralisation en Ni-Cu-EGP des indices de la region du Lac à Paul, suite anorthositique du Lac St-Jean: Unpublished M.Sc. thesis, Université du Québec à Chicoutimi, 232 p.

Keays, R.R., and Lightfoot, P.C., 2004, Formation of Ni-Cu-Platinum Group Element sulfide mineralization in the Sudbury impact Melt Sheet: Mineralogy and Petrology, v. 82, p. 217–258.

Lambert, D.D., Foster, J.G., Frick, L.R., Li, C., and Naldrett, A.J., 1999, Re-Os isotopic systematics of the Voisey's Bay Ni-Cu-Co magmatic ore system, Labrador, Canada: Lithos, v. 47, p. 67–88.

Lambert, I.B., Donnelly, T.H., Dunlop, J.S.W., and Groves, D.I., 1979, Stable isotope studies of early Archean sulphate deposits of probable evaporitic and volcanogenic origins: Nature, v. 276, p. 808–811.

Lavigne, M.J., and Michaud, M.J., 2001, Geology of North American Palladium Ltd.'s Roby Zone Deposit, Lac des Iles: Exploration and Mining Geology, v. 10, p. 1–17.

Layton-Matthews, D., Lesher, C.M., Burnham, O.M., Liwanag, J., Halden, N.M., Hulbert, L., and Peck, D.C., 2007, Magmatic Ni-Cu-platinum-group element deposits of the Thompson Nickel Belt, *in* Goodfellow W.D., ed., Mineral Deposits of Canada: A synthesis of major deposit-types, district metallogeny, the evolution of geological provinces, and exploration methods: Geological Association of Canada, Mineral Deposits Division, Special Publication, v. 5, p. 409–432.

Lesher, C.M., and Burnham, O.M., 2001, Multicomponent elemental and isotopic mixing in Ni-Cu-(PGE) ores at Kambalda, Western Australia: Canadian Mineralogist, v. 39, p. 421–446.

Lesher, C.M., and Campbell, I.H., 1993, Geochemical and fluid dynamic modelling of compositional variations in Archean komatiite-hosted nickel sulfide ores in Western Australia: Economic Geology, v. 88, p. 804–816.

Lesher, C.M., and Keays, R.R., 1984, Metamorphically and hydrothermally mobilized Fe-Ni-Cu sulphides at Kambalda, Western Australia, *in* Buchanan D.L., and Jones, M.J., ed., Sulphide deposits in mafic and ultramafic rocks: Institution of Mining and Metallurgy, p. 62-69.

Lesher, C.M., and Keays, R.R., 2002, Komatiite-associated Ni-Cu-(PGE) deposits:Geology, mineralogy, geochemistry and genesis: Canadian Institute of Mining, Metallurgy and Petroleum Special Volume 54, p. 579–618.

Lesher, C.M., Barnes, S.-J., Gillies, S.L., and Ripley, E.M., 1999, Ni-Cu-(PGE) sulphides in the Raglan Block, *in* Lesher, C.M., Komatiitic peridotite-hosted Fe-Ni-Cu-(PGE) sulphide deposits in the Raglan area, Cape Smith Belt, New Québec: Guidebook Series, 2, Mineral Exploration Research Centre, Laurentian University, p. 177-184.

Lesher, C.M., Burnham, O.M., Keays, R.R., Barnes, S.J., and Hulbert, L., 2001, Geochemical discrimination of barren and mineralized komatiites associated with magmatic Ni-Cu-(PGE) sulfide deposits: Canadian Mineralogist, v. 39, p. 673–696.

Li, C., and Naldrett, A.J., 2000, Melting reactions of gneissic inclusions with enclosing magma at Voisey's Bay: Implications with respect to ore genesis: Economic Geology, v. 95, p. 801–814.

Li, C., and Ripley, E.M., 2005, Empirical equations to predict the sulfur content of mafic magmas at sulfide saturation and applications to magmatic sulfide deposits: Mineralium Deposita, v. 40, p. 218–230.

Li, C., Lightfoot, P.C., Amelin, Y., and Naldrett, A.J., 2000, Contrasting petrological and geochemical relationships in the Voisey's Bay and Mushuau intrusions, Labrador, Canada: Implications for ore genesis: Economic Geology, v. 95, p. 771–799.

Li, C., Ripley, E.M., and Naldrett, A.J., 2003, Compositional variations of olivine and sulfur isotopes in the Noril'sk and Talnakh intrusions, Siberia: Implications for ore-forming processes in dynamic magmaconduits: Economic Geology, v. 98, p. 69–86.

Lightfoot, P.C., Naldrett, A.J., Gorbachev, N.S., Fedorenko, V.A., Hawkesworth, C.J., Hergt, J., and Doherty, W., 1994, Chemostratigraphy of Siberian trap lavas, Noril'sk district, Russia: Implications for the source of flood basalt magmas and their associated Ni-Cu mineralization: Ontario Geological Survey, Sudbury-Noril'sk Symposium Sudbury, Proceedings, p. 283–312.

Lightfoot, P.C., Keays, R.R., and Doherty, W., 2001, Chemical evolution and origin of nickel sulfide mineralization in the Sudbury Igneous Complex, Ontario, Canada: Economic Geology, v. 96, p. 1855–1875.

Lightfoot, P.C., Keays, R.R., Evans-Lamswood, D., and Wheeler, R., 2011, S saturation history of Nain Plutonic Suite mafic intrusions: origin of the Voisey's Bay Ni-Cu-Co sulfide deposit, Labrador, Canada: Mineralium Deposita, v. 47, p. 23–50.

Lorand, J.P., Alard, O., Luguet, A., and Keays, R.R., 2003, Sulfur and selenium systematics of the subcontinental lithospheric mantle: inferences from the Massif Central xenolith suite (France): Geochimica et Cosmochimica Acta, v. 67, p.4137–4151.

Lorand, J.P., and Alard, O., 2001, Geochemistry of platinum-group elements in the subcontinental lithospheric mantle; in-situ and whole-rock analyses of some spinel peridotite xenoliths, Massif Central, France: Geochimica et Cosmochimica Acta, v. 65, p. 2789–2806.

Lorand, J.P., and Alard, O., 2010, Determination of selenium and tellurium concentrations in Pyrenean peridotites (Ariege, France): New insight into S/Se/Te systematics of the upper in mantle sample: Chemical Geology, v. 278, p. 120–130.

Maier, W.D., 2000, Platinum-group elements in Cu-sulfide ores at Carolusberg and East Okiep, Namaqualand, South Africa: Mineralium Deposita, v. 35, p. 422–429.

Maier, W.D., and Barnes, S.-J., 1996, Unusually high concentrations of magnetite at Caraiba and other Cu-sulfide deposits in the Curaçá Valley, Bahia, Brazil: Canadian Mineralogist, v. 34, p. 717–731.

Maier, W.D., and Barnes, S.-J., 1999, The origin of Cu sulfide deposits in the Curaçà Valley, Bahia, Brazil: Evidence from Cu, Ni, Se, and platinum-group element concentrations: Economic Geology, v. 94, p. 165–183.

Maier, W.D., and Barnes, S.-J., 2010, The Kabanga Ni sulfide deposits, Tanzania: II. Chalcophile and sidérophile element geochemistry: Mineralium Deposita, v. 45, p. 443–460.

Maier, W.D., Barnes, S.-J., Chinyepi, G., Barton Jr, J.M., Eglington, B., and Setshedi, I., 2008, The composition of magmatic Ni-Cu-(PGE) sulfide deposits in the Tati and Selebi-Phikwe belts of eastern Botswana: Mineralium Deposita, v. 43, p. 37–60.

Mainwaring, P.R., and Naldrett, A.J., 1977, Country rock assimilation and genesis of Cu-Ni sulfides in the Water Hen Intrusion, Duluth Complex, Minnesota: Economic Geology, v. 72, p. 1269-1284.

McDonough, W.F., and Sun, S.S., 1995, The composition of the earth: Chemical Geology, v. 120, p. 223–253.

McGoldrick, P.J., and Keays, R.R., 1981, Precious and volatile metals in the Perseverance nickel deposit gossan: Implications for exploration in weathered terrains: Economic Geology, v. 76, p. 1752–1763.

Melezhick, V.A., Grinenko, L.N., and Fallick, A.E., 1998, 2000-Ma sulphide concretions from the 'Productive' Formation of the Pechenga Greenstone Belt, NW Russia: genetic history based on morphological and isotopic evidence: Chemical Geology, v. 148, p. 61–94.

Menard, T., Lesher, C.M., Stowell, H.H., Price, D.P., Pickell, J.R., and Hulbert, L., 1996, Geology, genesis, and metamorphic history of the Namew Lake Fe-Ni-CU-PGE deposit, Manitoba: Economic Geology, v. 91, p. 1394–1413.

Nabil, H., Clark, T., and Barnes, S.-J., 2004, A Ni-Cu-Co-PGE massive sulfide prospect in a gabbronorite dike at Lac Volant, eastern Grenville province, Québec: Geological Society of America Memoirs, v. 197, p. 145–162.

Naldrett, A.J., 1981, Nickel sulfide deposits: Classification, composition, and genesis: Economic Geology 75th Anniversary Volume, p. 628–685.

Naldrett, A.J., 1997, Key factors in the genesis of Noril'sk, Sudbury, Jinchuan, Voisey's Bay, and other world-class Ni-Cu-PGE deposits: Implications for exploration: Australian Journal of Earth Sciences, v. 44, p. 283–315.

Naldrett, A.J., 2004, Magmatic sulfide deposits: Geology, geochemistry, and exploration: Berlin, Springer, 727 p.

Naldrett, A.J., and Li, C., eds., 2000, A special issue on Voisey's Bay Ni-Cu-Co deposit: Economic Geology, v. 95, p. 673–916.

Naldrett,A.J., and Li, C., 2007, The Voisey's Bay deposit, Labrador, Canada, in Goodfellow, W.D., ed., Mineral Deposits of Canada: A Synthesis of Major Deposit-Types, District Metallogeny, the Evolution of Geological Provinces, and Exploration Methods: Geological Association of Canada, Mineral Deposits Division, Special Publication No. 5, p. 387–407.

Naldrett, A.J., Gasparrini, E.C., Barnes, S.J., Von Gruenewaldt, G., and Sharpe, M.R., 1986, The Upper Critical Zone of the Bushveld Complex and the origin of Merensky-type ores: Economic Geology, v. 81, p. 1105–1117.

Paktunc, A.D., Hulbert, L.J., and Harris, D.C., 1990, Partitioning of the platinum group and other trace elements in sulfides from the Bushveld Complex and Canadian occurrences of nickel-copper sulfides: Canadian Mineralogist, v. 28, p. 475–489.

Peach, C.L., Mathez, E.A., and Keays, R.R., 1990, Sulfide melt-silicate melt distribution coefficients for noble metals and other chalcophile elements as deduced from MORB: Implications for partial melting. Geochimica et Cosmochimica Acta, v. 54, p. 3379-3389.

Peach, C.L., Mathez, E.A., Keays, R.R., and Reeves, S.J., 1994, Experimentally determined sulfide melt-silicate melt partition coefficients for iridium and palladium. Chemical Geology, v. 117, p. 361-377.

Peck, D.C., and Keays, R.R., 1990, Insights into the behavior of precious metals in primitive, S-undersaturated magmas; evidence from the Heazlewood River Complex, Tasmania: Canadian Mineralogist, v. 28, p. 553–577.

Peck, D.C., Keays, R.R., James, R.S., Chubb, P.T., and Reeves, S.J., 2001, Controls on the formation of contact-type platinum-group element mineralization in the East Bull Lake intrusion: Economic Geology, v. 96, p. 559–581.

Peltonen, P., 1995, Magma-country rock interaction and the genesis of Ni-Cu deposits in the Vammala Nickel Belt, SW Finland: Mineralogy and Petrology, v. 52, p. 1–24.

Piña, R., Gervilla, F., Ortega, L., and Lunar, R., 2008, Mineralogy and geochemistry of platinum group elements in the Aguablanca Ni-Cu deposit (SW Spain): Mineralogy and Petrology, v. 92, p. 259–282.

Raith, J.G., and Harley, S.L., 1998, Low-P/high-T metamorphism in the Okiep Copper District, western Namaqualand, South Africa: Journal of Metamorphic Geology, v. 16, p. 281-305.

Ripley, E.M., 1981, Sulfur isotopic studies of the Dunka Road Cu-Ni deposit, Duluth Complex, Minnesota: Economic Geology, v. 76, p. 1222–1238.

Ripley, E.M., 1990b, Se/S ratios of the Virginia Formation and Cu-Ni mineralization in the Babbitt area, Duluth Complex, Minnesota: Economic Geology, v. 85, p. 1935–1940.

Ripley, E.M., 1999, Systematics of sulfur and oxygen isotopes in mafic igneous rocks and related Cu-Ni-PGE mineralization, *in* Keays, R.R., Lesher, C.M., Lightfoot, P.C., and Farrow, C.E.G., ed., Dynamic processes in magmatic ore deposits and their application in mineral exploration: Geological Association of Canada Short Course Notes, v. 13, p. 133–158.

Ripley, E.M., and Alawi, J.A., 1986, Sulfide mineralogy and chemical evolution of the Babbitt Cu–Ni deposit, Duluth Complex, Minnesota: Canadian Mineralogist, v. 24, p. 347–368.

Ripley, E.M., and Al-Jassar, T., 1987, Sulfur and oxygen isotopic studies of melt–country rock interaction, Babbitt Cu–Ni deposit, Duluth Complex, Minnesota: Economic Geology, v. 82, p. 87–107.

Ripley, E.M., and Li, C., 2003, Sulfur isotope exchange and metal enrichment in the formation of magmatic Cu-Ni-(PGE) deposits: Economic Geology, v. 98, p. 635–641.

Ripley, E.M., Park, Y.R., Li, C., and Naldrett, A.J., 1999, Sulfur and oxygen isotopic evidence of country rock contamination in the Voisey's Bay Ni-Cu-Co deposit, Labrador, Canada: Lithos, v. 47, p. 53–68.

Ripley, E.M., Li, C., and Shin, D., 2002, Paragneiss assimilation in the genesis of magmatic Ni–Cu–Co sulfide mineralization at Voisey's Bay, Labrador: δ34S, δ13C and Se/S evidence: Economic Geology, v. 97, p. 1307–1318.

Ripley, E.M., Sarkar, A., and Li, C., 2005, Mineralogic and stable isotope studies of hydrothermal alteration at the Jinchuan Ni-Cu deposit, China: Economic Geology, v. 100, p. 1349–1361.

Ripley, E.M., Taib, N.I., Li, C., and Moore, C.H., 2007, Chemical and mineralogical heterogeneity in the basal zone of the Partridge River Intrusion: implications for the origin of Cu–Ni mineralization in the Duluth Complex, Midcontinent rift system: Contributions to Mineralogy and Petrology, v. 154, p. 35–54.

Sappin, A-A., Constantin, M., and Clark, T., 2012, Origin of magmatic sulfides in a Proterozoic island arc – an example from the Portneuf-Mauricie Domain, Grenville Province, Canada: Mineralium Deposita, v. 56, p. 211–237.

Savard, D., Bédard, L.P., and Barnes, S.-J., 2006, TCF selenium preconcentration in geological materials for determination at sub-μg g−1 with INAA (Se/TCF-INAA): Talanta, v. 70, p. 566–571.

Schissel, D., Tsvetkov, A.A., Mitrofanov, F.P., and Korchagin, A.U., 2002, Basal platinum-group element mineralization in the Federov Pansky layered mafic intrusion, Kola Peninsula, Russia: Economic Geology, v. 97, p. 1657–1677.

Thériault, R.M., and Barnes, S.-J., 1998, Compositional variations in Cu–Ni–PGE sulfides of the Dunka Road deposit, Duluth Complex, Minnesota: the importance of combined assimilation and magmatic processes: Canadian Mineralogist, v. 36, p. 869–886.

Thériault, R.M., Barnes, S.-J., and Severson, M.J., 1997, The influence of country-rock assimilation and silicate to sulfide ratios *(R* factor) on the genesis of the Dunka Road Cu-Ni-platinum-group element deposit, Duluth Complex, Minnesota: Canadian Journal of Earth Sciences, v. 34, p. 375–389.

Thériault, R.M., Barnes, S.-J., and Severson, M.J., 2000, Origin of Cu-Ni-PGE sulfide mineralization in the Partridge River Intrusion, Duluth Complex, Minnesota: Economic Geolgy, v. 95, p. 929–943.

Tremblay, C., 1990, Les elements du groupe du platine dans le dyke de Méquillon, Ceinture de Cape Smith, Nouveau Québec: Unpublished M.Sc. thesis, Université du Québec à Chicoutimi, 90 p.

Vaillancourt, C., 2001, Etude géochimique et économique de la suite mafique et ultramafique de la baie à Cadie au lac Kenogami, Saguenay-Lac St-Jean, Québec: Unpublished M.Sc. thesis, Université du Québec à Chicoutimi, 187 p.

Walker, R.J., Morgan, J.W., Horan, M.F., Czamanske, G.K., Krogstad, E.J., Likhachev, A.P., and Kunilov, V.E., 1994, Re-Os isotopic evidence for an enriched-mantle plume source for the Noril'sk-type ore-bearing intrusions, Siberia: Geochimica et Cosmochimica Acta, v. 58, p. 4179–4197.

Watkinson, D.H., Lavigne, M.J., and Fox, P.E., 2002, Magmatic-hydrothermal Cu- and Pd-rich deposits in gabbroic rocks from North America, *in* Cabri, L.J., ed., The Geology, Geochemistry, Mineralogy and Mineral Beneficiation of Platinum-Group Elements. Canadian Institute of Mining, Metallurgy and Petroleum Special Volume 54, p. 299–320.

Yamamoto, M., 1976, Relationship between Se/S and sulfur isotope ratios of hydrothermal sulfide minerals: Mineralium Deposita, v. 11, p. 197–209.

Zientek, M.L. and Ripley, E.M., 1990, Sulfur isotope studies of the Stillwater Complex and associated rocks, Montana: Economic Geology, v. 85, p. 376–391.

CHAPITRE II

NOUVELLES MESURES DE CONCENTRATION EN S ET EN SE DANS LES ROCHES ENCAISSANTES DU COMPLEXE DE DULUTH, MINNESOTA, USA, ET IMPLICATIONS POUR LA FORMATION DES DÉPÔTS DE CU-NI-EGP

Titre du manuscrit (Soumis à Economic Geology, accepté et en cours de révision) :

"Selenium and sulfur concentrations in country rocks from the Duluth Complex, Minnesota, USA, and sulfide formation of the Cu-Ni-PGE deposits."

Auteurs:

Matthias Queffurus et Sarah-Jane Barnes

Résumé:

Il est régulièrement admis que la formation d'un gisement magmatique à sulfures de Ni-Cu nécessite une addition de soufre (S) d'origine externe provenant des roches encaissantes et contaminant le magma. Néanmoins, les mécanismes précis et la localisation exacte où le S est ajouté au magma demeurent mal compris. Un des indicateurs les plus évidents prouvant la contamination crustale est que de nombreux gisements possèdent des rapports S/Se plus élevés que les magmas primitifs et il est suggéré que ces valeurs élevées sont héritées des sédiments. Cependant, la majorité des études ne détermine pas les concentrations en Se dans les roches encaissantes des intrusions magmatiques à cause des difficultés analytiques. Nous avons mesurés

les concentrations en Se, S et les valeurs isotopiques du S ($\delta^{34}S$) sur les sulfures magmatiques du complexe de Duluth ainsi que sur les sédiments de la Formation de Virginia ayant contaminés le magma. Le Se a été déterminé par la méthode TCF-INAA (*Thiol Cotton Fiber - Instrumental Neutron Activation Analysis)*, une technique de haute précision pour les roches appauvries en Se. Nos résultats démontrent que les rapports S/Se et les valeurs en $\delta^{34}S$ de la plupart des sédiments et des xénolithes sont inférieurs à ceux des roches minéralisées, signifiant donc l'improbabilité des sédiments à être la source du S des roches intrusives minéralisées. Néanmoins l'horizon sédimentaire riche en S connu sous le nom d'Unité de Pyrrhotite Litée (UPL) localisé à la marge de l'intrusion possèdent des rapports S/Se et des valeurs $\delta^{34}S$ suffisamment élevés (18 438 et +18.22%, respectivement) pour augmenter les valeurs en S/Se et $\delta^{34}S$ des roches ignées sulfurées par contamination. L'examen des xénolithes de l'UPL et des gabbronorites autour de ces xénolithes suggère un mécanisme de transfert de S des sédiments au magma mafique. De plus, la plupart des xénolithes dérivés de l'UPL ont des rapports S/Se et $\delta^{34}S$ compris entre ceux de l'UPL et ceux des gabbronorites à sulfures disséminés. Les valeurs du rapport S/Se et du $\delta^{34}S$ diminuent progressivement depuis l'UPL, aux xénolithes, aux gabbronorites, aux gabbronorites à olivine et finalement jusqu'à l'horizon riche en Éléments du Groupe du Platine, indiquant un modèle de mélange entre les sulfures sédimentaires et le S magmatique. Ces résultats favorisent un mécanisme de contamination en S crustal par l'assimilation *in situ* de xénolithes de l'Unité de Pyrrhotite Litée.

Contributions des auteurs:

1er auteur : Matthias Queffurus

- Analyse en laboratoire du sélénium et du soufre.
- Traitement des données.

- Rédaction de l'ensemble du manuscrit.

- Production de tous les tableaux et figures.

- Mise en forme de l'article suivant les critères de l'éditeur.

2ème auteur : Sarah-Jane Barnes

- Direction et supervision du projet.

- Conseils à la rédaction du manuscrit.

- Révision de l'ensemble du manuscrit.

Selenium and sulfur concentrations in country rocks from the Duluth Complex, Minnesota, USA, and sulfide formation of the Cu-Ni-PGE deposits.

Matthias Queffurus* **and Sarah-Jane Barnes**

Université du Québec à Chicoutimi, 555 boulevard de l'Université, Saguenay, QC, G7H 2B1, Canada

(*corresponding author: e-mail: matthias.queffurus@uqac.ca)

Keywords: S/Se ratio, sulfur, selenium, contamination, assimilation, country rocks, TCF-INAA, Ni-Cu-PGE deposits, Duluth Complex, Virginia Formation.

Abstract

Various studies suggest that the formation of a magmatic Ni-Cu-Platinum Group Element (PGE) sulfide deposit require addition of S from the country rocks into the magma. However, exactly how and where this sulfur is added is not clear. One line of evidence for crustal contamination is that many deposits have S/Se ratios higher than primary magmas and it is suggested that these high ratios are inherited from crustal sediments. However, most studies do not determine Se in the country rocks to the intrusions because of analytical difficulties. We have determined Se abundances, using Thiol Cotton Fiber combined with Instrumental Neutron Activation Analysis (TCF-INAA), a high precision technique for rocks with low-Se concentration, S, and $\delta^{34}S$ on the magmatic sulfides of the Duluth Complex and on the sediments (i.e., Virginia Formation) which could have contaminated the magma. Our results show that the S/Se ratios and $\delta^{34}S$ for most of the sediments and xenoliths are lower than those of the ores and thus most of the sediments are unsuitable as a source of S for the ores. The S-rich layer known as the Bedded Pyrrhotite Unit of the Virginia Formation, which is found at the margins of the intrusion, has sufficiently high S/Se ratios and $\delta^{34}S$ values (18 438 and +18.22‰, respectively) to increase the S/Se ratios and $\delta^{34}S$ values of the sulfide-bearing igneous rocks by contamination. Examination of the xenoliths of Bedded Pyrrhotite Unit and gabbronorites around the xenoliths suggest a mechanism for transferring the S from the sediments to the mafic magma. Most of the xenoliths derived from the Bedded Pyrrhotite Unit have S/Se ratios and $\delta^{34}S$ values between those of the Bedded Pyrrhotite Unit and the gabbronorite-hosted disseminated sulfides. Values decrease progressively from the Bedded Pyrrhotite Unit, to xenoliths, to gabbronorite-hosted disseminated sulfide, to olivine gabbronorite-hosted disseminated sulfide and finally to a PGE-rich layer, indicating a model of mixing between sulfides from the sediments and S from the

magma. Our results favor a mechanism of crustal S contamination by *in situ* assimilation of Bedded Pyrrhotite Unit xenoliths.

Introduction

While many authors accept that much of the sulfur (S) found in magmatic Ni-Cu deposits is derived from the crust (e.g., Lesher and Burnham, 2001), the details of how this process occurs are not well established. The Cu-Ni deposits found at the margins of the Duluth Complex, Minnesota (Hauck et al., 1997) offer an opportunity to study how S could be added to the magma because there are numerous boreholes from the country rock into the deposits offering the possibility of detailed sampling. Previous work carried out on the Duluth Complex emphasized the importance of contamination by the country rocks in the genesis of the Cu-Ni-PGE mineralization (e.g., Mainwaring and Naldrett, 1977; Ripley, 1981; Tyson and Chang, 1984; Andrews and Ripley, 1989; Thériault et al., 1997; Thériault and Barnes, 1998; Ripley et al., 2007). Most of these studies highlighted the point that the source of the S which contaminated the mafic magma was probably the sediments of the underlying Virginia Formation. However, the authors differ in their opinions on the timing, location and mechanism involved in this S-contamination. Based on sulfur isotope data, some authors suggested that the initial S-contamination occurred at depth, by S-rich fluids produced during the devolatilization of the metasedimentary rocks of the Virginia Formation, and homogenized prior to magma emplacement (Ripley and Alawi, 1986; Ripley and Al-Jassar, 1987; Andrews and Ripley, 1989). In contrast, another hypothesis claims that S-contamination is caused by the assimilation of S-rich country rocks of the Virginia Formation into the magma (Mainwaring and Naldrett, 1977; Ripley, 1981; Rao and Ripley, 1983; Thériault et al., 1997; Thériault and Barnes, 1998; Thériault

et al., 2000). The high delta $\delta^{34}S$ and $\delta^{18}O$ values, and the presence of massive sulfides around a xenolith within the South Kawishiwi intrusion (SKI), are interpreted as strong evidence for at least some local *in situ* assimilation (Severson, 1994; Zanko et al., 1994).

Ripley (1990) and Thériault and Barnes (1998) showed that some of the Duluth Complex sulfide deposits have high S/Se ratios, which they interpreted to be the result of S-assimilation of the country rocks by the magma. Unfortunately, in these studies, the S/Se ratios of the Virginia Formation sediments could not be reliably estimated because the analytical methods of the time were not capable of accurately determining selenium (Se) in these sedimentary rocks. Modern analytical techniques allow Se determination to much lower levels (e.g., Hall and Pelchat, 1997; Savard et al., 2006; Fitzpatrick et al., 2009). Using TCF-INAA *(Thiol Cotton Fiber - Instrumental Neutron Activation Analysis)* method, we have determined the Se concentrations in a range of lithologic units: unmetamorphosed sediments away from the contact with the intrusion, metamorphosed sediments at the contact, xenoliths, and sulfide-bearing igneous rocks surrounding the xenoliths. The new Se data are combined with S and $\delta^{34}S$ data in order to consider how S was added to the magma.

Geological settings

The Duluth Complex

The Duluth Complex consists of a series of mafic intrusions, sporadically exposed along the northwestern margin of Lake Superior, Minnesota, USA (Fig. 1). This Keweenawan aged complex (1100 Ma) was emplaced during extensional tectonism of the Midcontinent Rift System. (Ojakangas et al., 2001). Rocks of the Duluth Complex were emplaced by two distinct magmatic episodes, each divided into two main series: an early stage (~1108 Ma) composed of the Felsic

Series and the Early Gabbro Series, followed by a main stage (~1099 Ma) consisting of the Anorthositic Series and the Layered Series (Fig. 1). Detailed documentation of the geology of the Duluth Complex is presented elsewhere (e.g., Miller and Severson, 2002a).

The Cu-Ni-PGE deposits

The Cu-Ni-PGE sulfide deposits consist of 4.4 billion tons at 0.66% Cu and 0.20% Ni (Listerud and Meineke, 1977), which represent one of the largest unexploited resources in the world. These deposits are located along the western margin of the complex in mafic cumulate rocks of the Layered Series, near the contact with the footwall metasedimentary rocks of the Animikie Group (Fig. 1). They are distributed among three intrusions, referred to as the Partridge River, the South Kawishiwi and the Bathtub (Severson and Hauck, 2008). The mineralized zones are 60 to 300 meters thick, located in the basal portion of each intrusion and consist mainly of mafic cumulates which contain interstitial magmatic sulfides (1-12%). In addition, lenses of semi-massive to massive sulfides occur towards the margins of the intrusion and in the footwall rocks.

The Partridge River and South Kawishiwi intrusions

The samples used in this study are mainly from the Partridge River intrusion (PRI; Fig. 1). The PRI is divided into at least eight subhorizontal igneous units (Severson and Hauck, 2008) on the basis of the different mafic lithology (Fig. 2). Detailed descriptions of these units can be found in Severson (1994), Hauck et al., (1997), Miller and Severson (2002), and Severson and Hauck (2008). Most of the disseminated Cu-Ni sulfide occurs in the lower 300 meters of the intrusion, in Unit 1, a heterogeneous assemblage consisting of mafic cumulate rocks with abundant xenoliths of the underlying Virginia Formation sediments. The mafic cumulate rocks

are predominantly olivine-bearing rocks (troctolites and olivine-gabbronorites, referred to informally as troctolites). But in some cases close to the xenoliths, no or very little olivine is present in the mafic cumulates and the rocks are gabbronorites with orthopyroxene as the dominant pyroxene. Towards the top of Unit 1, some PGE-rich layers are present just below the ultramafic layer that forms Unit 2 (Fig. 2). In a similar way, the basal section of South Kawishiwi intrusion (SKI) contains most of sulfide ore, in association with numerous xenoliths fragments, and detailed description of the igneous units can be found in Severson (1994) and Zanko et al. (1994).

The footwall rocks of the Animikie Group

Most of the footwall rocks of the PRI and part of the SKI, especially close to the Serpentine deposit, include the sedimentary rocks of the Animikie Group. The Animikie Group is composed of the Pokegama quartzite at the base, overlain by the Biwabik Iron Formation and its turn overlain the Virginia Formation. Rocks of the Virginia Formation are several thousands of meters thick, consisting of a sequence of bedded argillite, siltstone layers and fine-grained greywackes (Ojakangas et al., 2001). The Virginia Formation and its stratigraphic equivalents (Rove and Thomson Formations) are derived from the same episode of sedimentation but from different parts of the Middle Proterozoic sedimentary basin. Lucente and Morey (1983) divided the Virginia Formation into two members: 1) A lower lithosome, dominated by thin bedded carbonaceous argillite with visible sulfides formed by slow deep-sea pelagic sedimentation processes, and 2) An upper lithosome consisting of siltstone, sandstone and greywacke, formed by turbidity currents during basin subsidence. The mineral assemblage of the argillite rocks consist of chlorite, muscovite, quartz, plagioclase, ilmenite, kerogen and pyrite (Fig. 6A) (Lucente and Morey, 1983; Andrews and Ripley, 1989). Contact metamorphism of the intrusions

has led to the formation of cordierite and biotite at 1500m from the contact, followed by orthopyroxene and K-feldspar at 250m from the contact (Andrews and Ripley, 1989). Pyrite was converted into pyrrhotite by desulfurization reaction during the prograde metamorphism (Ripley, 1981). Close to the Duluth Complex, the effect of partial melting transformed the pre-existing sedimentary structures of the rocks considerably. Consequently, the Virginia Formation has been subdivided into several metamorphic units based on the degree of partial melting (Severson et al., 1994; Duschene, 2004). A particularly important layer in terms of the ore bodies is called the Bedded Pyrrhotite Unit (BPU). It contains between 5-15% thinly laminated pyrrhotite, and traces of chalcopyrite, sphalerite and galena. Several BPU horizons have been recognized locally in the footwall of the deposits (Severson, 1994; Thériault et al., 1997; Zanko et al., 1994), ranging from 10 to 60m in thickness and as xenoliths within the Duluth Complex (Severson et al., 1996; Williams et al., 2010). Hauck et al. (1997) suggests that the formation of this layer was syngenetic with the sedimentation in a closed basin.

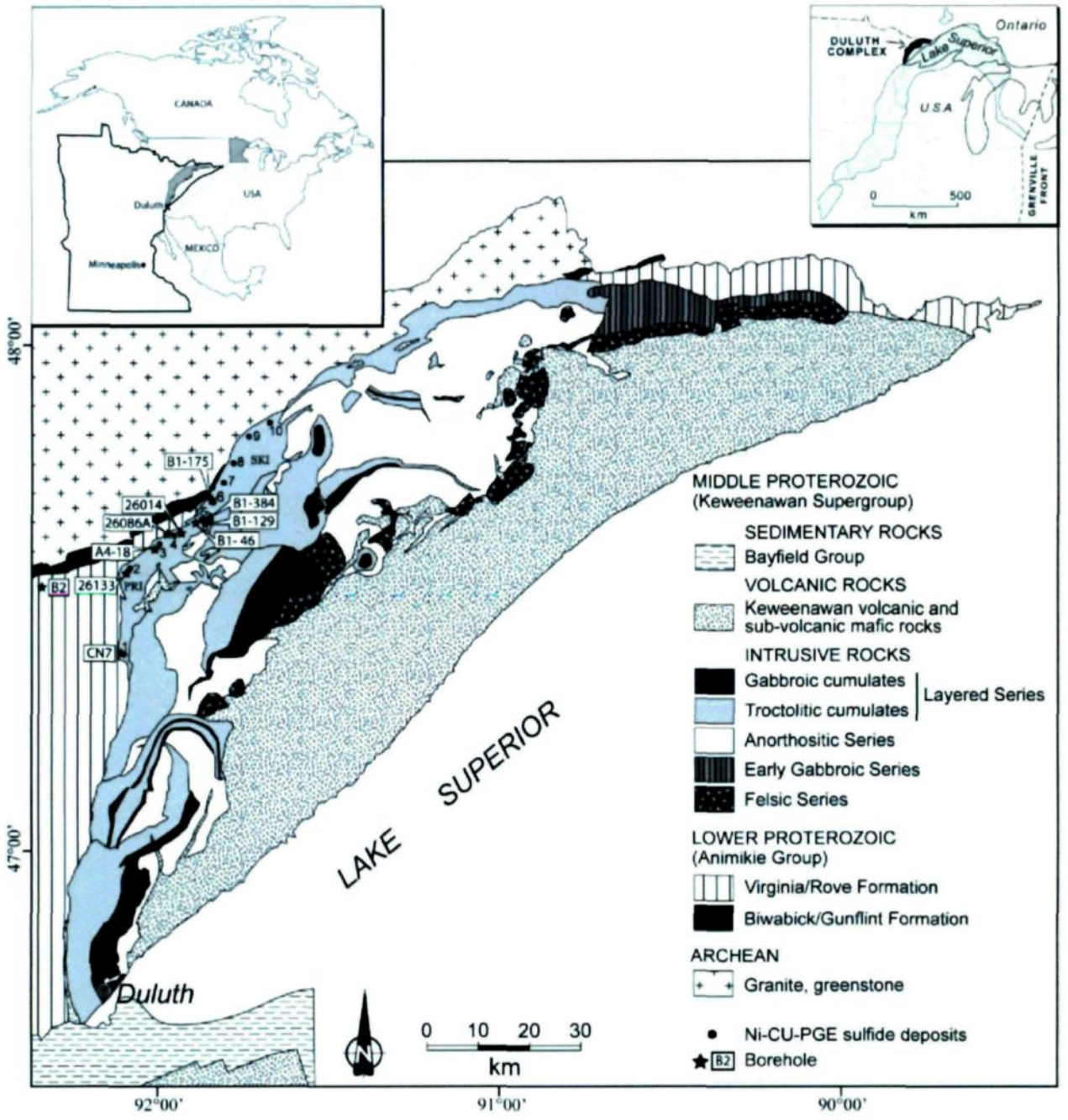

FIG. 1. Location map of the Duluth Complex (left inset), showing its position in the Midcontinent Rift System (right inset, simplified after Ojakangas et al., 2001) and its geology (modified after Miller and Severson, 2002a). Abbreviations for the Troctolitic Series: PRI = Partridge River intrusion, SKI = South Kawishiwi intrusion. Ni-Cu-PGE deposits : 1, Water Hen; 2, Wyman Creek; 3, Wetlegs; 4, Dunka Road (NorthMet); 5, Babbitt (Mesaba); 6, Serpentine; 7, Dunka Pit; 8, Birch Lake; 9, Nokomis; 10, Spruce Road. Boxes with stars indicate the location of boreholes.

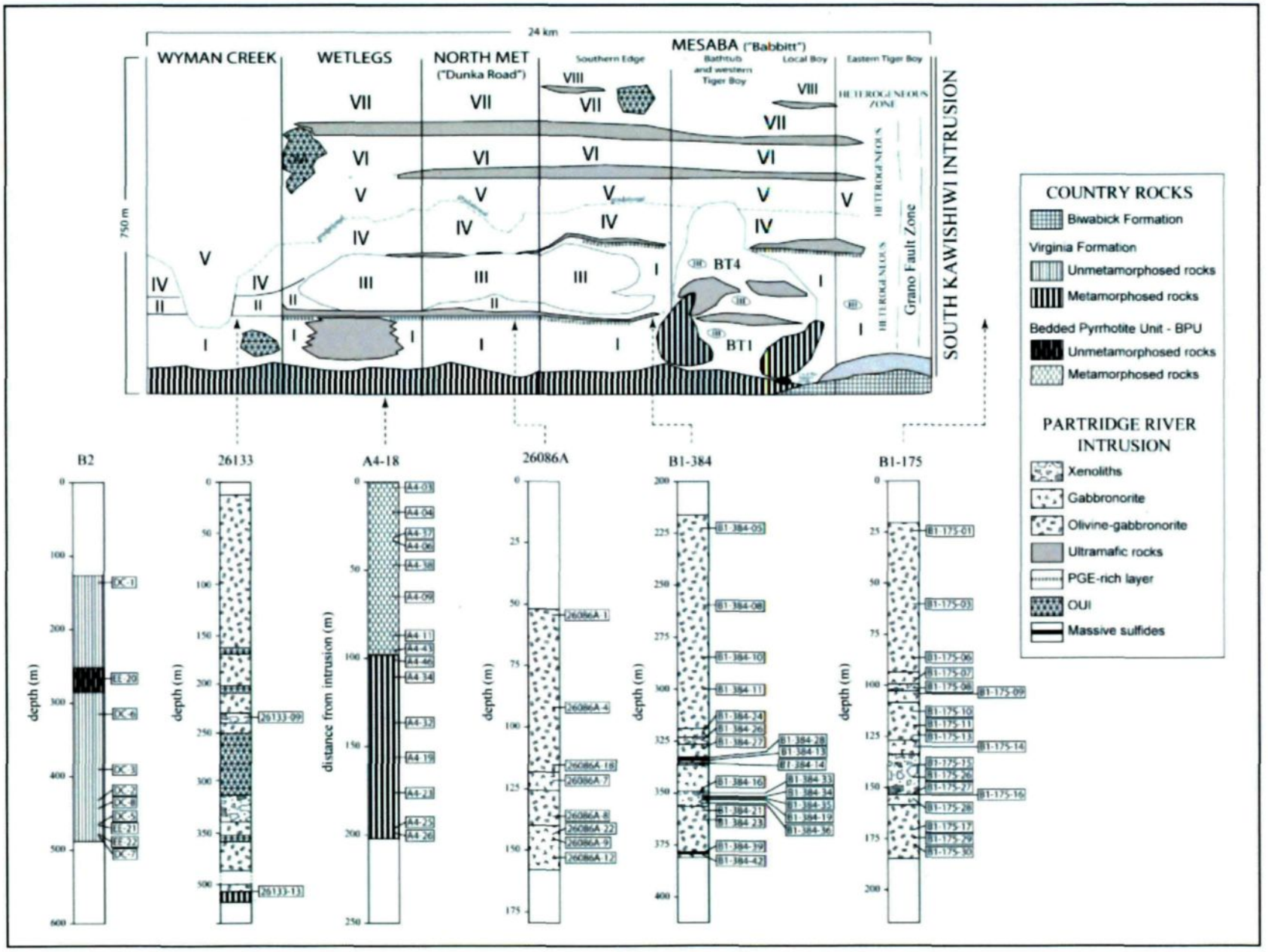

FIG. 2. Schematic cross section of the Partridge River intrusion and the stratigraphic position of the samples in the borehole sections analyzed in this study. Numbers I to VIII indicates igneous units of the PRI and BT indicate igneous units of the Bathtub intrusion. The locations of borehole sections are schematic. The few samples taken from LTV core, Dunka Pit, 26014, B1-46, B1-129 and CN7 are not indicated. Modified from Severson and Hauck (2008) after Severson (1994). Abbreviation: OUI = Oxide-bearing ultramafic intrusion

Sampling and Analytical Methods

Eighty-two samples from 12 borehole sections and three outcrop samples (DC-52, DC-54 and DC-70) were selected for Se and S analysis (Fig. 1, Table 2). The samples were chosen to cover the range of rock types and levels of metamorphism in the Virginia Formation, and to investigate the variation in S and Se concentrations around xenoliths. Unmetamorphosed samples were obtained from B2 borehole, LTV Pit and LTV core. Hornfelized and migmatized samples of the footwall were obtained from boreholes at Wetlegs (A4-18), Wyman Creek (26133) and Water Hen (CN7). The xenoliths and rocks surrounding the xenoliths were sampled at Dunka Road (26117, 26143, 26107 and 20686A), Babbitt (B1-46, B1-129, and B1-384) and Serpentine deposit (B1-175)

Each sample was crushed and 100g were pulverized in an aluminum carbide mill at the Université du Québec à Chicoutimi (UQAC). All analyses of Se and S were carried out at LabMaTer (Earth Materials Laboratory of UQAC). Whole-rock Se concentration was determined for 79 samples by TCF-INAA following the method of Savard et al. (2006). Three reference materials and three doped samples were also analyzed and results agree with the certified or estimated values (Table 1). Based on three sigma error for three blanks, the limit of detection is 0.003 ppm (+/- 0.002 ppm), consistent with the values of Savard et al. (2006). TCF-INAA is not an appropriate analytical method for S-rich samples, so Se in the three S-rich samples was determined using INAA at SLOWPOKE Laboratory (Ecole polytechnique, Montréal, Canada). Two reference materials (WMS-1 and WMS-1a) and a doped blank were also analyzed and results agree with the certified or expected values (Table 1).

For most samples, whole-rock S concentrations were determined at LabMaTer by the combustion iodometric procedure using a Laboratory Equipment Company (LECO) titrator

(Thériault and Barnes, 1998; Duschene, 2004; and unpublished studies). For the nine samples where S concentrations were not available from previous studies, S was determined by infrared spectrometry sulfur-carbon analyzer using an HORIBA EMIA-220V, according to the method of Bédard et al. (2008). The measured S concentration of the in-house reference material KPT-1 is consistent with the working value. Platinum-group element data were taken from previous studies (Thériault and Barnes, 1998) or unpublished studies carried out at UQAC.

In order to supplement our existing S isotope data base, $\delta^{34}S$ was determined for 16 rocks from the Virginia Formation at the Environmental Isotope Laboratory (University of Waterloo, ON, Canada) using a Micromass Isochrom-elemental Analyzer-Isotope Ratio Mass Spectrometer (EA-IRMS) with an analytical precision of ±0.3‰. All sulfur isotope compositions were calculated relative to the international standard Vienna Cañon Diablo Troilite (V-CDT). Reproducibility of the analytical results was controlled through duplicate measurements of internal Environmental Isotope Laboratory standards. To ensure consistency between the previously collected data and the new analyses, four samples from the Thériault and Barnes (1998) study were reanalyzed. The current results are consistent with the original results (Table 1).

Table 1. Se, S and $\delta^{34}S$ obtained for reference materials, blanks and fixed concentrations

Se-determination by TCF-INAA			
Sample	Se (ppm)	Se (ppm)	+/- (ppm)
	This study	Savard et al. (2009)	
SCo-1	0.793	0.841	0.071
MRG-1	0.220	0.199	0.008
		Certificate value	
WMS-1A	83.3	87.0	-
Doped blanks		Doped with	
Se - 0.97 ppm	0.93	0.97	-
Se - 3.7 ppm	3.708	3.70	-
Se - 3 ppm	2.870	3.00	-
Blank	0.003	-	-

Se-determination by INAA			
Sample	Se (ppm)	Se (ppm)	+/- (ppm)
	This study	Savard et al. (2006)	
WMS-1	105.4	111.0	17
		Certificate value	
WMS-1a	90.1	87.0	-
		Doped with	
Se - 100 ppm	101.9	100.0	-

S-determination by infrared spectrometry S-C analyser			
Sample	S (%)	S (%)	+/- (ppm)
	This study	UQAC working value	
KPT-1	1.10	1.03	0.03

Whole rock $\delta^{34}S$			
Sample	$\delta^{34}S$ (‰)	repeat	$\delta^{34}S$ (‰)
	This study		Thériault and Barnes (1998)
DC-8	5.70		5.10
DC-70	16.30	16.69	15.80
DC-66	9.55	9.40	9.80
DC-73	8.12	7.78	8.40

Results

S-Se concentrations and S/Se ratios

The S/Se ratios found in the BPU are higher than those of the rest of the Virginia Formation sediments. The S content of the BPU is much higher (1 to 8 wt %: Table 2) than the rest of the Virginia Formation (0.01 to 1.1 wt %: Table 2). The Se content in the BPU is slightly higher (0.8-8 ppm: Table 2) than the sedimentary and metasedimentary samples from rest of the Virginia Formation (0.04-6 ppm: Table 2). The net effect is that the S/Se ratios of the BPU samples are much higher than those of the rest of the Virginia Formation with many samples plotting along a trend approximating a ratio of S/Se = 20 000 (Fig. 3A). In contrast, samples from the rest of the Virginia Formation have S/Se ratios of less than 10 000, with many samples plotting along a trend of S/Se = 3000 (Fig. 3A), similar to mantle values (2850 - 4350: Eckstrand and Hulbert, 1987).

One point of particular interest for this study was whether S was removed preferentially with respect to Se during metamorphism of the sediments. A preferential loss of S could occur due to either the conversion of pyrite to pyrrhotite with S being released by the reaction or by partial melting of the sedimentary sulfides with Se being retained by the residual sulfides. The ranges of S and S/Se values for the BPU-xenoliths (Fig. 3B) are larger (S/Se = 9000-66 000, Table 2) than for the BPU rocks from the contact aureole and the unmetamorphosed BPU (Fig. 3B). This could be interpreted to suggest that some xenoliths are largely residual and some xenoliths contain injections of S enriched melt escaping from the xenolith, resulting in a large range in S/Se ratios. However, the majority of the samples analyzed were from xenoliths and this result may simply be a sampling effect. The range of S values for unmetamorphosed and metamorphosed sediments (Fig. 3) for the rest of the Virginia Formation are similar. There does not appear to have been a change in S concentrations or S/Se ratios with metamorphism for these samples.

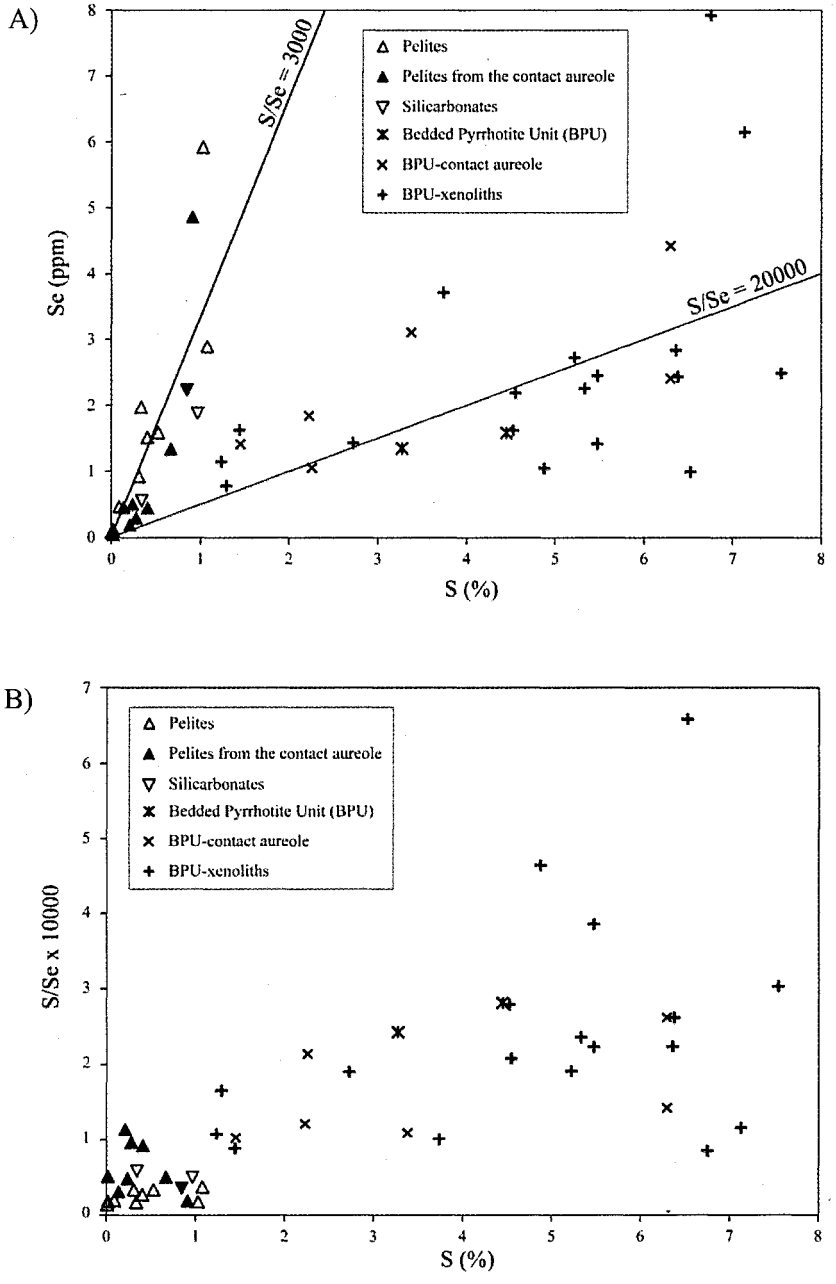

FIG. 3. Plots of (A) Se vs S and (B) S/Se vs S for sedimentary and metasedimentary rocks of the Virginia Formation, including the Bedded Pyrrhotite Unit and the BPU-xenoliths.

The range of S contents in gabbronorites (0.5 to 10 wt %, Table 2, Fig. 4) is greater than in the olivine-gabbronorites (0.1 to 5 wt %, Table 2, Fig. 4). While the range in Se values for both rock types is similar at 0.5 to 10 ppm (Table 2, Fig. 4). Thus, the S/Se ratios in the olivine-gabbronorites are generally lower than in the gabbronorites, with many olivine-gabbronorite samples plotting close to a S/Se ratio of 3000 (mantle values) while the gabbronorite samples plot close to a S/Se ratio of 10 000. These values are similar to those determined for gabbronorites and olivine-gabbronorites, referred to as norites and troctolites, (Thériault and Barnes, 1998).

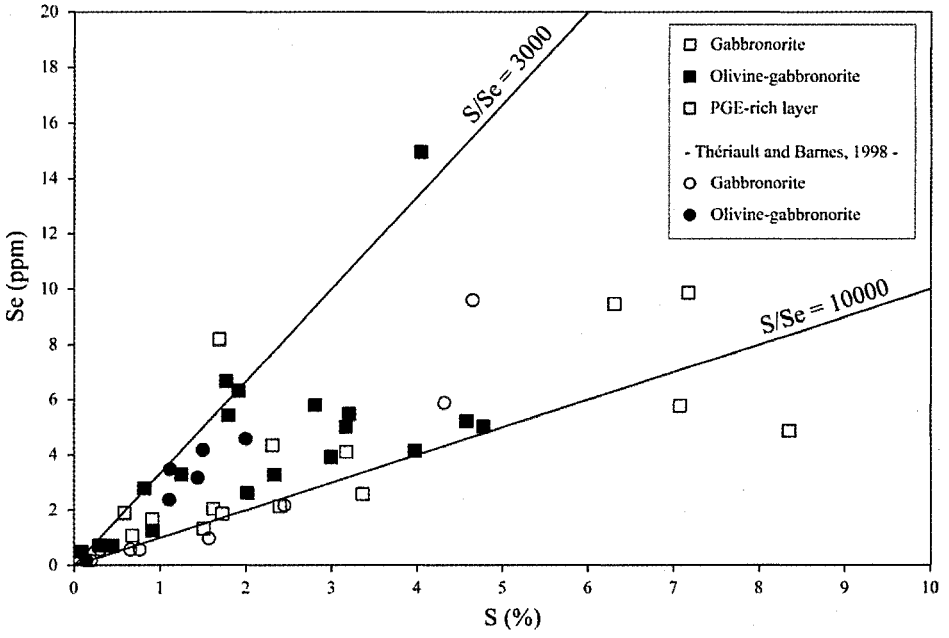

FIG. 4. Plots of Se vs S for sulfide-bearing igneous rocks.

Two massive sulfide samples from borehole B1-384 of the Babbitt deposit have the highest Se concentrations (21.4 ppm and 24.5 ppm: Table 2) of all the samples. The S/Se ratios of these two massive sulfides are high (~10 000) and similar to the values obtained for the gabbronorite samples. These results are consistent with S/Se ratios previously determined for the massive sulfides by Thériault and Barnes (1998).

Table 2. Whole-rock concentrations of Se, S, Pt, Pd and $\delta^{34}S$

Samples	Borehole	Depth (m)	Lithology	Unit	S (%)	Se (ppm)	S/Se	Pt (ppb)	Pd (ppb)	$\delta^{34}S$ (‰VCDT)
Virginia Formation										
DC-1	B2	135.9	pelites	Unmet VF.	0.02	0.1	1786	3.1	1.8	+ 5,30 [c]
EE-20	B2	266.4	BPU	Unmet VF.	3.28	1.4	24267	2.4	5.2	
DC-6	B2	314.6	pelites	Unmet VF.	0.01	0.1	1351	8.2	2.7	
DC-3	B2	390.3	pelites	Unmet VF.	0.31	0.9	3359	1.6	2.4	+ 8,60 [c]
DC-2	B2	432	pelites	Unmet VF.	0.97	1.9	5113	1.9	1.1	+ 9,01
DC-8	B2	443.2	pelites	Unmet VF.	1.08	2.9	3731	3.5	2.6	+ 5,70
DC-5	B2	464.8	pelites	Unmet VF.	0.53	1.6	3340	6.5	4.9	+ 7,20 [c]
EE-21	B2	465.1	pelites	Unmet VF.	1.03	5.9	1736	12.5	5.9	
EE-22	B2	478.5	pelites	Unmet VF.	0.34	2.0	1706	5.0	5.6	
DC-7	B2	479.7	pelites	Unmet VF.	0.09	0.5	1944	2.1	3.3	+ 4,50 [c]
DC-70	LTV Pit	outcrop	BPU	Unmet VF.	4.45	1.6	28143	2.4	3.5	+16,30
EE-25	LTV	7.9	pelites	Unmet VF.	0.40	1.5	2675	3.0	3.1	
EE-26	LTV	10.7	pelites	Unmet VF.	0.35	0.6	6000	2.3	2.3	
Virginia Formation (Wetlegs)										
A4-03	A4-18	3	diatexite (BPU)	RXTAL	2.26	1.1	21402	n.d.	n.d.	
A4-04	A4-18	17	metatexite (BPU)	DISRUPT	6.30	2.4	26195	n.d.	n.d.	+ 20,38
A4-37	A4-18	31.7	leucosome (BPU)		1.03	1.0	10239	n.d.	n.d.	
A4-06	A4-18	32.9	leucosome (BPU)		1.33	0.5	27254	n.d.	n.d.	+ 15,00
A4-38	A4-18	47.1	diatexite (BPU)	RXTAL	2.23	1.8	12120	n.d.	n.d.	+ 19,47
A4-09	A4-18	65	metatexite (BPU)	DISRUPT	3.38	3.1	10879	n.d.	n.d.	+ 16,71
A4-11	A4-18	86.9	metatexite (BPU)	DISRUPT	6.30	4.4	14241	n.d.	n.d.	
A4-43	A4-18	96	diatexite (BPU)	RXTAL	1.45	1.4	10262	n.d.	n.d.	
A4-46	A4-18	100.9	diatexite	RXTAL	0.14	0.5	3097	n.d.	n.d.	
A4-34	A4-18	110.6	leucosome		0.21	0.2	11351	n.d.	n.d.	+ 2,93
A4-32	A4-18	136.5	diatexite	RXTAL	0.02	0.0	5128	n.d.	n.d.	
A4-19	A4-18	155.7	metatexite	DISRUPT	0.24	0.5	4829	n.d.	n.d.	+ 6,48
A4-23	A4-18	175.7	metatexite	DISRUPT	0.41	0.4	9172	n.d.	n.d.	
A4-25	A4-18	196.6	hornfel	Met VF.	0.91	4.9	1871	n.d.	n.d.	+ 6,13
A4-26	A4-18	198.5	hornfel	Met VF.	0.67	1.3	5011	n.d.	n.d.	
NorthMet (Dunka Road)										
26086A-01	26086A	55.5	Ol-gabbronorite	PRI	0.09	0.5	1760	24.8	88.5	
26086A-04	26086A	93.6	Ol-gabbronorite	PRI	1.25	3.3	3782	71.6	2083.1	
26086A-18	26086A	117.2	Ol-gabbronorite	PRI	0.45	0.7	6310	9.9	42.8	
26086A-07	26086A	124.4	Gabbronorite	PRI	1.62	2.0	7941	141.8	282.3	
26086A-08	26086A	138.7	Ol-gabbronorite	PRI	0.82	2.8	2929	176.1	961.4	
26086A-22	26086A	146.1	Gabbronorite	PRI	3.36	2.6	13039	35.2	171.7	
26086A-09	26086A	147.8	Gabbronorite	PRI	1.51	1.3	11338	180.6	143.3	

Table 2. Whole-rock concentrations of Se, S, Pt, Pd and $\delta^{34}S$

Samples	Borehole	Depth (m)	Lithology	Unit	S (%)	Se (ppm)	S/Se	Pt (ppb)	Pd (ppb)	$\delta^{34}S$ (‰VCDT)
26086A-12	26086A	155.7	Gabbronorite	PRI	0.91	1.7	5494	38.6	151.2	
DC-52	-----	Outcrop	Gabbronorite	PRI	0.66	0,60 [b]	11000	3.7	11.0	+ 13,7 [c]
DC-54	-----	Outcrop	Gabbronorite	PRI	0.31	0,60 [b]	5167	6.9	8.1	+ 12,5 [c]
DC-64	26117	609.2	PGE-rich layer	PRI	0.59	1,90 [b]	3105	299.0	1630.0	+ 2,5 [c]
DC-61	26117	627.8	Ol-gabbronorite	PRI	1.50	4,20 [b]	3571	124.0	501.0	+ 7,5 [c]
DC-60	26117	683.4	Gabbronorite	PRI	1.57	1,00 [b]	15700	50.0	105.0	+ 10,4 [c]
DC-72	26117	703.5	Gabbronorite	PRI	4.65	9,60 [b]	4844	5.4	120.0	+ 13,6 [c]
DC-27	26117	708.3	Gabbronorite	PRI	0.77	0,60 [b]	12833	13.0	23.0	+ 14,5 [c]
DC-49	26117	727.5	Gabbronorite	PRI	0.20	0,20 [b]	10000	2.5	5.4	+ 8,2 [c]
DC-53	26117	741.2	Ol-gabbronorite	PRI	0.15	0,20 [b]	7500	10.0	39.0	+ 6,7 [c]
DC-55	26117	753.9	Ol-gabbronorite	PRI	1.11	2,40 [b]	4625	42.0	174.0	+ 9 [c]
DC-63	26143	252.3	Gabbronorite	PRI	2.45	2,20 [b]	11136	16.0	63.0	+ 7,1 [c]
DC-62	26107	627.5	PGE-rich layer	PRI	1.69	8,20 [b]	2061	560.0	2251.0	+ 1,6 [c]
DC-58	26107	682.5	Ol-gabbronorite	PRI	2.00	4,60 [b]	4348	161.0	712.0	+ 6,6 [c]
DC-56	26107	702.8	Ol-gabbronorite	PRI	1.44	3,20 [b]	4500	112.0	402.0	+ 9,2 [c]
DC-79	26107	718	Ol-gabbronorite	PRI	1.12	3,50 [b]	3200	164.0	583.0	+ 7,6 [c]
DC-66	26107	721.7	Gabbronorite	PRI	4.32	5,90 [b]	7322	35.0	464.0	+ 9,8 [c]
Mesaba (Babbitt)										
B1-46-05	B1-46	85.0	Xenolith (BPU)	PRI	2.72	1.4	19049	1.7	3.5	
B1-46-11	B1-46	93.3	Xenolith (BPU)	PRI	4,55 [a]	2.2	20801	n.d.	n.d.	
B1-129-18	B1-129	439.2	Xenolith (BPU)	PRI	7,55 [a]	2.5	30368	n.d.	n.d.	
B1-129-09	B1-129	558.5	Xenolith (BPU)	PRI	6,75 [a]	7.9	8522	n.d.	n.d.	
B1-384-05	B1-384	222.8	Ol-gabbronorite	PRI	1.77	6,66 [b]	2655	109.4	426.9	
B1-384-08	B1-384	260.0	Ol-gabbronorite	PRI	1.80	5,43 [b]	3308	422.5	1393.4	
B1-384-10	B1-384	285.3	Ol-gabbronorite	PRI	4.04	14,96 [b]	2703	58.6	296.1	
B1-384-11	B1-384	300.5	Ol-gabbronorite	PRI	1.91	6,32 [b]	3025	59.7	510.6	
B1-384-24	B1-384	322.2	Gabbronorite	PRI	3.17	4.1	7718	13.6	43.1	
B1-384-26	B1-384	325.3	Xenolith (BPU)	PRI	3.74	3.7	10059	9.3	41.7	+ 17,26
B1-384-27	B1-384	329.5	Gabbronorite	PRI	2.31	4,35 [b]	5315	105.5	1132.2	
B1-384-28	B1-384	334.2	Massive sulfide	PRI	19,75 [a]	21,44 [b]	9212	n.d.	n.d.	
B1-384-13	B1-384	335.4	Gabbronorite	PRI	1.72	1.9	9219	10.3	27.1	
B1-384-14	B1-384	336.3	Xenolith (BPU)	PRI	7,13 [a]	6.1	11595	n.d.	n.d.	
B1-384-16	B1-384	348.8	Gabbronorite	PRI	7.17	9,86 [b]	7274	9.3	36.8	
B1-384-33	B1-384	350.8	Xenolith (BPU)	PRI	5,33 [a]	2.3	23638	n.d.	n.d.	
B1-384-34	B1-384	352.3	Xenolith (BPU)	PRI	5.22	2.7	19156	1.5	3.8	+ 11,65
B1-384-35	B1-384	353.4	Xenolith (BPU)	PRI	6,38 [a]	2.4	26211	n.d.	n.d.	
B1-384-19	B1-384	354.1	Xenolith (BPU)	PRI	5.48	2.5	22351	0.9	12.5	+ 11,53

Table 2. Whole-rock concentrations of Se, S, Pt, Pd and $\delta^{34}S$

Samples	Borehole	Depth (m)	Lithology	Unit	S (%)	Se (ppm)	S/Se	Pt (ppb)	Pd (ppb)	$\delta^{34}S$ (‰VCDT)
B1-384-36	B1-384	355.6	Xenolith (BPU)	PRI	6,36 [a]	2.8	22425	n.d.	n.d.	
B1-384-21	B1-384	359.3	Ol-gabbronorite	PRI	0.29	0.7	4094	5.1	16.5	
B1-384-23	B1-384	363.9	Ol-gabbronorite	PRI	2.81	5,80 [b]	4841	168.3	39.0	
B1-384-39	B1-384	380.0	Massive sulfide	PRI	25,07 [a]	24,51 [b]	10228	n.d.	n.d.	
B1-384-42	B1-384	380.5	Gabbronorite		6.31	9,46 [b]	6668	1.9	92.0	
Wyman Creek										
26133-9	26133	217	Xenolith (Virg. F.)	PRI	0.85	2.3	3768	n.d.	n.d.	+ 7,11
26133-13	26133	481	Virginia Formation	Met VF.	0.28	0.3	9622	4.0	1.1	+ 5,91
Water Hen										
CN7-7	CN7	490	Xenolith (BPU)	PRI	1.44	1.6	8863	13.7	23.4	+ 16,57
Serpentine deposit										
B1-175-01	B1-175	23.9	Ol-gabbronorite	SKI	3.21	5.5	5854	18.4	133.0	
B1-175-03	B1-175	59.1	Ol-gabbronorite	SKI	3.98	4.2	9581	26.0	100.3	
B1-175-06	B1-175	85.3	Ol-gabbronorite	SKI	0.92	1.3	7328	17.4	60.0	
B1-175-07	B1-175	96.9	Gabbronorite	SKI	7.08	5.8	12263	6.7	84.3	
B1-175-08	B1-175	98.9	Xenolith (BPU)	SKI	1.29	0.8	16564	9.0	11.2	
B1-175-09	B1-175	102.7	Gabbronorite	SKI	8.35	4.9	17150	10.6	59.1	
B1-175-10	B1-175	111.3	Ol-gabbronorite	SKI	3.17	5.0	6323	38.8	88.1	
B1-175-11	B1-175	118.0	Ol-gabbronorite	SKI	2.02	2.6	7665	85.6	65.8	
B1-175-13	B1-175	122.8	Ol-gabbronorite	SKI	4.78	5.0	9495	16.2	49.4	
B1-175-14	B1-175	128.3	Gabbronorite	SKI	2.40	2.1	11196	2.6	13.8	
B1-175-15	B1-175	149.6	Xenolith (BPU)	SKI	4.53	1.6	27951	4.8	17.9	
B1-175-26	B1-175	148.6	Xenolith (BPU)	SKI	4.88	1.1	46438	0.9	8.2	
B1-175-27	B1-175	150.8	Xenolith (BPU)	SKI	5.48	1.4	38563	2.6	23.0	
B1-175-16	B1-175	151.5	Xenolith (BPU)	SKI	6.52	1.0	65832	0.7	39.2	
B1-175-28	B1-175	153.2	Gabbronorite	SKI	0.68	1.1	6296	2.3	7.1	
B1-175-17	B1-175	168.5	Ol-gabbronorite	SKI	4.58	5.2	8774	21.8	55.8	
B1-175-29	B1-175	172.2	Ol-gabbronorite	SKI	2.33	3.3	7088	70.4	91.8	
B1-175-30	B1-175	175.6	Ol-gabbronorite	SKI	3.00	3.9	7643	25.5	68.7	

[a] S-determination by infrared spectrometry sulfur-carbon analyzer (this study); all other S by LECO titration.

[b] Se-determination by INAA; all other Se by TCF-INAA.

[c] $\delta^{34}S$-determination from Thériault and Barnes (1998), all other $\delta^{34}S$ analyses from this study

PGE-determination by Ni-sulfide fire assay followed by INAA

Abbreviations: BPU = Bedded Pyrrhotite Unit, PRI = Partridge River intrusion, SKI = South Kawishiwi intrusion, Unmet VF = Unmetamorphosed Virginia Formation, Met VF = Metamorphosed Virginia Formation, RXTAL = Recrystallized Unit (Severson et al., 1994), DISRUPT = Disrupted Unit (Severson et al., 1994), Ol = Olivine, n.d. = no data.

S isotopes

The histogram in Figure 5 illustrates the range in whole rock $\delta^{34}S$ values for the different rock types. The $\delta^{34}S$ values of the unmetamorphosed Virginia Formation fall within the range +4.5 to +10‰, with an average value of +6.8‰. The contact aureole samples of the Virginia Formation have slightly lower, but similar $\delta^{34}S$ values, between +2.9 and +6.5‰ (average +5.4‰). The range in $\delta^{34}S$ values for the BPU samples is similar for samples from both unmetamorphosed (+16.3‰) and contact aureole (+15.0 to +20.4‰, average +17.9‰) samples. The $\delta^{34}S$ values of the xenolith samples overlap with those of the contact aureole samples, but have a slightly lower range (+11.5 to +17.3‰, average +14.3‰). These results are consistent with data compiled by Hauck et al. (1997).

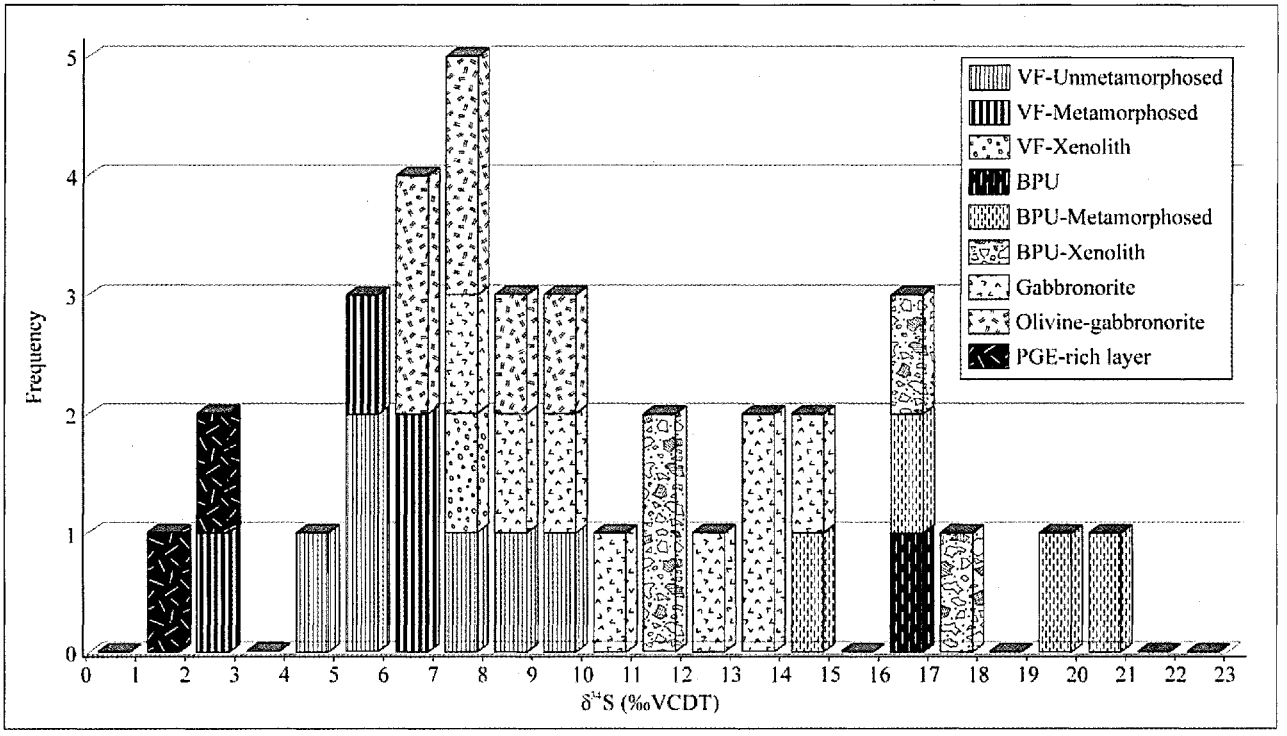

FIG. 5. Histogram showing the range of whole-rock $\delta^{34}S$ for unmetamorphosed and metamorphosed rocks of the Virginia Formation, including the Bedded Pyrrhotite Unit. The sulfide-bearing igneous rocks are fromThériault and Barnes (1998). Abbreviations: BPU = Bedded Pyrrhotite Unit, VF = Virginia Formation.

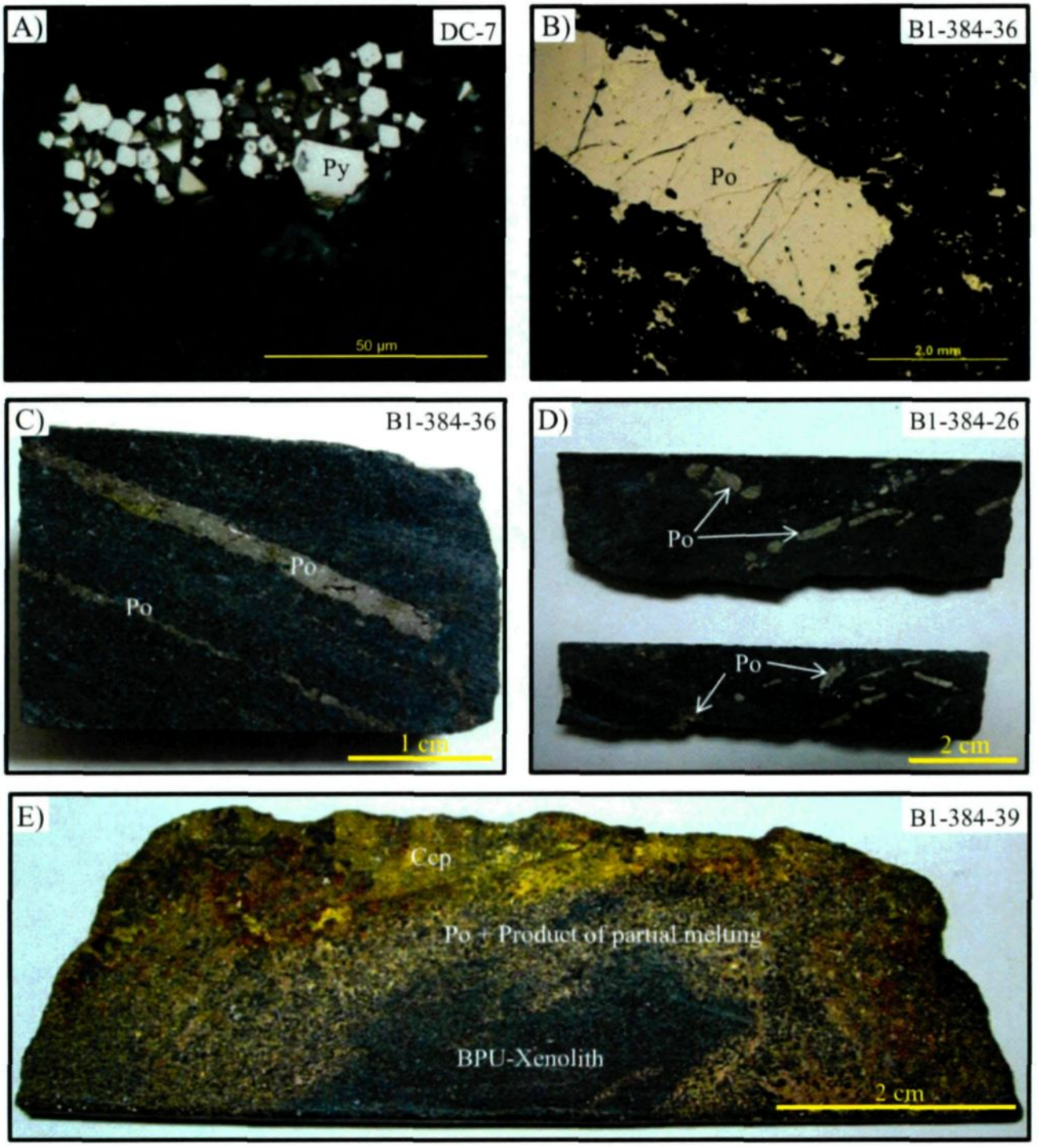

FIG. 6. Photographs and photomicrographs of rock textures from the Virginia Formation and the Bedded Pyrrhotite Unit. A. Cubic pyrite in unmetamorphosed pelites from B2 borehole. B. Bedded pyrrhotite within a BPU-xenolith. C. Lamination of pyrrhotite ranging 1-3 mm thick within a BPU-xenolith. D. Fragments of pyrrhotite beds within a BPU-xenolith. E. Crystallization of matrix sulfides (Po) with the product of the partial melting of the xenolith around a BPU-xenolith (Babbitt deposit). Sample numbers are indicated at top right. Abbreviations: Py = pyrite, Po = pyrrhotite, Ccp = chalcopyrite.

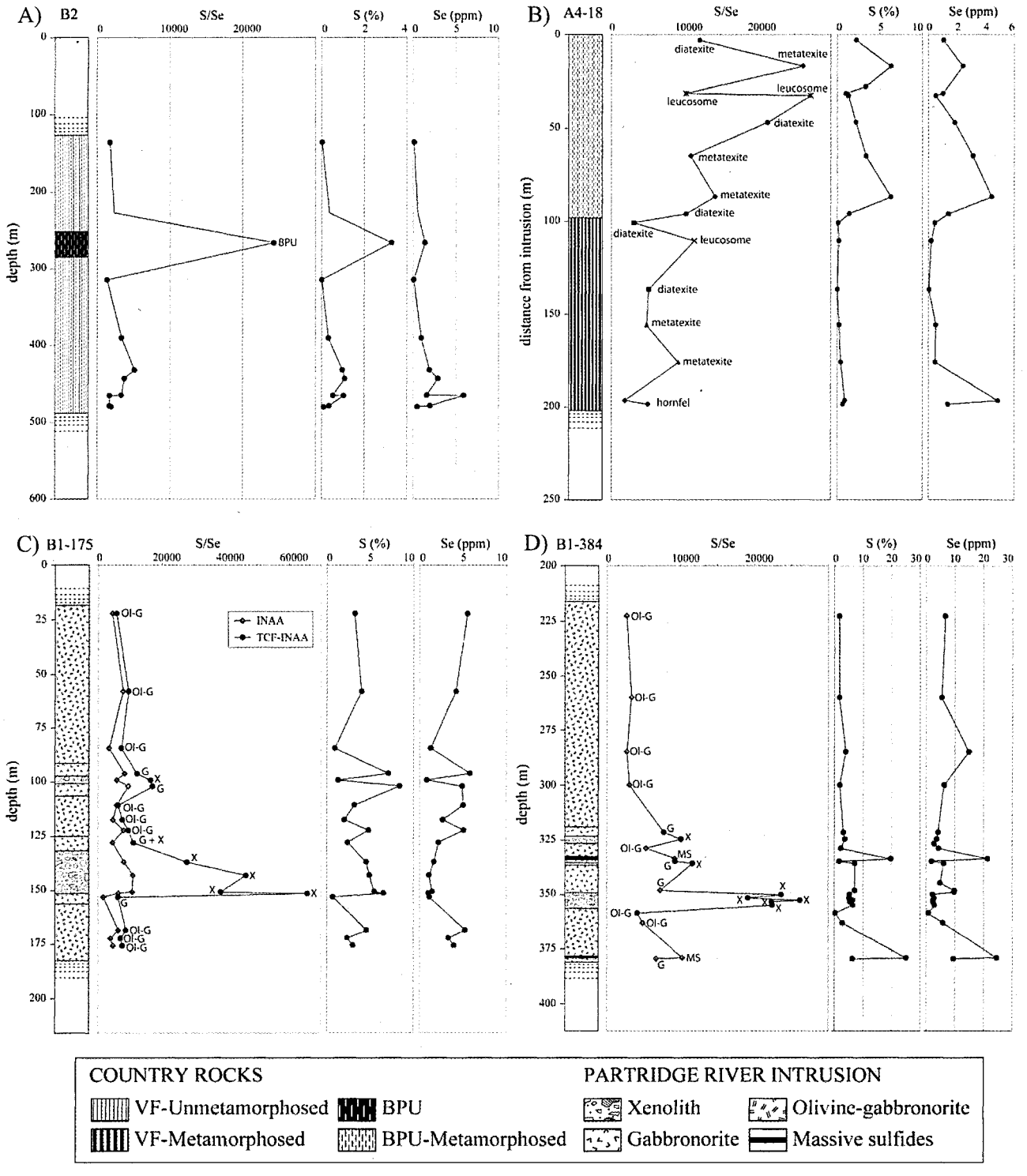

FIG. 7. Variations of S/Se, S and Se values with depth in meters in four borehole sections. A. B2 from unmetamorphosed Virginia Formation. B. A4-18 from Wetlegs (with depth replaced by distance from the PRI). C. B1-175 from Serpentine deposit. D. B1-384 from Babbitt. Simplified stratigraphic logs for each borehole are located to the left of each cross section. Abbreviations: BPU = Bedded Pyrrhotite Unit, Ol-G = Olivine-gabbronorite, G = Gabbronorite, X = xenolith, MS = massive sulfide.

Discussion

Contribution of Se-determination by TCF-INAA and its influence on S/Se ratios

The TCF-INAA technique provides better accuracy and precision for measuring low concentrations of Se in rocks. This can be illustrated by examining the results for the S/Se ratios from the borehole section B1-175 (Fig. 7C) as determined by TCF-INAA versus results for INAA alone. For the igneous rocks, both methods of determining Se have approximately the same S/Se ratio values. For the xenoliths, the values of S/Se ratios using Se-determination by TCF-INAA are significantly higher. We believe that the INAA results are incorrect, probably due to a combination of Se being too close to the detection limit of this method and due to interferences from the high incompatible element concentrations in the sediments. Similar differences were found in the S/Se ratios for other borehole sections where we have both INAA and TCF-INAA data. In general then, we believe that older Se data from sedimentary rocks should be discarded. Low quality Se data will affect the S/Se ratio and distort any following interpretation. Therefore, the accurate determination of Se in rocks is very important.

The S/Se ratios of the non-BPU Virginia Formation

In contrast to the findings of previous studies, we suggest that not all of the rocks of the Virginia Formation have high S/Se ratios. For the Virginia Formation, Ripley (1990) and Thériault and Barnes (1998) reported a wide range in the values of S/Se ratios (2333-67 000) in unmetamorphosed rocks, with most of the results being higher than 10 000. For samples not from the BPU, our results indicate a narrower range in the values of S/Se ratios (~3000: Table 2, Fig. 7A), which is lower than many of the mineralized samples. As discussed above, the older Se values for sedimentary rocks are probably incorrect.

The samples from the contact aureole of the Virginia Formation other than the BPU display approximately the same range in the values of S/Se ratios as unmetamorphosed samples (Table 2, Fig. 7B). These metapelitic rocks composed mainly of metatexite and diatexite, called Disrupted and Recrystallized Units respectively by Severson et al. (1994), are characterized by S/Se ratios lower than sulfide-bearing igneous rocks (< 10 000). The S and Se concentrations decrease progressively depending on the intensity of metamorphism, from hornfels to metatexite and to diatexite (Table 2, Fig. 7B). However, the S/Se ratios do not appear to be affected by the same decrease in the values and it seems to preserve its pre-partial melting values, as suggested by Ripley (1990).

These results show also that most of the pelitic and metapelitic rocks of the Virginia Formation are characterized by low, close to the mantle value, S/Se ratios. The S/Se ratios values of these sediments are much lower than most sulfide-bearing igneous rocks and massive sulfides (Fig. 7). Therefore, the contamination by these S-poor rocks cannot contribute to an increase of the S/Se ratio of the magma because any increase is limited and cannot exceed the maximum S/Se ratio of the sediments.

The S/Se and S isotope ratios of the BPU

Only the BPU samples have sufficiently high S/Se ratios to increase the S/Se ratio of gabbronorites to the current values by S-contamination. The average values of S/Se ratios of unmetamorphosed and metamorphosed rocks of the BPU are much higher than the average value of S/Se ratio of the gabbronorite-hosted disseminated sulfide from the Babbitt, the Dunka Road and the Serpentine deposits. Same as the footwall rocks without sulfides, S and Se concentrations decrease with an increase in the metamorphic grade (metatexite, diatexite, leucosome) but S/Se ratios seem to be unchanged and the values remain relatively high, despite the intensity of the

metamorphism. Even the two samples of leucosome, marked by an obvious S- and Se-depletion, have high S/Se ratios and seem to preserve their original high values.

The difference in the values of the S/Se ratios between the BPU and the rest of the Virginia Formation could be explained by the contrast in the depositional process of the sediments. During the sedimentation of the BPU, a significant contribution of S relative to Se, and thus an increase of S/Se ratio, has allowed the crystallization of laminated pyrrhotite, leading to the formation of the BPU. The specific conditions for the formation of the BPU remain unclear, but one hypothesis to explain the high S/Se ratio could be a distinct episode of chemical sedimentation during the clastic cycle of the Virginia Formation. Another hypothesis is the S-migration in preferential layers during the sedimentation cycle.

The $\delta^{34}S$ values of the BPU are very high compared to the unmetamorphosed metapelites and higher than the gabbronorites. The BPU is the only unit of the Virginia Formation with a range of values that can generate such significant deviations in the S/Se ratios and $\delta^{34}S$ values in the igneous rocks and could be the main source of additional crustal S in the PRI and the SKI.

The S/Se and S isotope ratios of the xenoliths

A large proportion of xenoliths are characterized by S/Se ratios intermediate between those of the BPU and the gabbronorites, suggesting a transition between the contaminating footwall rocks and the contaminated magma. The xenoliths of the Virginia Formation are mainly concentrated at the base of the intrusions and the volume proportion can reach 25% in the Babbitt deposit (Severson et al., 1996). Most of the xenoliths analyzed were derived from the BPU (Fig. 6B, C, D) and support the observation made by Williams et al. (2010) based on three drill-cores (B1-135, B1-189 and B1-127) from the Babbitt deposit. In B1-175 and B1-384 borehole sections, all the xenoliths have S/Se ratios higher than 10 000, some can exceed 65 000 (Fig. 4C, D; Table

2), making them the highest values found in the PRI and SKI. These S/Se ratios are generated by a high concentration of S relative to Se (Fig. 4B), proportion directly inherited from the BPU.

Most of the $\delta^{34}S$ values of the BPU-xenoliths are also intermediate between the BPU and the gabbronorite-hosted disseminated sulfide, demonstrating once more their transitional nature. The range in the values (+11.53‰ to +17.26‰, average of +14.25‰) falls within the same range of values (+6.3‰ to +29.1‰, average of +19.4‰) found by Zanko et al. (1994) in a BPU-xenolith from the Serpentine Deposit in the SKI. The thickness of the xenolith fragment (17 m) and thus the localization of the sampling could explain the slight difference in the values compared to this study.

There is a close stratigraphic association between the BPU-xenoliths and the gabbronorite, coupled with high values of S/Se ratios (Fig. 4). In both borehole sections, the gabbronorite has crystallized under and above fragments of xenoliths. The S/Se ratio decreases progressively from the BPU to the gabbronorites, which are highly contaminated by the S of the BPU-xenolith, and finally to the olivine-gabbronorites, which are less contaminated.

In addition, massive sulfides are found in close proximity to the BPU-xenolith. The B1-384-39 sample shows evidence of a genetic link between a BPU-xenolith and the crystallization of a large amount of magmatic sulfides at its periphery (Fig. 6E). A thin bed of pyrrhotite has been preserved in the center of the restitic core of this xenolith, while a large proportion of the border has undergone partial melting, resulting in the crystallization of matrix pyrrhotite and pods of chalcopyrite. Both of these are injected by an interstitial product of the partial melting of the xenolith (Fig. 6E). This textural association has not been highlighted in the Babbitt deposit until now. Thériault and Barnes (1998) reported the presence of pyrrhotite-rich massive sulfides as pods near the country-rock xenoliths in the Dunka Road deposit and Severson (1994) and Zanko et al. (1994) noted the distribution of basal massive sulfides around the BPU-xenoliths in the SKI.

The xenolith sample (26133-09) from borehole 26133 is characterized by a lower S/Se ratio (3768) and $\delta^{34}S$ value (+7.11‰), both close to the pelitic and metapelitic rocks of the non-BPU Virginia Formation. At Wyman Creek, the footwall rocks consist mainly of these metapelites, with values of S/Se ratio (9622) and $\delta^{34}S$ (+5.91‰) in the same range as the unmetamorphosed metapelites (B2 borehole) and metamorphosed metapelites (A4-18 borehole). There are few observations of BPU in the Wyman Creek area (Duschene, 2004), indicating that the xenolith is derived from the metapelite footwall rocks rather than the BPU, and thus explaining the low S/Se ratio and $\delta^{34}S$ values of this xenolith compared to the others described above. In addition, there is no association found between the xenolith and the gabbronorite hosted disseminated sulfides at this stratigraphic level (Fig. 2). Unfortunately, the hypothetical presence of xenoliths close to the sulfide mineralization, located below 350 meters, could not be examined due to a lack of samples.

Implication for the formation of the Cu-Ni deposits

These observations suggest a relationship between the S-rich BPU, the xenoliths derived from this BPU and the contamination by crustal S in the PRI and SKI. Plots of S/Se versus Pt+Pd and S/Se versus $\delta^{34}S$ (Figs. 8 and 9) show that the samples from the BPU and xenoliths derived from the BPU form a continuation of the linear trend. These trends indicate that the BPU is the source of the S in the mineralized zone. The eleven samples of S-poor pelitic rocks from the Virginia Formation are all located outside the field defined by the linear correlation. Their position in the diagrams, highlighting their low values of S/Se ratios and $\delta^{34}S$, indicates that these pelites cannot have contributed to an increase in the S/Se ratios and the $\delta^{34}S$ values of the gabbronorites, massive sulfides or most olivine-gabbronorites.

Based on these observations, we think that the key factor leading to the S-saturation into the

PRI and SKI is the *in situ* assimilation of S from BPU-xenoliths and not the contamination and homogenization by S prior to the emplacement of the intrusions. The regular decrease in S/Se ratios and $\delta^{34}S$ values from the BPU, to the BPU-xenoliths, to the gabbronorite, to the olivine-gabbronorite and to the PGE-rich layer point to a gradual mixing between S of crustal origin and S of mantle-origin. The S/Se ratios and $\delta^{34}S$ values of the S-rich BPU-xenoliths suggest that they represent transitional stages, and thus the mechanism of S-transfer between the BPU and the gabbronorite-hosted disseminated sulfide. A similar process of S-contamination triggered by xenoliths has been suggested by numerous studies on analogous types of magmatic Ni-Cu-PGE sulfides deposits (e.g., Barnes and Francis, 1995; Lesher and Burnham, 2001; Ripley et al., 2002; Barnes and Lightfoot, 2005). The melting of BPU-xenoliths released S and Se gradually and increased the S/Se ratio and the $\delta^{34}S$ value of the contaminated magma. The impact of crustal S and Se on the S/Se ratio of igneous rocks decreases progressively from the margin toward the interior of the intrusions.

Influence of the location of the BPU

Our results emphasize the important control the BPU had on the S-contamination of the PRI and the SKI. Assuming that *in situ* assimilation is responsible for the S-saturation of the mafic magma, both the location and the volume of the assimilated BPU have a critical influence. The BPU is not a continuous unit in the Virginia Formation (Severson et al., 2009) and is not present at all localities or stratigraphic levels in the vicinity of the intrusion. This heterogeneous distribution of the BPU could be one of the reasons for the erratic distribution of sulfide mineralization in the PRI (Rao and Ripley, 1983, Ripley and Alawi, 1986). Moreover, most of massive sulfides are found in the Local Boy/Tiger Boy area of the Babbitt deposit around and within large xenoliths in the lower portion of PRI (Hauck et al., 1997; Thériault et al., 2000), where the assimilation by

magmatic dissolution would have been the most effective. In contrast, the stratigraphic cross-section of the Babbitt deposit shows that the BPU is preserved in the upper portion (Severson et al., 1994), indicating a less marked magmatic digestion of the BPU at the boundary of the intrusion. The efficiency of the assimilation process, coupled with the location of the BPU, influence the degree of S-contamination in the surrounding magma.

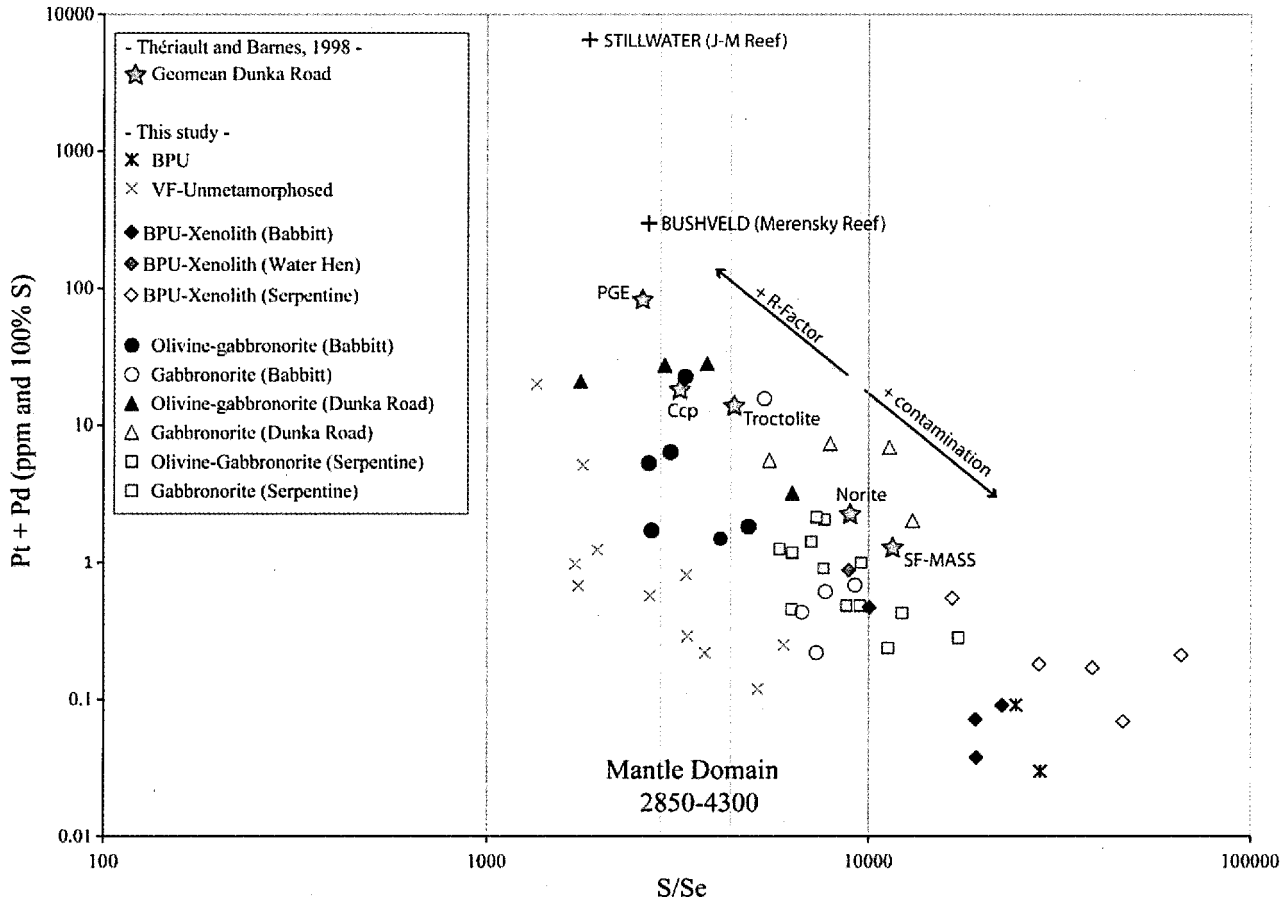

FIG. 8. Plot of Pt+Pd versus S/Se, illustrating the linear correlation between the BPU, the BPU-xenoliths with the sulfide-bearing igneous rocks and a PGE-rich layer. The mantle domain S/Se values are taken from Eckstrand and Hulbert (1987). The data of the J-M Reef and Merensky Reef are taken from Godel et al. (2007), Godel and Barnes (2008) and Barnes et al. (2009). Abbreviations: Ccp = chalcopyrite-rich sulfide, SF-MASS = pyrrhotite-rich massive sulfide, VF = Virginia Formation, BPU = Bedded Pyrrhotite Unit, Geomean = geometric mean, VCDT = Vienna Cañon Diablo Troilite (international standard).

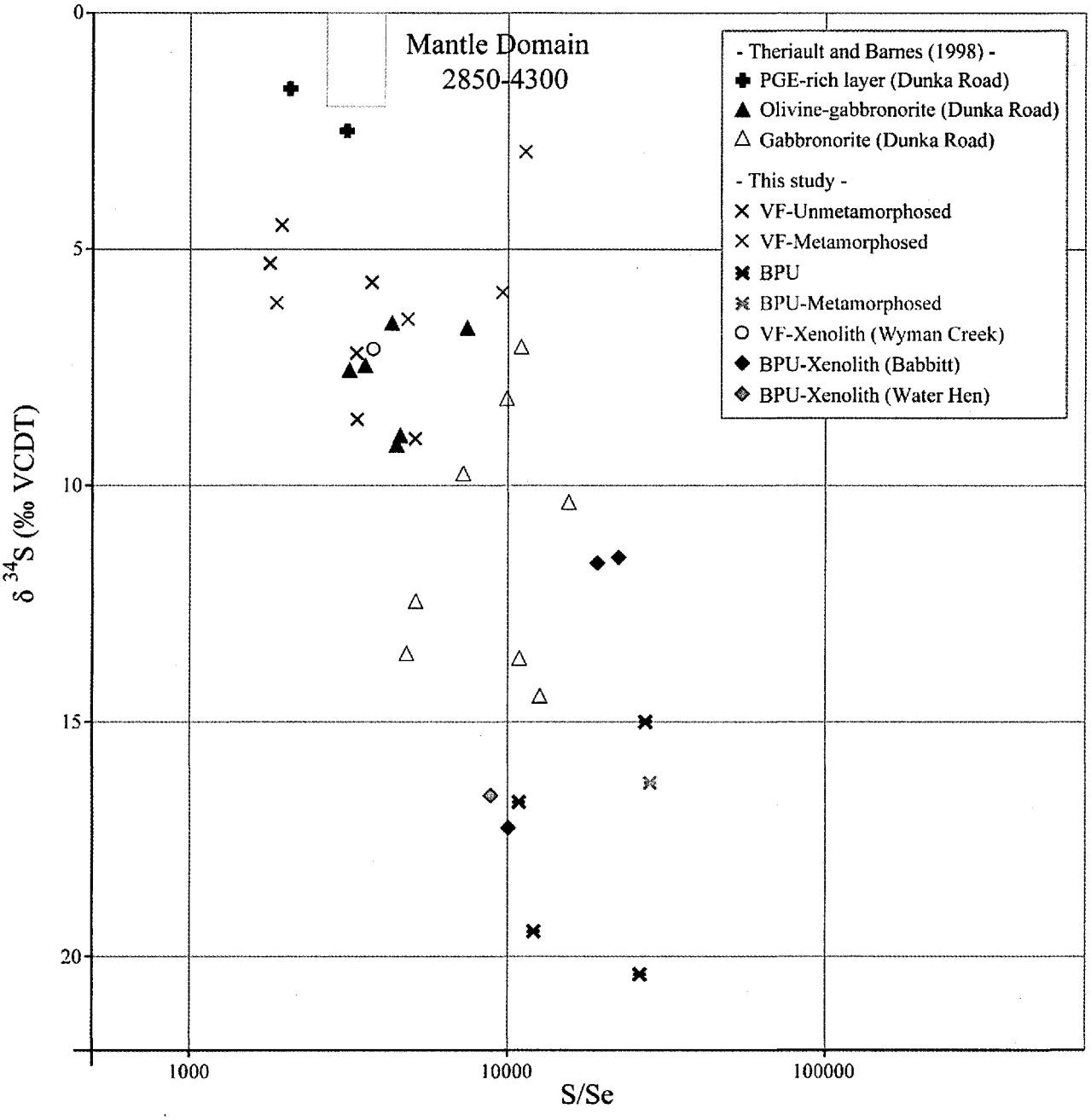

FIG. 9. Plot of $\delta^{34}S$ versus S/Se ratio illustrating the linear correlation between BPU and BPU-xenoliths with sulfide-bearing igneous rocks and PGE-rich layer from Dunka Road deposit. S/Se ratios and $\delta^{34}S$ values from the sulfide-bearing igneous rocks are taken from Thériault and Barnes (1998). Abbreviations: VF = Virginia Formation, BPU = Bedded Pyrrhotite Unit.

Proposed model for S-contamination of the PRI and SKI

The history of S-assimilation and the evolution of S/Se ratios in the PRI and the SKI can be described as follows and elaborates on the model suggested by Thériault and Barnes (1998) at Dunka Road:

1) The major pulse of S-undersaturated magma, with S/Se ratios similar to the mantle values (S/Se = 3000), was emplaced into the crust. The heat and turbulence of the magma caused an erosion of footwall rocks, leading to an extraction of rock fragments and their incorporation into the magma as xenoliths (Fig. 10A). In the PRI, the Virginia Formation makes up most of the underlying footwall rocks. These xenoliths were heated by the magma, causing melting. If only fractional melting took place, the unmelted portion of the xenolith was preserved as restitic fragments trapped in the intrusion, while the melted portion migrated into the surrounding magma, as xenomelt (Lesher and Burnham, 2001) and generated the contamination. In the case of total melting, the entire xenolith is dissolved and mixed into the magma, allowing optimal contamination.

2) The lithology of the rock assimilated, and especially the presence of sulfides, controlled the behavior of the S/Se ratio in the igneous rocks. The assimilation of metapelitic rocks of the Virginia Formation containing no sulfides (S-poor, low S/Se ratio and low $\delta^{34}S$ value) would not have released a significant concentration of S; the S/Se and $\delta^{34}S$ values of the adjacent magma would have remained more or less unchanged (Fig. 10C). These metapelitic rocks cannot be the main source of the assimilated S because their S/Se ratios and $\delta^{34}S$ values are too low with respect to the S/Se of the gabbronorites, the massive sulfides and even the olivine-gabbronorites. In contrast, a large amount of S was released into the magma by the dissolution of the S-rich

xenoliths of the BPU (high S/Se ratios and high $\delta^{34}S$ values), producing an increase in the S/Se ratios and $\delta^{34}S$ values into the mafic melt (Fig. 10B).

3) In both cases, the assimilation of xenoliths is accompanied by an important input of SiO_2 (Fig. 7A, B, C) causing the crystallization of orthopyroxene rather than olivine, and thus the crystallization of gabbronorites (Ripley and Alawi, 1988; Thériault and Barnes, 1998). Melts of gabbronoritic composition contaminated by the BPU-xenoliths see their S/Se ratios and $\delta^{34}S$ values increased significantly. This gabbronoritic melt is colder due to the crustal contamination and crystallizes rapidly, trapping the interstitial sulfide liquid with a high S/Se ratio. Where the amount of assimilated S is large, the segregation of a sulfide liquid may have occurred leading to the formation of lenses of massive sulfide (Fig. 10B), which flowed down into the mafic melt to the base of the intrusions.

4) The S/Se ratios and $\delta^{34}S$ values decreased progressively from the gabbronorites, to the olivine-gabbronorites and to the PGE-rich layers, and they are related to the gradual transport of S towards the interior of the intrusion (Fig. 10A). The S in the highly contaminated gabbronorite-hosted disseminated sulfides is mainly crustal in origin, while the olivine-gabbronorite-hosted disseminated sulfides are composed of a mixture of crustal- and mantle-derived S. The PGE-rich layer could have formed from mantle-derived S of an uncontaminated magma (Thériault and Barnes, 1998), linked to a new injection of olivine-gabbronoritic (troctolitic) magma (Fig. 10A). The decrease of contamination is associated with an increase in the R-factor, leading to an increase in the PGE content from the gabbronorite, to the olivine-gabbronorite and to the PGE-rich layer (Thériault et al., 1997).

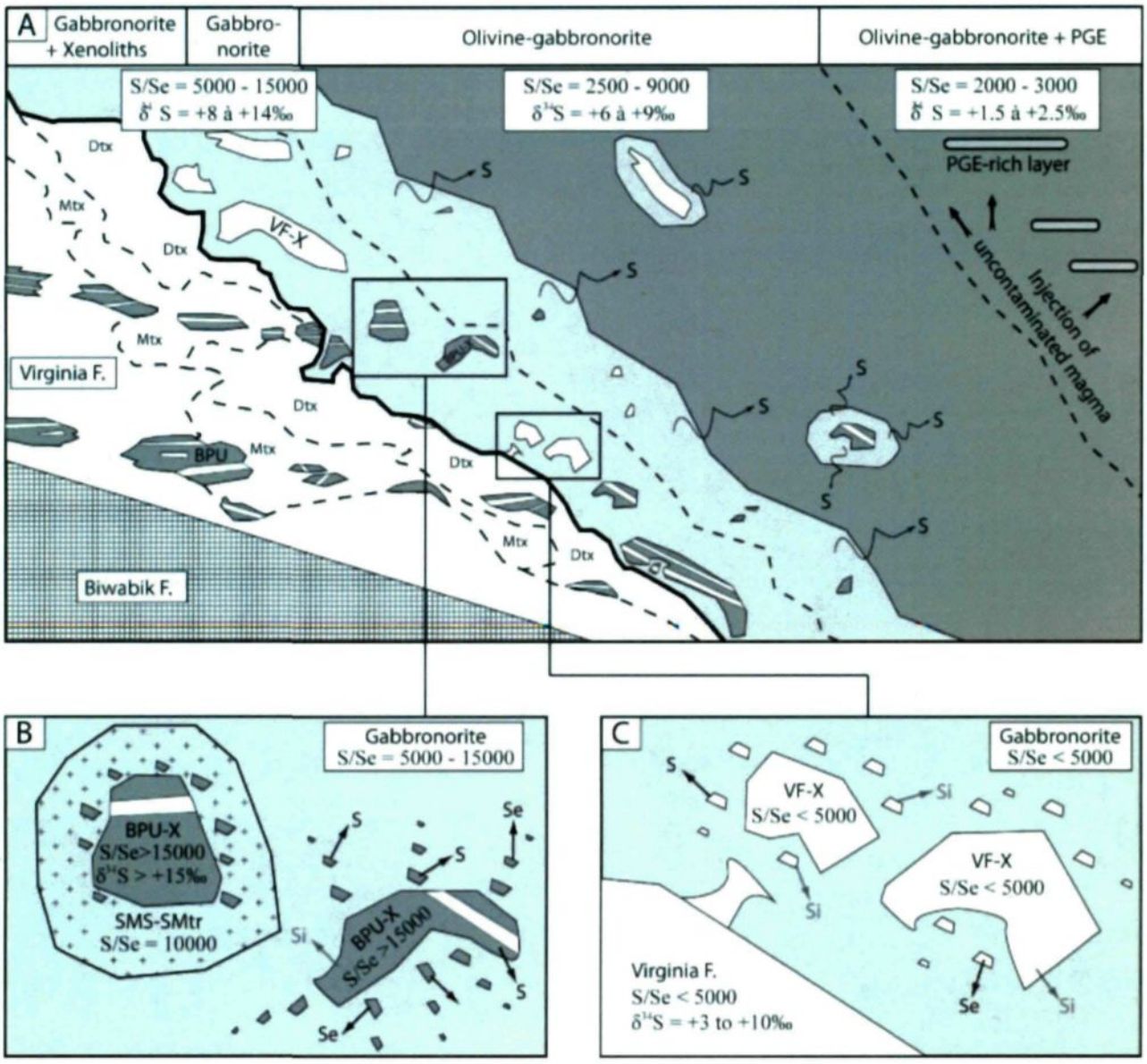

FIG. 10. Schematic model for the S-contamination of the PRI and SKI by country rocks and the evolution of the associated S/Se ratios. A. Assimilation of xenoliths from the Virginia Formation by the Partridge River intrusion. The input of Si promotes the crystallization of orthopyroxene and the formation of gabbronoritic melt. B. The contamination by BPU-xenoliths increases the S/Se ratios and the $\delta^{34}S$ values of the gabbronoritic melt. If the S-contamination is large, massive and matrix-related sulfides can form around BPU-xenoliths. C. The contamination by S-poor metapelitic rocks of the Virginia Formation cannot contribute to increased S/Se ratios and the $\delta^{34}S$ values of the gabbronoritic melt. Abbreviations: VF-X = Virginia Formation xenolith, BPU-X = Bedded Pyrrhotite Unit xenolith, Mtx = metatexite, Dtx = diatexite, SMS-SMtr = massive and matricial sulfides.

Conclusion

Based on the observed S/Se ratios and $\delta^{34}S$ values of the metapelitic rocks from the Virginia Formation, not all of its constituents can be the main source of S contaminating the Partridge River and South Kawishiwi intrusions. Only the BPU has sufficiently high S/Se ratios and $\delta^{34}S$ values to generate the S/Se ratios and $\delta^{34}S$ values found in the gabbronorite-hosted disseminated sulfides and massive sulfides. The BPU-xenoliths represent the transition phase between the BPU and the igneous rocks. The evolution of the S/Se ratios presented in this paper support the model for the formation of Cu-Ni sulfide deposits that involve S-saturation caused mainly by the *in situ* assimilation of xenoliths from the BPU. This conclusion is based on:

1) High S/Se ratios and $\delta^{34}S$ values of the BPU with respect to the values of most of the rocks of the Virginia Formation.

2) The S/Se ratios and $\delta^{34}S$ values of the xenoliths derived from the BPU, intermediate between the BPU and the gabbronorites, i.e., the most-contaminated igneous rocks.

3) The progressive decrease in the S/Se ratios and $\delta^{34}S$ values from the margin toward the interior of the intrusion, associated with an increase in the R-factor.

4) The stratigraphic proximity between the BPU-xenoliths and the gabbronorites, plus the high S/Se ratios associated with them.

5) The lack of decoupling between S and Se, and the apparent preservation of S/Se ratios, in the metamorphosed rocks, whatever the metamorphic grade.

6) The association of massive sulfides and xenomelts at the periphery of the BPU-xenoliths.

We suggest that the *in situ* assimilation is a more convincing alternative model of S-saturation than the early sulfide saturation model. The presence of the BPU in the vicinity of the Duluth Complex was critical to the formation of the Cu-Ni deposits.

Acknowledgments

Dr. Paul Bédard is thanked for his assistance with the preparation and the crushing of the samples. Dany Savard is thanked for his support with the TCF-INAA analyses and the sulfur determinations. Richard Heemskerk and the Environmental Isotope Laboratory are thanked for the sulfur isotope analyses. Dr. Sarah Dare and Dr. Philippe Pagé are also thanked for their helpful comments. This work was funded by the Canadian Research Chair in Magmatic Metallogeny and the Natural Sciences and Engineering Research Council of Canada.

REFERENCES

Andrews, M.S., and Ripley E.M., 1989, Mass transfer and sulfur fixation in the contact aureole of the Duluth Complex, Dunka Road Cu–Ni deposit, Minnesota: Canadian Mineralogist, v. 27, p. 293–310.

Barnes, S.-J., and Francis, D., 1995, The distribution of platinum-group elements, nickel, copper, and gold in the Muskox layered intrusion, Northwest Territories, Canada: Economic Geology, v. 90, p. 135–154.

Barnes, S.-J., and Lightfoot, P.C., 2005, Formation of magmatic nickel-sulfide ore deposits and processes affecting their copper and platinum-group element contents, *in* Hedenquist, J.W., Thompson, J.F.H., Goldfarb, R.J., and Richards, J.P., eds., Economic Geology 100th Anniversary Volume, p. 179–213.

Barnes, S.-J., and Maier, W.D., 2002, Platinum-group elements and microstructures of normal Merensky Reef from Impala platinum mines, Bushveld Complex: Journal of Petrology, v. 43, p.103–128.

Barnes, S.-J., Savard, D., Bédard, P., and Maier, W.D., 2009, Selenium and sulfur concentrations in the Bushveld Complex of South Africa and implications for formation of the platinum-group element deposits: Mineralium Deposita, v. 44, p. 647–663.

Bédard, L.P., Savard D.D., and Barnes, S.-J., 2008, Total sulfur concentration in geological reference materials by elemental infrared analyzer: Journal of Geostandards and Geoanalytical Research, v. 32, p. 203–208.

Duchesne, L., 2004. Fusion partielle et microstructures associées dans l'auréole de contact du complexe igné de Duluth, Minnesota: M.Sc. thesis, Université du Quebec à Chicoutimi, 217 p.

Eckstrand, O.R., and Hulbert, L.J., 1987, Selenium and the source of sulfur in magmatic nickel and platinum deposits (abs): Geological Association of Canada–Mineralogical Association Canada

Program with Abstracts, v.12, p.40.

Fitzpatrick, A.J., Kyser T.K., and Chipley, D., 2009, Selenium measurement in sulphides by hydride generation high-resolution inductively coupled plasma mass spectrometry: Geochemistry, Exploration, Environment Analysis, v. 9, p. 93–100.

Godel, B., and Barnes, S.-J., 2008, Platinum-group elements in sulfide minerals and the whole rocks of the J-M Reef (Stillwater Complex): implication for the formation of the reef: Chemical Geology, v. 248, p. 272–294.

Godel, B., Barnes, S.-J., and Maier, W.D., 2007, Platinum-group elements in sulphide minerals, platinum-group minerals, and the whole rocks of the Merensky Reef (Bushveld Complex, South Africa): Implication for the formation of the Reef: Journal of Petrology, v. 48, p. 1569–1604.

Hall, G.E.M., and Pelchat, J.-C., 1997a, Analysis of geological materials for bismuth, antimony, selenium and tellurium by continuous flow hydride generation inductively coupled plasma mass spectrometry; Part 2, Methodology and results: Journal of Analytical Atomic Spectrometry, v. 12, p. 103–106.

Hauck, S.A., Severson, M.J., Zanko, L., Barnes, S.-J., Morton, P., Alminas, H., Foord, E.E., and Dahlberg, E.H., 1997, An overview of the geology and oxide, sulfide, and platinum-group element mineralization along the western and northern contacts of the Duluth Complex, *in* Ojakangas, R.W., Dickas, A.B., and Green, J.C., eds., Middle Proterozoic to Cambrian rifting, central North America: Boulder, Colorado, Geological Society of America Special Paper 312, p. 137–185.

Lesher, C.M., and Burnham, O.M., 2001, Multicomponent elemental and isotopic mixing in Ni-Cu-(PGE) ores at Kambalda, Western Australia: Canadian Mineralogist, v. 39, p. 421–446.

Listerud, W.H., and Meineke, D.G., 1977, Mineral resources of a portion of the Duluth Complex and adjacent rocks in St. Louis and Lake Counties, northeastern Minnesota: Minnesota Department of Natural Resources, Division of Minerals, Report 93,74 p.

Lucente, M.E., and Morey, G.B., 1983, Stratigraphy and sedimentology of the Lower Proterozoic Virginia Formation, northern Minnesota: Minnesota Geological Survey, Report of Investigations RI-28, 28 p.

Mainwaring, P.R., and Naldrett, A.J., 1977, Country rock assimilation and genesis of Cu-Ni sulfides in the Water Hen Intrusion, Duluth Complex, Minnesota: Economic Geology, v. 72, p. 1269-1284.

McDonough, W.F., and Sun, S.S., 1995, The composition of the earth: Chemical Geology, v. 120, p. 223–253.

Miller, J.D., Jr. and Severson, M.J., 2002, Geology of the Duluth Complex *in* Miller, J.D., Jr., Green, J.C., Severson, M.J., Chandler, V.W., Hauck, S.A., Peterson, D.M., and Wahl, T.E., eds., Geology and mineral potential of the Duluth Complex and related rocks of northeastern Minnesota: Minnesota Geological Survey, Report of Investigations RI-58, p. 106-143.

Ojakangas, R.W., Morey, G.B., and Green, J.C., 2001, The Mesoproterozoic Midcontinent Rift System, Lake Superior Region, U.S.A., *in* Eriksson, P., Catuneanu, O., and Martins-Neto, M.,

eds., The influence of magmatism, tectonics, sea level change, and palaeoclimate on Precambrian basin evolution: change over time: Sedimentary Geology, v. 141.

Ojakangas, R.W., Morey, G.B., and Southwick, D.L., 2001, Paleoproterozoic basin development and sedimentation in the Lake Superior region, North America: Sedimentary Geology, v. 141, p. 319–341.

Paktunc, A.D., Hulbert, L.J., and Harris, D.C., 1990, Partitioning of the platinum group and other trace elements in sulfides from the Bushveld Complex and Canadian occurrences of nickel-copper sulfides: Canadian Mineralogist, v.28, p.475–489.

Rao, B.V., and Ripley, E.M., 1983, Petrochemical studies of the Dunka Road Cu-Ni deposit, Duluth Complex, Minnesota: Economic Geology, v. 78, p. 1222–1238.

Ripley, E.M., 1981, Sulfur isotopic studies of the Dunka Road Cu-Ni deposit, Duluth Complex, Minnesota: Economic Geology, v. 76, p. 610–620.

Ripley, E.M., 1990, Se/S ratios of the Virginia Formation and Cu-Ni mineralization in the Babbitt area, Duluth Complex, Minnesota: Economic Geology, v. 85, p.1935–1940.

Ripley, E.M., and Alawi, J.A., 1986, Sulfide mineralogy and chemical evolution of the Babbitt Cu–Ni deposit, Duluth Complex, Minnesota: Canadian Mineralogist, v. 24, p. 347–368.

Ripley, E.M., and Alawi, J.A., 1988, Petrogenesis of pelitic xenoliths at the Babbitt Cu–Ni deposit, Duluth Complex, Minnesota: Lithos, v. 21, p. 143–159.

Ripley, E.M., and Al-Jassar, T., 1987, Sulfur and oxygen isotopic studies of melt–country rock interaction, Babbitt Cu–Ni deposit, Duluth Complex, Minnesota: Economic Geology, v. 82, p. 87–107.

Ripley, E.M., Li, C., and Shin, D., 2002, Paragneiss assimilation in the genesis of magmatic Ni–Cu–Co sulfide mineralization at Voisey's Bay, Labrador: δ34S, δ13C and Se/S evidence: Economic Geology, v. 97, p. 1307–1318.

Ripley, E.M., Taib, N.I., Li, C., and Moore, C.H., 2007, Chemical and mineralogical heterogeneity in the basal zone of the Partridge River Intrusion: implications for the origin of Cu–Ni mineralization in the Duluth Complex, Midcontinent rift system: Contributions to Mineralogy and Petrology, v. 154, p. 35–54.

Savard, D., Bédard, L.P., and Barnes, S.-J., 2006, TCF selenium preconcentration in geological materials for determination at sub-μg g-1 with INAA (Se/TCF-INAA): Talanta, v. 70, p.566–571.

Severson, M.J., 1988, Geology and structure of a portion of the Partridge River intrusion: A progress report: University of Minnesota, Duluth, Natural Resources Research Institute, Technical Report, NRRI/GMIN-TR-88-08, 78 p.

Severson, M.J., 1994, Igneous stratigraphy of the South Kawishiwi Intrusion, Duluth Complex, northeastern Minnesota: University of Minnesota, Duluth, Natural Resources Research Institute, Technical Report, NRRI/TR-93/34, 210 p.

Severson, M.J., and Hauck, S.A., 2008, Finish logging of Duluth Complex drill core (and a reinterpretation of the geology at the Mesaba (Babbitt) deposit): University of Minnesota, Duluth, Natural Resources Research Institute, Technical Report, NRRI/TR-2008/17, 68 p.

Severson, M.J., Patelke, R.L., Hauck, S.A., and Zanko, L.M., 1996, The Babbitt copper-nickel deposit, part C: Igneous geology, footwall lithologies, and cross sections: Natural Resources Research Institute, Technical Report, NRRI/TR-94/21c, 79 p.

Severson, M.J., Oreskovich, J.A., and Patelke, M.M., 2009, Compile and make digital the lithologies for all NRRI drill logs, with emphasis on the Duluth Complex drill holes (An addendum to an earlier NRRI database): University of Minnesota, Duluth, Natural Resources Research Institute, Technical Report NRRI/TR-2009/33, 45 p.

Severson, M.J., Patelke, R.L., Hauck, S.A. and Zanko, L.M., 1994, The Babbitt Copper–Nickel deposit, Part B: Structural datums: University of Minnesota, Duluth, Natural Resources Research Institute, Technical Report NRRI/TR-94-21b, 51 p.

Thériault, R.M., and Barnes, S.-J., 1998, Compositional variations in Cu–Ni–PGE sulfides of the Dunka Road deposit, Duluth Complex, Minnesota: the importance of combined assimilation and magmatic processes: Canadian Mineralogist, v. 36, p. 869–886.

Thériault, R.M., Barnes, S.-J., and Severson, M.J., 1997, The influence of country-rock assimilation and silicate to sulfide ratios *(R* factor) on the genesis of the Dunka Road Cu-Ni-platinum-group element deposit, Duluth Complex, Minnesota: Canadian Journal of Earth Sciences, v. 34, p. 375–389.

Thériault, R.M., Barnes, S.-J., and Severson, M.J., 2000, Origin of Cu-Ni-PGE sulfide mineralization in the Partridge River Intrusion, Duluth Complex, Minnesota: Economic Geology, v. 95, p. 929–943.

Tyson, R.M., and Chang, L.L.Y., 1984, The petrology and sulfide mineralization of the Partridge River Troctolite, Duluth Complex, Minnesota: Canadian Mineralogist, v. 22, p. 23–38.

Williams, C.D., Ripley, E.M., and Li, C., 2010, Variations in Os isotope ratios of pyrrhotite as a result of water–rock and magma–rock interaction: Constraints from Virginia Formation–Duluth Complex contact zones: Geochimica et Cosmochimica Acta, v.74, p. 4772–4792.

Zanko, L.M., Severson, M.J., and Ripley, E.M., 1994, Geology and mineralization of the Serpentine Cu-Ni deposit: University of Minnesota, Duluth, Natural Resources Research Institute, Technical Report, NRRI/TR-93/52, 90 p.

CONCLUSION GÉNÉRALE

À travers les deux manuscrits proposés, ce mémoire de maîtrise retrace l'usage du rapport S/Se dans la caractérisation des processus pétrogénétiques des minéralisations de Ni-Cu-EGP puis propose une démarche scientifique originale avec la réalisation d'une étude consacrée au rapport S/Se des roches encaissantes du complexe de Duluth. Ces manuscrits s'intègrent de manière complémentaire dans un projet d'ensemble visant à accroître les connaissances sur l'utilisation du rapport S/Se dans les gisements magmatiques à sulfures de Ni-Cu-EGP.

Le manuscrit présenté au chapitre I synthétise les caractéristiques des rapports S/Se de la plupart des gisements magmatiques de Ni-Cu et d'EGP. En s'appuyant sur cette compilation, cette étude a permis de répertorier les différents processus affectant le rapport S/Se des dépôts Ni-Cu-EGP. Ces processus se divisent en 2 classes : 1) Les processus magmatiques incluent la contamination en S, l'influence du facteur R, la ségrégation du liquide sulfuré et le fractionnement du Se entre la MSS et l'ISS ; 2) Les processus tardi- à post-magmatiques englobent l'hydrothermalisme, le métamorphisme de haut grade, la serpentinisation et l'altération météorique. En fonction du type de dépôt, de l'origine du S et des processus subis, différents domaines du rapport S/Se ont été proposés. La majeure partie des gisements Ni-Cu possède des rapports S/Se élevés, des faibles concentrations en Pt+Pd, des faibles facteurs R et est formée par contamination en S, tandis que les gisements d'EGP ont des rapports S/Se faibles, des concentrations élevées en Pt+Pd, des facteurs R élevés et sont constitués de S dérivé du manteau. Entre ces deux domaines distincts, de nombreux gisements montrent un mélange entre le S d'origine crustale et le S d'origine mantellique. Un autre processus à considérer est la ségrégation du liquide sulfuré qui peut modifier significativement le rapport S/Se du magma fractionné

comme c'est le cas pour la Zone Supérieure du complexe du Bushveld. Enfin, les sulfures massifs de certains gisements (Sudbury, Noril'sk-Talnakh) montrent un fractionnement du Se entre la phase riche en Fe (solution solide monosulfurée : SSM) et la phase résiduelle riche en Cu (solution solide intermédiaire : SSI). Du fait de sa légère incompatibilité dans la SSM, le Se est enrichi dans la phase résiduelle riche en Cu et le rapport S/Se est donc plus faible dans la SSI que dans la SSM. Concernant les processus tardi- à post-magmatiques, le métamorphisme de haut grade ne concerne qu'un nombre restreint de gisements et demeure encore sujet à débat. Dans la plupart des gisements concernés, la remobilisation préférentielle du S par rapport au Se induit par l'hydrothermalisme, la serpentinisation et l'altération météorique entraîne une diminution modérée des valeurs du rapport S/Se. Tous les processus identifiés n'ont pas le même impact dans les variations du rapport S/Se et, dans la plupart des cas, l'origine du S contrôle en grande partie les valeurs du rapport S/Se. Ces processus se combinent et interagissent, simultanément ou successivement, et ils s'inscrivent donc dans un modèle dynamique témoignant de l'évolution du rapport S/Se depuis la fusion partielle mantellique et se poursuivant postérieurement à la mise en place du magma dans la croûte.

Les nombreuses applications du rapport S/Se lui confèrent un large éventail de possibilités de développement et de multiples investigations futures sont envisageables dont voici quelques pistes (liste non-exhaustive). De nombreux gisements restent à étudier où à réétudier en mettant en application les progrès analytiques dans la détermination du Se dans les roches. Plus particulièrement, les gisements dont les rapports S/Se datent de plus de 20 ans nécessiteraient une mise à jour des analyses en Se et la vérification des interprétations antérieures. Les roches minéralisées, ayant des concentrations en Se proches des limites de détection des techniques de mesures utilisées nécessiteraient également de nouvelles analyses. Des progrès dans la

compréhension des processus influençant les concentrations en S et en Se doivent être effectués, notamment lors d'épisodes métamorphiques de haut grade ou d'hydrothermalisme. Dans cette optique, de nouvelles études sur les gisements concernés (ex: O'Kiep, Curaçà Valley, Lac des Iles) se focalisant sur le rapport S/Se se révèleraient appropriées.

Le premier manuscrit s'achève sur quelques recommandations d'usage à respecter lors de l'utilisation du rapport S/Se. Parmi celles-ci, le couplage du rapport S/Se entre les roches minéralisées et les roches encaissantes est brièvement évoqué. En effet, le rapport S/Se des roches minéralisées utilisé indépendamment n'est pas un indicateur suffisamment fiable de la contamination s'il n'est pas comparé avec le rapport S/Se du contaminant potentiel. Le second manuscrit présenté dans ce mémoire et réalisé sur le complexe de Duluth s'inscrit donc comme un début d'investigation.

Le chapitre II a permis de mettre en évidence le rôle prépondérant exercé par les roches encaissantes du complexe de Duluth sur le développement des minéralisations et plus particulièrement sur les variations du rapport S/Se des roches minéralisées. La technique de dosage du Se par TCF-INAA a permis de distinguer des disparités importantes dans les valeurs du rapport S/Se entre les différentes lithologies composant la Formation de Virginia. Ces disparités n'avaient pas mises en évidence par les études antérieures car la technique de dosage du Se était inapproprié. La plupart des roches de la Formation de Virginia possède des rapports S/Se et des valeurs $\delta^{34}S$ inférieurs à ceux des roches magmatiques intrusives. L'Unité de Pyrrhotite Litée (UPL) est le seul horizon de la Formation de Virginia possédant des rapports S/Se et des valeurs $\delta^{34}S$ suffisamment élevés (18 438 et +18.22% respectivement) pour augmenter les valeurs en S/Se et $\delta^{34}S$ des roches ignées sulfurées par contamination crustale. Un

modèle impliquant un mélange entre le S magmatique et le S crustal est suggéré par la diminution progressive du rapport S/Se depuis la marge vers le cœur de l'intrusion magmatique, c'est-à-dire depuis l'UPL, aux xénolithes, aux gabbronorites, aux gabbronorites à olivine et finalement jusqu'aux horizons riches en EGP. Ces résultats soutiennent que la contamination en S crustal est principalement contrôlée par l'assimilation *in situ* de xénolithes dérivés de l'UPL. La réalisation de ce mécanisme est renforcée par les observations pétrographiques sur les xénolithes dérivés de l'UPL montrant des évidences de fusion partielle et le développement de sulfures semi-massifs au pourtour de ces xénolithes.

La présence de l'UPL joue un rôle fondamental dans la contamination en S de l'intrusion de *Partridge River* et, par incidence, sur le développement des dépôts Ni-Cu. Dans cette optique, la localisation de l'UPL peut donc représenter un outil d'exploration important dans la recherche de nouvelles zones minéralisées et donc dans l'accroissement des ressources potentielles du complexe intrusif de Duluth. Cette localisation peut cependant s'avérer difficile de par sa distribution erratique dans la formation de Virginia. Enfin, les mécanismes physiques de mélange permettant le transfert du S des sédiments encaissants vers le magma mafique sont encore mal compris et nécessitent une étude détaillée. Un projet de doctorat débute actuellement à l'Université du Québec à Chicoutimi pour déterminer les processus physico-chimiques de la fusion partielle des sédiments impliquée lors de l'assimilation *in situ* des roches encaissantes de la Formation de Virginia.

- ANNEXE 1 -

COMPILATION DES ANALYSES EN ÉLÉMENTS CHALCOPHILES (Ni, Cu, S, Se, Pt, Pd) DES GISEMENTS MAGMATIQUES À SULFURES DE Ni-Cu-EGP

Note : Dans un souci de cohérence avec la majeure partie des publications d'origines ainsi qu'avec les deux manuscrits présentés dans ce mémoire, les tableaux annexes sont renseignés en anglais.

Abbreviations

n	Number of samples
SF-MS	Massive sulfide
SF-Mtr	Matricial sulfide
SF-Diss	Disseminated sulfide
PGE	Platinum-Group Element
MSS	Monosulfide Solid-Solution
Inter	Mixing of MSS and ISS
ISS	Intermediate Solid-Solution
Ccp	Chalcopyrite
d.l.	Detection limit

Mining Camp	Rocktype/ore	Sample	n	Ni	Cu	Pt	Pd	S	Se	S/Se	references
Deposit				% wt	% wt	ppb	ppb	% wt	ppm		
North Range (Sudbury)											
Levack (N-Range)	Granophyre	212	-	0.00	0.00	d.l.	d.l.	0.01	0.01	10 833	Keays and Lightfoot, 2004
Levack (N-Range)	Granophyre	402	-	0.00	0.00	d.l.	0	0.02	0.02	11 765	Keays and Lightfoot, 2004
Levack (N-Range)	Granophyre	615	-	0.00	0.00	d.l.	1	0.02	0.05	4 348	Keays and Lightfoot, 2004
Levack (N-Range)	Granophyre	725	-	0.00	0.00	d.l.	d.l.	0.01	0.01	20 000	Keays and Lightfoot, 2004
Levack (N-Range)	Granophyre	1020	-	0.00	0.00	d.l.	d.l.	0.01	0.03	3 030	Keays and Lightfoot, 2004
Levack (N-Range)	Granophyre	1620	-	0.00	0.00	d.l.	d.l.	0.03	0.04	6 818	Keays and Lightfoot, 2004
Levack (N-Range)	Granophyre	1935	-	0.00	0.00	d.l.	d.l.	0.00	0.00	15 000	Keays and Lightfoot, 2004
Levack (N-Range)	Granophyre	2536	-	0.00	0.00	d.l.	d.l.	0.00	0.00	20 000	Keays and Lightfoot, 2004
Levack (N-Range)	Quartz Gabbro	3126	-	0.00	0.00	d.l.	d.l.	0.02	0.01	14 286	Keays and Lightfoot, 2004
Levack (N-Range)	Quartz Gabbro	3341	-	0.00	0.00	d.l.	1	0.07	0.05	13 000	Keays and Lightfoot, 2004
Levack (N-Range)	Quartz Gabbro	3495	-	0.00	0.00	d.l.	d.l.	0.13	0.08	16 250	Keays and Lightfoot, 2004
Levack (N-Range)	Quartz Gabbro	3598	-	0.00	0.00	d.l.	d.l.	0.11	0.07	15 493	Keays and Lightfoot, 2004
Levack (N-Range)	Quartz Gabbro	3703	-	0.00	0.00	d.l.	d.l.	0.06	0.07	9 275	Keays and Lightfoot, 2004
Levack (N-Range)	Quartz Gabbro	3804	-	0.00	-	d.l.	d.l.	0.01	0.01	10 000	Keays and Lightfoot, 2004
Levack (N-Range)	Quartz Gabbro	4360	-	0.00	0.00	d.l.	d.l.	0.02	0.02	8 947	Keays and Lightfoot, 2004
Levack (N-Range)	Felsic Norite	4655	-	0.00	0.00	0	d.l.	0.01	0.02	6 471	Keays and Lightfoot, 2004
Levack (N-Range)	Felsic Norite	4755	-	0.00	0.00	-	-	0.06	0.04	16 667	Keays and Lightfoot, 2004
Levack (N-Range)	Felsic Norite	4850	-	0.00	0.00	d.l.	d.l.	0.04	0.04	9 231	Keays and Lightfoot, 2004
Levack (N-Range)	Felsic Norite	5050	-	0.00	0.00	-	-	0.04	0.04	10 000	Keays and Lightfoot, 2004
Levack (N-Range)	Felsic Norite	5360	-	0.00	0.00	0	0	0.05	0.05	11 042	Keays and Lightfoot, 2004
Levack (N-Range)	Felsic Norite	5680	-	0.00	0.00	-	-	0.04	0.04	10 244	Keays and Lightfoot, 2004
Levack (N-Range)	Felsic Norite	5860	-	0.00	0.00	0	0	0.05	0.05	8 491	Keays and Lightfoot, 2004
Levack (N-Range)	Felsic Norite	6050	-	0.00	0.00	0	0	0.05	0.05	9 231	Keays and Lightfoot, 2004
Levack (N-Range)	Felsic Norite	6155	-	0.00	0.00	-	-	0.07	0.05	14 894	Keays and Lightfoot, 2004
Levack (N-Range)	Felsic Norite	6460	-	0.00	0.00	-	-	0.07	0.05	13 208	Keays and Lightfoot, 2004
Levack (N-Range)	Felsic Norite	6585	-	-	-	0	0	0.06	0.05	12 500	Keays and Lightfoot, 2004
Levack (N-Range)	Felsic Norite	6795	-	0.00	0.00	0	0	0.06	0.06	9 836	Keays and Lightfoot, 2004
Levack (N-Range)	Felsic Norite	7005	-	0.00	0.00	0	0	0.06	0.07	9 231	Keays and Lightfoot, 2004
Levack (N-Range)	Felsic Norite	7158	-	0.01	0.00	0	0	0.07	0.09	8 140	Keays and Lightfoot, 2004
Levack (N-Range)	Felsic Norite	7190	-	0.01	0.00	1	1	0.07	-	-	Keays and Lightfoot, 2004
Levack (N-Range)	Felsic Norite	7218	-	0.01	0.01	0	1	0.08	0.10	8 000	Keays and Lightfoot, 2004
Levack (N-Range)	Felsic Norite	7243	-	0.01	0.00	0	0	0.07	-	-	Keays and Lightfoot, 2004
Levack (N-Range)	Felsic Norite	7270	-	0.02	0.02	3	2	0.20	0.30	6 667	Keays and Lightfoot, 2004
Levack (N-Range)	Felsic Norite	7300	-	0.01	0.00	0	1	0.06	-	-	Keays and Lightfoot, 2004
Levack (N-Range)	Felsic Norite	7332	-	0.01	0.01	0	1	0.07	0.09	7 692	Keays and Lightfoot, 2004
Levack (N-Range)	Felsic Norite	7357	-	0.01	0.01	1	0	0.08	-	-	Keays and Lightfoot, 2004
Levack (N-Range)	Felsic Norite	7390	-	0.01	0.01	0	1	0.06	0.09	6 897	Keays and Lightfoot, 2004
Levack (N-Range)	Felsic Norite	7420	-	0.01	0.01	0	1	0.08	-	-	Keays and Lightfoot, 2004
Levack (N-Range)	Felsic Norite	7450	-	0.01	0.00	0	1	0.05	0.08	6 098	Keays and Lightfoot, 2004
Levack (N-Range)	Felsic Norite	7480	-	0.01	0.01	0	0	0.07	-	-	Keays and Lightfoot, 2004
Levack (N-Range)	Felsic Norite	7512	-	0.01	0.00	0	1	0.03	0.06	4 762	Keays and Lightfoot, 2004
Levack (N-Range)	Felsic Norite	7550	-	0.02	0.02	6	6	0.20	-	-	Keays and Lightfoot, 2004
Levack (N-Range)	Felsic Norite	7575	-	0.04	0.03	3	3	0.29	0.43	6 744	Keays and Lightfoot, 2004
Levack (N-Range)	Mafic Norite	7603	-	0.04	0.03	2	2	0.22	0.38	5 789	Keays and Lightfoot, 2004
Levack (N-Range)	Mafic Norite	7618	-	0.05	0.05	3	4	0.34	0.67	5 075	Keays and Lightfoot, 2004
Levack (N-Range)	Mafic Norite	7665	-	0.04	0.03	2	3	0.24	0.34	7 059	Keays and Lightfoot, 2004
Levack (N-Range)	Mafic Norite	7685	-	0.07	0.06	11	16	0.38	0.68	5 588	Keays and Lightfoot, 2004
Levack (N-Range)	Mafic Norite	7692	-	0.04	0.04	2	3	0.25	0.37	6 757	Keays and Lightfoot, 2004
Levack (N-Range)	Sublayer	7703	-	0.21	0.14	22	18	1.90	2.20	8 636	Keays and Lightfoot, 2004
Levack (N-Range)	Sublayer	7715	-	0.15	0.07	7	8	1.42	-	-	Keays and Lightfoot, 2004
Levack (N-Range)	Sublayer	7750	-	0.04	0.03	5	6	0.19	-	-	Keays and Lightfoot, 2004
Levack (N-Range)	Sublayer	7770	-	0.03	0.03	4	5	0.24	0.26	9 231	Keays and Lightfoot, 2004
Levack (N-Range)	Sublayer	7800	-	0.10	0.08	11	9	0.72	-	-	Keays and Lightfoot, 2004
Levack (N-Range)	Sublayer	7824	-	0.07	0.06	7	6	0.43	0.66	6 515	Keays and Lightfoot, 2004
Levack (N-Range)	Sublayer	7844	-	0.12	0.04	11	12	0.67	-	-	Keays and Lightfoot, 2004

Mining Camp	Rocktype/ore	Sample	n	Ni	Cu	Pt	Pd	S	Se	S/Se	references
Deposit				% wt	% wt	ppb	ppb	% wt	ppm		
Levack (N-Range)	Sublayer	7860	-	0.04	0.03	5	4	0.32	0.53	6 038	Keays and Lightfoot, 2004
Levack (N-Range)	Sublayer	7880	-	0.28	0.06	23	20	2.15	-	-	Keays and Lightfoot, 2004
Levack (N-Range)	Sublayer	7930	-	0.05	0.04	39	38	0.26	0.51	5 098	Keays and Lightfoot, 2004
Levack (N-Range)	Sublayer	7947	-	0.04	0.02	4	4	0.19	-	-	Keays and Lightfoot, 2004
Levack (N-Range)	Sublayer	7975	-	-	-	41	18	-	-	-	Keays and Lightfoot, 2004
Levack (N-Range)	Sublayer	8002	-	0.07	0.09	138	151	0.45	1.40	3 214	Keays and Lightfoot, 2004
Levack (N-Range)	Sublayer	8021	-	0.32	0.50	141	178	2.28	-	-	Keays and Lightfoot, 2004
Levack (N-Range)	Sublayer	8035	-	0.01	0.02	19	18	0.09	0.25	3 600	Keays and Lightfoot, 2004
Levack (N-Range)	Sublayer	8098	-	0.01	0.02	19	17	0.09	0.25	3 600	Keays and Lightfoot, 2004
Levack (N-Range)	Sublayer	8113	-	-	-	17	16	-	-	-	Keays and Lightfoot, 2004
Levack (N-Range)	Sublayer	8142	-	0.01	0.01	19	19	0.09	0.25	3 600	Keays and Lightfoot, 2004
Nickel Rim (N-Range)	Quartz Gabbro	94PCL-2045	-	0.00	0.00	d.l.	d.l.	0.03	0.05	6 711	Keays and Lightfoot, 2004
Nickel Rim (N-Range)	Quartz Gabbro	94PCL-2048	-	0.00	0.00	d.l.	d.l.	0.01	-	-	Keays and Lightfoot, 2004
Nickel Rim (N-Range)	Quartz Gabbro	94PCL-2049	-	0.00	0.00	d.l.	d.l.	0.12	0.09	13 721	Keays and Lightfoot, 2004
Nickel Rim (N-Range)	Quartz Gabbro	94PCL-2052	-	0.00	0.00	d.l.	d.l.	0.02	0.02	8 000	Keays and Lightfoot, 2004
Nickel Rim (N-Range)	Quartz Gabbro	94PCL-2055	-	0.00	0.00	d.l.	d.l.	0.10	0.08	12 895	Keays and Lightfoot, 2004
Nickel Rim (N-Range)	Quartz Gabbro	94PCL-2060	-	0.00	0.00	d.l.	1	0.09	-	-	Keays and Lightfoot, 2004
Nickel Rim (N-Range)	Quartz Gabbro	94PCL-2079	-	0.00	0.00	d.l.	d.l.	0.01	-	-	Keays and Lightfoot, 2004
Nickel Rim (N-Range)	Quartz Gabbro	94PCL-2061	-	0.00	0.00	d.l.	0	0.10	0.09	11 319	Keays and Lightfoot, 2004
Nickel Rim (N-Range)	Quartz Gabbro	94PCL-2064	-	0.00	0.01	0	d.l.	0.03	0.07	3 800	Keays and Lightfoot, 2004
Nickel Rim (N-Range)	Quartz Gabbro	94PCL-2065	-	0.00	0.00	d.l.	d.l.	0.10	-	-	Keays and Lightfoot, 2004
Nickel Rim (N-Range)	Felsic Norite	94PCL-2066	-	0.00	0.00	d.l.	d.l.	0.04	0.04	9 757	Keays and Lightfoot, 2004
Nickel Rim (N-Range)	Felsic Norite	94PCL-2068	-	0.00	0.00	d.l.	d.l.	0.06	-	-	Keays and Lightfoot, 2004
Nickel Rim (N-Range)	Felsic Norite	94PCL-2070	-	0.00	0.00	d.l.	d.l.	0.05	0.05	9 449	Keays and Lightfoot, 2004
Nickel Rim (N-Range)	Felsic Norite	94PCL-2072	-	0.00	0.00	0	d.l.	0.05	0.05	10 822	Keays and Lightfoot, 2004
Nickel Rim (N-Range)	Felsic Norite	94PCL-2077	-	0.00	0.00	d.l.	d.l.	0.05	0.04	13 571	Keays and Lightfoot, 2004
Nickel Rim (N-Range)	Felsic Norite	94PCL-2073	-	0.00	0.00	d.l.	d.l.	0.05	-	-	Keays and Lightfoot, 2004
Nickel Rim (N-Range)	Felsic Norite	94PCL-2076	-	0.00	0.00	d.l.	d.l.	0.06	-	-	Keays and Lightfoot, 2004
Nickel Rim (N-Range)	Felsic Norite	94PCL-2040	-	0.00	0.00	d.l.	d.l.	0.06	0.04	16 075	Keays and Lightfoot, 2004
Nickel Rim (N-Range)	Felsic Norite	94PCL-2039	-	0.00	0.00	d.l.	d.l.	0.06	-	-	Keays and Lightfoot, 2004
Nickel Rim (N-Range)	Felsic Norite	94PCL-2035	-	0.00	0.00	d.l.	0	0.06	0.04	14 372	Keays and Lightfoot, 2004
Nickel Rim (N-Range)	Felsic Norite	94PCL-2033	-	0.00	0.00	0	0	0.05	-	-	Keays and Lightfoot, 2004
Nickel Rim (N-Range)	Felsic Norite	94PCL-2031	-	0.00	0.00	d.l.	0	0.07	-	-	Keays and Lightfoot, 2004
Nickel Rim (N-Range)	Felsic Norite	94PCL-2028	-	0.01	0.01	1	1	0.12	0.14	8 156	Keays and Lightfoot, 2004
Nickel Rim (N-Range)	Felsic Norite	94PCL-2027	-	0.01	0.00	0	1	0.23	-	-	Keays and Lightfoot, 2004
Nickel Rim (N-Range)	Felsic Norite	94PCL-2026	-	0.01	0.01	5	6	0.16	-	-	Keays and Lightfoot, 2004
Nickel Rim (N-Range)	Felsic Norite	94PCL-2014	-	0.01	0.01	0	1	0.11	-	-	Keays and Lightfoot, 2004
Nickel Rim (N-Range)	Felsic Norite	94PCL-2012	-	0.03	0.03	1	1	0.27	0.50	5 427	Keays and Lightfoot, 2004
Nickel Rim (N-Range)	Mafic Norite	94PCL-2011	-	0.03	0.03	2	3	0.33	0.63	5 215	Keays and Lightfoot, 2004
Nickel Rim (N-Range)	Mafic Norite	94PCL-2010	-	0.03	0.03	2	2	0.35	-	-	Keays and Lightfoot, 2004
Nickel Rim (N-Range)	Mafic Norite	94PCL-2009	-	0.04	0.04	2	3	0.37	-	-	Keays and Lightfoot, 2004
Nickel Rim (N-Range)	Mafic Norite	94PCL-2003	-	0.06	0.06	6	8	0.49	0.86	5 748	Keays and Lightfoot, 2004
Nickel Rim (N-Range)	Mafic Norite	94PCL-2001	-	0.10	0.11	7	8	0.99	1.67	5 921	Keays and Lightfoot, 2004
Nickel Rim (N-Range)	Mafic Norite	94PCL-2016	-	0.05	0.04	3	3	0.43	0.63	6 873	Keays and Lightfoot, 2004
Nickel Rim (N-Range)	Sublayer	94PCL-2017	-	0.54	0.09	48	36	4.54	-	-	Keays and Lightfoot, 2004
Nickel Rim (N-Range)	Sublayer	94PCL-2018	-	0.22	0.18	58	45	1.58	2.57	6 143	Keays and Lightfoot, 2004
Nickel Rim (N-Range)	Sublayer	94PCL-2019	-	0.04	0.02	3	2	0.19	0.45	4 097	Keays and Lightfoot, 2004
Nickel Rim (N-Range)	Sublayer	94PCL-2020	-	0.09	0.07	15	15	0.73	1.04	7 064	Keays and Lightfoot, 2004
Nickel Rim (N-Range)	Sublayer	94PCL-2021	-	0.20	0.18	41	25	1.43	2.65	5 402	Keays and Lightfoot, 2004
Nickel Rim (N-Range)	Sublayer	94PCL-2022	-	0.01	0.01	19	22	0.06	0.24	2 354	Keays and Lightfoot, 2004
Nickel Rim (N-Range)	Sublayer	94PCL-2023	-	0.05	0.04	45	30	0.30	0.70	4 237	Keays and Lightfoot, 2004
Nickel Rim (N-Range)	Sublayer	94PCL-2024	-	0.03	0.03	24	28	0.20	0.66	3 070	Keays and Lightfoot, 2004
Creighton (Sudbury)											
Gertrude West	SF-Diss	CRTN1	-	0.51	0.28	14	20	4.79	10.00	4 789	Dare et al., 2010
Gertrude	SF-MS inclusion	CRTN2	-	1.10	1.55	107	37	10.23	16.00	6 392	Dare et al., 2010
Gertrude	SF-Diss	CRTN3	-	1.44	0.07	112	53	11.18	24.00	4 660	Dare et al., 2010

Mining Camp	Rocktype/ore	Sample	n	Ni	Cu	Pt	Pd	S	Se	S/Se	references
Deposit				% wt	% wt	ppb	ppb	% wt	ppm		
Gertrude	SF-MS	CRTN4	-	4.30	0.03	362	200	33.27	56.00	5 940	Dare et al., 2010
Upper 402	SF-MS inclusion	CRTN5	-	4.53	0.37	119	144	28.45	92.00	3 092	Dare et al., 2010
Upper 402	SF-Diss	CRTN6	-	1.13	0.31	72	24	5.35	12.00	4 454	Dare et al., 2010
Upper 402	SF-MS inclusion	CRTN7	-	3.15	4.28	8	143	18.70	63.00	2 968	Dare et al., 2010
Plum	SF-MS inclusion	CRTN8	-	4.88	2.93	10 570	8 314	24.32	139.00	1 749	Dare et al., 2010
Plum	SF-MS	CRTN9	-	5.16	21.82	68	1 188	32.46	108.00	3 005	Dare et al., 2010
Plum	SF-MS	CRTN10	-	7.43	1.54	49	157	33.32	99.00	3 365	Dare et al., 2010
Lower 402	SF-MS	CRTN11	-	5.65	3.59	42	622	31.14	96.00	3 244	Dare et al., 2010
Lower 402	SF-MS	CRTN12	-	7.50	0.27	44	214	36.47	103.00	3 541	Dare et al., 2010
Lower 402	SF-MS	CRTN13	-	5.98	0.40	41	88	36.79	106.00	3 471	Dare et al., 2010
Lower 402	SF-MS	CRTN14	-	11.80	6.72	43	801	33.85	101.00	3 351	Dare et al., 2010
Lower 402	SF-MS	CRTN15	-	9.12	1.85	36	232	35.09	102.00	3 440	Dare et al., 2010
Deep 400 East	SF-MS	CRTN16	-	14.75	0.96	21	834	33.71	109.00	3 093	Dare et al., 2010
Deep 400 East	SF-MS	CRTN17	-	8.05	1.80	15	117	32.13	91.00	3 531	Dare et al., 2010
Deep 400 East	SF-MS	CRTN18	-	4.95	20.71	13 690	310	34.16	94.00	3 634	Dare et al., 2010
Deep 400 East	SF-MS	CRTN19	-	12.68	8.07	11 770	783	34.12	89.00	3 833	Dare et al., 2010
Deep 400 East	SF-MS	CRTN20	-	10.68	6.95	39	448	32.94	98.00	3 361	Dare et al., 2010
Strathcona (Sudbury)											
Disseminated sulfides	SF-Diss	-	2	-	-	-	-	-	-	5 157	Barnes and Lightfoot, 2005
Creighton (Sudbury)											
Cu-rich veins 4550L	SF-MS - Mtr	MCR7B	-	1.32	16.45	853	298	34.72	106.90	3 248	Dare et al., 2011
Cu-rich veins 4550L	SF-MS - ISS	MCR7A	-	0.02	33.02	11 850	16 810	34.01	231.70	1 468	Dare et al., 2011
Cu-rich veins 4700L	SF-MS - ISS	MCR9	-	6.62	24.43	10 250	26 180	32.69	208.70	1 566	Dare et al., 2011
Cu-rich veins 4810L	SF-MS - ISS	MCR10	-	5.77	24.98	11 090	25 870	31.42	262.10	1 199	Dare et al., 2011
Cu-rich veins 4810L	SF-MS - ISS	MCR11	-	9.28	19.45	6 034	15 070	28.95	234.10	1 237	Dare et al., 2011
Cu-rich veins 4810L	SF-MS - ISS	MCR12	-	1.23	30.04	13 710	24 060	30.32	207.00	1 465	Dare et al., 2011
Cu-rich veins 4945L	SF-MS - ISS	MCR13	-	2.86	28.87	10 800	13 320	32.13	175.30	1 833	Dare et al., 2011
Cu-rich veins 4945L	SF-MS - ISS	MCR14	-	0.39	30.88	8 130	14 680	32.18	188.60	1 706	Dare et al., 2011
Main L1	SF-MS - MSS	MCR2	-	4.49	0.13	55	204	32.23	32.60	9 885	Dare et al., 2011
Main L2	SF-MS - MSS	MCR3	-	4.55	1.71	1 152	1 317	33.35	73.20	4 556	Dare et al., 2011
Main L2	SF-MS - MSS	MCR4	-	3.75	4.96	1 282	1 537	30.59	60.50	5 056	Dare et al., 2011
Main L2	SF-MS - MSS	MCR6	-	4.10	0.12	420	515	30.10	67.00	4 493	Dare et al., 2011
Main L3	SF-MS - MSS	MCR5	-	4.93	1.26	1 509	2 192	33.06	91.20	3 625	Dare et al., 2011
West L2	SF-MS - MSS	MCRE1	-	2.56	0.69	939	592	32.75	55.30	5 923	Dare et al., 2011
Duluth complex											
Dunka Road	Norite	DC-27	-	0.03	0.13	13	23	0.77	0.60	12 833	Thériault and Barnes, 1998
Dunka Road	Norite	DC-49	-	0.02	0.04	3	5	0.20	< 0.2	-	Thériault and Barnes, 1998
Dunka Road	Norite	DC-52	-	0.02	0.03	1	11	0.66	0.60	11 000	Thériault and Barnes, 1998
Dunka Road	Norite	DC-54	-	0.03	0.06	69	8	0.31	0.60	5 167	Thériault and Barnes, 1998
Dunka Road	Norite	DC-60	-	0.11	0.30	50	100	1.57	1.00	15 700	Thériault and Barnes, 1998
Dunka Road	Norite	DC-63	-	0.08	0.22	16	63	2.45	2.20	11 136	Thériault and Barnes, 1998
Dunka Road	Norite	DC-66	-	0.23	0.64	35	460	4.32	5.90	7 322	Thériault and Barnes, 1998
Dunka Road	Norite	DC-72	-	0.11	0.37	5	120	4.65	9.60	4 844	Thériault and Barnes, 1998
Dunka Road	Troctolite	DC-53	-	0.02	0.05	10	39	0.15	0.20	7 500	Thériault and Barnes, 1998
Dunka Road	Troctolite	DC-55	-	0.11	0.37	42	170	1.11	2.40	4 625	Thériault and Barnes, 1998
Dunka Road	Troctolite	DC-56	-	0.19	0.56	110	400	1.44	3.20	4 500	Thériault and Barnes, 1998
Dunka Road	Troctolite	DC-58	-	0.24	1.02	160	710	2.00	4.60	4 348	Thériault and Barnes, 1998
Dunka Road	Troctolite	DC-61	-	0.21	0.71	120	500	1.50	4.30	3 488	Thériault and Barnes, 1998
Dunka Road	Troctolite	DC-79	-	0.23	0.71	160	580	1.12	3.50	3 200	Thériault and Barnes, 1998
Dunka Road	PGE-rich layer	DC-62	-	0.37	1.22	560	2 300	1.69	8.20	2 061	Thériault and Barnes, 1998
Dunka Road	PGE-rich layer	DC-64	-	0.17	0.34	300	1 600	0.59	1.90	3 105	Thériault and Barnes, 1998
Dunka Road	SF-MS	DC-73	-	1.07	1.22	9	470	19.60	25.00	7 840	Thériault and Barnes, 1998
Dunka Road	SF-MS	DC-75	-	0.68	1.14	23	880	31.20	13.00	24 000	Thériault and Barnes, 1998
Dunka Road	SF-MS	DC-76	-	1.87	0.54	35	1 600	34.90	43.00	8 116	Thériault and Barnes, 1998
Dunka Road	Ccp-rich sulfides	DC-65	-	0.15	1.57	370	600	2.17	8.20	2 646	Thériault and Barnes, 1998
Dunka Road	Ccp-rich sulfides	DC-67	-	0.16	1.40	840	970	3.42	9.00	3 800	Thériault and Barnes, 1998

Mining Camp Deposit	Rocktype/ore	Sample	n	Ni % wt	Cu % wt	Pt ppb	Pd ppb	S % wt	Se ppm	S/Se	references
Dunka Road	Xenolith	DC-26	-	0.02	0.04	13	3	1.20	6.00	2 000	Thériault et al., 1997
Dunka Road	Xenolith	DC-69	-	0.10	0.13	7	36	10.09	1.90	53 105	Thériault et al., 1997
Dunka Road	Xenolith	DC-81	-	0.03	0.04	9	8	0.66	2.00	3 300	Thériault et al., 1997
Dunka Road	Xenolith	26082 - 117.9	-	-	-	-	-	1.38	1.70	8 118	Ripley, 1990
Dunka Road	Hornfel	26082 - 185.6	-	-	-	-	-	0.50	0.50	10 000	Ripley, 1990
Dunka Road	Hornfel	26082 - 187.4	-	-	-	-	-	3.78	1.80	21 000	Ripley, 1990
Dunka Road	Hornfel	26082 - 196.9	-	-	-	-	-	0.50	0.90	5 556	Ripley, 1990
Dunka Road	Hornfel	26082 - 222.5	-	-	-	-	-	1.14	4.70	2 426	Ripley, 1990
Dunka Road	Hornfel	26082 - 256.0	-	-	-	-	-	0.70	2.70	2 593	Ripley, 1990
Dunka Road	Hornfel	26082 - 256.6	-	-	-	-	-	0.05	0.10	5 000	Ripley, 1990
Dunka Road	Hornfel	26082 - 265.8	-	-	-	-	-	0.60	0.70	8 571	Ripley, 1990
Dunka Road	Hornfel	26082 - 274.9	-	-	-	-	-	1.04	0.90	11 556	Ripley, 1990
Babbitt	Xenolith	136 - 282.8	-	-	-	-	-	2.91	2.20	13 227	Ripley, 1990
Babbitt	Xenolith	136 - 284.4	-	-	-	-	-	4.45	2.80	15 893	Ripley, 1990
Babbitt	Xenolith	136 - 389.5	-	-	-	-	-	0.89	0.70	12 714	Ripley, 1990
Babbitt	Xenolith	136 - 514.5	-	-	-	-	-	0.94	0.60	15 667	Ripley, 1990
Babbitt	Xenolith	156 - 429.1	-	-	-	-	-	1.02	0.60	17 000	Ripley, 1990
Babbitt	Xenolith	156 - 449.6	-	-	-	-	-	1.15	0.90	12 778	Ripley, 1990
Babbitt	Xenolith	156 - 450.5	-	-	-	-	-	1.25	1.00	12 500	Ripley, 1990
Babbitt	Xenolith	156 - 486.1	-	-	-	-	-	1.05	0.50	21 000	Ripley, 1990
Babbitt	Xenolith	156 - 516.6	-	-	-	-	-	4.01	11.00	3 645	Ripley, 1990
Babbitt	Xenolith	156 - 532.5	-	-	-	-	-	2.39	8.00	2 988	Ripley, 1990
Babbitt	Xenolith	156 - 535.5	-	-	-	-	-	3.27	1.40	23 357	Ripley, 1990
Babbitt	Xenolith	146 - 519.7	-	-	-	-	-	3.15	11.00	2 864	Ripley, 1990
Babbitt	Xenolith	146 - 523.6	-	-	-	-	-	2.45	5.70	4 298	Ripley, 1990
Babbitt	Xenolith	146 - 528.2	-	-	-	-	-	1.48	1.30	11 385	Ripley, 1990
Babbitt	Xenolith	146 - 529.7	-	-	-	-	-	1.14	0.70	16 286	Ripley, 1990
Babbitt	Xenolith	146 - 532.8	-	-	-	-	-	1.37	0.50	27 400	Ripley, 1990
Babbitt	Xenolith	10120 - 130.4	-	-	-	-	-	0.49	0.30	16 333	Ripley, 1990
Babbitt	Xenolith	10134 - 20.7	-	-	-	-	-	0.83	1.50	5 533	Ripley, 1990
Babbitt	Xenolith	10134 - 68.6	-	-	-	-	-	0.18	0.20	9 000	Ripley, 1990
Babbitt	Xenolith	10134 - 75.3	-	-	-	-	-	0.57	1.00	5 700	Ripley, 1990
Babbitt	Xenolith	10134 - 83.8	-	-	-	-	-	0.09	0.40	2 250	Ripley, 1990
Babbitt	Xenolith	10172 - 119.5	-	-	-	-	-	0.42	0.80	5 250	Ripley, 1990
Babbitt	Xenolith	10152 - 7.9	-	-	-	-	-	0.42	0.70	6 000	Ripley, 1990
Babbitt	Xenolith	10152 - 32.0	-	-	-	-	-	0.37	0.40	9 250	Ripley, 1990
Babbitt	Xenolith	10053 - 9.1	-	-	-	-	-	0.50	0.90	5 556	Ripley, 1990
Babbitt	Xenolith	10053 - 32.9	-	-	-	-	-	0.06	0.30	2 000	Ripley, 1990
Babbitt	Xenolith	10039 - 16.4	-	-	-	-	-	0.31	0.30	10 333	Ripley, 1990
Babbitt	Hornfel	214 - 598.3	-	-	-	-	-	0.37	0.20	18 500	Ripley, 1990
Babbitt	Hornfel	214 - 599.2	-	-	-	-	-	0.45	0.90	5 000	Ripley, 1990
Babbitt	Hornfel	214 - 601.4	-	-	-	-	-	0.36	0.40	9 000	Ripley, 1990
Babbitt	Hornfel	214 - 602.9	-	-	-	-	-	0.40	0.30	13 333	Ripley, 1990
Virginia Formation	Pelites	DC-1	-	0.01	0.00	3	2	0.02	<0.2	-	Thériault and Barnes, 1998
Virginia Formation	Pelites	DC-3	-	0.01	0.00	<3.2	2	0.31	0.20	15 500	Thériault and Barnes, 1998
Virginia Formation	Pelites	DC-5	-	0.01	0.01	7	5	0.53	<0.2	-	Thériault and Barnes, 1998
Virginia Formation	Pelites	DC-7	-	0.00	0.00	<4.2	3	0.09	<0.2	-	Thériault and Barnes, 1998
Virginia Formation	Pelites	DC-8	-	0.01	0.01	4	3	1.08	0.20	54 000	Thériault and Barnes, 1998
Virginia Formation	Pelites	DC-9	-	0.01	0.01	4	<3.2	0.03	<0.2	-	Thériault and Barnes, 1998
Virginia Formation	Bedded Pyrrhotite	DC-70	-	0.01	0.02	<4.7	4	4.45	1.40	31 786	Thériault and Barnes, 1998
Virginia Formation	Pelites	MDD2 - 434.0	-	-	-	-	-	1.37	1.00	13 700	Ripley, 1990
Virginia Formation	Pelites	MDD2 - 477.0	-	-	-	-	-	0.07	0.30	2 333	Ripley, 1990
Virginia Formation	Pelites	MDD2 - 491.3	-	-	-	-	-	0.67	0.10	67 000	Ripley, 1990
Virginia Formation	Pelites	MDD5 - 137.7	-	-	-	-	-	0.35	1.40	2 500	Ripley, 1990
Virginia Formation	Pelites	MDD7 - 184.1	-	-	-	-	-	0.08	0.20	4 000	Ripley, 1990
Virginia Formation	Pelites	MDD7 - 225.2	-	-	-	-	-	0.23	0.10	23 000	Ripley, 1990

Mining Camp	Rocktype/ore	Sample	n	Ni	Cu	Pt	Pd	S	Se	S/Se	references
Deposit				% wt	% wt	ppb	ppb	% wt	ppm		
Virginia Formation	Pelites	24981 - 41.1	-	-	-	-	-	0.56	0.90	6 222	Ripley, 1990
Virginia Formation	Pelites	24981 - 47.5	-	-	-	-	-	0.41	0.60	6 833	Ripley, 1990
Virginia Formation	Pelites	24981 - 50.9	-	-	-	-	-	0.62	0.60	10 333	Ripley, 1990
Virginia Formation	Pelites	24981 - 53.6	-	-	-	-	-	0.47	0.30	15 667	Ripley, 1990
Virginia Formation	Pelites	24981 - 56.7	-	-	-	-	-	0.50	0.40	12 500	Ripley, 1990
Virginia Formation	Pelites	24981 - 59.7	-	-	-	-	-	0.24	0.30	8 000	Ripley, 1990
Virginia Formation	Pelites	24981 - 60.0	-	-	-	-	-	0.55	1.00	5 500	Ripley, 1990
Virginia Formation	Pelites	24981 - 62.8	-	-	-	-	-	1.40	2.80	5 000	Ripley, 1990
Virginia Formation	Pelites	24981 - 64.6	-	-	-	-	-	2.25	5.60	4 018	Ripley, 1990
Virginia Formation	Pelites	24981 - 68.0	-	-	-	-	-	1.14	3.20	3 563	Ripley, 1990
Noril'sk - Talnakh											
Oktyabr'sk (Kharaelakh)	SF-MS - MSS	90OC12	-	3.75	6.53	2 950	18 000	36.15	47.00	7 691	Czamanske et al., 1992
Oktyabr'sk (Kharaelakh)	SF-MS - MSS	90OMZS2-3	-	3.48	4.05	1 600	10 767	30.50	58.00	5 259	Czamanske et al., 1992
Komsolmolsky (Talnakh)	SF-MS - MSS	90KMZ5	-	4.97	3.94	5 200	26 000	32.00	59.00	5 424	Czamanske et al., 1992
Oktyabr'sk (Kharaelakh)	SF-MS - inter	90OC6A	-	1.39	22.25	4 100	10 500	32.93	72.00	4 573	Czamanske et al., 1992
Oktyabr'sk (Kharaelakh)	SF-MS - MSS	90OC4	-	3.03	12.30	4 191	21 256	32.45	76.00	4 270	Czamanske et al., 1992
Oktyabr'sk (Kharaelakh)	SF-MS - MSS	90OC6B	-	4.50	8.64	2 300	18 000	33.53	78.00	4 298	Czamanske et al., 1992
Oktyabr'sk (Kharaelakh)	SF-MS - inter	900MZS1-3	-	2.13	22.75	7 500	29 150	32.95	90.00	3 661	Czamanske et al., 1992
Oktyabr'sk (Kharaelakh)	SF-MS - inter	90OC29	-	1.82	21.47	4 300	39 000	34.00	104.00	3 269	Czamanske et al., 1992
Oktyabr'sk (Kharaelakh)	SF-MS - inter	90OC13	-	1.80	20.80	2 600	37 000	32.88	110.00	2 989	Czamanske et al., 1992
Oktyabr'sk (Kharaelakh)	SF-MS - ISS	90OMZS1-1	-	2.48	28.30	23 000	77 000	31.35	120.00	2 613	Czamanske et al., 1992
Medvezhy (Noril'sk 1)	SF-MS - inter	MC16	-	8.08	11.57	64 624	63 005	34.65	141.00	2 457	Czamanske et al., 1992
Oktyabr'sk (Kharaelakh)	SF-MS - ISS	90OC9	-	2.61	27.15	21 000	119 210	30.10	148.00	2 034	Czamanske et al., 1992
Oktyabr'sk (Kharaelakh)	SF-MS - ISS	90OC5	-	3.41	26.60	140 000	103 450	32.70	197.00	1 660	Czamanske et al., 1992
Oktyabr'sk (Kharaelakh)	SF-MS - ISS	90OC14	-	3.49	28.00	20 500	140 000	33.50	209.00	1 603	Czamanske et al., 1992
Medvezhy (Noril'sk 1)	SF-MS - ISS	90MC15	-	7.14	24.45	74 000	270 000	33.25	218.00	1 525	Czamanske et al., 1992
Medvezhy (Noril'sk 1)	SF-MS - ISS	90MC5	-	5.94	27.45	63 000	360 000	33.13	241.00	1 374	Czamanske et al., 1992
Medvezhy (Noril'sk 1)	SF-MS - ISS	90MCZC1	-	6.53	25.75	200 000	180 000	32.98	328.00	1 005	Czamanske et al., 1992
Jinchuan											
Jinchuan Ore	All ores	-	-	-	-	-	-	-	-	3 500	Chai and Naldrett, 1992
Molson Dykes											
Cuthbert Lake	SF-Diss	C1	-	-	-	-	-	0.09	0.21	4 410	Eckstrand et al., 1989
Cuthbert Lake	SF-Diss	C12	-	-	-	-	-	0.02	0.20	995	Eckstrand et al., 1989
Cuthbert Lake	SF-Diss	C15	-	-	-	-	-	0.03	0.13	2 546	Eckstrand et al., 1989
Cuthbert Lake	SF-Diss	C35	-	-	-	-	-	0.02	0.09	2 678	Eckstrand et al., 1989
Cuthbert Lake	SF-Diss	C53	-	-	-	-	-	0.33	0.53	6 266	Eckstrand et al., 1989
Sipiwesk Lake	SF-Diss	103	-	-	-	-	-	0.10	0.18	5 344	Eckstrand et al., 1989
Sipiwesk Lake	SF-Diss	105	-	-	-	-	-	0.06	0.25	2 396	Eckstrand et al., 1989
Sipiwesk Lake	SF-Diss	106	-	-	-	-	-	0.07	0.35	2 080	Eckstrand et al., 1989
Sipiwesk Lake	SF-Diss	109	-	-	-	-	-	0.12	0.48	2 590	Eckstrand et al., 1989
Sipiwesk Lake	SF-Diss	110	-	-	-	-	-	0.06	0.27	2 200	Eckstrand et al., 1989
Cross Lake	SF-Diss	219-1	-	-	-	-	-	0.04	0.16	2 806	Eckstrand et al., 1989
Cross Lake	SF-Diss	219-3	-	-	-	-	-	0.10	0.33	2 903	Eckstrand et al., 1989
Fox River Sill											
UCLZ	SF-Diss	1-7005	-	-	-	-	-	0.06	0.17	3 329	Eckstrand et al., 1989
UCLZ	SF-Diss	1-7025	-	-	-	-	-	0.82	2.33	3 514	Eckstrand et al., 1989
UCLZ	SF-Diss	1-7037	-	-	-	-	-	0.01	0.05	2 500	Eckstrand et al., 1989
UCLZ	SF-Diss	1-7049	-	-	-	-	-	0.01	0.01	18 600	Eckstrand et al., 1989
UCLZ	SF-Diss	1-7134	-	-	-	-	-	0.23	0.36	6 497	Eckstrand et al., 1989
UCLZ	SF-Diss	1-7164	-	-	-	-	-	0.60	0.71	8 442	Eckstrand et al., 1989
UCLZ	SF-Diss	1-7185	-	-	-	-	-	0.64	2.37	2 690	Eckstrand et al., 1989
UCLZ	SF-Diss	1-7200	-	-	-	-	-	1.24	2.61	4 767	Eckstrand et al., 1989
UCLZ	SF-Diss	1-7215	-	-	-	-	-	0.19	1.12	1 679	Eckstrand et al., 1989
UCLZ	SF-Diss	1-7218	-	-	-	-	-	0.20	0.92	2 211	Eckstrand et al., 1989
UCLZ	SF-Diss	1-7232	-	-	-	-	-	0.09	0.17	5 018	Eckstrand et al., 1989
UCLZ	SF-Diss	1-7247	-	-	-	-	-	0.10	0.34	3 050	Eckstrand et al., 1989

Mining Camp	Rocktype/ore	Sample	n	Ni	Cu	Pt	Pd	S	Se	S/Se	references
Deposit				% wt	% wt	ppb	ppb	% wt	ppm		
UCLZ	SF-Diss	2-7285	-	-	-	-	-	0.14	0.08	16 888	Eckstrand et al., 1989
UCLZ	SF-Diss	2-7491	-	-	-	-	-	0.34	0.51	6 629	Eckstrand et al., 1989
UCLZ	SF-Diss	2-7500	-	-	-	-	-	0.08	0.14	5 850	Eckstrand et al., 1989
UCLZ	SF-Diss	2-7533	-	-	-	-	-	0.76	1.49	5 113	Eckstrand et al., 1989
UCLZ	SF-Diss	2-7545	-	-	-	-	-	1.80	2.67	6 757	Eckstrand et al., 1989
UCLZ	SF-Diss	2-7554	-	-	-	-	-	0.06	0.20	2 975	Eckstrand et al., 1989
UCLZ	SF-Diss	5-7835	-	-	-	-	-	0.45	0.67	6 784	Eckstrand et al., 1989
UCLZ	SF-Diss	5-7850	-	-	-	-	-	0.41	0.46	8 902	Eckstrand et al., 1989
UCLZ	SF-Diss	5-7906	-	-	-	-	-	0.01	0.02	3 800	Eckstrand et al., 1989
UCLZ	SF-Diss	5-7913	-	-	-	-	-	0.05	0.35	1 494	Eckstrand et al., 1989
UCLZ	SF-Diss	5-7971	-	-	-	-	-	0.01	0.02	4 750	Eckstrand et al., 1989
UCLZ	SF-Diss	5-7972	-	-	-	-	-	0.00	0.02	1 250	Eckstrand et al., 1989
UCLZ	SF-Diss	5-9012	-	-	-	-	-	0.01	0.01	21 600	Eckstrand et al., 1989
UCLZ	SF-Diss	5-9027	-	-	-	-	-	0.02	0.31	626	Eckstrand et al., 1989
UCLZ	SF-Diss	5-9028	-	-	-	-	-	0.01	0.12	1 200	Eckstrand et al., 1989
LCLZ	Peridotite	1-7267	-	-	-	-	-	0.26	0.29	9 128	Eckstrand et al., 1989
LCLZ	Peridotite	1-7268	-	-	-	-	-	0.27	0.60	4 573	Eckstrand et al., 1989
LCLZ	Peridotite	2-7281	-	-	-	-	-	0.24	0.55	4 305	Eckstrand et al., 1989
Belleterre - Mine Lorraine											
Cu-poor	Altered sample	ML1	-	0.41	0.09	65	93	8.21	12.10	6 785	Bouchaib, 1992
Cu-rich	SF-Diss	ML2	-	1.09	4.04	-	-	20.60	32.90	6 261	Bouchaib, 1992
Cu-rich	SF-Diss	ML4	-	0.22	4.57	492	1 205	7.55	18.00	4 194	Bouchaib, 1992
Cu-poor	SF-MS	ML5	-	2.50	0.48	111	702	36.30	89.90	4 038	Bouchaib, 1992
Cu-rich	SF-Diss	ML6	-	0.61	4.20	172	273	12.60	29.90	4 214	Bouchaib, 1992
Cu-rich	SF-Diss	ML10	-	0.29	4.36	91	133	8.65	13.00	6 654	Bouchaib, 1992
Cu-poor	SF-MASS	ML11	-	2.47	0.29	100	233	34.20	69.00	4 957	Bouchaib, 1992
inter Cu	SF-MASS	ML12	-	1.60	2.56	77	162	26.40	41.40	6 377	Bouchaib, 1992
inter Cu	SF-MASS	ML13	-	1.37	1.77	172	683	22.30	39.40	5 660	Bouchaib, 1992
Cu-rich	SF-MASS	ML14	-	1.20	6.00	65	124	22.60	63.90	3 537	Bouchaib, 1992
inter Cu	SF-MASS	4A	-	2.02	1.68	290	303	27.50	100.00	2 750	Bouchaib, 1992
Cu-poor	SF-MASS	4B	-	2.78	0.03	128	278	36.00	100.00	3 600	Bouchaib, 1992
Cu-rich	SF-Diss	4D	-	0.68	7.42	340	< 1	19.30	< 60	-	Bouchaib, 1992
Cu-poor	SF-MASS	31B	-	2.00	0.28	86	433	29.40	100.00	2 940	Bouchaib, 1992
Cu-rich	SF-MASS	31C	-	1.73	10.10	1 983	928	29.20	100.00	2 920	Bouchaib, 1992
inter Cu	SF-MASS	31D	-	2.80	2.73	236	376	35.50	100.00	3 550	Bouchaib, 1992
Cu-rich	SF-MASS	31F	-	1.58	11.80	236	376	33.90	100.00	3 390	Bouchaib, 1992
Cu-poor	SF-MASS	31G	-	3.11	0.28	122	588	36.30	100.00	3 630	Bouchaib, 1992
Aguablanca											
leopardite-textured	SF-MS	Leopardite-6	-	4.63	3.19	1 581	1 438	20.26	57.00	3 554	Pina et al., 2008
leopardite-textured	SF-MS	AGU-55-136	-	3.70	3.67	1 337	1 438	25.15	74.00	3 399	Pina et al., 2008
leopardite-textured	SF-MS	Leopardite-2	-	5.85	0.62	1 187	1 771	20.12	64.00	3 144	Pina et al., 2008
leopardite-textured	SF-MS	6554-235	-	5.57	0.53	200	482	27.74	61.00	4 548	Pina et al., 2008
leopardite-textured	SF-MS	6580-279	-	6.24	0.93	446	621	30.01	67.00	4 479	Pina et al., 2008
leopardite-textured	SF-MS	6715-415	-	6.30	0.49	84	907	26.28	64.00	4 106	Pina et al., 2008
leopardite-textured	SF-MS	6580-281	-	5.70	1.83	467	676	30.42	65.00	4 680	Pina et al., 2008
leopardite-textured	SF-MS	6715-416	-	6.41	0.22	30	1 193	26.24	57.00	4 604	Pina et al., 2008
leopardite-textured	SF-MS	6730-198	-	3.46	0.24	823	891	14.68	39.00	3 764	Pina et al., 2008
Fragment-bearing	SF-Mtr	Breccia-4	-	3.93	0.95	952	1 244	16.32	49.00	3 331	Pina et al., 2008
Fragment-bearing	SF-Mtr	Breccia-1	-	3.09	0.73	681	823	12.74	36.00	3 539	Pina et al., 2008
Fragment-bearing	SF-Mtr	6629-39	-	3.44	0.82	2 244	768	15.24	36.00	4 233	Pina et al., 2008
Fragment-bearing	SF-Mtr	6758-544	-	2.59	2.51	603	711	13.86	33.00	4 200	Pina et al., 2008
Fragment-bearing	SF-Mtr	Breccia-10	-	2.73	2.06	576	699	16.49	36.00	4 581	Pina et al., 2008
Fragment-bearing	SF-Mtr	Breccia-11	-	4.21	0.71	352	793	21.54	47.00	4 583	Pina et al., 2008
Disseminated Ore	SF-Diss	6580-108	-	0.81	1.06	312	279	3.92	15.00	2 613	Pina et al., 2008
Disseminated Ore	SF-Diss	6749-390	-	0.41	1.48	346	216	3.17	12.00	2 642	Pina et al., 2008
Disseminated Ore	SF-Diss	6749-376	-	1.07	1.20	78	234	8.07	18.00	4 483	Pina et al., 2008

Mining Camp	Rocktype/ore	Sample	n	Ni	Cu	Pt	Pd	S	Se	S/Se	references
Deposit				% wt	% wt	ppb	ppb	% wt	ppm		
Disseminated Ore	SF-Diss	6758-548	-	0.43	1.13	276	128	3.56	12.00	2 967	Pina et al., 2008
Disseminated Ore	SF-Diss	6554-246	-	0.72	0.56	88	155	4.71	10.00	4 710	Pina et al., 2008
Disseminated Ore	SF-Diss	AGU-5-29	-	0.80	0.85	469	371	3.76	14.00	2 686	Pina et al., 2008
Disseminated Ore	SF-Diss	6554-169	-	0.52	0.46	147	132	2.37	7.00	3 386	Pina et al., 2008
Disseminated Ore	SF-Diss	6730-212	-	0.87	1.11	458	404	4.61	13.00	3 546	Pina et al., 2008
Disseminated Ore	SF-Diss	6715-452	-	1.23	0.99	185	386	5.77	18.00	3 206	Pina et al., 2008
Disseminated Ore	SF-Diss	6715-455	-	0.36	4.03	440	102	6.07	14.00	4 336	Pina et al., 2008
Veins	Ccp-veins	6479-44.2	-	0.99	1.62	45	371	4.70	12.00	3 917	Pina et al., 2008
Veins	Ccp-veins	6479-45.6	-	0.97	4.76	737	618	7.07	19.00	3 721	Pina et al., 2008
Veins	Ccp-veins	6554-221	-	0.79	10.60	150	2 513	16.90	-	-	Pina et al., 2008
Serie Negra Formation	Country rock	-	-	-	-	-	-	0.52	-	1 436	Pina et al., 2008
Voisey's Bay											
Ovoïd	SF-MS - MSS	VB-3	-	-	-	15	206	34.29	49.59	6 914	this study
Ovoïd	SF-MS - MSS	VB-4	-	-	-	15	206	32.94	45.40	7 256	this study
Ovoïd	SF-MS - ISS	VB-5	-	-	-	1	473	34.08	111.53	3 055	this study
Ovoïd	SF-MS - ISS	VB-6	-	-	-	1	254	28.57	72.00	3 968	this study
Tasiuyak Gneiss	Outcrop Sample	TG-1	-	-	-	-	-	0.12	3.29	365	Ripley et al., 2002
Tasiuyak Gneiss	Outcrop Sample	TG-2	-	-	-	-	-	0.29	1.03	2 816	Ripley et al., 2002
Tasiuyak Gneiss	Outcrop Sample	TG-3	-	-	-	-	-	0.07	0.71	986	Ripley et al., 2002
Tasiuyak Gneiss	Outcrop Sample	TG-4	-	-	-	-	-	0.01	2.86	35	Ripley et al., 2002
Tasiuyak Gneiss	Outcrop Sample	TG-5	-	-	-	-	-	0.28	1.14	2 456	Ripley et al., 2002
Tasiuyak Gneiss	Outcrop Sample	TG-6	-	-	-	-	-	0.02	9.95	20	Ripley et al., 2002
Tasiuyak Gneiss	Outcrop Sample	TG-7	-	-	-	-	-	0.50	4.99	1 002	Ripley et al., 2002
Tasiuyak Gneiss	Outcrop Sample	TG-8	-	-	-	-	-	0.04	1.59	252	Ripley et al., 2002
Tasiuyak Gneiss	Outcrop Sample	TG-9	-	-	-	-	-	0.01	5.72	17	Ripley et al., 2002
Country rock	Tasiuyak Gneiss	VB192/290.4	-	-	-	-	-	-	-	-	Ripley et al., 2002
Country rock	Tasiuyak Gneiss	VB192/293.0	-	-	-	-	-	0.01	-	-	Ripley et al., 2002
Country rock	Tasiuyak Gneiss	VB192/296.3	-	-	-	-	-	0.05	-	-	Ripley et al., 2002
Country rock	Tasiuyak Gneiss	VB192/331	-	-	-	-	-	1.67	-	-	Ripley et al., 2002
Country rock	Tasiuyak Gneiss	VB192/349.8	-	-	-	-	-	3.11	-	-	Ripley et al., 2002
Country rock	Tasiuyak Gneiss	VB192/350.0	-	-	-	-	-	3.56	1.56	22 821	Ripley et al., 2002
Country rock	Tasiuyak Gneiss	VB192/351	-	-	-	-	-	3.71	-	-	Ripley et al., 2002
Country rock	Tasiuyak Gneiss	VB192/357.5	-	-	-	-	-	1.89	-	-	Ripley et al., 2002
Country rock	Tasiuyak Gneiss	VB433/97	-	-	-	-	-	357.50	0.07	-	Ripley et al., 2002
Country rock	Tasiuyak Gneiss	VB433/98.5	-	-	-	-	-	0.05	0.04	12 500	Ripley et al., 2002
Country rock	Tasiuyak Gneiss	VB433/100.6	-	-	-	-	-	1.07	2.59	4 131	Ripley et al., 2002
Country rock	Tasiuyak Gneiss	VB433/107	-	-	-	-	-	0.16	-	-	Ripley et al., 2002
Country rock	Tasiuyak Gneiss	VB433/108.5	-	-	-	-	-	2.28	-	-	Ripley et al., 2002
Country rock	Tasiuyak Gneiss	VB433/109	-	-	-	-	-	0.33	0.10	33 000	Ripley et al., 2002
Country rock	Tasiuyak Gneiss	VB433/110.5	-	-	-	-	-	0.06	-	-	Ripley et al., 2002
Country rock	Tasiuyak Gneiss	VB433/112	-	-	-	-	-	0.05	-	-	Ripley et al., 2002
Country rock	Tasiuyak Gneiss	VB433/113.2	-	-	-	-	-	1.42	3.26	4 356	Ripley et al., 2002
Country rock	Tasiuyak Gneiss	VB433/115	-	-	-	-	-	0.75	0.77	9 740	Ripley et al., 2002
Country rock	Tasiuyak Gneiss	VB433/116	-	-	-	-	-	0.11	0.96	1 146	Ripley et al., 2002
Country rock	Tasiuyak Gneiss	VB433/117.5	-	-	-	-	-	0.08	-	-	Ripley et al., 2002
Country rock	Tasiuyak Gneiss	VB433/118	-	-	-	-	-	0.02	0.78	256	Ripley et al., 2002
Country rock	Tasiuyak Gneiss	VB433/119.5	-	-	-	-	-	0.61	0.29	21 034	Ripley et al., 2002
Country rock	Tasiuyak Gneiss	VB433/121	-	-	-	-	-	0.03	0.14	2 143	Ripley et al., 2002
Country rock	Tasiuyak Gneiss	VB433/122	-	-	-	-	-	0.02	0.01	20 000	Ripley et al., 2002
Country rock	Tasiuyak Gneiss	VB433/124.5	-	-	-	-	-	0.11	-	-	Ripley et al., 2002
Country rock	Tasiuyak Gneiss	VB433/152	-	-	-	-	-	0.22	-	-	Ripley et al., 2002
Country rock	Tasiuyak Gneiss	VB433/157	-	-	-	-	-	0.31	0.19	16 316	Ripley et al., 2002
Country rock	Tasiuyak Gneiss	VB433/173.5	-	-	-	-	-	6.47	8.03	8 057	Ripley et al., 2002
Country rock	Tasiuyak Gneiss	VB433/188	-	-	-	-	-	0.11	-	-	Ripley et al., 2002
Country rock	Tasiuyak Gneiss	VB487/99.5	-	-	-	-	-	1.02	2.06	4 951	Ripley et al., 2002
Country rock	Tasiuyak Gneiss	VB487/100.4	-	-	-	-	-	0.18	0.57	3 158	Ripley et al., 2002

Mining Camp / Deposit	Rocktype/ore	Sample	n	Ni % wt	Cu % wt	Pt ppb	Pd ppb	S % wt	Se ppm	S/Se	references
Country rock	Tasiuyak Gneiss	VB487/101	-	-	-	-	-	0.27	0.59	4 576	Ripley et al., 2002
Country rock	Tasiuyak Gneiss	VB487/101.5	-	-	-	-	-	0.41	0.94	4 362	Ripley et al., 2002
Country rock	Tasiuyak Gneiss	VB487/102.7	-	-	-	-	-	0.06	0.21	2 857	Ripley et al., 2002
Country rock	Tasiuyak Gneiss	VB487/103.3	-	-	-	-	-	1.06	3.31	3 202	Ripley et al., 2002
Country rock	Tasiuyak Gneiss	VB487/160.5	-	-	-	-	-	0.14	0.36	3 889	Ripley et al., 2002
Country rock	Tasiuyak Gneiss	VB487/316.0	-	-	-	-	-	0.18	0.40	4 500	Ripley et al., 2002
Country rock	Tasiuyak Gneiss	VB487/348.5	-	-	-	-	-	0.54	1.28	4 219	Ripley et al., 2002
Country rock	Tasiuyak Gneiss	VB487/407.5	-	-	-	-	-	0.15	0.36	4 167	Ripley et al., 2002
Country rock	Tasiuyak Gneiss	VB487/459	-	-	-	-	-	0.19	0.29	6 552	Ripley et al., 2002
Country rock	Tasiuyak Gneiss	VB487/550	-	-	-	-	-	0.38	0.67	5 672	Ripley et al., 2002
Country rock	Tasiuyak Gneiss	VB487/581.5	-	-	-	-	-	0.30	0.57	5 263	Ripley et al., 2002
Country rock	Tasiuyak Gneiss	VB487/605.4	-	-	-	-	-	0.06	0.10	6 000	Ripley et al., 2002
Country rock	Tasiuyak Gneiss	VB487/628.7	-	-	-	-	-	0.16	-	-	Ripley et al., 2002
Lac Volant											
Lac Volant Ore	SF-MS	Tc-319	-	2.12	0.58	-	-	38.20	37.00	10 324	Nabil et al., 2004
Lac Volant Ore	SF-MS	Tc-290	-	1.71	2.69	137	669	40.80	41.00	9 951	Nabil et al., 2004
Lac Volant Ore	SF-MS	Tc-291	-	1.88	0.57	214	375	36.60	36.00	10 167	Nabil et al., 2004
Lac Volant Ore	SF-MS	Tc-292	-	2.28	1.42	11	317	37.00	33.00	11 212	Nabil et al., 2004
Lac Volant Ore	SF-MS	Tc-294	-	1.58	0.71	47	176	40.80	30.00	13 600	Nabil et al., 2004
Lac Volant Ore	SF-MS	Tc-127	-	2.03	2.20	<3.1	314	41.40	36.00	11 500	Nabil et al., 2004
Lac Volant Ore	SF-MS	SM-d5	-	1.66	2.92	-	-	35.80	29.00	12 345	Nabil et al., 2004
Lac Volant Ore	SF-MS	SM-d8-9	-	1.76	1.82	46	295	36.90	30.00	12 300	Nabil et al., 2004
Lac Volant Ore	SF-MS	Sm-d123	-	1.82	1.32	1 704	326	36.90	29.00	12 724	Nabil et al., 2004
Lac Volant Ore	SF-MS	Sm-C12	-	1.68	1.56	-	-	36.40	25.00	14 560	Nabil et al., 2004
Lac Volant Ore	SF-MS	Sm-C3-4	-	1.65	2.89	16	328	36.40	29.00	12 552	Nabil et al., 2004
Lac Volant Ore	SF-MS	Sm-E	-	1.84	2.94	76	295	37.40	29.00	12 897	Nabil et al., 2004
Lac Volant Ore	SF-MS	Sm-G	-	1.94	0.61	263	231	36.00	22.00	16 364	Nabil et al., 2004
Lac Volant Ore	SF-MS	Sm-B	-	1.68	1J8	<14	349	36.80	26.00	14 154	Nabil et al., 2004
Lac Volant Ore	SF-MS	Sm-A1-3	-	1.63	1.63	19	326	35.20	26.00	13 538	Nabil et al., 2004
Lac Volant Ore	SF-MS	SM-A3-4	-	1.56	3.14	12	309	35.10	27.00	13 000	Nabil et al., 2004
Lac Volant Ore	SF-MS - ISS	Tc-291	-	0.30	19.40	<74	46	27.40	37.00	7 405	Nabil et al., 2004
Lac Volant Ore	SF-Mtr	Tc-168-a	-	0.97	1.59	43	312	15.70	15.00	10 467	Nabil et al., 2004
Lac Volant Ore	SF-Mtr	Tc-168-b	-	0.95	2.00	42	236	16.70	17.00	9 824	Nabil et al., 2004
Lac Volant Ore	SF-Mtr	TC-124-A1	-	0.88	1.31	<3.1	166	13.90	15.00	9 267	Nabil et al., 2004
Lac Volant Ore	SF-Mtr	Tc-309	-	0.91	0.61	15	20	12.60	10.00	12 600	Nabil et al., 2004
Lac Volant Ore	SF-Diss	Tc-315	-	0.45	0.14	<15	22	7.02	6.00	11 700	Nabil et al., 2004
Lac Volant Ore	SF-Diss	Tc-310	-	0.58	0.22	<2.9	38	7.73	9.00	8 589	Nabil et al., 2004
Lac Volant Ore	SF-Diss	Tc-293	-	0.23	0.14	<3.3	14	2.88	3.00	9 600	Nabil et al., 2004
Lac Volant Ore	SF-Diss	Tc-320	-	0.53	0.33	25	148	7.23	6.00	12 050	Nabil et al., 2004
Lac Volant Ore	SF-Diss	Tc-316	-	0.11	0.07	<6.7	4	1.79	3.00	5 967	Nabil et al., 2004
Lac Volant Ore	SF-Diss	Tc-318	-	0.34	0.32	33	59	5.08	8.00	6 350	Nabil et al., 2004
Country rock	Gabbronorite	Tc-101-a	-	0.01	0.01	<4.8	<1.5	0.11	3.60	306	Nabil et al., 2004
Country rock	Gabbronorite	Tc-153-a	-	0.01	0.01	<9	<1.3	0.02	3.70	54	Nabil et al., 2004
Country rock	Gabbronorite	Tc-184-a	-	0.01	0.00	7	<1.3	0.13	1.90	684	Nabil et al., 2004
Country rock	Gabbronorite dyke	Tc-234	-	0.01	0.00	<5	<2.4	0.15	3.00	500	Nabil et al., 2004
Country rock	Gabbronorite dyke	Tc-157-a	-	0.04	0.02	<3.2	2	< 0.01	1.60	-	Nabil et al., 2004
Country rock	Gabbronorite dyke	TC-173-A1	-	0.01	0.01	<4	<2.2	0.12	3.20	375	Nabil et al., 2004
Country rock	Gabbronorite dyke	Tc-231-a1	-	0.01	0.01	<7.5	2	0.13	4.30	302	Nabil et al., 2004
Country rock	Gabbronorite dyke	Tc-289-a	-	0.01	0.01	<6.1	<1.8	0.14	4.60	304	Nabil et al., 2004
Country rock	Gabbronorite dyke	Tc-311-c	-	0.01	0.01	<8.2	<2.7	0.11	4.80	229	Nabil et al., 2004
Country rock	Gabbronorite dyke	Tc-311-b	-	0.01	0.00	<4.6	<2.4	0.09	2.40	375	Nabil et al., 2004
Country rock	Gabbronorite dyke	Tc-263-a	-	0.01	0.01	<8.4	<2.8	0.18	4.50	400	Nabil et al., 2004
Country rock	Paragneiss	Met-1	-	0.01	0.02	-	-	3.41	3.60	9 472	Nabil et al., 2004
Lac à Paul											
Lac à Paul	Dunite	2349	-	0.05	0.05	3	3	1.37	1.47	9 320	Huss, 2002
Lac à Paul	Websterite	LH25	-	0.08	0.01	<2.5	<3.7	0.36	<1.6	-	Huss, 2002

Mining Camp	Rocktype/ore	Sample	n	Ni	Cu	Pt	Pd	S	Se	S/Se	references
Deposit				% wt	% wt	ppb	ppb	% wt	ppm		
Lac à Paul	Websterite	2568C	-	0.05	0.02	2	4	0.73	<1.2	-	Huss, 2002
Lac à Paul	Pyroxenite	2566A1	-	0.02	0.00	<2.0	<4.4	0.08	<3.0	-	Huss, 2002
Lac à Paul	Pyroxenite	2396A	-	0.02	0.04	<2.1	8	0.95	<1.7	-	Huss, 2002
Lac à Paul	Hornblendite	2497B	-	0.02	0.00	<3.4	<2.2	0.02	3.16	63	Huss, 2002
Lac à Paul	Hornblendite	2567D	-	0.02	0.08	<3.2	3	1.01	10.75	940	Huss, 2002
Lac à Paul	Hornblendite	2188C2	-	0.00	0.00	<2.0	4	1.52	0.82	18 537	Huss, 2002
Lac à Paul	Hornblendite	2188C1	-	0.01	0.00	<1.5	4	3.10	1.87	16 578	Huss, 2002
Lac à Paul	Hornblendite	2396B	-	0.01	0.03	1	1	0.55	0.00	-	Huss, 2002
Lac à Paul	Hornblendite	2474A1	-	0.17	0.17	3	5	3.19	2.36	13 517	Huss, 2002
Lac à Paul	Hornblendite	2474	-	0.25	0.19	<2.8	9	4.60	2.54	18 110	Huss, 2002
Lac à Paul	Norite	LH23	-	0.02	0.05	<1.8	6	0.06	1.85	324	Huss, 2002
Lac à Paul	Gabbronorite	2566A2	-	0.08	0.03	<2.1	4	1.31	0.76	17 237	Huss, 2002
Lac à Paul	Gabbronorite	2568A	-	0.01	0.01	<2.2	5	0.10	<2.4	-	Huss, 2002
Lac à Paul	Gabbronorite	2567B2	-	0.02	0.01	<0.99	1	0.42	<1.8	-	Huss, 2002
Lac à Paul	Gabbro	3229	-	0.07	0.22	<2.6	<6.9	0.98	1.19	8 235	Huss, 2002
Lac à Paul	Gabbro	2567B1	-	0.01	0.02	<1.7	3	0.13	1.14	1 140	Huss, 2002
Lac à Paul	Gabbro	2567A	-	0.01	0.08	<1.5	<4.6	0.11	<1.7	-	Huss, 2002
Lac à Paul	Gabbro	LH21	-	0.08	0.04	<1.5	1	1.72	5.42	3 173	Huss, 2002
Lac à Paul	Gabbro	2188A	-	0.00	0.00	2	<2.2	0.46	<1.4	-	Huss, 2002
Lac à Paul	Gabbro	2567C	-	0.00	0.00	<2.1	3	0.05	<1.2	-	Huss, 2002
Lac à Paul	Gabbro	2390	-	0.03	0.06	1	2	1.89	<1.9	-	Huss, 2002
Lac à Paul	Gabbro	690853	-	0.30	0.09	2	8	5.30	2.62	20 229	Huss, 2002
Lac à Paul	Gabbro	2566B1	-	1.22	0.38	<3.4	12	13.30	8.29	16 043	Huss, 2002
Lac à Paul	Gabbro	LH13	-	0.12	0.08	<5.4	20	4.34	3.21	13 520	Huss, 2002
Lac à Paul	Gabbro	690742	-	0.07	0.18	<2.1	17	1.56	1.11	14 054	Huss, 2002
Lac à Paul	Leucogabbro	690851	-	0.35	0.16	<4.0	14	6.22	3.09	20 129	Huss, 2002
Lac à Paul	Leucogabbro	2349B	-	0.00	0.00	<1.3	<2.2	0.38	0.88	4 318	Huss, 2002
Lac à Paul	Leucogabbro	2474A2	-	0.06	0.06	<2.3	5	0.86	1.44	5 972	Huss, 2002
Lac à Paul	Fe-Ti	LH17	-	0.02	0.05	<2.10	5	0.35	2.32	1 509	Huss, 2002
Lac à Paul	SF-Mtr	690741	-	0.59	0.70	16	73	14.80	6.02	24 585	Huss, 2002
Lac à Paul	SF-Mtr	689842	-	0.22	4.73	<6.0	6	15.60	6.70	23 284	Huss, 2002
Lac à Paul	SF-Mtr	690800	-	0.92	0.14	13	49	16.30	9.26	17 603	Huss, 2002
Lac à Paul	SF-Mtr	689841	-	0.43	0.68	182	68	20.40	7.96	25 628	Huss, 2002
Lac à Paul	SF-Mtr	2349C	-	0.45	1.87	<3.4	26	20.50	11.04	18 569	Huss, 2002
Lac à Paul	SF-MS	690739	-	1.34	0.10	3	92	29.90	13.93	21 464	Huss, 2002
Lac à Paul	SF-MS	690964	-	0.65	0.22	<3.4	71	32.20	13.08	24 618	Huss, 2002
Country rock	Syeno-Granite	2535	-	0.00	0.00	<1.6	4	0.01	1.44	69	Huss, 2002
Country rock	Granodiorite	3168	-	0.00	0.00	<1.1	3	0.01	1.89	53	Huss, 2002
Country rock	Monzogranite	3393	-	0.00	0.00	<3.1	<3.4	0.01	1.44	69	Huss, 2002
Country rock	Monzogranite	1063A	-	0.00	0.00	<5.0	4	0.02	2.51	80	Huss, 2002
Country rock	Granodiorite	2190A	-	0.00	0.00	<1.5	<2.1	0.01	2.92	34	Huss, 2002
Country rock	Monzogranite	LH18	-	0.00	0.00	<2.1	4	0.20	3.53	567	Huss, 2002
Country rock	Marble	2387A1	-	0.00	0.00	1	<4.5	0.37	1.21	3 058	Huss, 2002
Lac Kenogami											
Mafic/Ultramafic rocks	Harzburgite	2156	-	0.14	0.01	12	103	0.10	<1.1	-	Vaillancourt, 2001
Mafic/Ultramafic rocks	Dunite	2158	-	0.19	0.00	3	69	0.02	<1.0	-	Vaillancourt, 2001
Mafic/Ultramafic rocks	Harzburgite	2182	-	0.18	0.00	5	49	0.03	<1.0	-	Vaillancourt, 2001
Mafic/Ultramafic rocks	Harzburgite	2183	-	0.19	0.00	3	65	0.05	<1.5	-	Vaillancourt, 2001
Mafic/Ultramafic rocks	Harzburgite	2503	-	0.17	0.00	8	45	0.03	<0.7	-	Vaillancourt, 2001
Mafic/Ultramafic rocks	Harzburgite	2504	-	0.17	0.00	4	56	0.02	<0.5	-	Vaillancourt, 2001
Mafic/Ultramafic rocks	Dunite	2505	-	0.19	0.00	8	47	0.04	<0.1	-	Vaillancourt, 2001
Mafic/Ultramafic rocks	Harzburgite	2506	-	0.18	0.00	3	53	0.02	<1.1	-	Vaillancourt, 2001
Mafic/Ultramafic rocks	Harzburgite	2507	-	0.18	0.00	4	69	0.02	<1.0	-	Vaillancourt, 2001
Mafic/Ultramafic rocks	Dunite	2509	-	0.22	0.01	5	105	0.08	<0.7	-	Vaillancourt, 2001
Mafic/Ultramafic rocks	Harzburgite	2511	-	0.19	0.00	5	46	0.07	<1.3	-	Vaillancourt, 2001
Mafic/Ultramafic rocks	Harzburgite	2515	-	0.17	0.02	36	172	0.21	0.90	2 333	Vaillancourt, 2001

Mining Camp	Rocktype/ore	Sample	n	Ni	Cu	Pt	Pd	S	Se	S/Se	references
Deposit				% wt	% wt	ppb	ppb	% wt	ppm		
Mafic/Ultramafic rocks	Gabbronorite	2109	-	0.05	0.01	11	8	0.27	0.60	4 500	Vaillancourt, 2001
Mafic/Ultramafic rocks	Gabbronorite	2110	-	0.06	0.00	14	12	0.05	<0.6	-	Vaillancourt, 2001
Mafic/Ultramafic rocks	Gabbronorite	2311A	-	0.03	0.00	3	3	0.02	1.00	200	Vaillancourt, 2001
Mafic/Ultramafic rocks	Gabbronorite	2517A	-	0.04	0.00	6	4	<0.01	<0.9	-	Vaillancourt, 2001
Mafic/Ultramafic rocks	Gabbronorite	2519A	-	0.04	0.00	11	4	0.05	<0.5	-	Vaillancourt, 2001
Mafic/Ultramafic rocks	Gabbronorite	2185	-	0.01	0.00	3	2	0.06	3.00	200	Vaillancourt, 2001
Mafic/Ultramafic rocks	Gabbronorite	2520B	-	0.01	0.04	4	4	0.77	2.70	2 852	Vaillancourt, 2001
Mafic/Ultramafic rocks	Gabbronorite	2521	-	0.01	0.01	3	2	0.15	4.40	341	Vaillancourt, 2001
Dumont	Gabbronorite	2516A	-	0.09	0.02	4	54	0.43	<0.6	-	Vaillancourt, 2001
Dumont	Gabbronorite	2516C	-	0.15	0.03	4	27	0.60	4.00	1 500	Vaillancourt, 2001
Dumont	Gabbronorite	2516D	-	0.02	0.01	3	4	0.10	1.40	714	Vaillancourt, 2001
Dumont	Gabbronorite	2516E	-	0.05	0.03	3	17	0.87	1.40	6 214	Vaillancourt, 2001
Dumont	Gabbronorite	2516G	-	0.13	0.08	7	92	1.21	2.40	5 042	Vaillancourt, 2001
Dumont	Gabbronorite	2516H	-	0.39	0.10	11	123	1.17	9.10	1 286	Vaillancourt, 2001
Dumont	Gabbronorite	25161	-	0.19	0.20	3	44	1.64	3.10	5 290	Vaillancourt, 2001
Dumont	Gabbronorite	2516J	-	0.62	0.18	12	242	4.40	14.20	3 099	Vaillancourt, 2001
Dumont	Gabbronorite	2516K	-	2.81	1.14	13	749	28.20	49.80	5 663	Vaillancourt, 2001
Gagnon	Gabbronorite	2502E	-	0.16	0.28	23	78	0.54	3.40	1 588	Vaillancourt, 2001
Gagnon	Gabbronorite	2502F	-	0.68	0.27	30	92	1.91	8.80	2 170	Vaillancourt, 2001
Gagnon	Gabbronorite	2502G	-	0.24	0.13	11	27	0.67	3.50	1 914	Vaillancourt, 2001
Gagnon	Gabbronorite	2502I	-	0.05	0.08	5	3	0.23	1.20	1 917	Vaillancourt, 2001
Gagnon	Gabbronorite	2502J	-	0.07	0.10	14	28	0.26	2.30	1 130	Vaillancourt, 2001
Gagnon	Gabbronorite	2502K	-	0.16	0.21	159	938	0.51	3.40	1 500	Vaillancourt, 2001
Gagnon	Gabbronorite	2502L	-	0.03	0.05	8	<3.0	0.15	2.00	750	Vaillancourt, 2001
Other rock type	Migmatite	2502B	-	0.01	0.00	<6.0	<5.6	<0.01	2.90	-	Vaillancourt, 2001
Other rock type	Migmatite	2502C	-	<0.0047	0.00	<3.6	<3.7	<0.01	7.90	-	Vaillancourt, 2001
Other rock type	Migmatite	2502D	-	<0.0035	0.00	11	3	0.03	7.80	38	Vaillancourt, 2001
Other rock type	Quartzite	2513	-	<0.0004	0.00	<5.7	<2.2	<0.01	1.30	-	Vaillancourt, 2001
Other rock type	Quartzite	2514	-	0.00	0.00	<4.7	<1.6	<0.01	1.40	-	Vaillancourt, 2001
Other rock type	Migmatite	2515B	-	<0.0029	0.00	<11.0	1	0.02	10.40	19	Vaillancourt, 2001
Other rock type	Migmatite	2518	-	<0.0024	0.00	<6.7	<1.4	<0.01	6.90	-	Vaillancourt, 2001
Portneuf-Mauricie											
Réservoir Blanc	Gabbronorite	AS-04-470B	-	0.07	0.03	13	14	0.41	2.12	1 934	Sappin et al., 2011
Lac Matte	Orthopyroxenite	AS-04-431A	-	0.21	0.11	4	< 0,5	0.89	1.59	5 597	Sappin et al., 2011
Lac Matte	Gabbronorite	AS-04-431C	-	0.18	0.07	0	3	0.95	1.31	7 252	Sappin et al., 2011
Lac Matte	Websterite	AS-04-431D	-	0.42	0.20	6	2	1.91	3.84	4 974	Sappin et al., 2011
Lac Matte	Websterite	AS-05-608A	-	0.43	0.12	4	3	2.38	3.73	6 381	Sappin et al., 2011
Lac Kennedy	Harzburgite	AS-04-483A	-	0.15	0.00	1	1	0.10	<0,33	-	Sappin et al., 2011
Lac Kennedy	Gabbronorite	AS-04-516A2	-	0.40	0.39	1	5	3.16	5.44	5 809	Sappin et al., 2011
Lac Kennedy	Gabbronorite	AS-04-534B	-	0.06	0.03	1	1	0.33	1.13	2 920	Sappin et al., 2011
Lac Edouard	Orthopyroxenite	Bloc Edouard 1	-	1.54	0.29	1	28	15.40	22.00	7 000	Sappin et al., 2011
Lac Edouard	Gabbronorite	LE-40	-	0.14	0.05	1	< 0,5	0.61	1.18	5 169	Sappin et al., 2011
Lac Edouard	Websterite	LE-41	-	1.58	0.21	1	24	18.00	14.00	12 857	Sappin et al., 2011
Lac Edouard	Harzburgite	LE-44	-	0.32	0.14	4	1	2.31	3.71	6 226	Sappin et al., 2011
Boivin	Gabbronorite	AS-04-538A	-	0.13	0.03	1	1	0.54	0.95	5 684	Sappin et al., 2011
Rochette West	Websterite	AS-04-447A1	-	0.07	0.02	2	1	1.11	1.31	8 473	Sappin et al., 2011
Rochette West	Gabbronorite	AS-04-447B	-	0.04	0.03	6	7	1.03	0.47	21 915	Sappin et al., 2011
Rousseau	Orthopyroxenite	AS-03-317A	-	0.90	0.30	29	112	1.80	10.40	1 731	Sappin et al., 2011
Rousseau	Websterite	AS-05-681A2	-	0.27	0.09	36	60	0.70	4.37	1 602	Sappin et al., 2011
Rousseau	Orthopyroxenite	AS-05-766B	-	0.49	0.22	51	118	1.19	6.92	1 720	Sappin et al., 2011
Rousseau	Orthopyroxenite	LV-30	-	0.15	0.54	26	37	0.33	1.39	2 374	Sappin et al., 2011
Lac Nadeau	Gabbronorite	AS-03-99A	-	0.26	0.28	331	482	1.10	6.19	1 777	Sappin et al., 2011
Lac Nadeau	Gabbronorite	AS-03-101A	-	0.44	0.48	1 366	2 011	1.82	11.00	1 655	Sappin et al., 2011
Lac Nadeau	Gabbronorite	MC-03-1000	-	0.15	0.02	14	22	0.10	0.40	2 500	Sappin et al., 2011
Lac Nadeau	Lherzolite	TC-03-2016A	-	0.20	0.02	28	33	0.13	-	-	Sappin et al., 2011
Lac Nadeau	Lherzolite	TC-03-2029A	-	0.19	0.02	19	23	0.10	-	-	Sappin et al., 2011

Mining Camp	Rocktype/ore	Sample	n	Ni	Cu	Pt	Pd	S	Se	S/Se	references
Deposit				% wt	% wt	ppb	ppb	% wt	ppm		
Curaçà Valley											
Caraiba	Vein	7	-	0.19	24.70	121	74	24.47	113.00	2 165	Maier and Barnes, 1999
Caraiba	Vein	80	-	0.21	0.71	<24	47	10.20	10.00	10 200	Maier and Barnes, 1999
Caraiba	Vein	3909-34.65	-	0.01	49.41	45	72	19.48	175.00	1 113	Maier and Barnes, 1999
Caraiba	SF-MS	70	-	6.21	18.92	1 663	891	18.54	464.00	400	Maier and Barnes, 1999
Caraiba	SF-MS	17	-	0.07	35.43	121	185	13.28	121.00	1 098	Maier and Barnes, 1999
Caraiba	Orthopyroxenite	1620-9.1	-	0.09	0.16	62	5	0.33	3.00	1 100	Maier and Barnes, 1999
Caraiba	Orthopyroxenite	1620-19.0	-	0.11	0.25	17	6	0.34	4.00	850	Maier and Barnes, 1999
Caraiba	Orthopyroxenite	1620-26.3	-	0.10	0.35	<3	12	0.44	4.00	1 100	Maier and Barnes, 1999
Caraiba	Orthopyroxenite	1620-34.3	-	0.14	7.14	770	<2	2.51	62.00	405	Maier and Barnes, 1999
Caraiba	Orthopyroxenite	1620-38.7	-	0.23	6.95	1 352	<2	5.95	144.00	413	Maier and Barnes, 1999
Caraiba	Orthopyroxenite	1720-46.8	-	0.09	0.77	256	28	0.93	9.00	1 033	Maier and Barnes, 1999
Caraiba	Orthopyroxenite	3710-711	-	0.17	0.93	57	30	1.09	14.00	779	Maier and Barnes, 1999
Caraiba	Orthopyroxenite	3322-288.9	-	0.11	3.18	277	59	1.24	19.00	653	Maier and Barnes, 1999
Caraiba	Orthopyroxenite	3111-59	-	0.20	18.80	960	297	7.11	109.00	652	Maier and Barnes, 1999
Caraiba	Orthopyroxenite	4323-118.2	-	0.08	7.72	41	44	3.74	26.00	1 438	Maier and Barnes, 1999
Caraiba	Orthopyroxenite	4323-355.5	-	0.11	5.81	155	<2	2.91	23.00	1 265	Maier and Barnes, 1999
Caraiba	Orthopyroxenite	4323-360.4	-	0.12	5.22	99	<2	4.31	23.00	1 874	Maier and Barnes, 1999
Caraiba	Orthopyroxenite	4323-371.1	-	0.25	9.96	290	<2	7.20	52.00	1 385	Maier and Barnes, 1999
Caraiba	Orthopyroxenite	4323-379.4	-	0.19	10.69	<43	360	7.48	64.00	1 169	Maier and Barnes, 1999
Caraiba	Orthopyroxenite	mco12	-	0.03	1.97	55	42	2.99	28.00	1 068	Maier and Barnes, 1999
Caraiba	Orthopyroxenite	mco14	-	0.07	0.45	<3	<2	0.27	11.00	245	Maier and Barnes, 1999
Caraiba	Orthopyroxenite	mco8	-	0.11	3.99	760	1 112	5.83	22.00	2 650	Maier and Barnes, 1999
Caraiba	Orthopyroxenite	16	-	0.14	5.37	438	<2	1.56	18.00	867	Maier and Barnes, 1999
Sertaozinho	Orthopyroxenite	31	-	0.15	0.55	29	23	0.53	2.00	2 650	Maier and Barnes, 1999
Angico	Orthopyroxenite	337.1	-	0.12	3.15	<33	377	1.84	64.00	288	Maier and Barnes, 1999
Angico	Orthopyroxenite	338.5	-	0.09	2.59	74	67	1.20	48.00	250	Maier and Barnes, 1999
Angico	Orthopyroxenite	339.5	-	0.11	2.67	<3	106	1.79	68.00	263	Maier and Barnes, 1999
Surubim	Orthopyroxenite	65.3	-	0.11	3.92	41	41	2.31	12.00	1 925	Maier and Barnes, 1999
Surubim	Orthopyroxenite	28.6	-	0.03	0.50	32	12	0.29	3.00	967	Maier and Barnes, 1999
Susuarana	Orthopyroxenite	187.3	-	0.13	0.79	37	39	0.60	5.00	1 200	Maier and Barnes, 1999
Susuarana	Orthopyroxenite	196.2	-	0.12	1.01	38	37	0.62	5.00	1 240	Maier and Barnes, 1999
Susuarana	Orthopyroxenite	196.8	-	0.10	1.03	20	22	0.66	3.00	2 200	Maier and Barnes, 1999
Terra Do Sal	Orthopyroxenite	303.4	-	0.06	0.79	4	15	0.31	3.00	1 033	Maier and Barnes, 1999
Terra Do Sal	Orthopyroxenite	304.1	-	0.12	5.93	104	<2	1.82	25.00	728	Maier and Barnes, 1999
Vermelhos	Orthopyroxenite	16-71.3	-	0.08	1.63	40	113	0.80	28.00	286	Maier and Barnes, 1999
Vermelhos	Orthopyroxenite	38	-	0.08	1.14	39	29	0.62	13.00	477	Maier and Barnes, 1999
Vermelhos	Orthopyroxenite	65	-	0.08	1.53	104	45	0.84	12.00	700	Maier and Barnes, 1999
Vermelhos	Orthopyroxenite	67.1	-	0.10	2.66	55	91	1.32	31.00	426	Maier and Barnes, 1999
Caraiba	Meladiorite	mco1	-	0.36	3.46	199	143	3.75	36.00	1 042	Maier and Barnes, 1999
Caraiba	Meladiorite	mco10	-	0.03	0.99	11	33	1.10	3.00	3 667	Maier and Barnes, 1999
Terra Do Sal	Meladiorite	122.8	-	0.10	1.26	45	144	0.56	25.00	224	Maier and Barnes, 1999
Terra Do Sal	Meladiorite	325.6	-	0.12	3.65	35	131	1.03	11.00	936	Maier and Barnes, 1999
Caraiba	Diorite	4323-63.3	-	0.03	0.07	16	22	0.00	24.00	0	Maier and Barnes, 1999
Caraiba	Diorite	4323-370.1	-	0.00	0.17	32	<2	0.00	5.00	0	Maier and Barnes, 1999
Caraiba	Diorite	4323-381.1	-	< 0.0063	0.08	98	<2	0.17	5.00	340	Maier and Barnes, 1999
Caraiba	Diorite	4323-381.95	-	0.00	0.02	<3	<2	0.00	5.00	0	Maier and Barnes, 1999
Caraiba	Diorite	mco3	-	0.03	0.95	12	9	0.65	1.00	6 500	Maier and Barnes, 1999
Caraiba	Diorite	10	-	0.02	0.16	<3	<2	0.06	2.00	300	Maier and Barnes, 1999
Caraiba	Diorite	11	-	0.03	0.31	<3	<2	0.10	28.00	36	Maier and Barnes, 1999
Surubim	Diorite	13	-	0.00	0.11	15	<2	0.08	3.00	267	Maier and Barnes, 1999
Surubim	Diorite	43	-	0.03	1.47	<3	<2	0.80	13.00	615	Maier and Barnes, 1999
Santa Fe	Diorite	133.3	-	0.01	0.58	4	4	0.44	2.00	2 200	Maier and Barnes, 1999
Malha Santa Fe	Serpentinite	21	-	0.16	0.01	2	7	0.00	0.00	-	Maier and Barnes, 1999
Caraiba	Peridotite	6	-	0.23	0.04	12	16	0.08	0.00	-	Maier and Barnes, 1999
Malha Santa Fe	Websterite	20	-	0.15	0.01	2	8	0.01	0.00	-	Maier and Barnes, 1999

Mining Camp / Deposit	Rocktype/ore	Sample	n	Ni % wt	Cu % wt	Pt ppb	Pd ppb	S % wt	Se ppm	S/Se	references
Malha Santa Fe	Websterite	23	-	0.10	0.02	4	7	0.15	0.00	-	Maier and Barnes, 1999
Sertaozinho	Websterite	32	-	0.11	0.02	16	11	0.06	0.00	-	Maier and Barnes, 1999
Boa Sorte	Websterite	40	-	0.06	0.01	2	5	0.11	0.00	-	Maier and Barnes, 1999
Boa Sorte	Websterite	44	-	0.07	0.02	8	3	0.19	0.00	-	Maier and Barnes, 1999
Boa Sorte	Websterite	49	-	0.08	0.11	8	1	0.18	0.00	-	Maier and Barnes, 1999
Boa Sorte	Websterite	50	-	0.04	0.02	8	1	0.20	0.00	-	Maier and Barnes, 1999
Caraiba	Gabbro	mco13	-	0.00	0.51	2	1	0.00	4.00	-	Maier and Barnes, 1999
Caraiba	Gabbro	1620-30.2	-	0.01	0.11	2	1	0.09	2.00	450	Maier and Barnes, 1999
Caraiba	Gabbro	4323-264.4	-	0.01	0.01	14	18	0.00	1.00	-	Maier and Barnes, 1999
Caraiba	Gabbro	4323-299.6	-	0.00	0.02	21	13	0.00	2.00	-	Maier and Barnes, 1999
Caraiba	Gabbro	4323-322.1	-	0.01	0.01	8	13	0.07	1.00	700	Maier and Barnes, 1999
Susuarana	Gabbro	30	-	0.00	0.07	2	2	0.11	1.00	1 100	Maier and Barnes, 1999
Bagaicera	Gabbro	26	-	0.00	0.01	8	5	0.14	2.00	700	Maier and Barnes, 1999
Caraiba	Amphibolite	13	-	0.01	0.01	<3	<2	0.25	1.00	2 500	Maier and Barnes, 1999
Caraiba	Amphibolite	4323-24.4	-	0.02	0.01	21	14	0.00	1.00	-	Maier and Barnes, 1999
Caraiba	Amphibolite	4323-247.9	-	0.03	0.01	6	2	0.00	1.00	-	Maier and Barnes, 1999
Caidura Sul	Amphibolite	25	-	0.01	0.03	6	6	0.02	2.00	100	Maier and Barnes, 1999
Susuarana	Amphibolite	28	-	0.01	0.01	26	19	0.00	1.00	-	Maier and Barnes, 1999
Bagaicera	Amphibolite	27	-	0.12	0.01	15	7	0.05	3.00	167	Maier and Barnes, 1999
Boa Sorte	Amphibolite	55	-	0.10	0.03	11	4	0.01	2.00	50	Maier and Barnes, 1999
Caraiba	Amphibolite	mco11	-	0.04	1.88	54	82	2.92	7.00	4 171	Maier and Barnes, 1999
Caraiba	Amphibolite	mco9	-	0.05	1.90	150	219	3.02	15.00	2 013	Maier and Barnes, 1999
Vermelhos	Glimmerite	16-115	-	0.08	0.80	62	17	0.80	7.00	1 143	Maier and Barnes, 1999
Surubim	Glimmerite	118.3	-	0.10	3.66	<20	91	1.55	20.00	775	Maier and Barnes, 1999
Susuarana	Glimmerite	29	-	0.14	1.15	434	8	0.01	4.00	25	Maier and Barnes, 1999
Caraiba	Calc-silicate	3813-35.7	-	0.03	6.05	27	24	5.73	3.00	19 100	Maier and Barnes, 1999
Caraiba	Calc-silicate	3813-47.6	-	0.03	6.86	<3	39	6.45	10.00	6 450	Maier and Barnes, 1999
Caraiba	Calc-silicate	mco7	-	0.00	0.42	<3	<2	0.11	1.00	1 100	Maier and Barnes, 1999
Surubim	Calc-silicate	159.5	-	0.02	4.34	25	158	2.75	1.00	27 500	Maier and Barnes, 1999
Caraiba	Granite	3813-65.8	-	0.00	0.58	<3	<2	0.64	0.00	-	Maier and Barnes, 1999
Caraiba	Granite	4323-351.6	-	< 0.002	0.00	<3	<2	0.00	3.00	-	Maier and Barnes, 1999
Caraiba	Gneiss	4323-315.4	-	< 0.002	0.01	27	<2	0.00	2.00	-	Maier and Barnes, 1999
Santa Fe	Syenite	24	-	0.00	0.02	<3	4	0.02	2.00	100	Maier and Barnes, 1999
Rio Mulunga	Tonalite	62	-	0.01	0.05	<3	5	3.56	3.00	11 867	Maier and Barnes, 1999
Curaçà Valley	Peridotite	-	9	0.11	0.02	7	6	0.09	0.30	3 000	Maier and Barnes, 1996
Curaçà Valley	Pyroxénite	-	36	0.11	4.50	181	92	2.42	28.60	846	Maier and Barnes, 1996
Curaçà Valley	mélanorite	-	5	0.13	1.97	64	93	1.35	14.90	906	Maier and Barnes, 1996
Curaçà Valley	Norite	-	7	0.02	0.43	10	3	0.25	7.80	321	Maier and Barnes, 1996
Curaçà Valley	Gabbro	-	8	0.01	0.04	11	11	0.05	4.10	122	Maier and Barnes, 1996
Curaçà Valley	Amphibolite	-	3	0.02	0.02	13	9	0.01	1.30	77	Maier and Barnes, 1996
Curaçà Valley	Glimmerite	-	2	0.12	2.41	217	49	0.78	12.40	629	Maier and Barnes, 1996
Curaçà Valley	Calcsilicates	-	7	0.04	3.18	42	77	3.11	34.00	915	Maier and Barnes, 1996
Curaçà Valley	Syenite	-	1	0.00	0.02	<3	4	0.02	1.70	118	Maier and Barnes, 1996
Curaçà Valley	Granodiorite	-	1	< 0,002	0.00	<3	<2	0.00	2.70	-	Maier and Barnes, 1996
Curaçà Valley	Gneiss	-	1	< 0,002	0.01	27	<2	0.00	2.00	-	Maier and Barnes, 1996
Okiep											
Carolusberg Mine	Norite / Pyroxenite	CW19.05	-	0.08	4.88	90	93	1.27	20.00	635	Maier, 2000
Carolusberg Mine	Norite / Pyroxenite	CW26.62	-	0.02	1.85	< 20	44	0.88	-	-	Maier, 2000
Carolusberg Mine	Norite / Pyroxenite	CW27.10	-	0.03	2.39	13	29	0.82	-	-	Maier, 2000
Carolusberg Mine	Norite / Pyroxenite	CW27.60	-	0.04	3.14	20	45	0.80	-	-	Maier, 2000
Carolusberg Mine	Norite / Pyroxenite	CW29.30	-	0.02	1.34	< 26	25	0.36	-	-	Maier, 2000
Carolusberg Mine	Norite / Pyroxenite	CW36.90	-	0.03	2.35	-	-	0.90	-	-	Cawthorn and Meyer, 1993
Carolusberg Mine	Norite / Pyroxenite	CW50.30	-	0.08	6.86	-	-	2.18	24.00	908	Cawthorn and Meyer, 1993
Carolusberg Mine	Norite / Pyroxenite	CW50.8	-	0.08	5.55	< 10	< 130	1.78	21.00	848	Maier, 2000
Carolusberg Mine	Norite / Pyroxenite	CW57.7	-	0.07	3.37	-	-	1.31	-	-	Cawthorn and Meyer, 1993
Carolusberg Mine	Norite / Pyroxenite	CW58.2	-	0.07	3.62	-	-	1.36	24.00	567	Cawthorn and Meyer, 1993

Mining Camp / Deposit	Rocktype/ore	Sample	n	Ni % wt	Cu % wt	Pt ppb	Pd ppb	S % wt	Se ppm	S/Se	references
Koperberg Suite	Norite / Pyroxenite	CB3	-	0.01	0.32	-	-	-	-	-	Cawthorn and Meyer, 1993
West Okiep Mine	Norite / Pyroxenite	WO1	-	0.02	0.74	-	-	0.25	-	-	Cawthorn and Meyer, 1993
West Okiep Mine	Norite / Pyroxenite	WO2	-	0.04	4.17	-	-	1.12	17.00	659	Cawthorn and Meyer, 1993
West Okiep Mine	Norite / Pyroxenite	WO3	-	0.02	1.29	-	-	0.37	7.00	529	Cawthorn and Meyer, 1993
West Okiep Mine	Norite / Pyroxenite	WO4	-	0.04	4.26	-	-	1.40	11.00	1 273	Cawthorn and Meyer, 1993
West Okiep Mine	Norite / Pyroxenite	WO5	-	0.02	0.59	-	-	0.30	-	-	Cawthorn and Meyer, 1993
West Okiep Mine	Norite / Pyroxenite	WO6	-	0.02	0.91	-	-	0.30	7.00	429	Cawthorn and Meyer, 1993
West Okiep Mine	Norite / Pyroxenite	WO7	-	0.04	3.23	-	-	1.37	-	-	Cawthorn and Meyer, 1993
West Okiep Mine	Norite / Pyroxenite	WO8A	-	0.01	0.94	-	-	0.54	-	-	Cawthorn and Meyer, 1993
West Okiep Mine	Norite / Pyroxenite	WO8B	-	0.02	0.50	-	-	-	-	-	Cawthorn and Meyer, 1993
East Okiep Mine	Norite / Pyroxenite	EO1	-	0.02	1.17	-	-	1.24	7.00	1 771	Cawthorn and Meyer, 1993
East Okiep Mine	Norite / Pyroxenite	EO2	-	0.02	1.02	< 3	6	1.25	9.00	1 389	Maier, 2000
East Okiep Mine	Norite / Pyroxenite	EO3	-	0.01	1.00	< 3	< 3	1.12	-	-	Maier, 2000
East Okiep Mine	Norite / Pyroxenite	EO4	-	0.01	0.45	-	-	1.25	-	-	Cawthorn and Meyer, 1993
East Okiep Mine	Norite / Pyroxenite	EO5	-	0.01	0.95	-	-	1.05	-	-	Cawthorn and Meyer, 1993
East Okiep Mine	Norite / Pyroxenite	EO6	-	0.01	1.23	9	5	1.26	7.00	1 800	Maier, 2000
East Okiep Mine	Norite / Pyroxenite	EO7	-	0.01	0.82	-	-	1.19	-	-	Cawthorn and Meyer, 1993
East Okiep Mine	Norite / Pyroxenite	EO8	-	0.01	1.33	< 3	7	1.47	7.00	2 100	Maier, 2000
Vammala											
Deep Ore	SF-Diss	V204	-	-	-	-	-	1.96	-	-	Peltonen, 1995
Deep Ore	SF-Diss	V208	-	-	-	-	-	1.48	4.50	3 289	Peltonen, 1995
Deep Ore	SF-Diss	V219	-	-	-	-	-	3.14	-	-	Peltonen, 1995
Deep Ore	SF-Diss	V238	-	-	-	-	-	5.37	14.98	3 584	Peltonen, 1995
Deep Ore	SF-Diss	V248	-	-	-	-	-	6.56	14.50	4 525	Peltonen, 1995
Sotka Ore	SF-Diss	294/6	-	-	-	-	-	3.18	8.40	3 788	Peltonen, 1995
Sotka Ore	SF-Diss	294/7	-	-	-	-	-	7.94	37.48	2 119	Peltonen, 1995
Sotka Ore	SF-Diss	294/10	-	-	-	-	-	5.82	27.30	2 132	Peltonen, 1995
Sotka Ore	SF-Diss	294/11	-	-	-	-	-	8.09	33.90	2 387	Peltonen, 1995
Sotka Ore	SF-Diss	294/14	-	-	-	-	-	10.40	36.61	2 841	Peltonen, 1995
Ekojoki Ore	SF-Diss	E22a	-	-	-	-	-	4.35	19.49	2 232	Peltonen, 1995
Ekojoki Ore	SF-Diss	E24	-	-	-	-	-	11.30	47.23	2 392	Peltonen, 1995
Ekojoki Ore	SF-Diss	E69	-	-	-	-	-	6.96	19.21	3 623	Peltonen, 1995
Ekojoki Ore	SF-Mtr	E73	-	-	-	-	-	14.20	24.57	5 780	Peltonen, 1995
Ekojoki Ore	SF-Diss	E82	-	-	-	-	-	4.08	9.91	4 115	Peltonen, 1995
Ekojoki Ore	SF-Diss	E93	-	-	-	-	-	3.13	11.21	2 793	Peltonen, 1995
Ekojoki Ore	SF-Diss	El03	-	-	-	-	-	2.38	8.78	2 710	Peltonen, 1995
Sulfide vein	vein	E75.4	-	-	-	-	-	22.00	33.88	6 494	Peltonen, 1995
Sulfide vein	vein	E76.4	-	-	-	-	-	8.08	17.37	4 651	Peltonen, 1995
Sulfide vein	vein	294/13	-	-	-	-	-	16.10	40.73	3 953	Peltonen, 1995
Sulfide vein	vein	294/83	-	-	-	-	-	34.70	92.65	3 745	Peltonen, 1995
Sulfide vein	vein	294/78	-	-	-	-	-	23.40	52.18	4 484	Peltonen, 1995
Sulfide vein	vein	V238b	-	-	-	-	-	23.90	60.71	3 937	Peltonen, 1995
Murto	(unmineralised)	M41	-	-	-	-	-	0.32	0.42	7 692	Peltonen, 1995
Murto	(unmineralised)	M72	-	-	-	-	-	0.17	0.20	8 403	Peltonen, 1995
Murto	(unmineralised)	M76	-	-	-	-	-	0.65	0.36	17 857	Peltonen, 1995
Murto	(unmineralised)	M100	-	-	-	-	-	0.40	0.24	16 667	Peltonen, 1995
Posionlahti	(unmineralised)	P137	-	-	-	-	-	0.43	0.18	23 810	Peltonen, 1995
Posionlahti	(unmineralised)	P279	-	-	-	-	-	0.73	0.04	200 000	Peltonen, 1995
Posionlahti	(unmineralised)	P368	-	-	-	-	-	0.80	0.60	13 333	Peltonen, 1995
Posionlahfi	(unmineralised)	P396	-					0.28	0.18	15 625	Peltonen, 1995
Svecofennian Formation	Mica schist	Ms20b	-	-	-	-	-	0.74	0.70	10 526	Peltonen, 1995
Svecofennian Formation	Mica schist	U300	-	-	-	-	-	1.67	2.10	7 937	Peltonen, 1995
Svecofennian Formation	Mica schist	L3d	-	-	-	-	-	3.69	3.10	11 905	Peltonen, 1995
Svecofennian Formation	Mica schist	Ek135	-	-	-	-	-	1.50	2.40	6 250	Peltonen, 1995
Svecofennian Formation	Black schist	Kla	-	-	-	-	-	5.34	2.30	23 256	Peltonen, 1995
Svecofennian Formation	Black schist	Klc	-	-	-	-	-	2.87	2.61	10 989	Peltonen, 1995

Mining Camp / Deposit	Rocktype/ore	Sample	n	Ni % wt	Cu % wt	Pt ppb	Pd ppb	S % wt	Se ppm	S/Se	references
Svecofennian Formation	Black schist	Un182	-	-	-	-	-	4.53	15.81	2 865	Peltonen, 1995
Svecofennian Formation	Black schist	M62	-	-	-	-	-	4.35	4.09	10 638	Peltonen, 1995
Svecofennian Formation	Black schist	M104	-	-	-	-	-	4.60	5.98	7 692	Peltonen, 1995
Svecofennian Formation	Black schist	Ek26	-	-	-	-	-	5.25	4.10	12 821	Peltonen, 1995
Svecofennian Formation	Black schist	Ek55	-	-	-	-	-	3.48	7.10	4 902	Peltonen, 1995
Svecofennian Formation	Black schist	R25	-	-	-	-	-	5.28	6.18	8 547	Peltonen, 1995
Svecofennian Formation	Black schist	R26	-	-	-	-	-	4.76	10.28	4 630	Peltonen, 1995
Svecofennian Formation	Black schist	R29	-	-	-	-	-	13.70	9.45	14 493	Peltonen, 1995
Svecofennian Formation	Mica schist	E2b	-	-	-	-	-	0.66	0.60	10 989	Peltonen, 1995
Svecofennian Formation	Mica schist	E2e	-	-	-	-	-	0.96	0.90	10 638	Peltonen, 1995
Svecofennian Formation	Mica schist	E2f	-	-	-	-	-	0.31	0.60	5 155	Peltonen, 1995
Svecofennian Formation	Mica schist	E2c	-	-	-	-	-	4.01	4.21	9 524	Peltonen, 1995
Svecofennian Formation	Mica schist	E2d	-	-	-	-	-	4.14	5.01	8 264	Peltonen, 1995
Svecofennian Formation	Mica schist	29414	-	-	-	-	-	1.25	2.00	6 250	Peltonen, 1995
Svecofennian Formation	Mica schist	476 3	-	-	-	-	-	1.55	1.40	11 111	Peltonen, 1995
Svecofennian Formation	Black schist	Sm2a	-	-	-	-	-	6.36	26.20	2 427	Peltonen, 1995
Svecofennian Formation	Black schist	L2c	-	-	-	-	-	6.09	16.20	3 759	Peltonen, 1995
Svecofennian Formation	Black schist	47614	-	-	-	-	-	3.90	3.71	10 526	Peltonen, 1995
Svecofennian Formation	Black schist	47615	-	-	-	-	-	4.02	9.00	4 464	Peltonen, 1995
Svecofennian Formation	Black schist	47617	-	-	-	-	-	4.41	15.92	2 770	Peltonen, 1995
Svecofennian Formation	Contact zone	294116	-	-	-	-	-	2.94	8.91	3 300	Peltonen, 1995
Svecofennian Formation	Contact zone	29415	-	-	-	-	-	5.71	13.99	4 082	Peltonen, 1995
Selebi-Phikwe											
Lentswe (Phikwe Belt)	Peridotite	LT-7	-	0.05	0.04	10	61	0.04	<0.2	-	Maier et al., 2008
Phoenix (Tati Belt)	Gabbronorite	148–247.2	-	0.01	0.02	9	11	0.03	<0.2	-	Maier et al., 2008
Phoenix (Tati Belt)	Gabbronorite	148–237.3	-	0.02	0.01	13	29	0.03	<0.2	-	Maier et al., 2008
Phoenix (Tati Belt)	Gabbronorite	148–100.8	-	0.06	0.03	47	162	0.16	0.78	2 051	Maier et al., 2008
Phoenix (Tati Belt)	Gabbronorite	148–191.6	-	0.02	0.00	22	25	0.02	<0.2	-	Maier et al., 2008
Phoenix (Tati Belt)	Granite	148–270.3	-	0.00	0.00	<1.9	4	0.01	0.92	109	Maier et al., 2008
Phoenix (Tati Belt)	Granite	119–222	-	0.51	0.33	154	809	2.94	11.34	2 593	Maier et al., 2008
Phoenix (Tati Belt)	Granite	148–261.2	-	0.19	0.30	226	979	0.95	4.18	2 273	Maier et al., 2008
Dikoloti (Phikwe Belt)	SF-Diss	DK–17	-	0.29	1.07	81	488	11.11	3.17	35 047	Maier et al., 2008
Phikwe (Phikwe Belt)	SF-Diss	SP-21	-	0.55	3.36	<40	18	13.66	11.55	11 827	Maier et al., 2008
Phikwe (Phikwe Belt)	SF-Diss	Sp13-1	-	0.13	0.02	124	24	3.31	3.64	9 093	Maier et al., 2008
Phikwe (Phikwe Belt)	SF-Diss	SP-9	-	0.08	0.02	7	7	0.64	<2	-	Maier et al., 2008
Phokoje	SF-Diss	112–733	-	0.37	0.29	36	13	5.39	3.73	14 450	Maier et al., 2008
Phoenix (Tati Belt)	SF-Diss	148–215.9	-	3.93	0.94	2	8	16.48	40.66	4 053	Maier et al., 2008
Phoenix (Tati Belt)	SF-Diss	148–196.3	-	0.17	1.14	246	1	1.68	5.05	3 327	Maier et al., 2008
Phoenix (Tati Belt)	SF-Diss	148–135.4	-	0.17	0.00	140	551	0.59	2.77	2 130	Maier et al., 2008
Phoenix (Tati Belt)	SF-Diss	148–156.7	-	0.01	0.63	373	2	3.75	14.42	2 601	Maier et al., 2008
Phoenix (Tati Belt)	SF-Diss	148–162.4	-	0.20	0.16	140	565	0.87	3.27	2 661	Maier et al., 2008
Selkirk (Tati belt)	SF-Diss	S8	-	0.29	0.02	125	500	3.62	7.06	5 127	Maier et al., 2008
Selkirk (Tati belt)	SF-Diss	S1	-	0.48	0.32	188	681	5.35	8.36	6 400	Maier et al., 2008
Selkirk (Tati belt)	SF-Diss	S11	-	0.13	0.13	78	287	1.09	2.35	4 638	Maier et al., 2008
Selkirk (Tati belt)	SF-Diss	S2	-	0.49	0.97	182	819	6.56	10.76	6 097	Maier et al., 2008
Selkirk (Tati belt)	SF-Diss	S3	-	0.11	0.26	90	439	1.14	3.43	3 324	Maier et al., 2008
Selkirk (Tati belt)	SF-Diss	S6	-	0.27	0.24	143	526	5.35	5.70	9 386	Maier et al., 2008
Tekwane (Tati Belt)	SF-Diss	TW-9	-	0.30	0.25	162	816	1.31	2.95	4 441	Maier et al., 2008
Tekwane (Tati Belt)	SF-Diss	TW-7	-	0.27	0.01	283	1	1.42	4.46	3 184	Maier et al., 2008
Dikoloti (Phikwe Belt)	SF-MS	DK-17-2	-	0.55	0.37	110	1	20.48	6.29	32 560	Maier et al., 2008
Phikwe (Phikwe Belt)	SF-MS	SP-13b	-	1.75	0.28	20	83	30.71	103.00	2 982	Maier et al., 2008
Phikwe (Phikwe Belt)	SF-MS	SP-18	-	1.77	1.21	9	44	28.67	27.89	10 280	Maier et al., 2008
Phikwe (Phikwe Belt)	SF-MS	SP-16	-	1.45	0.24	9	29	26.03	24.19	10 761	Maier et al., 2008
Phokoje (Phikwe Belt)	SF-MS	112–738	-	2.03	0.04	15	167	30.29	43.10	7 028	Maier et al., 2008
Phoenix (Tati Belt)	SF-MS	P3	-	3.88	14.02	208	5	33.83	83.63	4 045	Maier et al., 2008
Phoenix (Tati Belt)	SF-MS	119–217.14	-	1.05	28.27	<1.5	435	31.38	66.78	4 699	Maier et al., 2008

Mining Camp	Rocktype/ore	Sample	n	Ni	Cu	Pt	Pd	S	Se	S/Se	references
Deposit				% wt	% wt	ppb	ppb	% wt	ppm		
Phoenix (Tati Belt)	SF-MS	P8	-	7.93	0.04	122	8	36.19	115.00	3 147	Maier et al., 2008
Phoenix (Tati Belt)	SF-MS	P10	-	6.84	0.05	53	6	36.01	80.26	4 487	Maier et al., 2008
Phoenix (Tati Belt)	SF-MS	P4	-	6.95	1.83	25	6	35.66	81.41	4 380	Maier et al., 2008
Phoenix (Tati Belt)	SF-MS	P6	-	0.69	0.03	437	6	35.48	98.66	3 596	Maier et al., 2008
Phoenix (Tati Belt)	SF-MS	P1	-	7.79	2.12	<28	7	35.29	88.95	3 967	Maier et al., 2008
Phoenix (Tati Belt)	SF-MS	119-217.3	-	6.66	0.18	619	6	33.90	72.11	4 701	Maier et al., 2008
Phoenix (Tati Belt)	SF-MS	P2	-	7.70	0.99	271	7	35.28	82.53	4 275	Maier et al., 2008
Selkirk (Tati belt)	SF-MS	S12	-	2.77	0.02	472	3	32.60	55.11	5 915	Maier et al., 2008
Selkirk (Tati belt)	SF-MS	233-13.3	-	3.00	0.73	52	2	35.16	48.71	7 218	Maier et al., 2008
Selkirk (Tati belt)	SF-MS	S13	-	1.78	0.00	522	5	35.58	52.71	6 750	Maier et al., 2008
Selkirk (Tati belt)	SF-MS	S9	-	2.83	2.41	231	3	33.91	58.41	5 806	Maier et al., 2008
Selkirk (Tati belt)	SF-MS	S4	-	2.96	0.07	228	2	36.47	37.68	9 679	Maier et al., 2008
Phoenix (Tati Belt)	Vein	P5	-	1.09	6.32	148	2	12.54	32.69	3 836	Maier et al., 2008
Phoenix (Tati Belt)	Vein	P7	-	0.21	0.05	33	5	15.26	37.75	4 042	Maier et al., 2008
Phoenix (Tati Belt)	Vein	P9	-	1.75	8.67	3	5	16.76	42.38	3 955	Maier et al., 2008
Kambalda											
Kambalda	All ores	-	11	-	-	-	-	-	-	9 430	Cowden et al., 1986
Kambalda	interpillow sulfide	-	-	-	-	-	-	-	-	8 805	Lesher and Keays, 1984
Kambalda	MS sdt-enriched	-	-	-	-	-	-	-	-	7 435	Lesher and Keays, 1984
Kambalda	Ni sdt enriched	-	-	-	-	-	-	-	-	1 250	Lesher and Keays, 1984
Kambalda	Hydrothermal veins	-	3	-	-	-	-	-	-	3 469	Lesher and Keays, 1984
Lunnon Shoot	Ni-Ore	-	-	-	-	-	-	-	-	12 900	Bavinton, 1981
Country rock	Sediment	-	-	-	-	-	-	-	-	16 800	Bavinton, 1981
Mt Keith											
Mt Keith	Dunite	MKD52-1524	-	1.18	0.00	-	65	0.66	0.52	12 761	Groves and Keays, 1979
Mt Keith	Dunite	MKD52-1596	-	1.42	0.02	-	79	0.99	0.61	16 187	Groves and Keays, 1979
Mt Keith	Dunite	MKD52-1699	-	0.37	0.00	-	0	0.01	0.02	9 333	Groves and Keays, 1979
Mt Keith	Serpentinized Dunite	MKD52-666	-	0.92	0.02	-	35	0.50	-	-	Groves and Keays, 1979
Mt Keith	Serpentinized Dunite	MKD52-1268	-	1.87	0.03	-	114	1.35	-	-	Groves and Keays, 1979
Mt Keith	Serpentinized Dunite	MKD52-1292.5	-	1.24	0.02	-	137	0.90	0.66	13 616	Groves and Keays, 1979
Mt Keith	Serpentinized Dunite	MKD52-1577	-	1.16	0.01	-	65	0.96	-	-	Groves and Keays, 1979
Mt Keith	Black Serpentinite	MKD19-1381	-	0.98	0.03	-	96	1.05	0.71	14 851	Groves and Keays, 1979
Mt Keith	Black Serpentinite	MKD19-1394	-	0.75	0.06	-	61	0.84	0.62	13 505	Groves and Keays, 1979
Mt Keith	Black Serpentinite	MKD19-1461	-	0.63	0.03	-	34	1.70	0.55	30 853	Groves and Keays, 1979
Mt Keith	Black Serpentinite	MKD34-942	-	0.80	0.02	-	62	0.82	0.53	15 414	Groves and Keays, 1979
Mt Keith	Black Serpentinite	MKD34-991	-	0.69	0.03	-	38	0.96	0.53	18 079	Groves and Keays, 1979
Mt Keith	Black Serpentinite	MKD34-1032	-	0.72	0.03	-	41	1.15	-	-	Groves and Keays, 1979
Mt Keith	Black Serpentinite	Winze specimen	-	0.77	0.02	-	64	1.59	0.55	29 174	Groves and Keays, 1979
Mt Keith	Green Serpentinite	MKD19-958	-	0.20	0.00	-	2	0.17	0.14	12 028	Groves and Keays, 1979
Mt Keith	Green Serpentinite	MKD34-1063	-	0.69	0.01	-	36	0.77	-	-	Groves and Keays, 1979
Mt Keith	Green Serpentinite	MKD34-1173	-	0.40	0.00	-	13	0.31	-	-	Groves and Keays, 1979
Mt Keith	Talc-carbonate	MKD19-1220	-	0.69	0.00	-	90	1.13	0.58	19 416	Groves and Keays, 1979
Mt Keith	Talc-carbonate rock	MKD19-1429	-	0.58	0.03	-	61	1.57	0.67	23 294	Groves and Keays, 1979
Mt Keith	Talc-carbonate rock	MKD19-1436	-	0.34	0.02	-	17	1.11	0.25	43 701	Groves and Keays, 1979
Mt Keith	Talc-carbonate rock	MKD19-1498	-	0.82	0.01	-	88	1.10	0.65	16 871	Groves and Keays, 1979
Mt Keith	Talc-carbonate rock	MKD19-1735	-	0.25	0.00	-	1	0.05	0.00	112 500	Groves and Keays, 1979
Mt Keith	Talc-carbonate rock	MKD34-1241	-	0.34	0.00	-	11	0.30	-	-	Groves and Keays, 1979
Mt Keith	Talc-carbonate rock	MKD48A-1245	-	0.79	0.02	-	52	0.99	0.43	22 900	Groves and Keays, 1979
Langmuir											
Langmuir 1 and 2	All ores	-	42	6.52	0.26	322	606	19.50	10.50	18 571	Green and Naldrett, 1981
Langmuir 1 and 3	Mill concentrate	-	1	8.80	0.44	350	900	29.00	10.40	27 885	Green and Naldrett, 1982
Langmuir 1 and 4	Pyrrhotite-rich ores	-	18	7.97	0.25	395	566	25.60	11.00	23 273	Green and Naldrett, 1983
Langmuir 1 and 5	Pyrite-rich ores	-	8	8.20	0.29	256	703	23.50	9.80	23 980	Green and Naldrett, 1984
Langmuir 1 and 6	Millerite-rich ores	-	12	5.54	0.21	386	720	11.60	11.60	10 000	Green and Naldrett, 1985
Langmuir 1 and 7	Metasedimentary ores	-	4	1.79	0.26	125	350	6.50	6.50	10 000	Green and Naldrett, 1986
Mc Watters	Pyrite-rich ores	-	1	10.60	0.24	174	474	21.30	13.00	16 385	Green and Naldrett, 1988

Mining Camp / Deposit	Rocktype/ore	Sample	n	Ni % wt	Cu % wt	Pt ppb	Pd ppb	S % wt	Se ppm	S/Se	references
South End Fault Zone	SF-MS	328	-	13.70	0.11	20	199	35.20	16.00	22 000	Green and Naldrett, 1990
South End Fault Zone	SF-MS	329	-	14.70	0.14	295	350	33.20	15.81	21 000	Green and Naldrett, 1991
South End Fault Zone	SF-MS	347C	-	6.30	0.41	520	350	24.30	10.13	24 000	Green and Naldrett, 1992
South End Fault Zone	SF-MS	346A	-	11.20	0.07	430	210	36.20	18.10	20 000	Green and Naldrett, 1993
South End Fault Zone	SF-MS	345A	-	11.65	0.07	300	650	35.20	16.76	21 000	Green and Naldrett, 1994
Country rock (Close)	Iron Formation	345B	-	1.22	0.07	24	11	3.40	1.70	20 000	Green and Naldrett, 1995
Country rock (Close)	Iron Formation	319	-	0.15	0.06	98	20	5.50	1.38	40 000	Green and Naldrett, 1996
Country rock	Iron Formation	326	-	0.01	0.01	20	2	7.10	5.92	12 000	Green and Naldrett, 1998
Country rock	Iron Formation	350	-	0.07	0.59	20	17	11.20	10.98	10 200	Green and Naldrett, 1999
Country rock	Iron Formation	351	-	0.03	0.07	34	7	9.90	10.00	9 900	Green and Naldrett, 2000
Country rock	Metasediment	327	-	2.10	0.73	220	930	7.80	7.09	11 000	Green and Naldrett, 2001
Country rock	Metasediment	346B	-	2.40	0.10	60	130	14.10	11.75	12 000	Green and Naldrett, 2002
Country rock	Metasediment	347B	-	3.36	0.13	250	350	8.50	9.04	9 400	Green and Naldrett, 2003
Country rock	Altered andesite	321	-	0.08	0.07	5	1	5.20	4.00	13 000	Green and Naldrett, 2004
Country rock	Altered andesite	343	-	0.05	0.04	10	11	5.20	5.20	10 000	Green and Naldrett, 2005
Thompson											
Thompson	SF-MS	-	6	-	-	-	-	-	-	12 800	Bleeker, 1990
Thompson	SF-breccia	-	7	-	-	-	-	-	-	16 186	Bleeker, 1990
Thompson	Ni-SED	-	14	-	-	-	-	-	-	30 659	Bleeker, 1990
Pipe II											
Pipe II	SF-MS	-	3	-	-	-	-	-	-	23 926	Bleeker, 1990
Namew Lake											
Namew Lake	SF-Diss	-	18	-	-	-	-	-	-	1 851	Menard et al., 1996
Cape Smith (Raglan)											
Cape Smith (Raglan)	Disseminated	-	89	-	-	-	-	-	-	3 189	Barnes et al., 1997b
Cape Smith (Raglan)	Massive and matrix	-	57	-	-	-	-	-	-	3 093	Barnes et al., 1997b
Cape Smith (Raglan)	Fe-rich Pd/Ir < diss	-	32	-	-	-	-	-	-	3 342	Barnes et al., 1997b
Cape Smith (Raglan)	Cu-rich Pd/Ir > diss	-	17	-	-	-	-	-	-	2 790	Barnes et al., 1997b
Cape Smith (Raglan)	Vein	-	5	-	-	-	-	-	-	4 628	Barnes et al., 1997b
Delta Horizon (Cape Smith Belt)											
Delta 8 (77-29)	SF-MS	3	-	5.92	0.60	792	1 064	29.48	73.20	4 027	Giovenazzo, 1991
Delta 8 (77-29)	SF-MS	4	-	6.26	0.71	1 140	1 044	26.60	78.90	3 371	Giovenazzo, 1991
Delta 8 (77-29)	SF-MS	5	-	8.70	1.35	793	653	29.70	95.40	3 113	Giovenazzo, 1991
Delta 8 (77-29)	SF-MS	6	-	7.26	0.99	1 251	746	30.44	73.30	4 153	Giovenazzo, 1991
Delta 8 (77-29)	SF-MS	9	-	6.98	1.33	762	251	27.75	69.90	3 970	Giovenazzo, 1991
Delta 8 (77-29)	SF-MS	11	-	8.06	0.46	534	202	32.63	82.30	3 965	Giovenazzo, 1991
Delta 8 (77-29)	SF-MS	13	-	5.73	0.60	1 204	98	30.42	79.60	3 822	Giovenazzo, 1991
Delta 8 (77-29)	SF-MS	15	-	10.48	0.46	256	261	31.84	76.90	4 140	Giovenazzo, 1991
Delta 8 (77-29)	SF-MS	16	-	7.34	0.60	1 816	105	31.78	77.10	4 122	Giovenazzo, 1991
Delta 8 (77-29)	SF-MS	18	-	6.97	1.84	1 172	286	31.89	84.30	3 783	Giovenazzo, 1991
Delta 8 (77-29)	SF-MS	19	-	6.19	0.51	695	554	31.00	75.50	4 106	Giovenazzo, 1991
Delta 8 (77-29)	SF-MS	21	-	6.32	1.48	794	2 741	30.01	79.50	3 775	Giovenazzo, 1991
Delta 8 (77-29)	Granophyre/SF-MS	22	-	2.35	1.04	480	3 905	11.41	21.60	5 282	Giovenazzo, 1991
Delta 8 (77-29)	Pyroxenite	23	-	0.57	0.43	240	330	2.60	10.90	2 385	Giovenazzo, 1991
Delta 8 (77-29)	Pyroxenite	24	-	0.74	0.80	293	482	2.23	ld	-	Giovenazzo, 1991
Delta 8 (77-29)	Pyroxenite	25	-	1.17	0.80	< 15	34	4.92	12.10	4 066	Giovenazzo, 1991
Delta 8 (77-29)	Gabbro/veins/SF-Diss	26	-	0.80	1.92	566	879	3.58	12.60	2 841	Giovenazzo, 1991
Delta 8 (77-29)	Gabbro/veins/SF-Diss	27	-	0.52	0.88	660	1 320	1.89	ld	-	Giovenazzo, 1991
Delta 8 (77-29)	Gabbro/veins/SF-Diss	28	-	1.03	1.07	400	5 808	2.42	11.10	2 180	Giovenazzo, 1991
Delta 8 (87-86)	Granophyre	21	-	0.55	0.41	349	926	3.08	14.20	2 169	Giovenazzo, 1991
Delta 8 (87-86)	Granophyre	22	-	0.10	0.60	116	196	0.90	7.30	1 233	Giovenazzo, 1991
Delta 8 (87-86)	Granophyre	24	-	0.10	0.76	1 084	3 122	1.22	5.80	2 103	Giovenazzo, 1991
Delta 8 (87-86)	Granophyre/Veins	25	-	3.01	8.87	-		15.00	140.46	1 068	Giovenazzo, 1991
Delta 8 (87-86)	Pyroxenite/Veins	26	-	0.33	0.49	3 250	17 465	2.02	15.67	1 289	Giovenazzo, 1991
Delta 9 (77-24)	Siltstone	OO	-	0.09	0.02	4	3	0.60	7.70	779	Giovenazzo, 1991

Mining Camp / Deposit	Rocktype/ore	Sample	n	Ni % wt	Cu % wt	Pt ppb	Pd ppb	S % wt	Se ppm	S/Se	references
Delta 9 (77-24)	Siltstone/Veins	0	-	0.14	1.06	12	36	1.30	5.20	2 500	Giovenazzo, 1991
Delta 9 (77-24)	Granophyre	1	-	0.10	0.09	107	532	0.20	< 5	-	Giovenazzo, 1991
Delta 9 (77-24)	SF-MS	2	-	5.21	0.85	2 320	8 240	27.93	122.10	2 287	Giovenazzo, 1991
Delta 9 (77-24)	SF-MS	3	-	4.07	0.75	2 586	6 452	27.23	121.90	2 234	Giovenazzo, 1991
Delta 9 (77-24)	SF-MS	4	-	5.05	2.66	2 760	9 800	22.64	97.00	2 334	Giovenazzo, 1991
Delta 9 (77-24)	SF-MS	5	-	4.13	0.73	4 500	6 990	18.20	71.60	2 542	Giovenazzo, 1991
Delta 9 (77-24)	SF-MS	6	-	5.16	0.25	2 466	6 425	29.82	138.50	2 153	Giovenazzo, 1991
Delta 9 (77-24)	Pyroxenite	7	-	2.52	0.98	1 201	2 975	12.59	63.50	1 983	Giovenazzo, 1991
Delta 9 (77-24)	SF-MS	8	-	5.95	0.60	300	660	31.00	100.50	3 085	Giovenazzo, 1991
Delta 9 (77-24)	SF-MS	9	-	7.51	0.54	651	747	31.01	92.60	3 349	Giovenazzo, 1991
Delta 9 (77-24)	SF-MS	10	-	2.70	3.18	5 480	3 981	22.38	108.80	2 057	Giovenazzo, 1991
Delta 9 (77-24)	SF-MS	11	-	7.89	0.43	1 220	2 100	32.70	93.00	3 516	Giovenazzo, 1991
Delta 9 (77-24)	SF-MS	12	-	6.76	2.44	597	182	29.71	185.40	1 602	Giovenazzo, 1991
Delta 9 (77-24)	SF-MS	13	-	4.84	0.50	20	264	34.14	101.30	3 370	Giovenazzo, 1991
Delta 9 (77-24)	SF-MS	14	-	6.09	0.96	81	369	34.65	131.30	2 639	Giovenazzo, 1991
Delta 9 (77-24)	SF-MS	15	-	6.55	2.19	1 081	1 013	33.92	119.30	2 843	Giovenazzo, 1991
Delta 9 (77-24)	Granophyre/SF-MS	16	-	1.89	5.62	135	235	14.95	61.30	2 439	Giovenazzo, 1991
Méquillon (Cape Smith Belt)											
Dyke	SF-Diss	CT-65-i	-	0.15	0.07	104	250	0.72	1.80	3 986	Tremblay, 1990
Dyke	SF-Diss	CT-04-i	-	0.16	0.26	196	391	1.43	3.40	4 210	Tremblay, 1990
Dyke	SF-Diss	CT-99-i	-	0.22	0.12	189	293	1.72	4.50	3 832	Tremblay, 1990
Dyke	SF-Diss	CT-18-i	-	0.15	0.04	23	27	0.85	2.00	4 238	Tremblay, 1990
Dyke	SF-Diss	CT-36-i	-	0.38	0.29	200	930	2.61	5.60	4 653	Tremblay, 1990
Country rock	Sediment	CT-61-s	-	0.01	0.03	14	17	4.13	3.00	13 781	Tremblay, 1990
Country rock	Sediment	CT-173-s	-	-	-	-	-	1.65	1.60	10 321	Tremblay, 1990
Country rock	Sediment	CT-24-s	-	-	-	-	-	2.26	1.40	16 114	Tremblay, 1990
2-3 (Cape Smith Belt)											
2-3	All ores	-	12	-	-	-	-	-	-	6 343	Barnes et al., 1992
Donaldson West (Cape Smith Belt)											
Donaldson West	SF-Diss	-	14	-	-	-	-	-	-	3 834	Dillon-Leitch et al., 1986
Donaldson West	SF-Net textured	-	12	-	-	-	-	-	-	12 471	Dillon-Leitch et al., 1986
Donaldson West	SF-MS	-	3	-	-	-	-	-	-	4 957	Dillon-Leitch et al., 1986
Donaldson West	Veins	-	11	-	-	-	-	-	-	5 626	Dillon-Leitch et al., 1986
Frontier Zone (Cape Smith Belt)											
Frontier Zone	Mesocumulat	C-05-53	-	0.28	0.04	19	62	0.57	0.90	6 333	Dionne-Foster, 2007
Frontier Zone	Orthocumulat	C-04-36	-	0.19	0.02	5	22	0.41	0.60	6 833	Dionne-Foster, 2007
Frontier Zone	Orthocumulat	C-04-37	-	0.36	0.18	21	187	2.89	3.40	8 500	Dionne-Foster, 2007
Frontier Zone	Metacumulat	20787	-	0.31	0.09	28	155	1.17	1.40	8 357	Dionne-Foster, 2007
Frontier Zone	Metacumulat	C-04-04	-	0.26	0.08	8	121	0.66	1.20	5 500	Dionne-Foster, 2007
Frontier Zone	Metacumulat	C-04-05	-	0.26	0.08	8	121	0.66	1.20	5 500	Dionne-Foster, 2007
Frontier Zone	Metacumulat	C-05-66	-	0.31	0.10	37	146	0.73	1.60	4 563	Dionne-Foster, 2007
Frontier Zone	Metacumulat	C-05-57	-	0.54	0.23	41	263	2.09	3.10	6 742	Dionne-Foster, 2007
Frontier Zone	Metaborder	26725	-	0.96	0.41	66	504	4.39	6.40	6 859	Dionne-Foster, 2007
Frontier Zone	Metaborder	C-04-34	-	0.24	0.39	68	428	1.41	1.70	8 294	Dionne-Foster, 2007
Frontier Zone	Metaborder	C-04-48	-	0.20	0.05	18	60	2.54	1.90	13 368	Dionne-Foster, 2007
Frontier Zone	Metaborder	C-05-61	-	0.12	0.01	7	19	0.67	0.40	16 750	Dionne-Foster, 2007
Frontier Zone	Metaborder	C-05-59	-	0.14	0.01	4	5	0.74	0.90	8 222	Dionne-Foster, 2007
Frontier Zone	Komatiitic basalt	C-04-28	-	0.10	0.01	8	5	0.38	0.20	19 000	Dionne-Foster, 2007
Frontier Zone	Komatiitic basalt	C-04-29	-	0.10	0.00	3	5	0.58	0.30	19 333	Dionne-Foster, 2007
Frontier Zone	Komatiitic basalt	C-04-47	-	0.07	0.01	4	5	1.80	1.40	12 857	Dionne-Foster, 2007
Frontier Zone	Komatiitic basalt	C-04-50	-	0.04	0.01	4	5	1.60	0.60	26 667	Dionne-Foster, 2007
Frontier Zone	Ophitic basalt	S-04-13	-	0.00	0.00	1	5	0.49	0.60	8 167	Dionne-Foster, 2007
Frontier Zone	Ophitic basalt	C-04-18	-	0.00	0.01	1	5	1.34	0.90	14 889	Dionne-Foster, 2007
Frontier Zone	Ophitic basalt	C-04-19	-	0.00	0.01	1	5	0.94	0.70	13 429	Dionne-Foster, 2007
Frontier Zone	Ophitic basalt	C-04-20	-	0.01	0.00	5	5	0.77	0.40	19 250	Dionne-Foster, 2007
Frontier Zone	Ophitic basalt	C-04-30	-	0.01	0.01	1	5	0.60	0.60	10 000	Dionne-Foster, 2007

Mining Camp / Deposit	Rocktype/ore	Sample	n	Ni % wt	Cu % wt	Pt ppb	Pd ppb	S % wt	Se ppm	S/Se	references
Frontier Zone	SF-Diss	C-04-49	-	0.11	0.02	10	31	0.17	0.40	4 250	Dionne-Foster, 2007
Frontier Zone	Schist SF-Diss	C-04-31	-	0.26	0.29	19	143	0.80	1.60	5 000	Dionne-Foster, 2007
Frontier Zone	Schist SF-Diss	C-04-31	-	0.26	0.29	19	143	0.80	1.60	5 000	Dionne-Foster, 2007
Frontier Zone	SF-Diss	C-04-32	-	3.45	1.57	434	3 377	10.84	29.60	3 662	Dionne-Foster, 2007
Frontier Zone	SF-Diss	C-04-33	-	2.37	0.75	385	2 137	9.99	20.90	4 780	Dionne-Foster, 2007
Frontier Zone	SF-Mtr	C-04-43	-	3.06	0.84	536	2 042	14.73	28.40	5 187	Dionne-Foster, 2007
Frontier Zone	SF-Mtr	C-04-38	-	1.14	0.46	62	682	10.22	14.70	6 952	Dionne-Foster, 2007
Frontier Zone	SF-Mtr	C-04-39	-	1.17	0.57	108	835	10.20	13.50	7 556	Dionne-Foster, 2007
Frontier Zone	Schist SF-Mtr	C-04-42	-	2.97	0.87	280	1 884	15.22	25.60	5 945	Dionne-Foster, 2007
Frontier Zone	SF-MS	C-04-44	-	6.01	1.29	419	1 669	31.11	46.30	6 719	Dionne-Foster, 2007
Frontier Zone	SF-MSR	C-04-22	-	0.18	1.30	83	449	3.28	3.20	10 250	Dionne-Foster, 2007
Frontier Zone	SF-MSR	C-04-40	-	2.04	0.97	409	2 266	19.41	30.20	6 427	Dionne-Foster, 2007
Frontier Zone	SF-MSR	C-04-23	-	1.89	0.46	438	1 816	35.84	29.40	12 190	Dionne-Foster, 2007
Frontier Zone	SF-MSR	C-04-24	-	1.55	1.02	413	2 163	32.86	32.50	10 111	Dionne-Foster, 2007
Frontier Zone	SF-MSR	C-04-25	-	1.98	0.53	357	2 368	33.63	30.60	10 990	Dionne-Foster, 2007
Frontier Zone	SF-MSR	C-04-41	-	1.34	2.10	34	404	23.46	11.80	19 881	Dionne-Foster, 2007
Frontier Zone	Sedimentary SF-MS	C-04-21	-	0.00	0.01	1	5	2.08	2.70	7 704	Dionne-Foster, 2007
Frontier Zone	Sedimentary SF-MS	C-04-26	-	0.33	0.05	6	16	21.71	30.60	7 095	Dionne-Foster, 2007
Frontier Zone	Sedimentary SF-MS	C-04-27	-	0.02	0.01	9	5	34.97	14.70	23 789	Dionne-Foster, 2007
Frontier Zone	Litharenite	26761	-	0.00	0.01	1	5	2.10	0.60	35 000	Dionne-Foster, 2007
Frontier Zone	Litharenite	C-04-51	-	0.00	0.02	1	5	2.59	1.00	25 900	Dionne-Foster, 2007
Pechenga											
Flows (West Ore)	SF-MS	-	13	6.75	1.17	373	421	29.90	62.00	4 823	Barnes et al., 2001b
Flows (West Ore)	SF-Diss	-	16	1.54	0.64	142	149	6.09	15.53	3 921	Barnes et al., 2001b
Flows (West Ore)	SF-Breccia	-	6	3.63	0.22	154	132	21.09	31.00	6 803	Barnes et al., 2001b
Flows (West Ore)	SF-Breccia	-	10	3.26	1.14	281	83	16.01	34.00	4 709	Barnes et al., 2001b
Flows (West Ore)	Ferropicrite tuffs	-	2	0.11	0.02	4	4	0.80	1.00	8 000	Barnes et al., 2001b
Country rock	Black schists	-	4	0.04	0.05	4	4	2.63	2.00	13 150	Barnes et al., 2001b
Intrusions (East Ore)	SF-MS	-	4	9.57	4.35	131	219	31.44	70.00	4 491	Barnes et al., 2001b
Intrusions (East Ore)	SF-Diss	-	3	1.98	0.64	127	182	5.26	15.90	3 308	Barnes et al., 2001b
Intrusions (East Ore)	SF-Breccia	-	1	9.93	1.78	306	405	22.23	61.00	3 644	Barnes et al., 2001b
Intrusions (East Ore)	SF-Breccia	-	1	5.21	1.24	408	348	22.79	67.00	3 401	Barnes et al., 2001b
Intrusions (East Ore)	Veins	-	1	2.49	19.90	156	78	20.43	40.00	5 108	Barnes et al., 2001b
Intrusions (East Ore)	Ferropicrite	-	3	0.89	1.58	266	306	2.59	10.00	2 590	Barnes et al., 2001b
Country rock	Black schists	-	1	0.04	0.02	12	7	18.71	10.00	18 710	Barnes et al., 2001b
Country rock	Conglomerate	-	1	0.01	0.01	2	< 3	1.98	2.00	9 900	Barnes et al., 2001b
Kabanga											
Kabanga North	Andalusite schist	KN 98-48	-	0.00	0.00	<1.8	2	0.04	0.16	2 244	Maier et al., 2010
Main North Body	Banded pelite	KN 01-05	-	0.04	0.00	-	-	0.97	0.19	52 079	Maier et al., 2010
Kabanga North	Breccia	KN 98-48	-	0.89	0.07	1 230	970	13.92	8.70	15 994	Maier et al., 2010
Kabanga North	Gabbronorite	KN 98-48	-	0.79	0.06	359	232	7.59	4.36	17 409	Maier et al., 2010
Main North Body	Gabbronorite	KN 01-01b	-	0.37	0.05	88	29	4.69	0.79	59 162	Maier et al., 2010
Kabanga North	Gabbronorite	KN 95-66	-	0.09	0.03	-	-	0.33	0.39	8 421	Maier et al., 2010
Kabanga North	Gabbronorite	KN 95-66	-	0.05	0.00	<3.5	<4.3	0.40	0.08	48 575	Maier et al., 2010
Kabanga North	Gabbronorite	KN 95-66	-	0.00	0.00	<2.5	<1.6	0.01	0.71	75	Maier et al., 2010
Kabanga North	Gabbronorite	KN 95-66	-	0.01	0.00	<1.5	<2.7	0.07	0.95	772	Maier et al., 2010
Kabanga Main	Gabbronorite	KN 92-27	-	0.01	0.00	<3.9	<3.5	0.19	2.31	824	Maier et al., 2010
Kabanga Main	Gabbronorite	KN 98-74	-	0.13	0.12	161	129	7.36	2.71	27 151	Maier et al., 2010
Kabanga Main	Harzburgite	KN 98-74	-	0.17	0.03	33	18	2.47	0.62	39 765	Maier et al., 2010
Kabanga Main	Harzburgite	KN 98-74	-	0.25	0.02	46	25	0.97	0.48	20 183	Maier et al., 2010
Kabanga Main	Harzburgite	KN 98-74	-	0.18	0.01	100	33	3.27	0.71	46 117	Maier et al., 2010
Kabanga Main	Harzburgite	KN 98-74	-	0.22	0.02	62	13	4.95	1.00	49 499	Maier et al., 2010
Kabanga Main	Harzburgite	KN 98-74	-	0.19	0.03	27	16	1.30	0.09	152 694	Maier et al., 2010
Block 1	Harzburgite	KB 007	-	0.13	0.02	2	1	1.09	0.45	24 271	Maier et al., 2010
Block 1	Harzburgite	KB 007	-	0.07	0.01	2	<1.6	1.57	0.13	120 977	Maier et al., 2010
Block 1	Harzburgite	KB 007	-	0.15	0.03	4	2	3.43	0.47	72 983	Maier et al., 2010

Mining Camp	Rocktype/ore	Sample	n	Ni	Cu	Pt	Pd	S	Se	S/Se	references
Deposit				% wt	% wt	ppb	ppb	% wt	ppm		
Block 1	Harzburgite	KB 007	-	0.09	0.01	<3.8	<2.8	2.34	0.32	73 194	Maier et al., 2010
Block 1	Harzburgite	KB 007	-	0.09	0.02	25	12	3.22	0.19	169 532	Maier et al., 2010
Kabanga North	Harzburgite	KN 94-51	-	0.70	0.11	1 003	1 415	13.44	6.65	20 211	Maier et al., 2010
Main North Body	Harzburgite	KN 01-01b	-	0.06	0.01	<1.3	<2.1	3.32	0.08	425 423	Maier et al., 2010
Main North Body	Harzburgite	KN 01-01b	-	0.17	0.02	<1.3	2	1.87	0.29	63 901	Maier et al., 2010
Main North Body	Harzburgite	KN 01-01b	-	0.39	0.04	77	35	2.74	1.42	19 257	Maier et al., 2010
Main North Body	Harzburgite	KN 01-01b	-	0.18	0.02	-	-	2.45	0.44	55 802	Maier et al., 2010
Main North Body	Harzburgite	KN 01-05	-	0.26	0.02	77	58	0.88	0.01	1 760 000	Maier et al., 2010
Main North Body	Harzburgite	KN 01-05	-	0.14	0.02	<1.4	2	2.85	0.00	9 493 333	Maier et al., 2010
Kabanga North	Harzburgite	KN 95-66	-	0.13	0.00	-	-	0.21	0.00	3 016 518	Maier et al., 2010
Kabanga North	Harzburgite	KN 95-66	-	0.12	0.04	-	-	1.53	0.07	228 090	Maier et al., 2010
Kabanga Main Upper	Harzburgite	KSM 04	-	0.07	0.01	<1.8	<3.1	2.96	0.32	93 532	Maier et al., 2010
Kabanga Main Upper	Harzburgite	KN 91-16	-	0.08	0.03	<2.1	7	6.82	0.69	99 615	Maier et al., 2010
Kabanga Main Upper	Harzburgite	KN 91-16	-	0.12	0.03	2	5	6.12	0.91	67 082	Maier et al., 2010
Kabanga Main	Harzburgite	KN95-78	-	0.23	0.06	3	6	10.87	0.45	239 577	Maier et al., 2010
Kabanga North	Harzburgite breccia	KN 01-17	-	1.65	0.19	1 564	1 686	11.60	8.80	13 182	Maier et al., 2010
Kabanga North	Harzburgite	KN 01-17	-	1.10	0.27	3 216	1 837	9.00	7.70	11 688	Maier et al., 2010
Main North Body	Schist	KN 01-05	-	0.00	0.00	-	-	0.80	0.14	55 521	Maier et al., 2010
Kabanga Main	Olivine-pyroxenite	KN95-78	-	0.27	0.08	<5	9	18.85	0.66	285 174	Maier et al., 2010
Kabanga Main	Pyroxenite	KN 98-74	-	0.09	0.03	25	10	4.01	0.48	83 621	Maier et al., 2010
Kabanga Main	Pyroxenite	KN 98-74	-	0.17	0.02	93	30	3.77	0.58	64 955	Maier et al., 2010
Kabanga North	Pyroxenite	KN 98-48	-	0.71	0.17	44	41	14.59	5.37	27 163	Maier et al., 2010
Kabanga North	Pyroxenite	KN 98-48	-	0.75	0.17	119	81	12.34	5.45	22 636	Maier et al., 2010
Block 1	Pyroxenite	KB 007	-	0.01	0.00	3	4	3.53	0.24	146 904	Maier et al., 2010
Block 1	Pyroxenite	KB 007	-	0.09	0.08	15	11	13.40	1.67	80 227	Maier et al., 2010
Main North Body	Pyroxenite	KN 01-01b	-	0.11	0.01	-	-	1.07	0.00	5 363 000	Maier et al., 2010
Kabanga Main Upper	Pyroxenite	KN 91-16	-	0.14	0.03	<2.5	<2.8	17.05	1.25	136 481	Maier et al., 2010
Kabanga Main	Pyroxenite	KN98-56	-	0.13	0.02	<5	<7	7.65	0.33	235 446	Maier et al., 2010
Kabanga Main	Pyroxenite	KN95-78	-	0.41	0.14	<5	12	17.85	0.86	208 478	Maier et al., 2010
Kabanga Main	Pyroxenite	KN95-78	-	0.16	0.04	11	4	7.51	0.38	196 415	Maier et al., 2010
Kabanga Main	Pyroxenite	KN95-78	-	0.23	0.04	<5	5	8.38	0.49	171 933	Maier et al., 2010
Main North Body	Pyroxenite-breccia	KN 01-08	-	0.49	0.25	9	29	16.30	3.10	52 581	Maier et al., 2010
Kabanga North	Pyroxenite-breccia	KN 98-48	-	0.74	0.16	83	66	11.49	4.63	24 825	Maier et al., 2010
Kabanga Main	SF-MS	KN 98-74	-	0.59	0.05	<5.4	<16	31.70	6.30	50 317	Maier et al., 2010
Kabanga Main	SF-MS	KN 98-74	-	0.41	0.20	2	-	15.80	2.80	56 429	Maier et al., 2010
Kabanga Main	SF-MS	KN 98-74	-	0.49	0.06	68	59	15.62	4.90	31 878	Maier et al., 2010
Kabanga Main	SF-MS	KN 98-74	-	1.94	0.07	74	100	29.30	9.30	31 505	Maier et al., 2010
Kabanga Main	SF-MS	KN 98-74	-	1.45	0.20	11	33	38.10	6.80	56 029	Maier et al., 2010
Kabanga Main	SF-MS	KN 98-74	-	2.63	0.14	12	78	36.00	8.50	42 353	Maier et al., 2010
Kabanga Main	SF-MS	KN 98-74	-	2.18	0.11	110	135	34.50	10.80	31 944	Maier et al., 2010
Kabanga Main	SF-MS	KN 98-74	-	0.73	0.16	21	33	12.20	2.00	61 000	Maier et al., 2010
Kabanga Main	SF-MS	KN 98-74	-	2.72	0.22	30	41	34.80	4.40	79 091	Maier et al., 2010
Kabanga Main	SF-MS	KN 98-74	-	2.42	0.11	88	140	32.30	7.80	41 410	Maier et al., 2010
Kabanga Main	SF-MS	KN 98-74	-	1.71	0.27	51	79	26.30	4.80	54 792	Maier et al., 2010
Kabanga Main	SF-MS	KN 98-74	-	2.06	0.12	16	28	28.50	7.80	36 538	Maier et al., 2010
Kabanga North	SF-MS	KN 98-48	-	4.01	0.14	3 119	-	32.50	0.62	524 194	Maier et al., 2010
Kabanga North	SF-MS	KN 98-48	-	5.33	0.37	342	1 523	34.00	15.20	22 368	Maier et al., 2010
Kabanga North	SF-MS	KN 98-48	-	4.20	0.14	275	407	20.30	7.00	29 000	Maier et al., 2010
Kabanga North	SF-MS	KN 98-48	-	2.34	0.31	75	64	34.40	5.70	60 351	Maier et al., 2010
Kabanga North	SF-MS	KN 98-48	-	7.22	0.35	32	166	32.70	9.90	33 030	Maier et al., 2010
Kabanga North	SF-MS	KN 98-48	-	2.92	0.25	75	89	34.00	7.00	48 571	Maier et al., 2010
Kabanga North	SF-MS	KN 98-48	-	2.69	0.13	178	216	33.20	7.00	47 429	Maier et al., 2010
Kabanga North	SF-MS	KN 98-48	-	1.92	0.32	32	41	11.70	1.50	78 000	Maier et al., 2010
Luhuma	SF-MS	Luh 001	-	0.32	0.16	4	<2.4	9.69	3.20	30 281	Maier et al., 2010
Luhuma	SF-MS	Luh 001	-	0.98	0.11	<14	<42	32.16	8.50	37 834	Maier et al., 2010
Luhuma	SF-MS	Luh 006	-	0.06	0.10	<6.4	<7.1	17.59	3.60	48 868	Maier et al., 2010

Mining Camp / Deposit	Rocktype/ore	Sample	n	Ni % wt	Cu % wt	Pt ppb	Pd ppb	S % wt	Se ppm	S/Se	references
Block 1	SF-MS	KB 007	-	0.28	0.03	5	<11	25.49	2.20	115 865	Maier et al., 2010
Kabanga Main	SF-MS	KN 92-26	-	7.94	0.05	1 522	7 179	35.40	25.70	13 774	Maier et al., 2010
Kabanga North	SF-MS	KN 95-59	-	2.67	0.23	7 133	-	35.51	26.60	13 351	Maier et al., 2010
Main North Body	SF-MS	KN01-01b	-	1.53	0.04	42	51	28.20	2.60	108 462	Maier et al., 2010
Main North Body	SF-MS	KN 01-05	-	2.01	0.12	37	168	34.60	6.40	54 063	Maier et al., 2010
Main North Body	SF-MS	KN 01-05	-	1.47	0.09	<14	<21	36.10	2.70	133 704	Maier et al., 2010
Kabanga North	SF-MS	KN 01-18	-	3.26	0.41	215	57	35.50	6.80	52 206	Maier et al., 2010
Kabanga North	SF-MS	KN 01-18	-	1.91	0.38	12	14	36.60	8.00	45 750	Maier et al., 2010
Kabanga North	SF-MS	KN 02-01	-	2.38	0.02	12	50	35.30	9.80	36 020	Maier et al., 2010
Kabanga Main	SF-MS	KN 95-82	-	0.00	0.26	3 875	-	36.30	20.60	17 621	Maier et al., 2010
Kabanga North	SF-MS Breccia	KN 93-36	-	6.50	0.25	11 174	9 495	31.40	17.70	17 740	Maier et al., 2010
Block 1	SF-MS Breccia	KB1 023	-	1.13	0.08	59	25	26.76	3.90	68 611	Maier et al., 2010
Main North Body	SF-MS Breccia	KN 01-05	-	1.82	0.10	94	74	34.50	5.90	58 475	Maier et al., 2010
Kabanga North	SF-MS Breccia	KN 01-17	-	2.90	0.23	11	69	35.30	9.40	37 553	Maier et al., 2010
Kabanga North	SF-MS Breccia	KN 01-17	-	1.20	0.06	5 150	-	35.30	20.00	17 650	Maier et al., 2010
Kabanga North	SF-MS Breccia	KN 02-01	-	1.42	0.08	56	89	13.20	2.50	52 800	Maier et al., 2010
Kabanga North	SF-MS Breccia	KN 02-01	-	2.50	0.03	8	66	28.80	4.80	60 000	Maier et al., 2010
Kabanga Main Upper	SF-MS Breccia	KN 91-16	-	0.48	0.12	<14	<9.3	33.30	3.10	107 419	Maier et al., 2010
Kabanga North	SF-MS	KN 01-17	-	5.29	0.37	24 470	-	34.20	21.00	16 286	Maier et al., 2010
Windarra											
Windarra	Ore	-	6	-	-	-	-	-	-	1 500	Groves et al., 1979
Windarra	Ore	-	6	-	-	-	-	-	-	2 000	Groves et al., 1979
Windarra	Ore	-	5	-	-	-	-	-	-	2 500	Groves et al., 1979
Windarra	Ore	-	2	-	-	-	-	-	-	3 500	Groves et al., 1979
Windarra	Ore	-	2	-	-	-	-	-	-	4 000	Groves et al., 1979
Windarra	Ore	-	2	-	-	-	-	-	-	5 500	Groves et al., 1979
Country rock	Metasediment	-	1	-	-	-	-	-	-	2 500	Groves et al., 1979
Country rock	Metasediment	-	2	-	-	-	-	-	-	3 000	Groves et al., 1979
Country rock	Metasediment	-	1	-	-	-	-	-	-	3 500	Groves et al., 1979
Country rock	Metasediment	-	1	-	-	-	-	-	-	4 000	Groves et al., 1979
Country rock	Metasediment	-	1	-	-	-	-	-	-	6 500	Groves et al., 1979
Country rock	Metasediment	-	1	-	-	-	-	-	-	7 500	Groves et al., 1979
Country rock	Metasediment	-	1	-	-	-	-	-	-	8 500	Groves et al., 1979
Country rock	Metasediment	-	2	-	-	-	-	-	-	13 000	Groves et al., 1979
Country rock	Metasediment	-	1	-	-	-	-	-	-	13 500	Groves et al., 1979
Country rock	Metasediment	-	1	-	-	-	-	-	-	14 500	Groves et al., 1979
Country rock	Metasediment	-	1	-	-	-	-	-	-	15 000	Groves et al., 1979
Country rock	Metasediment	-	1	-	-	-	-	-	-	18 500	Groves et al., 1979
Nepean											
Nepean	Ore	-	2	-	-	-	-	-	-	500	Groves et al., 1979
Nepean	Ore	-	19	-	-	-	-	-	-	1 000	Groves et al., 1979
Nepean	Ore	-	2	-	-	-	-	-	-	1 500	Groves et al., 1979
Nepean	Ore	-	2	-	-	-	-	-	-	2 500	Groves et al., 1979
Country rock	Metasediment	-	1	-	-	-	-	-	-	500	Groves et al., 1979
Country rock	Metasediment	-	3	-	-	-	-	-	-	1 000	Groves et al., 1979
Country rock	Metasediment	-	1	-	-	-	-	-	-	1 500	Groves et al., 1979
Country rock	Metasediment	-	1	-	-	-	-	-	-	2 000	Groves et al., 1979
Widgiemooltha											
Widgiemooltha	Ore	-	30	-	-	-	-	-	-	1 000	Groves et al., 1979
Widgiemooltha	Ore	-	13	-	-	-	-	-	-	1 500	Groves et al., 1979
Widgiemooltha	Ore	-	9	-	-	-	-	-	-	2 000	Groves et al., 1979
Widgiemooltha	Ore	-	5	-	-	-	-	-	-	2 500	Groves et al., 1979
Country rock	Metasediment	-	2	-	-	-	-	-	-	500	Groves et al., 1979
Country rock	Metasediment	-	6	-	-	-	-	-	-	1 000	Groves et al., 1979
Country rock	Metasediment	-	4	-	-	-	-	-	-	1 500	Groves et al., 1979
Wannaway											

Mining Camp	Rocktype/ore	Sample	n	Ni	Cu	Pt	Pd	S	Se	S/Se	references
Deposit				% wt	% wt	ppb	ppb	% wt	ppm		
Wannaway	Ore	-	-	-	-	-	-	-	-	8 700	McQueen, 1981
Redross											
Redross	Ore	-	-	-	-	-	-	-	-	11 500	McQueen, 1981
Stillwater											
J-M reef	Reef	ST-12	-	0.23	0.18	166 355	248 678	0.75	5.33	1 411	Godel and Barnes, 2008
J-M reef	Reef	ST-14	-	0.09	0.06	7 811	40 757	0.33	1.47	2 259	Godel and Barnes, 2008
J-M reef	Reef	ST-16	-	0.34	0.17	23 007	45 007	1.01	6.03	1 673	Godel and Barnes, 2008
J-M reef	Reef	ST-17	-	0.06	0.04	11 391	37 134	0.27	1.23	2 187	Godel and Barnes, 2008
Bushveld											
Upper Zone C	Diorite	103.88	-	-	0.00	-	-	0.13	0.14	9 621	Barnes et al., 2009
Upper Zone C	Diorite	157.07	-	-	0.02	-	-	0.16	0.31	5 182	Barnes et al., 2009
Upper Zone C	Diorite	269.28	-	-	0.01	-	-	0.56	0.77	7 353	Barnes et al., 2009
Upper Zone C	Diorite	269.96	-	-	0.01	-	-	0.58	0.42	13 818	Barnes et al., 2009
Upper Zone C	Xenolith	272.58	-	-	0.05	-	-	2.71	2.15	12 628	Barnes et al., 2009
Upper Zone C	Diorite	304.72	-	-	0.03	-	-	1.20	2.02	5 929	Barnes et al., 2009
Upper Zone C	Mag layer R	305.44	-	-	0.01	-	-	0.39	0.46	8 426	Barnes et al., 2009
Upper Zone C	Gabbronorite	328.87	-	-	0.09	-	-	6.79	9.76	6 957	Barnes et al., 2009
Upper Zone C	Gabbronorite	351.13	-	-	0.04	-	-	1.95	3.31	5 895	Barnes et al., 2009
Upper Zone C	Gabbronorite	351.7	-	-	0.02	-	-	0.66	1.01	6 509	Barnes et al., 2009
Upper Zone C	Anorthosite	352.1	-	-	0.00	-	-	0.15	0.11	14 162	Barnes et al., 2009
Upper Zone C	Gabbronorite	443.87	-	-	0.00	-	-	0.03	0.05	6 148	Barnes et al., 2009
Upper Zone C	Gabbronorite	559.16	-	-	0.01	-	-	0.48	0.83	5 867	Barnes et al., 2009
Upper Zone C	Mag layer Q	603.67	-	-	0.02	-	-	0.54	0.84	6 427	Barnes et al., 2009
Upper Zone B	Mag layer P	611.56	-	-	0.10	-	-	5.83	8.12	7 178	Barnes et al., 2009
Upper Zone B	Mag layer P	611.76	-	-	0.03	-	-	1.02	1.30	7 796	Barnes et al., 2009
Upper Zone B	Mag layer O	644.8	-	-	0.01	-	-	0.16	0.30	5 330	Barnes et al., 2009
Upper Zone B	Gabbronorite	687.3	-	-	0.01	-	-	0.25	0.36	6 906	Barnes et al., 2009
Upper Zone B	Gabbronorite	806.02	-	-	0.02	-	-	0.47	0.54	8 743	Barnes et al., 2009
Upper Zone B	Mag layer M	830.57	-	-	0.01	-	-	0.19	0.26	7 389	Barnes et al., 2009
Upper Zone B	Mag layer M	830.75	-	-	0.01	-	-	0.16	0.27	5 815	Barnes et al., 2009
Upper Zone B	Mag layer L	848.8	-	-	0.00	-	-	0.03	0.03	9 226	Barnes et al., 2009
Upper Zone B	Gabbronorite	882.05	-	-	0.00	-	-	0.02	0.06	4 069	Barnes et al., 2009
Upper Zone B	Mag layer J	903.08	-	-	0.03	-	-	0.23	0.46	5 055	Barnes et al., 2009
Upper Zone B	Gabbronorite	920.83	-	-	0.12	-	-	0.55	1.71	3 191	Barnes et al., 2009
Upper Zone B	Mag layer I	930.4	-	-	0.03	-	-	0.16	0.48	3 361	Barnes et al., 2009
Upper Zone B	Mag layer II	978	-	-	0.00	-	-	0.02	0.03	6 839	Barnes et al., 2009
Upper Zone B	Mag layer H	1002.5	-	-	0.01	-	-	0.08	0.20	3 949	Barnes et al., 2009
Upper Zone A	Gabbronorite	1028.03	-	-	0.00	-	-	0.05	0.05	11 717	Barnes et al., 2009
Upper Zone A	Gabbronorite	1048.81	-	-	0.01	-	-	0.03	0.12	2 675	Barnes et al., 2009
Upper Zone A	Gabbronorite	1049.26	-	-	0.02	-	-	0.24	0.53	4 494	Barnes et al., 2009
Upper Zone A	Gabbronorite	1070.95	-	-	0.14	-	-	0.39	1.51	2 583	Barnes et al., 2009
Upper Zone A	Gabbronorite	1144.8	-	-	0.01	-	-	0.05	0.12	4 367	Barnes et al., 2009
Upper Zone A	Gabbronorite	1216.3	-	-	0.03	-	-	0.11	0.43	2 582	Barnes et al., 2009
Upper Zone A	Mag layer	1224	-	-	0.15	-	-	0.21	1.33	1 555	Barnes et al., 2009
Upper Zone A	Gabbronorite	1279.93	-	-	0.05	-	-	0.20	0.60	3 356	Barnes et al., 2009
Upper Zone A	Gabbronorite	1316.52	-	-	0.16	-	-	0.49	2.28	2 159	Barnes et al., 2009
Upper Zone A	Mag layer E	1334.55	-	-	0.19	-	-	0.54	2.27	2 382	Barnes et al., 2009
Upper Zone A	Gabbronorite	1374.84	-	-	0.03	-	-	0.17	0.44	3 881	Barnes et al., 2009
Upper Zone A	Anorthosite	1382.24	-	-	0.04	-	-	0.15	0.60	2 500	Barnes et al., 2009
Upper Zone A	Mag layer C	1397.05	-	-	0.02	-	-	0.07	0.27	2 675	Barnes et al., 2009
Upper Zone A	Mag layer B	1403.17	-	-	0.10	-	-	1.12	2.28	4 910	Barnes et al., 2009
Upper Zone A	Gabbronorite	1404.35	-	-	0.22	-	-	0.52	2.02	2 569	Barnes et al., 2009
Upper Zone A	Gabbronorite	1483.34	-	-	0.02	-	-	0.07	0.25	2 722	Barnes et al., 2009
Upper Zone A	Anorthosite	1517.08	-	-	0.00	-	-	0.04	0.10	4 632	Barnes et al., 2009
Upper Zone A	Anorthosite	1520.33	-	-	0.35	-	-	0.87	4.96	1 745	Barnes et al., 2009
Upper Zone A	Gabbronorite	1530.27	-	-	0.16	-	-	0.19	2.02	942	Barnes et al., 2009

Mining Camp	Rocktype/ore	Sample	n	Ni	Cu	Pt	Pd	S	Se	S/Se	references
Deposit				% wt	% wt	ppb	ppb	% wt	ppm		
Upper Zone A	Gabbronorite	1530.47	-	-	0.13	-	-	0.18	1.60	1 129	Barnes et al., 2009
Upper Zone A	Gabbronorite	1534.54	-	-	0.08	-	-	0.10	0.66	1 511	Barnes et al., 2009
Upper Zone A	Gabbronorite	1547.7	-	-	0.07	-	-	0.06	0.58	1 078	Barnes et al., 2009
Main Zone	Gabbronorite	1618.43	-	-	0.00	-	-	0.01	0.02	3 000	Barnes et al., 2009
Main Zone	Gabbronorite	1708.75	-	-	0.00	-	-	0.02	0.05	4 170	Barnes et al., 2009
Main Zone	Gabbronorite	1745.45	-	-	0.00	-	-	0.01	0.03	2 172	Barnes et al., 2009
Main Zone	Gabbronorite	1745.45	-	-	0.01	-	-	0.05	0.10	5 179	Barnes et al., 2009
Main Zone	Norite	1967.1	-	-	0.00	-	-	0.01	0.03	3 214	Barnes et al., 2009
Main Zone	Norite	1973.68	-	-	0.01	-	-	0.01	0.03	3 593	Barnes et al., 2009
Main Zone	Anorthosite	1973.78	-	-	0.03	-	-	0.06	0.24	2 353	Barnes et al., 2009
Main Zone	Gabbro	mz7	-	-	0.00	-	-	0.00	0.03	1 000	Barnes et al., 2009
Main Zone	Gabbro	mz4	-	-	0.00	-	-	0.00	0.08	295	Barnes et al., 2009
Main Zone	Gabbro	sp11	-	-	0.00	-	-	0.01	0.02	3 235	Barnes et al., 2009
Main Zone	Gabbro	a1	-	-	0.00	-	-	0.00	0.02	2 438	Barnes et al., 2009
Main Zone	Gabbro	a35	-	-	0.00	-	-	0.00	0.01	3 000	Barnes et al., 2009
Main Zone	Gabbro	a65	-	-	0.00	-	-	0.00	0.03	1 152	Barnes et al., 2009
Main Zone	Gabbro	a79	-	-	0.00	-	-	0.01	0.02	4 409	Barnes et al., 2009
Main Zone	Gabbro	a106	-	-	0.00	-	-	0.01	0.03	4 360	Barnes et al., 2009
Main Zone	Gabbro	a141	-	-	0.00	-	-	0.01	0.02	3 056	Barnes et al., 2009
Main Zone	Gabbro	a168	-	-	0.00	-	-	0.01	0.02	4 000	Barnes et al., 2009
Main Zone	Gabbro	a206	-	-	0.00	-	-	0.01	0.01	5 889	Barnes et al., 2009
Main Zone	Gabbro	a238	-	-	0.01	-	-	0.03	0.11	2 456	Barnes et al., 2009
Main Zone	Gabbro	a254	-	-	0.00	-	-	0.01	0.04	1 432	Barnes et al., 2009
Main Zone	Gabbro	a255	-	-	-	-	-	0.01	0.02	3 261	Barnes et al., 2009
Main Zone	Gabbro	a261	-	-	-	-	-	0.01	0.02	4 211	Barnes et al., 2009
Main Zone	Gabbro	a262	-	-	-	-	-	0.01	0.02	3 938	Barnes et al., 2009
Main Zone	Gabbro	a271	-	-	0.00	-	-	0.01	0.02	3 158	Barnes et al., 2009
Main Zone	Gabbro	a275	-	-	-	-	-	0.01	0.01	7 250	Barnes et al., 2009
Main Zone	Norite	a297	-	-	-	-	-	0.01	0.06	1 825	Barnes et al., 2009
Main Zone	Pyroxenite	a298	-	-	0.01	-	-	0.11	0.21	5 076	Barnes et al., 2009
Main Zone	Norite	a301	-	-	0.00	-	-	0.01	0.02	3 053	Barnes et al., 2009
Main Zone	Norite	a315	-	-	-	-	-	0.01	0.02	6 000	Barnes et al., 2009
Main Zone	Norite	a334	-	-	0.00	-	-	0.01	0.02	3 318	Barnes et al., 2009
Critical Zone	Norite	ua2	-	-	0.00	-	-	0.01	0.03	2 438	Barnes et al., 2009
Bastard Unit	Norite	ua20	-	-	0.00	-	-	0.02	0.03	5 455	Barnes et al., 2009
Bastard Unit	Pyroxenite	ua25	-	-	0.02	-	-	0.11	0.45	2 395	Barnes et al., 2009
Merensky Reef	Anorthosite	ua31	-	-	0.00	-	-	0.02	0.07	2 537	Barnes et al., 2009
Merensky Reef	Norite	ua36	-	-	0.01	-	-	0.03	0.11	2 385	Barnes et al., 2009
Merensky Reef	Norite	ua41	-	-	0.02	-	-	0.08	0.42	1 971	Barnes et al., 2009
Merensky Reef	Melanorite	m-4	-	0.42	0.14	5 210	2 160	1.45	4.38	3 320	Barnes et al., 2009
Merensky Reef	Melanorite	m-3	-	0.41	0.11	2 480	2 360	1.58	3.89	4 074	Barnes et al., 2009
Merensky Reef	Melanorite	m-2	-	0.29	0.10	3 140	2 220	0.80	3.01	2 660	Barnes et al., 2009
Merensky Reef	Melanorite	m-1	-	1.37	0.28	16 550	11 900	4.03	14.57	2 764	Barnes et al., 2009
Merensky Reef	Melanorite	CGM-2	-	0.44	0.43	8 840	5 940	1.48	5.51	2 692	Barnes et al., 2009
Merensky Reef	Melanorite	GGM-1	-	1.31	0.35	42 080	16 290	2.98	14.32	2 082	Barnes et al., 2009
Merensky Reef	Anorthosite	An	-	0.13	0.09	5 340	4 030	0.59	1.75	3 385	Barnes et al., 2009
Merensky Reef	composite	SARM-7	-	-	0.07	-	-	0.42	1.99	2 097	Barnes et al., 2009
Pseudoreef	Anorthosite	ua48	-	-	0.00	-	-	0.01	0.03	2 059	Barnes et al., 2009
UG-2	Pyroxenite	ua63	-	-	0.00	-	-	0.01	0.06	1 724	Barnes et al., 2009
UG-2	Pyroxenite	ua66	-	-	0.00	-	-	0.02	0.06	3 750	Barnes et al., 2009
UG-2	Harzburgite	ua70	-	-	0.00	-	-	0.02	0.06	3 770	Barnes et al., 2009
UG-1	Pyroxenite	b235/34	-	-	0.00	-	-	0.01	0.02	6 208	Barnes et al., 2009
UG-1	Pyroxenite	b235/36	-	-	0.00	-	-	0.01	0.02	4 375	Barnes et al., 2009
MG4	Norite	b235/39	-	-	0.00	-	-	0.00	0.01	1 125	Barnes et al., 2009
MG4	Norite	s11	-	-	0.00	-	-	0.00	0.01	2 429	Barnes et al., 2009
MG4	Norite	s20	-	-	0.00	-	-	0.00	0.01	1 286	Barnes et al., 2009

Mining Camp	Rocktype/ore	Sample	n	Ni	Cu	Pt	Pd	S	Se	S/Se	references
Deposit				% wt	% wt	ppb	ppb	% wt	ppm		
MG4	Norite	s30	-	-	0.00	-	-	0.00	0.01	1 250	Barnes et al., 2009
MG4	Pyroxenite	s40	-	-	0.00	-	-	0.00	0.01	1 900	Barnes et al., 2009
MG4	Pyroxenite	s52	-	-	0.00	-	-	0.00	0.01	2 231	Barnes et al., 2009
MG4	Pyroxenite	ng3 146.5	-	-	0.00	-	-	0.00	0.02	941	Barnes et al., 2009
MG3	Pyroxenite	ng3 159.4	-	-	0.00	-	-	0.01	0.03	3 103	Barnes et al., 2009
MG3	Norite	ng3 176.45	-	-	0.00	-	-	0.01	0.04	2 400	Barnes et al., 2009
MG3	Norite	ng3 194.7	-	-	0.00	-	-	0.01	0.02	3 125	Barnes et al., 2009
MG2	Pyroxenite	ng3 214.25	-	-	0.00	-	-	0.01	0.02	2 636	Barnes et al., 2009
MG1	Pyroxenite	ng3 220.17	-	-	0.00	-	-	0.01	0.01	3 846	Barnes et al., 2009
MG1	Pyroxenite	ng3 232	-	-	0.00	-	-	0.01	0.02	4 826	Barnes et al., 2009
MG1	Pyroxenite	ng1 25	-	-	0.00	-	-	0.01	0.04	1 955	Barnes et al., 2009
LG7	Harzburgite	ng1 95.1	-	-	0.00	-	-	0.02	0.02	10 563	Barnes et al., 2009
LG6	Pyroxenite	ng1 163.27	-	-	0.00	-	-	0.01	0.04	2 622	Barnes et al., 2009
LG6	Pyroxenite	ng1 233.6	-	-	0.00	-	-	0.01	0.03	3 385	Barnes et al., 2009
LG6	Pyroxenite	ng1 245.25	-	-	0.00	-	-	0.00	0.01	2 385	Barnes et al., 2009
LG5	Pyroxenite	ng1 257.7	-	-	0.00	-	-	0.01	0.02	3 333	Barnes et al., 2009
LG5	Pyroxenite	ng1 292.3	-	-	0.00	-	-	0.00	0.01	3 222	Barnes et al., 2009
LG5	Pyroxenite	ng1 327.45	-	-	0.00	-	-	0.01	0.03	3 231	Barnes et al., 2009
LG4	Pyroxenite	ng1 380.35	-	-	0.00	-	-	0.01	0.03	3 531	Barnes et al., 2009
LG4	Pyroxenite	ng1 421	-	-	0.00	-	-	0.01	0.05	1 904	Barnes et al., 2009
LG2	Pyroxenite	ng1 500.5	-	-	0.00	-	-	0.01	0.03	1 724	Barnes et al., 2009
LG2	Harzburgite	ng1 509.8	-	-	0.00	-	-	0.01	0.06	1 967	Barnes et al., 2009
LG1	Pyroxenite	ng1 528.5	-	-	0.00	-	-	0.01	0.02	3 045	Barnes et al., 2009
LG1	Pyroxenite	ng1 558.78	-	-	0.00	-	-	0.01	0.02	3 529	Barnes et al., 2009
Critical Zone	Pyroxenite	ng1 575.35	-	-	0.00	-	-	0.01	0.02	4 706	Barnes et al., 2009
Critical Zone	Pyroxenite	ng1 619.85	-	-	0.00	-	-	0.01	0.02	3 188	Barnes et al., 2009
Lower Zone	Pyroxenite	ng1 670.1	-	-	0.00	-	-	0.01	0.02	6 174	Barnes et al., 2009
Lower Zone	Harzburgite	ng1 698	-	-	0.00	-	-	0.01	0.03	2 593	Barnes et al., 2009
Lower Zone	Dunite	ng1 773.38	-	-	0.00	-	-	0.00	0.02	1 471	Barnes et al., 2009
Lower Zone	Dunite	ng1 793.8	-	-	0.00	-	-	0.00	0.01	5 143	Barnes et al., 2009
Lower Zone	Pyroxenite	ng2 115.25	-	-	-	-	-	0.00	-	-	Barnes et al., 2009
Lower Zone	Pyroxenite	ng2 171.5	-	-	0.00	-	-	0.01	0.03	3 929	Barnes et al., 2009
Lower Zone	Pyroxenite	ng2 253.05	-	-	0.00	-	-	0.02	0.08	2 100	Barnes et al., 2009
Lower Zone	Pyroxenite	ng2 332.25	-	-	0.00	-	-	0.02	0.08	1 928	Barnes et al., 2009
Lower Zone	Pyroxenite	ng2 373	-	-	0.00	-	-	0.02	0.04	5 778	Barnes et al., 2009
Lower Zone	Pyroxenite	ng2 409.79	-	-	-	-	-	0.01	0.02	8 875	Barnes et al., 2009
Lower Zone	Harzburgite	ng2 449.4	-	-	0.00	-	-	0.03	0.08	4 139	Barnes et al., 2009
Lower Zone	Pyroxenite	ng2 490.05	-	-	-	-	-	0.03	0.06	5 714	Barnes et al., 2009
Lower Zone	Harzburgite	ng2 557.1	-	-	0.00	-	-	0.02	0.04	5 310	Barnes et al., 2009
Lower Zone	Harzburgite	ng2 626.12	-	-	0.00	-	-	0.03	0.06	4 839	Barnes et al., 2009
Lower Zone	Pyroxenite	ng2 678.64	-	-	-	-	-	0.03	0.10	2 647	Barnes et al., 2009
Marginal Zone	B1-QT	CD-017	-	-	0.01	-	-	0.05	0.18	2 713	Barnes et al., 2009
Marginal Zone	B1-QT	CD-001	-	-	0.00	-	-	0.05	0.16	2 968	Barnes et al., 2009
Marginal Zone	B1-QT	DI-225	-	-	0.01	-	-	0.06	0.10	6 516	Barnes et al., 2009
Marginal Zone	B-1	CO-114	-	-	0.00	-	-	0.04	0.15	3 007	Barnes et al., 2009
Marginal Zone	B-1	DI-204	-	-	0.00	-	-	0.05	0.13	3 550	Barnes et al., 2009
Marginal Zone	B1-UM	CD-005	-	-	0.01	-	-	0.04	0.14	2 517	Barnes et al., 2009
Marginal Zone	B1-UM	bc-5	-	-	0.00	-	-	0.04	0.07	4 863	Barnes et al., 2009
Marginal Zone	B1-UM	CO-113	-	-	0.00	-	-	0.02	0.07	2 875	Barnes et al., 2009
Marginal Zone	B-2	bc-6	-	-	0.01	-	-	0.02	0.07	2 435	Barnes et al., 2009
Marginal Zone	B-2	bc-25	-	-	0.01	-	-	0.01	0.06	949	Barnes et al., 2009
Marginal Zone	B-2	CO-66	-	-	0.01	-	-	0.02	0.05	3 173	Barnes et al., 2009
Marginal Zone	B-3	CO-48	-	-	0.00	-	-	0.00	0.02	2 588	Barnes et al., 2009
Marginal Zone	B-3	CO-252	-	-	0.00	-	-	0.01	0.01	6 625	Barnes et al., 2009
Great Dyke											
Mimosa Mine	Main Sulfide Zone	GD-10	-	0.26	0.23	470	631	0.82	3.30	2 485	Barnes et al., 2008

Mining Camp	Rocktype/ore	Sample	n	Ni	Cu	Pt	Pd	S	Se	S/Se	references
Deposit				% wt	% wt	ppb	ppb	% wt	ppm		
Penikat											
AP-reef	Reef	FI-02-06	-	0.35	0.58	6 150	26 060	1.51	11.60	1 302	Barnes et al., 2008
PV-reef	Reef	FI-03-04	-	0.71	1.20	10 550	11 450	3.83	24.60	1 557	Barnes et al., 2008
Munni Munni											
UM Zone	Gabbro	0179	-	0.05	0.02	4	3	0.09	0.15	5 885	Hoatson and Keays, 1989
UM Zone	Gabbronorite	0100	-	0.04	0.08	35	58	0.83	1.83	4 553	Hoatson and Keays, 1989
UM Zone	Gabbronorite	0102	-	0.06	0.16	15	0	1.24	2.46	5 049	Hoatson and Keays, 1989
UM Zone	Websterite	0001	-	0.07	0.00	3	6	0.01	0.03	4 069	Hoatson and Keays, 1989
UM Zone	Websterite	0003	-	0.09	0.00	1	2	0.01	-	-	Hoatson and Keays, 1989
UM Zone	Websterite	0005	-	0.09	0.00	1	2	0.01	0.03	2 308	Hoatson and Keays, 1989
UM Zone	Websterite	0007	-	0.08	0.00	2	3	0.01	0.01	5 333	Hoatson and Keays, 1989
Serpentinite (UM Zone)	Websterite	0011	-	0.13	0.00	2	2	<0.02	0.01	1 429	Hoatson and Keays, 1989
Serpentinite (UM Zone)	Websterite	0016	-	0.11	0.00	1	2	<0.02	0.02	625	Hoatson and Keays, 1989
Serpentinite (UM Zone)	Websterite	0018	-	0.11	0.00	1	2	0.00	<0.005	-	Hoatson and Keays, 1989
Serpentinite (UM Zone)	Websterite	0020	-	0.08	0.00	2	2	0.00	<0.005	-	Hoatson and Keays, 1989
Serpentinite (UM Zone)	Websterite	0022	-	0.10	0.00	1	2	0.00	<0.005	-	Hoatson and Keays, 1989
Serpentinite (UM Zone)	Clinopyroxenite	0024	-	0.10	0.00	2	3	0.00	<0.005	-	Hoatson and Keays, 1989
UM Zone	Clinopyroxenite	0028	-	0.07	0.00	2	2	0.00	<0.005	-	Hoatson and Keays, 1989
Serpentinite (UM Zone)	Websterite	0031	-	0.11	0.00	2	3	0.00	0.02	909	Hoatson and Keays, 1989
Serpentinite (UM Zone)	Websterite	0032	-	0.09	0.00	2	3	0.00	0.01	2 300	Hoatson and Keays, 1989
Serpentinite (UM Zone)	Lherzolite	0034	-	0.19	0.00	2	3	0.02	0.04	3 905	Hoatson and Keays, 1989
UM Zone	Websterite	0036	-	0.08	0.00	2	2	0.01	0.01	9 417	Hoatson and Keays, 1989
UM Zone	Websterite	0037	-	0.08	0.00	1	3	0.01	<0.005	-	Hoatson and Keays, 1989
Serpentinite (UM Zone)	Websterite	0041	-	0.07	0.00	2	3	0.01	0.04	2 976	Hoatson and Keays, 1989
Serpentinite (UM Zone)	Websterite	0042	-	0.07	0.00	4	2	0.02	0.03	5 294	Hoatson and Keays, 1989
PGE-rich (UM Zone)	Websterite	0044	-	0.05	0.01	3	17	0.01	0.09	1 600	Hoatson and Keays, 1989
PGE-rich (UM Zone)	Websterite	0143	-	0.09	0.12	525	1 854	-	0.24	-	Hoatson and Keays, 1989
PGE-rich (UM Zone)	Websterite	0094	-	0.10	0.28	88	6	0.39	1.63	2 417	Hoatson and Keays, 1989
Gabbroïc Zone	Gabbronorite	0048	-	0.02	0.02	1	2	0.03	0.13	2 792	Hoatson and Keays, 1989
Gabbroïc Zone	Gabbronorite	0049	-	0.02	0.02	0	2	0.03	0.11	2 642	Hoatson and Keays, 1989
Gabbroïc Zone	Gabbronorite	0051	-	0.01	0.02	2	4	0.04	0.10	3 778	Hoatson and Keays, 1989
Gabbroïc Zone	Gabbronorite	0051	-	0.01	0.02	1	3	0.04	0.09	3 967	Hoatson and Keays, 1989
Gabbroïc Zone	Gabbronorite	0055	-	0.01	0.03	1	2	0.04	0.13	3 068	Hoatson and Keays, 1989
Gabbroïc Zone	Gabbronorite	0058	-	0.01	0.04	1	2	0.06	0.15	4 093	Hoatson and Keays, 1989
Gabbroïc Zone	Gabbronorite	0061	-	0.01	0.04	1	2	0.06	0.16	3 677	Hoatson and Keays, 1989
Gabbroïc Zone	Gabbronorite	0064	-	0.00	0.03	0	1	0.07	0.16	4 081	Hoatson and Keays, 1989
Gabbroïc Zone	Gabbronorite	0066	-	0.00	0.03	1	2	0.07	0.13	5 589	Hoatson and Keays, 1989
Gabbroïc Zone	Gabbronorite	0131	-	0.01	0.01	6	4	0.03	0.12	2 422	Hoatson and Keays, 1989
Other rock types	Orthopyroxenite	0046	-	0.07	0.00	1	3	0.00	0.01	7 833	Hoatson and Keays, 1989
Other rock types	Chromitite	0156	-	0.00	0.00	0	3	0.00	0.12	270	Hoatson and Keays, 1989
Other rock types	Chromitite	0159	-	0.07	0.00	0	3	0.00	0.01	3 538	Hoatson and Keays, 1989
Other rock types	Shear	0088	-	0.14	0.37	50	12	0.58	1.66	3 474	Hoatson and Keays, 1989
Other rock types	Shear	0163	-	0.08	0.16	0	3	0.12	0.73	1 597	Hoatson and Keays, 1989
Federov Pansky											
Federov Pansky Ore	Silicified gabbronorite	P-86/177	-	-	-	-	-	0.41	< 1	-	Schissel et al., 2002
Federov Pansky Ore	Mesogabbronorite	P-117/19	-	-	-	-	-	1.17	9.00	1 300	Schissel et al., 2002
Federov Pansky Ore	Mesogabbronorite	P-110/162	-	-	-	-	-	0.20	< 1	-	Schissel et al., 2002
Federov Pansky Ore	Mesogabbronorite	P-107/ 63	-	-	-	-	-	0.53	2.00	2 650	Schissel et al., 2002
Federov Pansky Ore	Mesogabbronorite	P-106/46.6	-	-	-	-	-	0.26	< 1	-	Schissel et al., 2002
Federov Pansky Ore	Mesogabbronorite	P-113/36	-	-	-	-	-	0.05	< 1	-	Schissel et al., 2002
Federov Pansky Ore	Mesogabbronorite	P-116/128	-	-	-	-	-	0.22	2.00	1 100	Schissel et al., 2002
Federov Pansky Ore	Mesogabbronorite	P-106/42	-	-	-	-	-	0.66	2.00	3 300	Schissel et al., 2002
Federov Pansky Ore	Mesogabbronorite	P-86/164.3	-	-	-	-	-	0.47	1.00	4 700	Schissel et al., 2002
Federov Pansky Ore	Mesogabbronorite	P-113/101.3	-	-	-	-	-	0.32	< 1	-	Schissel et al., 2002
Federov Pansky Ore	Mesogabbronorite	P-86/146	-	-	-	-	-	0.43	< 1	-	Schissel et al., 2002
Federov Pansky Ore	Mesogabbronorite	P-110/163	-	-	-	-	-	0.39	< 1	-	Schissel et al., 2002

Mining Camp / Deposit	Rocktype/ore	Sample	n	Ni % wt	Cu % wt	Pt ppb	Pd ppb	S % wt	Se ppm	S/Se	references
Federov Pansky Ore	Mesogabbronorite	P-115/17.5	-	-	-	-	-	0.44	1.00	4 400	Schissel et al., 2002
Federov Pansky Ore	Mesogabbronorite	P-115/26.5	-	-	-	-	-	0.82	5.00	1 640	Schissel et al., 2002
Federov Pansky Ore	Leucogabbronorite	P-106/141	-	-	-	-	-	0.53	5.00	1 060	Schissel et al., 2002
East Bull Lake											
Marginal Series. B Zone	Gabbronorite	90DCP-050	-	0.07	0.17	258	475	0.56	1.75	3 200	Peck et al., 2001
Marginal Series. B Zone	Pyroxenite	91DCP-533	-	0.06	0.12	29	52	0.11	0.94	1 170	Peck et al., 2001
Marginal Series. B Zone	Leucogabbronorite	91DCP-548	-	0.05	0.11	77	180	0.34	1.20	2 830	Peck et al., 2001
Marginal Series. B Zone	Gabbronorite	91DCP-525	-	0.08	0.20	95	200	0.40	3.80	1 050	Peck et al., 2001
Marginal Series. B Zone	Leucogabbronorite	90DCP-373	-	0.07	0.05	139	342	0.07	-	-	Peck et al., 2001
Marginal Series	SF-Diss	AMEAN	17	0.06	0.10	94	188	0.22	1.78	1 240	Peck et al., 2001
Marginal Series	SF-Diss	GMEAN	17	0.05	0.08	67	115	0.15	1.33	1 350	Peck et al., 2001
Lower Series. IB Zone	Pyroxenite	91DCP-469	-	0.09	0.54	781	2 460	0.89	5.30	1 680	Peck et al., 2001
Lower Series. IB Zone	Pyroxenite	91DCP-487	-	0.01	0.22	965	1 170	0.44	3.40	1 290	Peck et al., 2001
Lower Series. IB Zone	Pyroxenite	91DCP-492	-	0.06	0.26	500	765	0.46	6.60	697	Peck et al., 2001
Lower Series. IB Zone	Pyroxenite	91DCP-496	-	g	0.14	1 230	631	0.13	-	-	Peck et al., 2001
Lower Series	SF-Diss	AMEAN	20	0.05	0.26	402	627	0.50	3.31	1 500	Peck et al., 2001
Lower Series	SF-Diss	GMEAN	20	0.04	0.21	301	515	0.37	2.54	1 160	Peck et al., 2001
Lower Series. IB Zone	Gabbronorite	91DCP-500	-	0.10	0.19	390	665	0.41	2.80	1 460	Peck et al., 2001
Lower Series. IB Zone	Leucogabbronorite	91DCP-396	-	0.33	0.05	39	117	0.12	0.32	3 750	Peck et al., 2001
Lower Series. IB Zone	Leucogabbronorite	91DCP-398	-	0.59	0.17	177	365	0.69	2.60	2 650	Peck et al., 2001
Lower Series. IB Zone	Gabbronorite	91DCP-603	-	0.14	0.54	555	2 660	0.97	-	-	Peck et al., 2001
Lower Series	SF-Diss	AMEAN	8	0.26	0.16	189	724	0.47	1.82	2 600	Peck et al., 2001
Lower Series	SF-Diss	GMEAN	8	0.15	0.11	114	498	0.35	1.37	2 240	Peck et al., 2001
Lower Series. AN Zone	Anorthosite	90DCP-348	-	0.19	0.45	282	725	0.55	3.08	1 790	Peck et al., 2001
Lower Series. AN Zone	Anorthosite	91DCP-508	-	0.01	0.07	900	3 200	0.06	-	-	Peck et al., 2001
Lower Series. AN Zone	Anorthosite	91DCP-560	-	0.04	0.12	2 140	8 690	0.23	1.30	1 770	Peck et al., 2001
Lower Series. AN Zone	Anorthosite	91DCP-567	-	0.09	0.33	690	2 920	0.77	5.10	1 510	Peck et al., 2001
Lower Series. AN Zone	Anorthosite	91DCP-586	-	0.01	0.01	100	480	0.03	0.09	3 330	Peck et al., 2001
Lower Series	SF-Diss	AMEAN	23	0.07	0.23	562	1 835	0.45	2.71	1 660	Peck et al., 2001
Lower Series	SF-Diss	GMEAN	23	0.04	0.15	383	1 260	0.31	1.73	1 780	Peck et al., 2001
Lower Series. AN Zone	Anorthosite	90DCP-303	-	0.01	0.04	80	390	0.05	0.41	1 220	Peck et al., 2001
Lower Series. AN Zone	Leucogabbronorite	91DCP-302	-	0.02	0.12	625	2 420	0.22	1.90	1 160	Peck et al., 2001
Lower Series. AN Zone	Leucogabbronorite	91DCP-600	-	0.12	0.22	224	1 240	0.65	-	-	Peck et al., 2001
Lower Series. AN Zone	Leucogabbronorite	91DCP-601	-	0.07	0.19	90	500	0.64	-	-	Peck et al., 2001
Lower Series. AN Zone	Leucogabbronorite	91DCP-384	-	0.04	0.09	236	1 110	0.30	1.50	2 000	Peck et al., 2001
Lower Series	SF-Diss	AMEAN	13	0.04	0.10	138	586	0.29	1.02	2 840	Peck et al., 2001
Lower Series	SF-Diss	GMEAN	13	0.03	0.07	86	379	0.19	0.75	1 730	Peck et al., 2001
Lower Series. AN Zone	Leucogabbronorite	90DCP-372	-	0.13	0.35	355	1 440	1.17	1.47	7 960	Peck et al., 2001
Lower Series. AN Zone	Leucogabbronorite	90DCP-407	-	0.10	0.28	343	1 750	0.46	2.29	2 010	Peck et al., 2001
Lower Series. AN Zone	Leucogabbronorite	91DCP-433	-	0.06	0.20	500	1 200	0.25	4.30	581	Peck et al., 2001
Lower Series. AN Zone	Leucogabbronorite	91DCP-475	-	0.12	0.39	606	2 270	0.80	6.80	1 180	Peck et al., 2001
Lower Series. AN Zone	Leucogabbronorite	91DCP-517	-	0.23	0.50	435	2 600	1.17	10.00	1 170	Peck et al., 2001
Lower Series. AN Zone	Leucogabbronorite	91DCP-555	-	0.18	0.93	984	6 200	2.58	14.00	1 840	Peck et al., 2001
Lower Series. AN Zone	Leucogabbronorite	91DCP-556	-	0.06	0.06	105	550	0.32	1.60	2 000	Peck et al., 2001
Lower Series. AN Zone	Leucogabbronorite	91DCP-405	-	0.74	0.18	110	1 200	0.88	2.60	3 390	Peck et al., 2001
Lower Series	SF-Diss	AMEAN	77	0.08	0.19	224	726	0.52	2.69	1 940	Peck et al., 2001
Lower Series	SF-Diss	GMEAN	77	0.07	0.14	171	501	0.40	2.02	2 130	Peck et al., 2001
Lower Series. AN Zone	Gabbronorite	91DCP-179B	-	0.21	0.19	493	2 220	1.56	2.07	7 540	Peck et al., 2001
Lower Series. AN Zone	Gabbronorite	91DCP-476	-	0.15	0.28	225	1 250	0.66	3.50	1 890	Peck et al., 2001
Lower Series. AN Zone	Gabbronorite	91DCP-481	-	0.04	0.12	170	450	0.28	2.70	1 040	Peck et al., 2001
Lower Series. AN Zone	Gabbronorite	90DCP-324	-	0.02	0.01	98	158	0.03	-	-	Peck et al., 2001
Lower Series. AN Zone	Gabbronorite	91DCP-304	-	0.07	0.28	113	390	0.61	2.60	2 350	Peck et al., 2001
Lower Series	SF-Diss	AMEAN	11	0.07	0.13	158	593	0.36	2.31	1 570	Peck et al., 2001
Lower Series	SF-Diss	GMEAN	11	0.05	0.08	120	405	0.15	2.02	2 000	Peck et al., 2001
Main Series. LG Zone	Gabbronorite	91DCP-099	-	0.08	0.05	175	290	0.05	0.18	2 780	Peck et al., 2001
Main Series. LG Zone	Gabbronorite	91DCP-428	-	0.04	0.02	17	55	0.04	0.17	2 350	Peck et al., 2001

Mining Camp	Rocktype/ore	Sample	n	Ni	Cu	Pt	Pd	S	Se	S/Se	references
Deposit				% wt	% wt	ppb	ppb	% wt	ppm		
Main Series. LG Zone	Gabbronorite	91DCP-393	-	0.02	0.03	93	132	0.04	0.16	2 500	Peck et al., 2001
Main Series. LG Zone	Gabbronorite	91DCP-392	-	0.02	0.05	50	217	0.05	0.54	930	Peck et al., 2001
Mains Series	SF-Diss	AMEAN	8	0.04	0.04	68	148	0.51	4.03	1 270	Peck et al., 2001
Mains Series	SF-Diss	GMEAN	8	0.04	0.04	45	110	0.12	0.82	1 450	Peck et al., 2001
Structurally PGE-rich	SF-MS	90DCP-353	-	0.38	3.36	275	1 520	11.40	30.40	3 750	Peck et al., 2001
Structurally PGE-rich	SF-Diss	90DCP-485	-	0.07	0.13	318	600	1.46	4.26	3 430	Peck et al., 2001
Structurally PGE-rich	SF-MS	90DCP-488	-	0.17	5.63	475	2 180	7.30	27.60	2 650	Peck et al., 2001
Structurally PGE-rich	SF-MS	90DCP-497	-	0.48	14.50	171	2 300	24.40	52.10	4 680	Peck et al., 2001
Structurally PGE-rich	SF-MS	90DCP-500	-	0.29	3.93	189	1 600	8.16	25.20	3 240	Peck et al., 2001
Structurally PGE-rich	SF-MS	91DCP-573	-	0.11	0.55	680	3 760	39.80	48.90	8 140	Peck et al., 2001
Structurally PGE-rich	massive magnetite	91DCP-579	-	0.09	0.84	788	1 050	1.90	19.40	979	Peck et al., 2001
Structurally PGE-rich	SF-MS	91DCP-581	-	0.91	0.13	500	2 000	28.60	35.40	8 080	Peck et al., 2001
Structurally PGE-rich	SF-MS	91DCP-583	-	0.30	0.53	200	2 480	21.00	82.50	2 550	Peck et al., 2001
Structurally PGE-rich	SF-MS	AMEAN	37	0.35	1.58	271	1 080	10.00	26.30	5 850	Peck et al., 2001
Structurally PGE-rich	SF-MS	GMEAN	37	0.21	0.69	212	768	5.50	14.50	4 600	Peck et al., 2001
Lac des Iles											
Roby Zone	Melanogabbro	JH02-037	-	0.10	0.14	190	1 460	0.60	2.90	2 069	Hinchey and Hattori, 2005
Roby Zone	Melanogabbro	JH02-140	-	0.15	0.24	752	6 940	0.67	5.60	1 196	Hinchey and Hattori, 2005
Roby Zone	Clinopyroxenite	JH02-138	-	0.21	0.34	1 020	8 790	1.35	9.00	1 500	Hinchey and Hattori, 2005
Roby Zone	Clinopyroxenite	JH02-089	-	0.18	0.23	382	3 280	0.82	4.60	1 783	Hinchey and Hattori, 2005
Roby Zone	Dark gabbro	JH02-148	-	0.22	0.24	998	9 160	0.77	6.70	1 149	Hinchey and Hattori, 2005
Roby Zone	Dark gabbro	JH02-146	-	0.31	0.34	1 370	11 720	1.02	9.30	1 097	Hinchey and Hattori, 2005
Twilight Zone	Melanorite	JH-02-181	-	0.14	0.18	449	3 560	0.67	3.80	1 763	Hinchey and Hattori, 2005
Twilight Zone	Melanorite	JH-02-173	-	0.17	0.23	587	4 570	0.57	4.90	1 163	Hinchey and Hattori, 2005
High Grade Zone	Gabbro / Pyroxenite	JH-02-SZ3	-	0.80	0.35	355	1 100	0.86	16.20	531	Hinchey and Hattori, 2005
High Grade Zone	Gabbro / Pyroxenite	JH-02-SZ1	-	0.23	0.25	912	9 300	2.27	9.30	2 441	Hinchey and Hattori, 2005
High Grade Zone	Gabbro / Pyroxenite	JH-02-SZ2	-	0.13	0.17	1 026	19 700	1.67	5.80	2 879	Hinchey and Hattori, 2005
High Grade Zone	Gabbro / Pyroxenite	JH-02-SZ4	-	0.17	0.24	1 186	17 100	1.05	7.20	1 458	Hinchey and Hattori, 2005
High Grade Zone	Gabbro / Pyroxenite	JHC-02-035	-	0.35	0.29	1 204	20 800	0.77	15.60	494	Hinchey and Hattori, 2005
High Grade Zone	Gabbro / Pyroxenite	JHC-03-050	-	0.32	0.27	582	10 100	0.95	10.30	922	Hinchey and Hattori, 2005
High Grade Zone	Gabbro / Pyroxenite	JHC-03-063	-	0.16	0.15	811	16 600	0.47	6.20	758	Hinchey and Hattori, 2005
High Grade Zone	Gabbro / Pyroxenite	JHC-03-070	-	0.37	0.31	1 984	48 600	0.58	11.10	523	Hinchey and Hattori, 2005

- ANNEXE 2 -

TABLEAU RECAPITULATIF DES ANALYSES ISOTOPIQUES DU SOUFRE ($\delta^{34}S$)

Note : Dans un souci de cohérence avec la majeure partie des publications d'origines ainsi qu'avec les deux manuscrits présentés dans ce mémoire, les tableaux annexes sont renseignés en anglais.

Abbreviations

stdev	Standard Deviation
n	Number of samples
SF-MS	Massive sulfide
SF-Mtr	Matricial sulfide
SF-Diss	Disseminated sulfide
PGE	Platinum-Group Element
WR	Whole Rock
Py	Pyrite
Ccp	Chalcopyrite
Po	Pyrrhotite
Pn	Pentlandite
Sieg	Siegenite

Deposit	Rocktype/ore	Sample	Target	$\delta^{34}S$	stdev	references
Sudbury						
Sudbury	All ores	average	-	+0.00	2.00	Naldrett, 1981
Duluth Complex						
Dunka Road	Norite	DC-27	WR	+14.50	-	Thériault and Barnes, 1998
Dunka Road	Norite	DC-49	WR	+8.20	-	Thériault and Barnes, 1998
Dunka Road	Norite	DC-52	WR	+13.70	-	Thériault and Barnes, 1998
Dunka Road	Norite	DC-54	WR	+12.50	-	Thériault and Barnes, 1998
Dunka Road	Norite	DC-60	WR	+10.40	-	Thériault and Barnes, 1998
Dunka Road	Norite	DC-63	WR	+7.10	-	Thériault and Barnes, 1998
Dunka Road	Norite	DC-66	WR	+9.60	-	Thériault and Barnes, 1998
Dunka Road	Norite	DC-72	WR	+13.50	-	Thériault and Barnes, 1998
Dunka Road	Troctolite	DC-53	WR	+6.70	-	Thériault and Barnes, 1998
Dunka Road	Troctolite	DC-55	WR	+9.00	-	Thériault and Barnes, 1998
Dunka Road	Troctolite	DC-56	WR	+9.20	-	Thériault and Barnes, 1998
Dunka Road	Troctolite	DC-58	WR	+6.60	-	Thériault and Barnes, 1998
Dunka Road	Troctolite	DC-61	WR	+7.50	-	Thériault and Barnes, 1998
Dunka Road	Troctolite	DC-79	WR	+7.60	-	Thériault and Barnes, 1998
Dunka Road	PGE-rich layer	DC-62	WR	+1.60	-	Thériault and Barnes, 1998
Dunka Road	PGE-rich layer	DC-64	WR	+2.50	-	Thériault and Barnes, 1998
Dunka Road	SF-MS	DC-73	WR	+8.40	-	Thériault and Barnes, 1998
Dunka Road	SF-MS	DC-75	WR	+16.00	-	Thériault and Barnes, 1998
Dunka Road	SF-MS	DC-76	WR	+12.00	-	Thériault and Barnes, 1998
Dunka Road	Ccp-rich sulfides	DC-65	WR	+11.00	-	Thériault and Barnes, 1998
Dunka Road	Ccp-rich sulfides	DC-67	WR	+11.90	-	Thériault and Barnes, 1998
Virginia Formation	Pelites	DC-1	WR	+5.30	-	Thériault and Barnes, 1998
Virginia Formation	Pelites	DC-3	WR	+8.60	-	Thériault and Barnes, 1998
Virginia Formation	Pelites	DC-5	WR	+7.20	-	Thériault and Barnes, 1998
Virginia Formation	Pelites	DC-7	WR	+4.50	-	Thériault and Barnes, 1998
Virginia Formation	Pelites	DC-8	WR	+5.10	-	Thériault and Barnes, 1998
Virginia Formation	Pelites	DC-9	WR	+4.70	-	Thériault and Barnes, 1998
Virginia Formation	Bedded Pyrrhotite	DC-70	WR	+15.80	-	Thériault and Barnes, 1998
Babbitt	Xenolith	136 - 282.8	WR	+7.10	-	Ripley, 1990
Babbitt	Xenolith	156 - 450.5	WR	+8.50	-	Ripley, 1990
Babbitt	Xenolith	146 - 528.2	WR	+9.10	-	Ripley, 1990
Babbitt	Xenolith	10120 - 130.4	WR	+3.30	-	Ripley, 1990
Babbitt	Xenolith	10134 - 20.7	WR	+6.20	-	Ripley, 1990
Babbitt	Xenolith	10134 - 68.6	WR	+2.90	-	Ripley, 1990
Babbitt	Xenolith	10134 - 75.3	WR	+5.40	-	Ripley, 1990
Babbitt	Xenolith	10134 - 83.8	WR	+4.10	-	Ripley, 1990
Babbitt	Xenolith	10172 - 119.5	WR	+5.40	-	Ripley, 1990
Babbitt	Xenolith	10152 - 7.9	WR	+4.90	-	Ripley, 1990
Babbitt	Xenolith	10152 - 32.0	WR	+5.90	-	Ripley, 1990
Babbitt	Xenolith	10053 - 9.1	WR	+4.60	-	Ripley, 1990
Babbitt	Xenolith	10053 - 32.9	WR	+4.70	-	Ripley, 1990
Babbitt	Xenolith	10039 - 16.4	WR	+3.90	-	Ripley, 1990
Babbitt	Hornfel	214 - 599.2	WR	+6.40	-	Ripley, 1990
Virginia Formation	Pelites	MDD2 - 434.0	WR	+13.50	-	Ripley, 1990
Virginia Formation	Pelites	MDD2 - 491.3	WR	-1.00	-	Ripley, 1990
Virginia Formation	Pelites	24981 - 47.5	WR	+5.60	-	Ripley, 1990
Virginia Formation	Pelites	24981 - 50.9	WR	+6.50	-	Ripley, 1990
Virginia Formation	Pelites	24981 - 53.6	WR	+7.10	-	Ripley, 1990
Virginia Formation	Pelites	24981 - 62.8	WR	+8.80	-	Ripley, 1990
Virginia Formation	Pelites	24981 - 64.6	WR	+8.00	-	Ripley, 1990
Virginia Formation	Pelites	24981 - 68.0	WR	+6.50	-	Ripley, 1990
Jinchuan						
Jinchuan	SF-Diss	CBZHS-20	Po	+1.80	-	Chai and Naldrett, 1992
Jinchuan	Net textured	CBZHS-7	Po	+2.20	-	Chai and Naldrett, 1992
Jinchuan	Net textured	CBZHS-4	Pn	+2.10	-	Chai and Naldrett, 1992
Jinchuan	Net textured	CBZHS-5	Pn	-0.30	-	Chai and Naldrett, 1992
Jinchuan	Net textured	CBZHS-5	Ccp	+2.50	-	Chai and Naldrett, 1992
Jinchuan	Net textured	CBZHS-6	Pn	+2.40	-	Chai and Naldrett, 1992

Deposit	Rocktype/ore	Sample	Target	$\delta^{34}S$	stdev	references
Jinchuan	Net textured	CBZHS-8	Py	+1.00	-	Chai and Naldrett, 1992
Jinchuan	SF-Diss	CBZHS-10	Pn	+2.50	-	Chai and Naldrett, 1992
Jinchuan	SF-Diss	CBZHS-10	Ccp	+2.40	-	Chai and Naldrett, 1992
Jinchuan	SF-Diss	CBZHS-11	Ccp	+2.70	-	Chai and Naldrett, 1992
Jinchuan	SF-Diss	CBZHS-11	Po	+3.10	-	Chai and Naldrett, 1992
Jinchuan	SF-MS	CBZHS-14	Pn	+1.60	-	Chai and Naldrett, 1992
Jinchuan	SF-MS	CBZHS-15	Pn	+1.80	-	Chai and Naldrett, 1992
Jinchuan	SF-Diss	CBZHS-16	Ccp	+1.80	-	Chai and Naldrett, 1992
Jinchuan	SF-Diss	CBZHS-16	Py	-2.60	-	Chai and Naldrett, 1992
Jinchuan	SF-MS	CBZHS-16	Po	+2.30	-	Chai and Naldrett, 1992
Jinchuan	SF-MS	CBZHS- 18	Py	+1.80	-	Chai and Naldrett, 1992
Jinchuan	Ore	I14-16-60	Po-Ccp	+0.80	-	Ripley et al., 2005
Jinchuan	Ore	I14-16-77	Po-Ccp	+2.20	-	Ripley et al., 2005
Jinchuan	Ore	I14-16-85	Po-Ccp	+6.00	-	Ripley et al., 2005
Jinchuan	Ore	I14-16-106	Po-Ccp	+0.80	-	Ripley et al., 2005
Jinchuan	Ore	I14-16-114	Py	-8.80	-	Ripley et al., 2005
Jinchuan	Ore	I14-16-124	Py	-11.30	-	Ripley et al., 2005
Jinchuan	Ore	I14-16-133	Po-Ccp	-0.30	-	Ripley et al., 2005
Jinchuan	Ore	I14-16-143	Po-Ccp	+0.50	-	Ripley et al., 2005
Jinchuan	Ore	I14-16-153	Po-Ccp	-0.70	-	Ripley et al., 2005
Jinchuan	Ore	I14-16-158	Po-Ccp	-2.60	-	Ripley et al., 2005
Jinchuan	Ore	I14-16-175	-	-	-	Ripley et al., 2005
Jinchuan	Ore	I14-16-195	Po-Ccp	+0.30	-	Ripley et al., 2005
Jinchuan	Ore	I14-16-209	Po-Ccp	+6.00	-	Ripley et al., 2005
Jinchuan	Ore	I14-16-220	Po-Ccp	+1.60	-	Ripley et al., 2005
Jinchuan	Ore	I14-16-234	Po-Ccp	+2.50	-	Ripley et al., 2005
Jinchuan	Ore	I14-16-257	Po-Ccp	+5.40	-	Ripley et al., 2005
Jinchuan	Ore	I14-16-271	Po-Ccp	-2.30	-	Ripley et al., 2005
Jinchuan	Ore	I14-16-291	Po-Ccp	+0.10	-	Ripley et al., 2005
Jinchuan	Ore	I14-16-299	Po-Ccp	+1.20	-	Ripley et al., 2005
Jinchuan	Ore	I14-16-306	Py	-27.00	-	Ripley et al., 2005
Jinchuan	Ore	I14-16-315	Po-Ccp	+0.80	-	Ripley et al., 2005
Jinchuan	Ore	I14-16-330	Po-Ccp	+0.30	-	Ripley et al., 2005
Jinchuan	Ore	I14-16-335	Po-Ccp	+0.60	-	Ripley et al., 2005
Jinchuan	Ore	I14-16-335	Po-Ccp	+2.10	-	Ripley et al., 2005
Jinchuan	Ore	I14-16-345	Po-Ccp	+0.80	-	Ripley et al., 2005
Jinchuan	Ore	I14-16-366	Po-Ccp	+4.90	-	Ripley et al., 2005
Jinchuan	Ore	I14-16-377	Po-Ccp	+0.20	-	Ripley et al., 2005
Jinchuan	Ore	II14-83-360	Po-Ccp	-0.10	-	Ripley et al., 2005
Jinchuan	Ore	II14-83-370	Po-Ccp	+4.80	-	Ripley et al., 2005
Jinchuan	Ore	II14-83-435	Po-Ccp	+1.90	-	Ripley et al., 2005
Jinchuan	Ore	II14-83-459	Po-Ccp	+2.80	-	Ripley et al., 2005
Jinchuan	Ore	II14-83-473	Po-Ccp	+2.70	-	Ripley et al., 2005
Jinchuan	Ore	II14-83-483	Po-Ccp	+0.90	-	Ripley et al., 2005
Jinchuan	Ore	II14-83-493	Po-Ccp	+2.80	-	Ripley et al., 2005
Jinchuan	Ore	II14-83-519	Po-Ccp	+3.20	-	Ripley et al., 2005
Jinchuan	Ore	II14-83-528	Po-Ccp	+2.50	-	Ripley et al., 2005
Jinchuan	Ore	II14-83-551	Po-Ccp	+0.70	-	Ripley et al., 2005
Jinchuan	Ore	II14-83-559	Po-Ccp	+0.30	-	Ripley et al., 2005
Jinchuan	Ore	II14-83-569	Po-Ccp	+0.10	-	Ripley et al., 2005
Jinchuan	Ore	II14-83-573	Po-Ccp	+0.30	-	Ripley et al., 2005
Jinchuan	Ore	II14-83-589	Po-Ccp	+1.00	-	Ripley et al., 2005
Jinchuan	Ore	II14-83-598	Po-Ccp	+2.20	-	Ripley et al., 2005
Jinchuan	Ore	II14-83-610	Po-Ccp	+3.00	-	Ripley et al., 2005
Jinchuan	Ore	II14-83-620	Po-Ccp	+1.20	-	Ripley et al., 2005
Jinchuan	Ore	II14-83-634	Po-Ccp	+2.90	-	Ripley et al., 2005
Jinchuan	Ore	II14-83-644	Po-Ccp	+1.20	-	Ripley et al., 2005
Jinchuan	Ore	II14-83-656	Po-Ccp	+2.10	-	Ripley et al., 2005
Jinchuan	Ore	II14-83-668	Po-Ccp	+2.50	-	Ripley et al., 2005
Jinchuan	Ore	II14-83-681	Po-Ccp	+1.00	-	Ripley et al., 2005
Jinchuan	Ore	II14-83-702	Po-Ccp	+1.70	-	Ripley et al., 2005

Deposit	Rocktype/ore	Sample	Target	$\delta^{34}S$	stdev	references
Jinchuan	Ore	II14-83-722	Po-Ccp	+2.00	-	Ripley et al., 2005
Jinchuan	Ore	II14-83-751	Po-Ccp	+1.90	-	Ripley et al., 2005
Jinchuan	Ore	II14-83-770	Po-Ccp	+1.10	-	Ripley et al., 2005
Jinchuan	Ore	II14-83-783	Po-Ccp	+1.90	-	Ripley et al., 2005
Jinchuan	Ore	II14-83-790	Po-Ccp	+2.20	-	Ripley et al., 2005
Jinchuan	Ore	II14-83-802	Po-Ccp	+2.00	-	Ripley et al., 2005
Jinchuan	Ore	II14-83-809	Po-Ccp	+1.80	-	Ripley et al., 2005
Jinchuan	Ore	II14-83-817	Po-Ccp	-0.50	-	Ripley et al., 2005
Jinchuan	Ore	II14-83-822	Po-Ccp	+0.90	-	Ripley et al., 2005
Jinchuan	Ore	II14-83-840	Po-Ccp	+0.50	-	Ripley et al., 2005
Jinchuan	Ore	II14-83-854	Po-Ccp	+1.50	-	Ripley et al., 2005
Jinchuan	Ore	II14-83-867	Po-Ccp	+8.30	-	Ripley et al., 2005
Jinchuan	Ore	II48-136-93	Py	-11.70	-	Ripley et al., 2005
Jinchuan	Ore	II48-136-107	Po-Ccp	+2.00	-	Ripley et al., 2005
Jinchuan	Ore	II48-136-114	Po-Ccp	-0.10	-	Ripley et al., 2005
Jinchuan	Ore	II48-136-124	-	-	-	Ripley et al., 2005
Jinchuan	Ore	II48-136-130	Po-Ccp	+1.60	-	Ripley et al., 2005
Jinchuan	Ore	II48-136-158	Po-Ccp	-0.30	-	Ripley et al., 2005
Jinchuan	Ore	II48-136-175	-	-	-	Ripley et al., 2005
Jinchuan	Ore	II48-136-188	Po-Ccp	-1.30	-	Ripley et al., 2005
Jinchuan	Ore	II48-136-231	Po-Ccp	+0.30	-	Ripley et al., 2005
Jinchuan	Ore	II48-136-238	Po-Ccp	+2.10	-	Ripley et al., 2005
Jinchuan	Ore	II48-136-241	Po-Ccp	+3.80	-	Ripley et al., 2005
Jinchuan	Ore	II48-136-255	Po-Ccp	+4.00	-	Ripley et al., 2005
Jinchuan	Ore	II48-136-294	-	-	-	Ripley et al., 2005
Jinchuan	Ore	II48-136-320	Py	-8.90	-	Ripley et al., 2005
Jinchuan	Ore	II48-136-323	Po-Ccp	+1.50	-	Ripley et al., 2005
Jinchuan	Ore	II48-136-340	Po-Ccp	+0.70	-	Ripley et al., 2005
Jinchuan	Ore	II48-136-351	Po-Ccp	-0.40	-	Ripley et al., 2005
Jinchuan	Ore	II48-136-395	Po-Ccp	-4.00	-	Ripley et al., 2005
Jinchuan	Ore	II48-136-410	Po-Ccp	+1.20	-	Ripley et al., 2005
Jinchuan	Ore	II48-136-442	-	-	-	Ripley et al., 2005
Jinchuan	Ore	II48-136-450	Po-Ccp	+1.60	-	Ripley et al., 2005
Jinchuan	Ore	II48-136-461	Po-Ccp	+1.50	-	Ripley et al., 2005
Jinchuan	Ore	II48-136-465	Po-Ccp	+1.80	-	Ripley et al., 2005
Jinchuan	Ore	II48-136-473	Po-Ccp	+2.60	-	Ripley et al., 2005
Jinchuan	Ore	II48-136-476	Po-Ccp	-0.10	-	Ripley et al., 2005
Jinchuan	Ore	II48-136-486	-	-	-	Ripley et al., 2005
Jinchuan	Ore	II48-136-497	-	-	-	Ripley et al., 2005
Jinchuan	Ore	II48-136-505	Po-Ccp	+3.00	-	Ripley et al., 2005
Jinchuan	Ore	II48-136-516	Po-Ccp	+2.70	-	Ripley et al., 2005
Jinchuan	Ore	II48-136-528	Po-Ccp	+2.40	-	Ripley et al., 2005
Jinchuan	Ore	II48-136-538	Po-Ccp	+1.10	-	Ripley et al., 2005
Jinchuan	Ore	II48-136-548	Po-Ccp	+1.90	-	Ripley et al., 2005
Jinchuan	Ore	II48-136-552	Po-Ccp-Py	-3.50	-	Ripley et al., 2005
Jinchuan	Ore	II48-136-557	Po-Ccp	+1.10	-	Ripley et al., 2005
Jinchuan	Ore	II48-136-568	Po-Ccp	+1.90	-	Ripley et al., 2005
Jinchuan	Ore	II48-136-577	Po-Ccp	+1.10	-	Ripley et al., 2005
Jinchuan	Ore	II48-136-588	Po-Ccp-Py	-4.30	-	Ripley et al., 2005
Jinchuan	Ore	II48-136-599	Po-Ccp	+0.80	-	Ripley et al., 2005
Jinchuan	Ore	II48-136-607	Po-Ccp	+1.70	-	Ripley et al., 2005
Jinchuan	Ore	II48-136-622	Po-Ccp	+1.50	-	Ripley et al., 2005
Jinchuan	Ore	II48-136-623	Po-Ccp	+0.70	-	Ripley et al., 2005
Jinchuan	Ore	II48-136-630	Po-Ccp	+1.20	-	Ripley et al., 2005
Jinchuan	Ore	II48-136-634	Po-Ccp	+2.90	-	Ripley et al., 2005
Jinchuan	Ore	II48-136-646	Po-Ccp	+0.50	-	Ripley et al., 2005
Jinchuan	Ore	II48-136-651	Po-Ccp	+0.00	-	Ripley et al., 2005
Jinchuan	Ore	II48-136-655	Po-Ccp	+1.30	-	Ripley et al., 2005
Jinchuan	Ore	II48-136-659	Po-Ccp	+0.30	-	Ripley et al., 2005
Molson Dykes					-	
Cuthbert Lake	SF-Diss	C1	WR	+0.22	-	Eckstrand et al., 1989

Deposit	Rocktype/ore	Sample	Target	$\delta^{34}S$	stdev	references
Cuthbert Lake	SF-Diss	C12	WR	-0.32	-	Eckstrand et al., 1989
Cuthbert Lake	SF-Diss	C15	WR	-3.86	-	Eckstrand et al., 1989
Cuthbert Lake	SF-Diss	C35	WR	-0.72	-	Eckstrand et al., 1989
Cuthbert Lake	SF-Diss	C53	WR	+0.11	-	Eckstrand et al., 1989
Sipiwesk Lake	SF-Diss	103	WR	-0.36	-	Eckstrand et al., 1989
Sipiwesk Lake	SF-Diss	105	WR	-0.99	-	Eckstrand et al., 1989
Sipiwesk Lake	SF-Diss	106	WR	-1.26	-	Eckstrand et al., 1989
Sipiwesk Lake	SF-Diss	109	WR	-1.19	-	Eckstrand et al., 1989
Sipiwesk Lake	SF-Diss	110	WR	-1.01	-	Eckstrand et al., 1989
Cross Lake	SF-Diss	219-1	WR	-2.55	-	Eckstrand et al., 1989
Cross Lake	SF-Diss	219-3	WR	-0.67	-	Eckstrand et al., 1989
Fox River Sill						
UCLZ	SF-Diss	1-7005	WR	+4.80	-	Eckstrand et al., 1989
UCLZ	SF-Diss	1-7025	WR	+9.20	-	Eckstrand et al., 1989
UCLZ	SF-Diss	1-7037	WR	+8.30	-	Eckstrand et al., 1989
UCLZ	SF-Diss	1-7049	WR	+0.70	-	Eckstrand et al., 1989
UCLZ	SF-Diss	1-7134	WR	+10.70	-	Eckstrand et al., 1989
UCLZ	SF-Diss	1-7164	WR	+10.90	-	Eckstrand et al., 1989
UCLZ	SF-Diss	1-7185	WR	+12.10	-	Eckstrand et al., 1989
UCLZ	SF-Diss	1-7200	WR	+12.30	-	Eckstrand et al., 1989
UCLZ	SF-Diss	1-7215	WR	+11.70	-	Eckstrand et al., 1989
UCLZ	SF-Diss	1-7218	WR	+11.80	-	Eckstrand et al., 1989
UCLZ	SF-Diss	1-7232	WR	+7.90	-	Eckstrand et al., 1989
UCLZ	SF-Diss	1-7247	WR	+9.50	-	Eckstrand et al., 1989
UCLZ	SF-Diss	2-7285	WR	+4.10	-	Eckstrand et al., 1989
UCLZ	SF-Diss	2-7491	WR	+10.10	-	Eckstrand et al., 1989
UCLZ	SF-Diss	2-7500	WR	+8.40	-	Eckstrand et al., 1989
UCLZ	SF-Diss	2-7533	WR	+10.10	-	Eckstrand et al., 1989
UCLZ	SF-Diss	2-7545	WR	+10.50	-	Eckstrand et al., 1989
UCLZ	SF-Diss	2-7554	WR	+9.20	-	Eckstrand et al., 1989
UCLZ	SF-Diss	5-7835	WR	+9.20	-	Eckstrand et al., 1989
UCLZ	SF-Diss	5-7850	WR	+10.10	-	Eckstrand et al., 1989
UCLZ	SF-Diss	5-7906	WR	+6.10	-	Eckstrand et al., 1989
UCLZ	SF-Diss	5-7913	WR	+10.90	-	Eckstrand et al., 1989
UCLZ	SF-Diss	5-7971	WR	+3.90	-	Eckstrand et al., 1989
UCLZ	SF-Diss	5-7972	WR	+3.60	-	Eckstrand et al., 1989
UCLZ	SF-Diss	5-9012	WR	+6.00	-	Eckstrand et al., 1989
UCLZ	SF-Diss	5-9027	WR	+6.50	-	Eckstrand et al., 1989
UCLZ	SF-Diss	5-9028	WR	+8.20	-	Eckstrand et al., 1989
LCLZ	Peridotite	1-7267	WR	+17.40	-	Eckstrand et al., 1989
LCLZ	Peridotite	1-7268	WR	+16.60	-	Eckstrand et al., 1989
LCLZ	Peridotite	2-7281	WR	+17.30	-	Eckstrand et al., 1989
Aguablanca						
Aguablanca	Ore	91	Ccp	+7.43	-	Casquet et al., 1998
Aguablanca	Ore	91	Po	+7.45	-	Casquet et al., 1998
Aguablanca	Ore	92	Po	+7.14	-	Casquet et al., 1998
Aguablanca	Ore	92	Py	+7.23	-	Casquet et al., 1998
Aguablanca	Ore	93	Po	+7.20	-	Casquet et al., 1998
Aguablanca	Ore	93	Ccp	+7.33	-	Casquet et al., 1998
Aguablanca	Ore	94	Po	+7.60	-	Casquet et al., 1998
Aguablanca	Ore	94	Ccp	+7.73	-	Casquet et al., 1998
Aguablanca	Ore	95	Po	+7.11	-	Casquet et al., 1998
Aguablanca	Ore	95	Ccp	+7.24	-	Casquet et al., 1998
Aguablanca	Ore	100	Po	+7.50	-	Casquet et al., 1998
Aguablanca	Ore	100	Ccp	+7.64	-	Casquet et al., 1998
Aguablanca	Ore	101	Po	+7.49	-	Casquet et al., 1998
Aguablanca	Ore	101	Ccp	+7.63	-	Casquet et al., 1998
Aguablanca	Ore	102	Po	+7.50	-	Casquet et al., 1998
Aguablanca	Ore	102	Ccp	+7.18	-	Casquet et al., 1998
Aguablanca	Ore	102	Pn	+7.38	-	Casquet et al., 1998
Aguablanca	Ore	103	Po	+7.49	-	Casquet et al., 1998

Deposit	Rocktype/ore	Sample	Target	$\delta^{34}S$	stdev	references
Aguablanca	Ore	104	Po	+7.75	-	Casquet et al., 1998
Voisey's Bay						
Ovoïd	SF-MS	VB-10-18	Po	-1.40	-	Ripley et al., 1999
Ovoïd	SF-MS	VB-10-18	Pn	+0.00	-	Ripley et al., 1999
Ovoïd	SF-MS	VB-10-18	Ccp	-1.50	-	Ripley et al., 1999
Ovoïd	SF-MS	VB-10-38	Ccp	-1.50	-	Ripley et al., 1999
Ovoïd	SF-MS	VB-10-38	Po-Pn	-1.50	-	Ripley et al., 1999
Ovoïd	SF-MS	VB-10-58	Pn	-1.70	-	Ripley et al., 1999
Ovoïd	SF-MS	VB-10-58	Ccp	-1.70	-	Ripley et al., 1999
Ovoïd	SF-MS	VB-10-58	Po	-1.40	-	Ripley et al., 1999
Ovoïd	SF-MS	VB-10-75	Po	-1.90	-	Ripley et al., 1999
Ovoïd	SF-MS	VB-10-75	Pn	-1.90	-	Ripley et al., 1999
Ovoïd	SF-MS	VB-10-75	Ccp	-1.80	-	Ripley et al., 1999
Ovoïd	SF-MS	VB-10-90	Po	-1.80	-	Ripley et al., 1999
Ovoïd	SF-MS	VB-10-90	Pn-Ccp	-2.10	-	Ripley et al., 1999
Ovoïd	SF-MS	VB-10-110	Pn	-1.30	-	Ripley et al., 1999
Ovoïd	SF-MS	VB-10-110	Ccp	-1.50	-	Ripley et al., 1999
Ovoïd	SF-MS	VB-10-110	Po	-1.60	-	Ripley et al., 1999
Ovoïd	SF-MS	VB-10-126	Ccp	-1.40	-	Ripley et al., 1999
Ovoïd	SF-MS	VB-10-126	Po	-1.40	-	Ripley et al., 1999
Tasiuyak Gneiss	Country rock	TG-1	WR/Po	-17.00	-	Ripley et al., 2002
Tasiuyak Gneiss	Country rock	TG-2	WR/Po	-7.40	-	Ripley et al., 2002
Tasiuyak Gneiss	Country rock	TG-3	WR/Po	-6.50	-	Ripley et al., 2002
Tasiuyak Gneiss	Country rock	TG-4	WR/Po	-2.30	-	Ripley et al., 2002
Tasiuyak Gneiss	Country rock	TG-5	WR/Po	-1.30	-	Ripley et al., 2002
Tasiuyak Gneiss	Country rock	TG-6	WR/Po	-3.30	-	Ripley et al., 2002
Tasiuyak Gneiss	Country rock	TG-7	WR/Po	-2.40	-	Ripley et al., 2002
Tasiuyak Gneiss	Country rock	TG-8	WR/Po	-4.10	-	Ripley et al., 2002
Tasiuyak Gneiss	Country rock	TG-9	WR/Po	-4.40	-	Ripley et al., 2002
Tasiuyak Gneiss	Country rock	VB192/293.0	WR/Po	+15.30	-	Ripley et al., 2002
Tasiuyak Gneiss	Country rock	VB192/296.3	WR/Po	+7.40	-	Ripley et al., 2002
Tasiuyak Gneiss	Country rock	VB192/331	WR/Po	-16.30	-	Ripley et al., 2002
Tasiuyak Gneiss	Country rock	VB192/349.8	WR/Po	-14.10	-	Ripley et al., 2002
Tasiuyak Gneiss	Country rock	VB192/350.0	WR/Po	-17.00	-	Ripley et al., 2002
Tasiuyak Gneiss	Country rock	VB192/351	WR/Po	-11.30	-	Ripley et al., 2002
Tasiuyak Gneiss	Country rock	VB192/357.5	WR/Po	-6.50	-	Ripley et al., 2002
Tasiuyak Gneiss	Country rock	VB433/97	WR/Po	+5.40	-	Ripley et al., 2002
Tasiuyak Gneiss	Country rock	VB433/98.5	WR/Po	+14.60	-	Ripley et al., 2002
Tasiuyak Gneiss	Country rock	VB433/100.6	WR/Po	+6.60	-	Ripley et al., 2002
Tasiuyak Gneiss	Country rock	VB433/107	WR/Po	+18.30	-	Ripley et al., 2002
Tasiuyak Gneiss	Country rock	VB433/108.5	WR/Po	+4.50	-	Ripley et al., 2002
Tasiuyak Gneiss	Country rock	VB433/109	WR/Po	+8.70	-	Ripley et al., 2002
Tasiuyak Gneiss	Country rock	VB433/110.5	WR/Po	-4.20	-	Ripley et al., 2002
Tasiuyak Gneiss	Country rock	VB433/112	WR/Po	-0.40	-	Ripley et al., 2002
Tasiuyak Gneiss	Country rock	VB433/113.2	WR/Po	+1.70	-	Ripley et al., 2002
Tasiuyak Gneiss	Country rock	VB433/115	WR/Po	-4.70	-	Ripley et al., 2002
Tasiuyak Gneiss	Country rock	VB433/116	WR/Po	+4.30	-	Ripley et al., 2002
Tasiuyak Gneiss	Country rock	VB433/117.5	WR/Po	-3.20	-	Ripley et al., 2002
Tasiuyak Gneiss	Country rock	VB433/118	WR/Po	-2.60	-	Ripley et al., 2002
Tasiuyak Gneiss	Country rock	VB433/119.5	WR/Po	+8.60	-	Ripley et al., 2002
Tasiuyak Gneiss	Country rock	VB433/121	WR/Po	+4.00	-	Ripley et al., 2002
Tasiuyak Gneiss	Country rock	VB433/122	WR/Po	+7.00	-	Ripley et al., 2002
Tasiuyak Gneiss	Country rock	VB433/124.5	WR/Po	+4.50	-	Ripley et al., 2002
Tasiuyak Gneiss	Country rock	VB433/152	WR/Po	-2.60	-	Ripley et al., 2002
Tasiuyak Gneiss	Country rock	VB433/157	WR/Po	-2.20	-	Ripley et al., 2002
Tasiuyak Gneiss	Country rock	VB433/173.5	WR/Po	-6.60	-	Ripley et al., 2002
Tasiuyak Gneiss	Country rock	VB433/188	WR/Po	+3.50	-	Ripley et al., 2002
Tasiuyak Gneiss	Country rock	VB487/99.5	WR/Po	+1.00	-	Ripley et al., 2002
Tasiuyak Gneiss	Country rock	VB487/100.4	WR/Po	+0.40	-	Ripley et al., 2002
Tasiuyak Gneiss	Country rock	VB487/101	WR/Po	+7.50	-	Ripley et al., 2002
Tasiuyak Gneiss	Country rock	VB487/101.5	WR/Po	+1.50	-	Ripley et al., 2002

Deposit	Rocktype/ore	Sample	Target	$\delta^{34}S$	stdev	references
Tasiuyak Gneiss	Country rock	VB487/102.7	WR/Po	+5.00	-	Ripley et al., 2002
Tasiuyak Gneiss	Country rock	VB487/103.3	WR/Po	-1.10	-	Ripley et al., 2002
Tasiuyak Gneiss	Country rock	VB487/160.5	WR/Po	-4.70	-	Ripley et al., 2002
Tasiuyak Gneiss	Country rock	VB487/316.0	WR/Po	-4.50	-	Ripley et al., 2002
Tasiuyak Gneiss	Country rock	VB487/348.5	WR/Po	-7.70	-	Ripley et al., 2002
Tasiuyak Gneiss	Country rock	VB487/407.5	WR/Po	-6.00	-	Ripley et al., 2002
Tasiuyak Gneiss	Country rock	VB487/459	WR/Po	-6.20	-	Ripley et al., 2002
Tasiuyak Gneiss	Country rock	VB487/550	WR/Po	-7.20	-	Ripley et al., 2002
Tasiuyak Gneiss	Country rock	VB487/581.5	WR/Po	-5.20	-	Ripley et al., 2002
Tasiuyak Gneiss	Country rock	VB487/605.4	WR/Po	-6.50	-	Ripley et al., 2002
Tasiuyak Gneiss	Country rock	VB487/628.7	WR/Po	-6.20	-	Ripley et al., 2002
Lac Volant						
Lac Volant	SF-MS	Tc-294	WR	+1.40	-	Nabil et al., 2004
Lac Volant	SF-MS	SM-d8-9	WR	+1.30	-	Nabil et al., 2004
Lac Volant	SF-MS	Sm-C3-4	WR	+1.20	-	Nabil et al., 2004
Lac Volant	SF-MS	Sm-E	WR	+1.30	-	Nabil et al., 2004
Lac Volant	SF-MS	Sm-G	WR	+1.40	-	Nabil et al., 2004
Lac Volant	SF-MS	Sm-A1-3	WR	+1.50	-	Nabil et al., 2004
Lac Volant	SF-MS	SM-A3-4	WR	+1.40	-	Nabil et al., 2004
Lac Volant	Vein	Tc-291	WR	+1.40	-	Nabil et al., 2004
Lac Volant	SF-Mtr	Tc-168-a	WR	+1.00	-	Nabil et al., 2004
Lac Volant	SF-Mtr	Tc-168-b	WR	+1.00	-	Nabil et al., 2004
Lac Volant	SF-Mtr	Tc-315	WR	+1.70	-	Nabil et al., 2004
Lac Volant	SF-Diss	Tc-318	WR	+1.00	-	Nabil et al., 2004
Lac Volant	SF-Diss	Tc-306	WR	+1.80	-	Nabil et al., 2004
Paragneiss	Country rock	-	WR	+3.20	-	Nabil et al., 2004
Portneuf-Mauricie						
Réservoir Blanc	Gabbronorite	AS-04-470B	WR	+2.20	-	Sappin et al., 2011
Lac Matte	Orthopyroxenite	AS-04-431A	WR	+1.80	-	Sappin et al., 2011
Lac Matte	Gabbronorite	AS-04-431C	WR	+1.40	-	Sappin et al., 2011
Lac Matte	Websterite	AS-04-431D	WR	+1.20	-	Sappin et al., 2011
Lac Matte	Websterite	AS-05-608A	WR	-	-	Sappin et al., 2011
Lac Kennedy	Harzburgite	AS-04-483A	WR	-	-	Sappin et al., 2011
Lac Kennedy	Gabbronorite	AS-04-516A2	WR	+1.90	-	Sappin et al., 2011
Lac Kennedy	Gabbronorite	AS-04-534B	WR	+0.16	-	Sappin et al., 2011
Lac Edouard	Orthopyroxenite	Bloc Edouard 1	WR	+2.40	-	Sappin et al., 2011
Lac Edouard	Gabbronorite	LE-40	WR	-	-	Sappin et al., 2011
Lac Edouard	Websterite	LE-41	WR	+0.48	-	Sappin et al., 2011
Lac Edouard	Harzburgite	LE-44	WR	-	-	Sappin et al., 2011
Boivin	Gabbronorite	AS-04-538A	WR	+2.00	-	Sappin et al., 2011
Rochette West	Websterite	AS-04-447A1	WR	+2.90	-	Sappin et al., 2011
Rochette West	Gabbronorite	AS-04-447B	WR	-	-	Sappin et al., 2011
Rousseau	Orthopyroxenite	AS-03-317A	WR	+0.60	-	Sappin et al., 2011
Rousseau	Websterite	AS-05-681A2	WR	-2.60	-	Sappin et al., 2011
Rousseau	Orthopyroxenite	AS-05-766B	WR	-1.10	-	Sappin et al., 2011
Rousseau	Orthopyroxenite	LV-30	WR	+1.00	-	Sappin et al., 2011
Lac Nadeau	Gabbronorite	AS-03-99A	WR	+0.70	-	Sappin et al., 2011
Lac Nadeau	Gabbronorite	AS-03-101A	WR	+0.90	-	Sappin et al., 2011
Lac Nadeau	Gabbronorite	MC-03-1000	WR	+1.10	-	Sappin et al., 2011
Lac Nadeau	Lherzolite	TC-03-2016A	WR	-2.90	-	Sappin et al., 2011
Lac Nadeau	Lherzolite	TC-03-2029A	WR	+0.50	-	Sappin et al., 2011
Vammala						
Deep Ore	SF-Diss	average	Sulfides	-0.90	0.95	Peltonen, 1995
Sokta Ore	SF-Diss	average	Sulfides	-1.00	0.66	Peltonen, 1995
Veins	SF-Diss	average	Sulfides	+0.30	0.85	Peltonen, 1995
Svecofennian Formation	Schist	average	Sulfides	+0.70	3.65	Peltonen, 1995
Kambalda						
Kambalda	All ores	average	-	+2.50	1.50	Groves et al., 1979
Mt Keith						
Mt Keith	All ores	average (n = 2)	-	-2.30	0.00	Donnelly et al., 1978

Deposit	Rocktype/ore	Sample	Target	$\delta^{34}S$	stdev	references
Langmuir						
Langmuir	All ores	average (n = 17)	WR	+0.00	2.20	Green and Naldrett, 1981
Country rock	Iron Formation	average (n = 5)	WR	-4.81	2.35	Green and Naldrett, 1981
Thompson						
Thompson	All ores	average	-	+4.25	1.75	Bleeker, 1990
Méquillon (Cape Smith Belt)						
Dyke	SF-Diss	CT-65-i	Sulfides	+4.00	-	Tremblay, 1990
Dyke	SF-Diss	CT-04-i	Sulfides	+5.10	-	Tremblay, 1990
Dyke	SF-Diss	CT-99-i	Sulfides	+4.10	-	Tremblay, 1990
Dyke	SF-Diss	CT-18-i	Sulfides	+4.70	-	Tremblay, 1990
Dyke	SF-Diss	CT-36-i	Sulfides	+4.70	-	Tremblay, 1990
Country rock	Sediment	CT-61-s	Sulfides	+0.80	-	Tremblay, 1990
Country rock	Sediment	CT-173-s	Sulfides	+0.20	-	Tremblay, 1990
Country rock	Sediment	CT-24-s	Sulfides	+3.00	-	Tremblay, 1990
Raglan (Cape Smith Belt)						
Raglan	All ores	average	-	+4.50	1.50	Lesher et al., 1999a
Pechenga						
Flows (West Ore)	SF-MS	average (n = 13)	-	+0.00	-	Barnes et al., 2001b
Flows (West Ore)	SF-Diss	average (n = 16)	-	-0.30	-	Barnes et al., 2001b
Flows (West Ore)	SF-Breccia	average (n = 16)	-	+0.00	-	Barnes et al., 2001b
Country rocks	Black schists	average (n = 4)	-	-1.25	-	Barnes et al., 2001b
Intrusions (East Ore)	SF-MS	average (n = 4)	-	+4.05	-	Barnes et al., 2001b
Intrusions (East Ore)	SF-Diss	average (n = 3)	-	+5.40	-	Barnes et al., 2001b
Intrusions (East Ore)	SF-Breccia	average (n = 2)	-	+3.55	-	Barnes et al., 2001b
Intrusions (East Ore)	Veins	average (n = 1)	-	+4.00	-	Barnes et al., 2001b
Country rocks	Black schists	average (n = 1)	-	+11.07	-	Barnes et al., 2001b
Drillhole 2905	Synsed/Early layer	23a	Py	-1.10	-	Melezhik et al., 1998
Drillhole 2905	Synsed/Early layer	23b	Py	-1.20	-	Melezhik et al., 1998
Drillhole 2905	Synsed/Early layer	23c	Py	-2.50	-	Melezhik et al., 1998
Drillhole 2905	Synsed/Early layer	23d	Py	-1.90	-	Melezhik et al., 1998
Drillhole 2905	Synsed/Early layer	23e	Py	-0.90	-	Melezhik et al., 1998
Drillhole 2905	Synsed/Early layer	23g	Py	-2.20	-	Melezhik et al., 1998
Drillhole 2905	Synsed/Early layer	23h	Py	-1.80	-	Melezhik et al., 1998
Drillhole 2905	Synsed/Early layer	24a	Py	+0.30	-	Melezhik et al., 1998
Drillhole 2905	Synsed/Early layer	24b	Py	-0.50	-	Melezhik et al., 1998
Drillhole 2905	Synsed/Early layer	24c	Py	-0.50	-	Melezhik et al., 1998
Drillhole 2905	Synsed/Early layer	24d	Py	-1.10	-	Melezhik et al., 1998
Zhdanovsky	Early diagenetic	1a	Py	-2.10	-	Melezhik et al., 1998
Zhdanovsky	Early diagenetic	1b	Py	-1.40	-	Melezhik et al., 1998
Zhdanovsky	Early diagenetic	2a	Py	-0.60	-	Melezhik et al., 1998
Zhdanovsky	Early diagenetic	2b	Py	-0.60	-	Melezhik et al., 1998
Zhdanovsky	Early diagenetic	2c	Py	-0.50	-	Melezhik et al., 1998
Zhdanovsky	Early diagenetic	3a	Py	-1.30	-	Melezhik et al., 1998
Zhdanovsky	Early diagenetic	3b	Po	-1.30	-	Melezhik et al., 1998
Zhdanovsky	Early diagenetic	45a	Py	-1.40	-	Melezhik et al., 1998
Zhdanovsky	Early diagenetic	46a	Py	-0.90	-	Melezhik et al., 1998
Zhdanovsky	Early diagenetic	46b	Py	-0.90	-	Melezhik et al., 1998
Zhdanovsky	Early diagenetic	46c	Py	-0.80	-	Melezhik et al., 1998
Zhdanovsky	Early diagenetic	46d	Py	-1.10	-	Melezhik et al., 1998
Zhdanovsky	Early diagenetic	46e	Po	-0.30	-	Melezhik et al., 1998
Zhdanovsky	Early diagenetic	47a	Py	-2.10	-	Melezhik et al., 1998
Zhdanovsky	Early diagenetic	47b	Py	-2.10	-	Melezhik et al., 1998
Zhdanovsky	Early diagenetic	47c	Py	-1.00	-	Melezhik et al., 1998
Zhdanovsky	Early diagenetic	47d	Py	-1.90	-	Melezhik et al., 1998
Zhdanovsky	Early diagenetic	4	Py	-0.80	-	Melezhik et al., 1998
Zhdanovsky	Early diagenetic	6b	Py	-0.80	-	Melezhik et al., 1998
Zhdanovsky	Early diagenetic	7a	Po	-2.10	-	Melezhik et al., 1998
Zhdanovsky	Early diagenetic	7b	Py	-1.60	-	Melezhik et al., 1998
Zhdanovsky	Early diagenetic	8a	Py	-1.90	-	Melezhik et al., 1998
Zhdanovsky	Early diagenetic	8c	Py	-0.90	-	Melezhik et al., 1998

Deposit	Rocktype/ore	Sample	Target	$\delta^{34}S$	stdev	references
Zhdanovsky	Early diagenetic	9a	Po	-1.00	-	Melezhik et al., 1998
Zhdanovsky	Early diagenetic	9b	Py	-1.00	-	Melezhik et al., 1998
Zhdanovsky	Early diagenetic	40	Py	-1.90	-	Melezhik et al., 1998
Zhdanovsky	Early diagenetic	41a	Py	-1.40	-	Melezhik et al., 1998
Zhdanovsky	Early diagenetic	41b	Py	-1.00	-	Melezhik et al., 1998
Zhdanovsky	Early diagenetic	41c	Py	-1.90	-	Melezhik et al., 1998
Zhdanovsky	Early diagenetic	43	Py	-0.30	-	Melezhik et al., 1998
Zhdanovsky	Early diagenetic	44a	Py	-0.80	-	Melezhik et al., 1998
Zhdanovsky	Early diagenetic	44b	Py	-2.70	-	Melezhik et al., 1998
Zhdanovsky	Early diagenetic	44d	Py	-1.60	-	Melezhik et al., 1998
Zhdanovsky	Early diagenetic	44e	Py	-0.40	-	Melezhik et al., 1998
Zhdanovsky	Early diagenetic	13a	Po–Py	+3.80	-	Melezhik et al., 1998
Zhdanovsky	Early diagenetic	13b	Po–Py	+2.20	-	Melezhik et al., 1998
Zhdanovsky	Early diagenetic	13c	Po–Py	+2.60	-	Melezhik et al., 1998
Zhdanovsky	Early diagenetic	13d	Po–Py	+2.00	-	Melezhik et al., 1998
Zhdanovsky	Early diagenetic	14a	Po–Py	+2.90	-	Melezhik et al., 1998
Zhdanovsky	Early diagenetic	14b	Po–Py	+2.30	-	Melezhik et al., 1998
Zhdanovsky	Early diagenetic	14c	Po–Py	+2.50	-	Melezhik et al., 1998
Zhdanovsky	Early diagenetic	14d	Po	+1.60	-	Melezhik et al., 1998
Zhdanovsky	Early diagenetic	14e	Po	+2.50	-	Melezhik et al., 1998
Zhdanovsky	Early diagenetic	14f	Po	+2.50	-	Melezhik et al., 1998
Zhdanovsky	Early diagenetic	15a	Po–Py	+2.70	-	Melezhik et al., 1998
Zhdanovsky	Early diagenetic	15b	Po–Py	+3.10	-	Melezhik et al., 1998
Zhdanovsky	Early diagenetic	15c	Po	+2.10	-	Melezhik et al., 1998
Zhdanovsky	Early diagenetic	16a	Po–Py	+2.20	-	Melezhik et al., 1998
Zhdanovsky	Early diagenetic	16b	Po–Py	+3.00	-	Melezhik et al., 1998
Zhdanovsky	Early diagenetic	16c	Po–Py	+2.50	-	Melezhik et al., 1998
Zhdanovsky	Early diagenetic	16d	Po	+1.00	-	Melezhik et al., 1998
Zhdanovsky	Early diagenetic	16e	Po–Py	+3.10	-	Melezhik et al., 1998
Zhdanovsky	Early diagenetic	16f	Po	+2.70	-	Melezhik et al., 1998
Zhdanovsky	Early diagenetic	16g	Po–Py	+2.50	-	Melezhik et al., 1998
Zhdanovsky	Early diagenetic	16h	Po–Py	+2.50	-	Melezhik et al., 1998
Zhdanovsky	Early diagenetic	16i	Po	+2.60	-	Melezhik et al., 1998
Zhdanovsky	Early diagenetic	16j	Po–Py	+2.40	-	Melezhik et al., 1998
Zhdanovsky	Early diagenetic	17a	Po–Py	+2.70	-	Melezhik et al., 1998
Zhdanovsky	Early diagenetic	17b	Po–Py	+2.60	-	Melezhik et al., 1998
Zhdanovsky	Early diagenetic	17c	Po–Py	+2.70	-	Melezhik et al., 1998
Zhdanovsky	Early diagenetic	17d	Po–Py	+2.00	-	Melezhik et al., 1998
Zhdanovsky	Early diagenetic	18a	Po–Py	+2.40	-	Melezhik et al., 1998
Zhdanovsky	Early diagenetic	18b	Po–Py	+2.40	-	Melezhik et al., 1998
Zhdanovsky	Early diagenetic	18c	Po–Py	+2.30	-	Melezhik et al., 1998
Zhdanovsky	Early diagenetic	18d	Po	+1.30	-	Melezhik et al., 1998
Zhdanovsky	Early diagenetic	19b	Po–Py	+2.40	-	Melezhik et al., 1998
Zhdanovsky	Early diagenetic	19c	Po–Py	+2.60	-	Melezhik et al., 1998
Zhdanovsky	Early diagenetic	22a	Po–Py	+2.70	-	Melezhik et al., 1998
Zhdanovsky	Early diagenetic	22b	Po–Py	+2.50	-	Melezhik et al., 1998
Zhdanovsky	Early diagenetic	22c	Po–Py	+2.10	-	Melezhik et al., 1998
Zhdanovsky	Early diagenetic	22d	Po	+2.00	-	Melezhik et al., 1998
Zhdanovsky	Early diagenetic	48a	Po–Py	+2.00	-	Melezhik et al., 1998
Zhdanovsky	Early diagenetic	48b	Po–Py	+1.00	-	Melezhik et al., 1998
Zhdanovsky	Early diagenetic	48c	Po–Py	+3.20	-	Melezhik et al., 1998
Zhdanovsky	Early diagenetic	48d	Po	+2.50	-	Melezhik et al., 1998
Zhdanovsky	Early diagenetic	48e	Po	+2.40	-	Melezhik et al., 1998
Zhdanovsky	Mudstones	20a	Po	+1.90	-	Melezhik et al., 1998
Zhdanovsky	Mudstones	20b	Po	+1.70	-	Melezhik et al., 1998
Zhdanovsky	Mudstones	21	Po	+2.30	-	Melezhik et al., 1998
Drillhole 2794	Early diagenetic	10a	Po	-3.40	-	Melezhik et al., 1998
Drillhole 2794	Early diagenetic	10b	Po	-2.50	-	Melezhik et al., 1998
Drillhole 2794	Early diagenetic	10c	Po	-3.90	-	Melezhik et al., 1998
Drillhole 2794	Early diagenetic	10d	Py	-5.60	-	Melezhik et al., 1998
Drillhole 2794	Early diagenetic	10e	Py	-7.40	-	Melezhik et al., 1998

Deposit	Rocktype/ore	Sample	Target	$\delta^{34}S$	stdev	references
Drillhole 2700	Early diagenetic	60a	Py	-2.40	-	Melezhik et al., 1998
Drillhole 2700	Early diagenetic	60b	Py	-4.10	-	Melezhik et al., 1998
Drillhole 2700	Early diagenetic	60c	Py	-1.00	-	Melezhik et al., 1998
Drillhole 2700	Early diagenetic	60d	Py	+9.60	-	Melezhik et al., 1998
Drillhole 2700	Early diagenetic	60e	Py	+11.80	-	Melezhik et al., 1998
Drillhole 2700	Early diagenetic	60f	Py	+12.40	-	Melezhik et al., 1998
Drillhole 2700	Early diagenetic	60g	Py	+0.00	-	Melezhik et al., 1998
Drillhole 2700	Early diagenetic	60h	Py	+0.00	-	Melezhik et al., 1998
Drillhole 2700	Early diagenetic	60i	Py	-3.10	-	Melezhik et al., 1998
Drillhole 2700	Early diagenetic	60j	Py	+2.00	-	Melezhik et al., 1998
Drillhole 2700	Early diagenetic	60k	Py	+2.60	-	Melezhik et al., 1998
Drillhole 2700	Early diagenetic	60l	Py	-5.70	-	Melezhik et al., 1998
Drillhole 2700	Early diagenetic	61a	Py	-8.30	-	Melezhik et al., 1998
Drillhole 2700	Early diagenetic	61b	Py	-2.30	-	Melezhik et al., 1998
Drillhole 2700	Early diagenetic	61c	Py	-3.20	-	Melezhik et al., 1998
Drillhole 2700	Early diagenetic	61d	Py	-2.50	-	Melezhik et al., 1998
Drillhole 2700	Early diagenetic	61e	Py	-4.10	-	Melezhik et al., 1998
Drillhole 2700	Early diagenetic	61f	Py	-3.10	-	Melezhik et al., 1998
Drillhole 2700	Early diagenetic	61g	Py	+2.40	-	Melezhik et al., 1998
Drillhole 2700	Early diagenetic	61h	Py	+12.80	-	Melezhik et al., 1998
Drillhole 2700	Early diagenetic	62a	Py	-1.40	-	Melezhik et al., 1998
Drillhole 2700	Early diagenetic	62b	Py	-5.50	-	Melezhik et al., 1998
Drillhole 2700	Early diagenetic	62c	Py	-3.20	-	Melezhik et al., 1998
Drillhole 2700	Early diagenetic	62d	Py	-1.80	-	Melezhik et al., 1998
Drillhole 2700	Early diagenetic	62e	Py	-3.10	-	Melezhik et al., 1998
Drillhole 2900	Mid-diagenetic	535-1c	Po	+6.20	-	Melezhik et al., 1998
Drillhole 2900	Mid-diagenetic	535-2c	Po	+8.20	-	Melezhik et al., 1998
Drillhole 2900	Mid-diagenetic	535-1	Po	+7.10	-	Melezhik et al., 1998
Drillhole 2900	Mid-diagenetic	535-2	Po	+6.50	-	Melezhik et al., 1998
Drillhole 2900	Mid-diagenetic	535-3	Po	+6.70	-	Melezhik et al., 1998
Drillhole 2900	Mid-diagenetic	535-4	Po	+3.30	-	Melezhik et al., 1998
Drillhole 2900	Mid-diagenetic	535-5	Po	+7.80	-	Melezhik et al., 1998
Drillhole 2900	Mid-diagenetic	535-6	Po	+7.70	-	Melezhik et al., 1998
Drillhole 2900	Mid-diagenetic	535-7	Po	+7.30	-	Melezhik et al., 1998
Drillhole 2900	Mid-diagenetic	535-8	Po	+3.80	-	Melezhik et al., 1998
Drillhole 2900	Mid-diagenetic	539-9	Po	+7.90	-	Melezhik et al., 1998
Drillhole 2900	Mid-diagenetic	535-10	Po	+7.90	-	Melezhik et al., 1998
Drillhole 2900	Mid-diagenetic	535-11	Po	+5.70	-	Melezhik et al., 1998
Drillhole 2900	Mid-diagenetic	535-12	Po	+3.90	-	Melezhik et al., 1998
Drillhole 2900	Mid-diagenetic	535-13	Po	+4.30	-	Melezhik et al., 1998
Drillhole 2900	Mid-diagenetic	535-14	Po	+6.60	-	Melezhik et al., 1998
Drillhole 2900	Mid-diagenetic	535-15	Po	+5.70	-	Melezhik et al., 1998
Drillhole 2900	Mid-diagenetic	535-16	Po	+6.50	-	Melezhik et al., 1998
Drillhole 2900	Mid-diagenetic	535-17	Po	+3.80	-	Melezhik et al., 1998
Drillhole 2900	Mid-diagenetic	535-18	Po	+7.00	-	Melezhik et al., 1998
Drillhole 2900	Mid-diagenetic	535-19	Po	+7.10	-	Melezhik et al., 1998
Drillhole 2900	Mid-diagenetic	535-20	Po	+3.70	-	Melezhik et al., 1998
Drillhole 2900	Mid-diagenetic	535-21	Po	+6.80	-	Melezhik et al., 1998
Drillhole 2900	Mid-diagenetic	535-22	Po	+5.40	-	Melezhik et al., 1998
Drillhole 2900	Mid-diagenetic	535-23	Po	+0.90	-	Melezhik et al., 1998
Drillhole 2900	Mid-diagenetic	535-24	Po	+7.00	-	Melezhik et al., 1998
Drillhole 2900	Mid-diagenetic	535-25	Po	+6.90	-	Melezhik et al., 1998
Drillhole 2900	Mid-diagenetic	535-26	Po	+6.30	-	Melezhik et al., 1998
Drillhole 2900	Mid-diagenetic	535-27	Po	+6.30	-	Melezhik et al., 1998
Drillhole 2900	Mid-diagenetic	535-28	Po	+2.10	-	Melezhik et al., 1998
Drillhole 2900	Mid-diagenetic	535-29	Po	+7.50	-	Melezhik et al., 1998
Drillhole 2900	Mid-diagenetic	535-1	Po	+7.50	-	Melezhik et al., 1998
Drillhole 2900	Mid-diagenetic	535-2	Po	+7.30	-	Melezhik et al., 1998
Drillhole 2900	Mid-diagenetic	535-3	Po	+6.60	-	Melezhik et al., 1998
Drillhole 2900	Mid-diagenetic	535-5	Po	+5.70	-	Melezhik et al., 1998
Drillhole 2900	Mid-diagenetic	535-6	Po	+6.30	-	Melezhik et al., 1998

Deposit	Rocktype/ore	Sample	Target	$\delta^{34}S$	stdev	references
Drillhole 2900	Mid-diagenetic	535-7	Po	+7.20	-	Melezhik et al., 1998
Raysoaivi	Late diagenetic	11a	Po	+8.30	-	Melezhik et al., 1998
Raysoaivi	Late diagenetic	11b	Po	+7.30	-	Melezhik et al., 1998
Raysoaivi	Late diagenetic	11c	Po	+9.10	-	Melezhik et al., 1998
Raysoaivi	Late diagenetic	11d	Po	+7.70	-	Melezhik et al., 1998
Raysoaivi	Late diagenetic	11e	Po	+9.30	-	Melezhik et al., 1998
Drillhole 2794	Late diagenetic	33a	Po–Py	+9.30	-	Melezhik et al., 1998
Drillhole 2794	Late diagenetic	33b	Po–Py	+9.20	-	Melezhik et al., 1998
Drillhole 2794	Late diagenetic	33c	Po–Py	+10.80	-	Melezhik et al., 1998
Drillhole 2794	Late diagenetic	33d	Po–Py	+8.90	-	Melezhik et al., 1998
Drillhole 2794	Late diagenetic	33e	Po–Py	+13.80	-	Melezhik et al., 1998
Drillhole 2794	Late diagenetic	33f	Po–Py	+9.00	-	Melezhik et al., 1998
Drillhole 2794	Late diagenetic	33g	Po–Py	+8.50	-	Melezhik et al., 1998
Drillhole 2794	Late diagenetic	33j	Po–Py	+7.80	-	Melezhik et al., 1998
Drillhole 2794	Late diagenetic	33k	Po–Py	+9.30	-	Melezhik et al., 1998
Drillhole 2400	Late diagenetic	50a	Py	+8.90	-	Melezhik et al., 1998
Drillhole 2400	Late diagenetic	50b	Py	+5.80	-	Melezhik et al., 1998
Drillhole 2400	Late diagenetic	50c	Py	+12.40	-	Melezhik et al., 1998
Drillhole 2400	Late diagenetic	50d	Py	+8.10	-	Melezhik et al., 1998
Drillhole 2400	Late diagenetic	50e	Py	+9.30	-	Melezhik et al., 1998
Drillhole 2400	Late diagenetic	51a	Py	+9.30	-	Melezhik et al., 1998
Drillhole 2400	Late diagenetic	51b	Py	+7.20	-	Melezhik et al., 1998
Drillhole 2400	Late diagenetic	51c	Py	+10.30	-	Melezhik et al., 1998
Drillhole 2400	Late diagenetic	51d	Py	+7.70	-	Melezhik et al., 1998
Drillhole 2400	Late diagenetic	51e	Py	+8.80	-	Melezhik et al., 1998
Kotselvaara	Late diagenetic	34a	Py	+12.40	-	Melezhik et al., 1998
Kotselvaara	Late diagenetic	34c	Py	+23.80	-	Melezhik et al., 1998
Kotselvaara	Late diagenetic	34d	Po	+8.40	-	Melezhik et al., 1998
Kotselvaara	Late diagenetic	35a	Po	+7.10	-	Melezhik et al., 1998
Kotselvaara	Late diagenetic	35c	Po	+8.30	-	Melezhik et al., 1998
Kotselvaara	Late diagenetic	35g	Po	+7.40	-	Melezhik et al., 1998
Kotselvaara	Late diagenetic	35h	Po	+7.60	-	Melezhik et al., 1998
Kotselvaara	Late diagenetic	35i	Po	+8.20	-	Melezhik et al., 1998
Kotselvaara	Late diagenetic	35k	Po	+8.00	-	Melezhik et al., 1998
Kotselvaara	Late diagenetic	35l	Po	+8.50	-	Melezhik et al., 1998
Kotselvaara	Late diagenetic	35m	Po	+7.90	-	Melezhik et al., 1998
Kotselvaara	Late diagenetic	35n	Po	+7.50	-	Melezhik et al., 1998
Kotselvaara	Late diagenetic	36a	Po	+8.70	-	Melezhik et al., 1998
Kotselvaara	Late diagenetic	36b	Po	+8.10	-	Melezhik et al., 1998
Kotselvaara	Late diagenetic	36c	Po	+8.60	-	Melezhik et al., 1998
Kotselvaara	Late diagenetic	36d	Po	+8.90	-	Melezhik et al., 1998
Kotselvaara	Late diagenetic	36e	Po	+8.80	-	Melezhik et al., 1998
Kotselvaara	Late diagenetic	36f	Po	+8.40	-	Melezhik et al., 1998
Kotselvaara	Late diagenetic	36g	Po	+8.30	-	Melezhik et al., 1998
Kotselvaara	Late diagenetic	36h	Po	+8.10	-	Melezhik et al., 1998
Kotselvaara	Late diagenetic	36i	Po	+8.60	-	Melezhik et al., 1998
Kotselvaara	Late diagenetic	36j	Po	+7.60	-	Melezhik et al., 1998
Kotselvaara	Late diagenetic	36k	Po	+7.80	-	Melezhik et al., 1998
Kotselvaara	Late diagenetic	36l	Po	+9.40	-	Melezhik et al., 1998
Kotselvaara	Late diagenetic	36m	Po	+8.10	-	Melezhik et al., 1998
Kotselvaara	Late diagenetic	36n	Po	+8.70	-	Melezhik et al., 1998
Kotselvaara	Late diagenetic	36o	Po	+8.40	-	Melezhik et al., 1998
Kotselvaara	Late diagenetic	36p	Po	+8.90	-	Melezhik et al., 1998
Kotselvaara	Late diagenetic	36q	Po	+7.40	-	Melezhik et al., 1998
Kotselvaara	Late diagenetic	37a	Po	+8.00	-	Melezhik et al., 1998
Kotselvaara	Late diagenetic	37b	Po	+8.80	-	Melezhik et al., 1998
Kotselvaara	Late diagenetic	37c	Po	+7.80	-	Melezhik et al., 1998
Kotselvaara	Late diagenetic	37d	Po	+8.20	-	Melezhik et al., 1998
Kotselvaara	Late diagenetic	37e	Po	+7.40	-	Melezhik et al., 1998
Kotselvaara	Late diagenetic	37f	Po	+7.80	-	Melezhik et al., 1998
Kotselvaara	Late diagenetic	37g	Po	+7.90	-	Melezhik et al., 1998

Deposit	Rocktype/ore	Sample	Target	$\delta^{34}S$	stdev	references
Kotselvaara	Late diagenetic	37h	Po	+8.40	-	Melezhik et al., 1998
Kotselvaara	Late diagenetic	37i	Po	+7.40	-	Melezhik et al., 1998
Kotselvaara	Late diagenetic	37k	Po	+8.00	-	Melezhik et al., 1998
Kotselvaara	Late diagenetic	37l	Po	+9.30	-	Melezhik et al., 1998
Kotselvaara	Late diagenetic	37n	Po	+7.80	-	Melezhik et al., 1998
Kotselvaara	Late diagenetic	37o	Po	+8.00	-	Melezhik et al., 1998
Kotselvaara	Late diagenetic	37p	Po	+7.70	-	Melezhik et al., 1998
Kotselvaara	Late diagenetic	37q	Po	+6.00	-	Melezhik et al., 1998
Kotselvaara	Late diagenetic	38a	Po	+8.40	-	Melezhik et al., 1998
Kotselvaara	Late diagenetic	38b	Po	+8.60	-	Melezhik et al., 1998
Kotselvaara	Late diagenetic	38c	Po	+9.90	-	Melezhik et al., 1998
Kotselvaara	Late diagenetic	38d	Po	+8.20	-	Melezhik et al., 1998
Kotselvaara	Late diagenetic	38e	Po	+8.00	-	Melezhik et al., 1998
Kotselvaara	Late diagenetic	38f	Po	+12.10	-	Melezhik et al., 1998
Kotselvaara	Late diagenetic	38g	Po	+7.90	-	Melezhik et al., 1998
Kotselvaara	Late diagenetic	38h	Po	+8.00	-	Melezhik et al., 1998
Kotselvaara	Late diagenetic	38i	Po	+8.30	-	Melezhik et al., 1998
Kotselvaara	Late diagenetic	38j	Po	+8.40	-	Melezhik et al., 1998
Kotselvaara	Late diagenetic	38k	Po	+7.50	-	Melezhik et al., 1998
Kotselvaara	Late diagenetic	38l	Po	+8.20	-	Melezhik et al., 1998
Kotselvaara	Late diagenetic	38m	Po	+8.10	-	Melezhik et al., 1998
Kotselvaara	Late diagenetic	38n	Po	+7.80	-	Melezhik et al., 1998
Kotselvaara	Late diagenetic	38o	Po	+8.40	-	Melezhik et al., 1998
Kotselvaara	Late diagenetic	38p	Po	+8.10	-	Melezhik et al., 1998
Kotselvaara	Late diagenetic	38q	Po	+7.80	-	Melezhik et al., 1998
Kotselvaara	Late diagenetic	38r	Po	+8.40	-	Melezhik et al., 1998
Kotselvaara	Py-Po lens	39a	Po-Py	+22.50	-	Melezhik et al., 1998
Kotselvaara	Py-Po lens	39b	Po-Py	+20.10	-	Melezhik et al., 1998
Kotselvaara	Py-Po lens	39c	Po-Py	+23.20	-	Melezhik et al., 1998
Kotselvaara	Py-Po lens	39d	Po-Py	+19.50	-	Melezhik et al., 1998
Kotselvaara	Py-Po lens	39e	Po-Py	+22.20	-	Melezhik et al., 1998
Kotselvaara	Py-Po lens	39f	Po-Py	+19.30	-	Melezhik et al., 1998
Kotselvaara	Py-Po lens	39g	Po-Py	+18.00	-	Melezhik et al., 1998
Kotselvaara	Py-Po lens	39h	Po-Py	+18.70	-	Melezhik et al., 1998
Drillhole 2400	Dyke	12a	Py–Po	+13.00	-	Melezhik et al., 1998
Drillhole 2400	Dyke	12c	Py–Po	+13.50	-	Melezhik et al., 1998
Drillhole 2400	Dyke	12d	Py–Po	+14.20	-	Melezhik et al., 1998
Drillhole 2400	Dyke	12f	Py–Po	+23.40	-	Melezhik et al., 1998
Drillhole 2400	Dyke	12g	Py–Po	+24.90	-	Melezhik et al., 1998
Drillhole 2400	Dyke	12h	Py–Po	+10.00	-	Melezhik et al., 1998
Drillhole 2400	Dyke	12i	Py–Po	+11.40	-	Melezhik et al., 1998
Kabanga						
Kabanga North	Schist	KN 98-48	-	+9.10	-	Maier et al., 2010
Main North Body	Banded pelite	KN 01-05	-	+20.20	-	Maier et al., 2010
Kabanga Main	Gabbronorite	KN 98-74	-	+13.40	-	Maier et al., 2010
Kabanga Main	Harzburgite	KN 98-74	-	+21.20	-	Maier et al., 2010
Kabanga Main	Harzburgite	KN 98-74	-	+17.50	-	Maier et al., 2010
Kabanga Main	Harzburgite	KN 98-74	-	+19.20	-	Maier et al., 2010
Block 1	Harzburgite	KB 007	-	+19.60	-	Maier et al., 2010
Block 1	Harzburgite	KB 007	-	+16.50	-	Maier et al., 2010
Block 1	Harzburgite	KB 007	-	+12.10	-	Maier et al., 2010
Main North Body	Harzburgite	KN 01-01b	-	+11.20	-	Maier et al., 2010
Kabanga Main Upper	Harzburgite	KN 91-16	-	+16.90	-	Maier et al., 2010
Kabanga North	Harzburgite breccia	KN 01-17	-	+22.20	-	Maier et al., 2010
Main North Body	Schist	KN 01-05	-	-0.10	-	Maier et al., 2010
Kabanga Main	Pyroxenite	KN 98-74	-	+10.50	-	Maier et al., 2010
Kabanga Main	Pyroxenite	KN 98-74	-	+19.80	-	Maier et al., 2010
Kabanga North	Pyroxenite	KN 98-48	-	+22.50	-	Maier et al., 2010
Kabanga Main Upper	Pyroxenite	KN 91-16	-	+18.60	-	Maier et al., 2010
Kabanga Main	SF-MS	KN 98-74	-	+14.50	-	Maier et al., 2010
Kabanga Main	SF-MS	KN 98-74	-	+14.20	-	Maier et al., 2010

Deposit	Rocktype/ore	Sample	Target	$\delta^{34}S$	stdev	references
Kabanga Main	SF-MS	KN 98-74	-	+17.90	-	Maier et al., 2010
Kabanga Main	SF-MS	KN 98-74	-	+21.30	-	Maier et al., 2010
Kabanga Main	SF-MS	KN 98-74	-	+21.10	-	Maier et al., 2010
Kabanga North	SF-MS	KN 98-48	-	+22.50	-	Maier et al., 2010
Luhuma	SF-MS	Luh 001	-	+17.70	-	Maier et al., 2010
Luhuma	SF-MS	Luh 006	-	+18.70	-	Maier et al., 2010
Block 1	SF-MS	KB 007	-	+15.40	-	Maier et al., 2010
Kabanga North	SF-MS	KN 01-18	-	+22.20	-	Maier et al., 2010
Kabanga North	SF-MS	KN 02-01	-	+21.70	-	Maier et al., 2010
Block 1	SF-MS Breccia	KB1 023	-	+15.40	-	Maier et al., 2010
Kabanga North	SF-MS Breccia	KN 01-17	-	+21.70	-	Maier et al., 2010
Kabanga North	SF-MS Breccia	KN 01-17	-	+22.50	-	Maier et al., 2010
Kabanga North	SF-MS Breccia	KN 02-01	-	+22.40	-	Maier et al., 2010
Stillwater					-	
J-M reef	Reef	5102-E #2	Sulfides	+1.20	-	Zientek and Ripley, 1990
J-M reef	Reef	5102-E #2	Sulfides	+0.90	-	Zientek and Ripley, 1990
J-M reef	Reef	5104W-C	Sulfides	+1.50	-	Zientek and Ripley, 1990
J-M reef	Reef	5104W-G	Sulfides	+1.20	-	Zientek and Ripley, 1990
J-M reef	Reef	5110W	Sulfides	+1.40	-	Zientek and Ripley, 1990
J-M reef	Reef	5112 EL	Sulfides	+0.80	-	Zientek and Ripley, 1990
J-M reef	Reef	5112 EM	Sulfides	+1.10	-	Zientek and Ripley, 1990
J-M reef	Reef	5112 EM	Sulfides	+1.40	-	Zientek and Ripley, 1990
J-M reef	Reef	FPA-1	Sulfides	+0.50	-	Zientek and Ripley, 1990
J-M reef	Reef	FPA-2	Sulfides	+0.00	-	Zientek and Ripley, 1990
J-M reef	Reef	77-79-2	Sulfides	+0.50	-	Zientek and Ripley, 1990
J-M reef	Reef	77-79-3	Sulfides	+0.50	-	Zientek and Ripley, 1990
J-M reef	Reef	77-79-3	Sulfides	+0.70	-	Zientek and Ripley, 1990
J-M reef	Reef	77-79-6	Sulfides	+0.10	-	Zientek and Ripley, 1990
J-M reef	Reef	77-79-6	Sulfides	+0.70	-	Zientek and Ripley, 1990
J-M reef	Reef	77-79-6WA	Sulfides	+3.70	-	Zientek and Ripley, 1990
J-M reef	Reef	77-79-14	Sulfides	+0.30	-	Zientek and Ripley, 1990
J-M reef	Reef	85-80-3	Sulfides	+1.00	-	Zientek and Ripley, 1990
J-M reef	Reef	77-79-7W	Sulfides	+1.20	-	Zientek and Ripley, 1990
J-M reef	Reef	77-79-7W	Sulfides	+0.80	-	Zientek and Ripley, 1990
J-M reef	Reef	77-79-9W	Sulfides	+0.50	-	Zientek and Ripley, 1990
J-M reef	Reef	77-79-9W	Sulfides	+0.40	-	Zientek and Ripley, 1990
J-M reef	Reef	77-79-11W	Sulfides	+0.50	-	Zientek and Ripley, 1990
J-M reef	Reef	85-80-8	Sulfides	+1.80	-	Zientek and Ripley, 1990
J-M reef	Reef	77-79-12W	Sulfides	+2.60	-	Zientek and Ripley, 1990
J-M reef	Reef	77-79-15W	Sulfides	+0.60	-	Zientek and Ripley, 1990
J-M reef	Reef	77-79-15W	Sulfides	+0.70	-	Zientek and Ripley, 1990
J-M reef	Reef	77-79-17W	Sulfides	-1.00	-	Zientek and Ripley, 1990
J-M reef	Reef	77-79-17W	Sulfides	+2.10	-	Zientek and Ripley, 1990
J-M reef	Reef	77-75-23W	Sulfides	+0.70	-	Zientek and Ripley, 1990
J-M reef	Reef	77-75-23W	Sulfides	+0.90	-	Zientek and Ripley, 1990
J-M reef	Reef	77-79-20W	Sulfides	+1.10	-	Zientek and Ripley, 1990
J-M reef	Reef	77-79-20W	Sulfides	+0.30	-	Zientek and Ripley, 1990
J-M reef	Reef	77-74-14	Sulfides	+0.90	-	Zientek and Ripley, 1990
J-M reef	Reef	77-74-16	Sulfides	+7.20	-	Zientek and Ripley, 1990
J-M reef	Reef	77-74-16	Sulfides	+1.80	-	Zientek and Ripley, 1990
J-M reef	Reef	77-75-20W	Sulfides	+0.40	-	Zientek and Ripley, 1990
J-M reef	Reef	77-75-20W	Sulfides	+0.60	-	Zientek and Ripley, 1990
J-M reef	Reef	77-74-2W	Sulfides	+1.00	-	Zientek and Ripley, 1990
J-M reef	Reef	77-74-2W	Sulfides	+0.60	-	Zientek and Ripley, 1990
J-M reef	Reef	77-74-6W	Sulfides	+1.00	-	Zientek and Ripley, 1990
J-M reef	Reef	77-74-6W	Sulfides	+0.80	-	Zientek and Ripley, 1990
J-M reef	Reef	77-75-1WD	Sulfides	+0.30	-	Zientek and Ripley, 1990
J-M reef	Reef	77-75-1WD	Sulfides	+0.30	-	Zientek and Ripley, 1990
J-M reef	Reef	77-75-7W	Sulfides	+0.80	-	Zientek and Ripley, 1990
J-M reef	Reef	77-74-8W	Sulfides	+0.20	-	Zientek and Ripley, 1990
J-M reef	Reef	77-74-8W	Sulfides	+0.80	-	Zientek and Ripley, 1990

Deposit	Rocktype/ore	Sample	Target	$\delta^{34}S$	stdev	references
J-M reef	Reef	77-75-2W	Sulfides	+0.80	-	Zientek and Ripley, 1990
J-M reef	Reef	77-75-2W	Sulfides	+0.00	-	Zientek and Ripley, 1990
J-M reef	Reef	77-75-24WB	Sulfides	+1.10	-	Zientek and Ripley, 1990
J-M reef	Reef	77-75-24WC	Sulfides	+3.90	-	Zientek and Ripley, 1990
J-M reef	Reef	77-79-1W	Sulfides	+0.50	-	Zientek and Ripley, 1990
J-M reef	Reef	85-80-1	Sulfides	+0.40	-	Zientek and Ripley, 1990
J-M reef	Reef	76-41W	Sulfides	+0.40	-	Zientek and Ripley, 1990
Bushveld						
Merensky Reef	Reef	-	-	-0.60	0.00	Buchanan et al., 1981
Munni-Munni						
Munni-Munni	All ores	-	-	+2.40	0.10	Hoatson and Keays, 1989
Federov Pansky						
Federov Block - Upper	Gabbronorite	4946	WR	+0.20	-	Schissel et al., 2002
Federov Block - Upper	Gabbronorite	4958	WR	+0.30	-	Schissel et al., 2002
Federov Block - Upper	Gabbronorite	4977	WR	+0.70	-	Schissel et al., 2002
Federov Block - Upper	Gabbronorite	4979	WR	+0.70	-	Schissel et al., 2002
Federov Block - Upper	Gabbronorite	2928	WR	+0.80	-	Schissel et al., 2002
Federov Block - Upper	Gabbronorite	3202	WR	+0.80	-	Schissel et al., 2002
Federov Block - Upper	Gabbronorite	5024	WR	+0.80	-	Schissel et al., 2002
Federov Block - Lower	Gabbronorite	5026	WR	+0.80	-	Schissel et al., 2002
Federov Block - Lower	Gabbronorite	3195	WR	+1.40	-	Schissel et al., 2002
Federov Block - Lower	Gabbronorite	4787	WR	-0.20	-	Schissel et al., 2002
Federov Block - Lower	Gabbronorite	1824	WR	+0.00	-	Schissel et al., 2002
Federov Block - Lower	Gabbronorite	1822	WR	+0.30	-	Schissel et al., 2002
Federov Block - Lower	Gabbronorite	1952	WR	+0.50	-	Schissel et al., 2002
Federov Block - Lower	Gabbronorite	166508	WR	+0.50	-	Schissel et al., 2002
Federov Block - Lower	Gabbronorite	166509	WR	+0.60	-	Schissel et al., 2002
Federov Block - Lower	Gabbronorite	1355	WR	+0.70	-	Schissel et al., 2002
Federov Block - Lower	Gabbronorite	5314	WR	+0.80	-	Schissel et al., 2002
Federov Block - Lower	Gabbronorite	1958	WR	+1.00	-	Schissel et al., 2002
Federov Block - Lower	Gabbronorite	5312A	WR	+1.20	-	Schissel et al., 2002
Federov Block - Lower	Gabbronorite	5320	WR	+1.20	-	Schissel et al., 2002
Federov Block - Lower	Gabbronorite	166510	WR	+1.40	-	Schissel et al., 2002
Federov Block - Lower	Gabbronorite	1835	WR	+0.40	-	Schissel et al., 2002
Federov Block - Lower	Gabbronorite	4788	WR	+0.50	-	Schissel et al., 2002
Country rock	Archean Gneiss	5171	WR	-2.00	-	Schissel et al., 2002
Country rock	Archean Gneiss	5172	WR	-1.70	-	Schissel et al., 2002
Country rock	Archean Gneiss	5173	WR	-0.50	-	Schissel et al., 2002
Country rock	Archean Gneiss	1358	WR	+1.70	-	Schissel et al., 2002
Country rock	Archean Gneiss	1359	WR	+2.70	-	Schissel et al., 2002
West Pansky	Anorthosite	2067	WR	+0.00	-	Schissel et al., 2002
West Pansky	Anorthosite	2064	WR	+0.10	-	Schissel et al., 2002
West Pansky	Anorthosite	2077	WR	+0.20	-	Schissel et al., 2002
West Pansky	Anorthosite	2041	WR	+0.50	-	Schissel et al., 2002
West Pansky	Anorthosite	2024	WR	+0.80	-	Schissel et al., 2002
West Pansky	Anorthosite	2031	WR	+0.90	-	Schissel et al., 2002
West Pansky	Anorthosite	370/480	WR	+1.30	-	Schissel et al., 2002
Country rock	Schist	1300/3418	WR	+0.40	-	Schissel et al., 2002
Country rock	Schist	284/484	WR	+1.20	-	Schissel et al., 2002
Country rock	Schist	900/1360-7	WR	+2.90	-	Schissel et al., 2002
Lac des Iles						
Roby Zone	Dark gabbro	JH02-146	Py	+0.31	-	Hinchey and Hattori, 2005
Roby Zone	Dark gabbro	JH02-146	Ccp	+0.83	-	Hinchey and Hattori, 2005
Roby Zone	Dark gabbro	JH02-146	Po	+0.53	-	Hinchey and Hattori, 2005
Roby Zone	Dark gabbro	JH02-146	Po	+0.10	-	Hinchey and Hattori, 2005
High Grade Zone	Gabbro / Pyroxenite	JH-02-SZ3	Py	+0.60	-	Hinchey and Hattori, 2005
High Grade Zone	Gabbro / Pyroxenite	JH-02-SZ1	Py	+0.95	-	Hinchey and Hattori, 2005
High Grade Zone	Gabbro / Pyroxenite	JH-02-SZ2	Py	+0.99	-	Hinchey and Hattori, 2005
High Grade Zone	Gabbro / Pyroxenite	JH-02-SZ2	Ccp	+1.52	-	Hinchey and Hattori, 2005
High Grade Zone	Gabbro / Pyroxenite	JHC-03-063	Py	+0.30	-	Hinchey and Hattori, 2005

Deposit	Rocktype/ore	Sample	Target	$\delta^{34}S$	stdev	references
High Grade Zone	Gabbro / Pyroxenite	JHC-03-063	Ccp	+0.30	-	Hinchey and Hattori, 2005
High Grade Zone	Gabbro / Pyroxenite	JHC-03-070	Sieg	+0.80	-	Hinchey and Hattori, 2005
High Grade Zone	Gabbro / Pyroxenite	JHC-03-070	Ccp	+0.85	-	Hinchey and Hattori, 2005